

# Development of Versatile Bio-stable Oral Polymeric Delivery Systems for Proteins

By

***Pierre Pavan Demarco Kondiah***



***A Thesis submitted to the Faculty of Health Sciences, University of the Witwatersrand, in fulfillment of the requirements for the degree of Doctor of Philosophy***

**Supervisor:**

Professor Viness Pillay  
Department of Pharmacy and Pharmacology, Faculty of Health Sciences, University of the Witwatersrand, South Africa

**Co-Supervisors:**

Professor Yahya E. Choonara  
Department of Pharmacy and Pharmacology, Faculty of Health Sciences, University of the Witwatersrand, South Africa

Professor Girish Modi  
Department of Neurosciences, Division: Neurology, Faculty of Health Sciences, University of the Witwatersrand, South Africa

**Johannesburg, 2014**

## DECLARATION

I, Pierre Pavan Demarco Kondiah declare that this thesis is my own work. It has being submitted for the degree of Doctor of Philosophy in the Faculty of Health Sciences in the University of the Witwatersrand, Johannesburg. It has not been submitted before for any degree or examination at this or any other University.



.....  
This..20th.. day of .Dec..2014

## RESEARCH OUTPUTS

Pierre P.D. Kondiah, Lomas K. Tomar, Charu Tyagi, Yahya E. Choonara, Girish Modi, Lisa C. du Toit, Pradeep Kumar, Viness Pillay, A novel pH-sensitive interferon- $\beta$  (INF-  $\beta$ ) oral delivery system for application in multiple sclerosis International Journal of Pharmaceutics 456 (2013) 459– 472 [Research Article]. Accreditation: ISI; IF: 3.785

### Research Output Presentation

Pierre P.D. Kondiah, Viness Pillay, Yahya E. Choonara, Development of a Versatile Proteomatrix Oral Polymeric Delivery System for advances in the field of Multiple Sclerosis (Podium Presentation). Cross-Faculty Postgraduate Research Day, University of the Witwatersrand, Johannesburg, South Africa, 2014

### Patent Filed

Oral Protein Polymeric Delivery System, Pierre P.D. Kondiah, Viness Pillay, Yahya E. Choonara, Lisa C. du Toit, Pradeep Kumar, Lomas K. Tomar, Charu Tyagi. SA Patent Application Number (SA 2013, 05584). PCT filed.

## DEDICATION

Dedication to Bhagawan Sri Sathya Sai Baba



## Acknowledgments

**I would like to acknowledge my family, friends, and all supervisors in supporting me throughout my PhD endeavor. My sincere thanks and appreciation!**



## Abstract

An oral proteomatrix drug delivery platform was formulated using pH responsive biostable polymers for slow release kinetics for the treatment of the neurodegenerative disease, multiple sclerosis (MS), which was the primary aim. After successful design and optimization for utilizing this system for MS, this system was further applied as a versatile platform for oral protein delivery. Interferon beta (INF- $\beta$ ) was selected as the oral treatment for MS. The fundamental effect of INF- $\beta$  in the treatment of MS is based on reducing the immune response that is directed against central nervous system myelin, i.e. the fatty sheath that surrounds and protects nerve fibers. Damage of nerve fibers, resulting in demyelination, consequently causes nerve impulses to be slowed or halted, thus producing symptoms of MS (Jongen et al., 2011). To date, INF- $\beta$  is effectively being used to treat MS subcutaneously or as intramuscular injections. These forms of administration have commonly been associated with multiple problems of pain, allergic reactions, poor patient compliance and chances of infection (Chiu et al., 2007). It was thus concluded to design an oral platform for the delivery of multiple protein therapeutic formulations. To prove the versatility of the proteomatrix system, two other demanding protein therapeutics for oral delivery, insulin and erythropoietin, were selected for further *in vitro* Box-Behnken series of formulations and *in vivo* analysis. By administration of these oral protein systems, a greater patient compliance can be achieved, thus enhancing the therapeutic profiles of patients with conditions of MS, diabetes and chronic renal failure resulting in chronic anemia. All studies consisted of *in vitro* drug release studies, characterization using specific analytical techniques for testing the mechanical properties, as well as the physicochemical characteristics of the copolymeric system. All proteins, INF- $\beta$ , insulin and erythropoietin, were analyzed *in vivo* using New Zealand White rabbits (NZW) with determination of the protein from serum obtained during regular blood sampling intervals.

The polymers chitosan (CHT), trimethyl-chitosan (TMC), poly(ethylene glycol)dimethacrylate (PEGDMA) and methacrylic acid (MAA) was used in synthesis-free radical polymerization reaction, to obtain crosslinked copolymeric systems of CHT-PEGDMA-MAA and TMC-PEGDMA-MAA. The polymerization of CHT-PEGDMA-MAA produced a microgel formulation, thereby loading INF- $\beta$ , insulin and erythropoietin as separate formulations for further evaluation. TMC-PEGDMA-MAA polymerization produced microparticles, loading the three proteins as separate drug delivery formulations for further *in vivo* and *in vitro* analysis. Mucoadhesive studies were undertaken on the proteomatrix systems, confirming greater mucoadhesion in the TMC crosslinked polymer than the CHT.

For insulin studies, rabbits were induced with diabetes according to the protocol approved by the university ethics committee, and evaluated for a decrease in blood glucose levels in relation to time of 24 hours. *In vivo* studies were undertaken comparing the oral experimental formulations, against a leading commercial product on the market for all protein formulations, administered subcutaneously, as well as compared to a control (n=3 rabbits for each group in the study). Results obtained from copolymeric TMC-PEGDMA-MAA proteomatrix microparticles concluded a greater peak absorption concentration and greater sustained release profiles for each protein formulation *in vivo*, as opposed to the copolymeric CHT-PEGDMA-MAA proteomatrix microgel formulation. Both TMC-PEGDMA-MAA and CHT-PEGDMA-MAA copolymeric proteomatrix formulations proved successful for all *in vitro* and *in vivo* studies to significant degrees, thus producing a versatile platform for oral protein delivery.

## TABLE OF CONTENTS

DECLARATION	ii
RESEARCH OUTPUTS	iii
DEDICATION	iv
ACKNOWLEDGEMENTS	v
ABSTRACT	vii
TABLE OF CONTENTS	viii
LIST OF FIGURES	xiv
LIST OF TABLES	xxii
LIST OF COMMONLY-USED ABBREVIATIONS	xxiv
CHAPTER 1	1
1. INTRODUCTION	1
1.1. Background into Protein Therapeutics	1
1.2. Rational and Motivation of Study	4
1.3. Possible Therapeutic Agent Application of the Delivery System	8
1.4. Aim and Objectives	8
1.5. Novelty of the delivery systems	9
1.6. Overview of the Thesis	10
1.7. Concluding Remarks	12
CHAPTER 2	13
2. A LITERATURE REVIEW OF CRITICAL EVALUATION OF THERAPEUTIC MULTIPLE SCLEROSIS INTERVENTIONS: DIAGNOSIS AND TREATMENT OPTIONS	13
2.1. Introduction	13
2.2. Multiple Sclerosis Symptoms and Prognosis	14
2.3. Advances in Diagnosis	17
2.3.1. Pathophysiology of MS	19
2.3.2. Immunological studies	21
2.3.3. Genetic predisposing factors	21
2.3.4. Experimental autoimmune encephalomyelitis (EAE) and viral animal modeling for multiple sclerosis	22
2.4. Current Line of Treatment	26

2.4.1. Anti-CD20 antibodies	28
2.4.2. Disease Modifying Treatments	30
2.4.2.1. Glatiramer acetate (GA)	32
2.4.2.2. Beta-Interferon treatment	34
2.4.2.3. Natalizumab treatment	36
2.4.2.4. Mitoxantrone treatment	38
2.5. Fingolimod Therapy	39
2.6. 4-aminopyridine (4-AP) (Fampridine-SR) and 3,4 diaminopyridine	40
2.7. Teriflunomide	42
2.8. Dimethyl fumarate	43
2.9. Vitamin D therapy	44
2.10. Fatigue in MS	45
2.11. Concluding Remarks	48
 CHAPTER 3	 49
 CRITICAL EVALUATION OF PHYSICOCHEMICAL AND PHYSICOMECHANICAL PROPERTIES OF NOVEL MICROGEL AND MICROPARTICULATE SYSTEMS	 49
3.1. Introduction	49
3.2. Materials and Methods	50
3.2.1. Materials	50
3.2.2. Synthesis of TMC for microparticulate formation	51
3.2.3. Synthesis of PEGdimethacrylate (PEGDMA)	51
3.2.4. Preparation of CHT-PEGDMA-MAA/TMC-PEGDMA-MAA copolymeric particles	52
3.2.5. Box-Behnken Design of copolymeric particles	52
3.2.6. Attenuated Total Reflectance-Fourier Transform Infrared (ATR-FTIR) spectroscopy	54
3.2.7. Particle size and zeta potential analysis of copolymeric systems	54
3.2.8. Mucoadhesion studies	55
3.2.9. Porositometric analysis	55
3.2.10. Morphological Characteristics of the Particles using Scanning Electron Microscopy (SEM)	57
3.2.11. Thermal Properties of the Monomers, Polymers and Copolymeric Systems	57

using Differential Scanning Calorimetry (DSC) analysis	
3.2.12. Thermogravimetric analysis (TGA)	57
3.2.13. Matrix hardness (MH) and Matrix resilience (MR)	58
3.2.14. Rheological Evaluation	58
3.2.15. X-Ray Diffraction (XRD) analysis	60
3.2.16. NMR Evaluation	61
3.3. Results and Discussion	61
3.3.1 PART A: Evaluation of TMC-PEGDMA-MAA Copolymeric Microparticulate System	61
3.3.1.1. Box-Behnken optimization evaluation	61
3.3.1.2. ATR-FTIR Spectroscopy	63
3.3.1.3 Particle size and zeta potential analysis	64
3.3.1.4. Porosity analysis of optimized copolymeric delivery system	66
3.3.1.5. Morphological characteristic determination using SEM techniques	69
3.3.1.6. Mucoadhesive properties of optimized copolymeric delivery system	70
3.3.1.7. Thermal evaluation using Differential Scanning Calorimetry (DSC) analysis	72
3.3.1.8. Thermogravimetric analysis (TGA)	74
3.3.1.9. Matrix hardness (MH) and Matrix resilience (MR)	76
3.3.1.10. Rheological Evaluation	78
3.3.1.11. X-Ray Diffraction (XRD) analysis	80
3.3.1.12. NMR analysis	82
3.3.1.13. Concluding Remarks	85
3.3.2 PART B: Evaluation of CHT-PEGDMA-MAA Copolymeric Microgel System	86
3.3.2.1. Box-Behnken optimization analysis	86
3.3.2.2. ATR-FTIR Spectroscopy of monomers and copolymeric microgel formulation	88
3.3.2.3. Particle size and zeta potential analysis	89
3.3.2.4. Porosity analysis of optimized copolymeric delivery system	91
3.3.2.5. Scanning Electron Microscopy (SEM) of the microgel formulation	93
3.3.2.6. Mucoadhesive properties of optimized copolymeric delivery system	94
3.3.2.7. Differential Scanning Calorimetry (DSC) analysis of monomers and copolymeric microgel formulation	95

3.3.2.8. Thermogravimetric analysis (TGA)	98
3.3.2.9. Mechanical evaluation of the copolymeric microgel tablet	100
3.3.2.10. Rheological evaluation of the microgel formulation	102
3.3.2.11. X-Ray Diffraction (XRD) analysis of the microgel formulation	104
3.3.2.12. NMR analysis	105
3.3.3. Concluding Remarks	107
CHAPTER 4	108
PROTEIN LOADING AND <i>IN VITRO</i> RELEASE ANALYSIS OF THE ORAL MICROPARTICULATE AND MICROGEL DRUG DELIVERY PLATFORMS	108
4.1. Introduction	108
4.2. Materials and Methods	109
4.2.1. Materials	109
4.2.2. Protein-loading in copolymeric microgel and microparticulate systems	109
4.2.3. Protein release studies undertaken on all Box-Behnken design and optimized formulations	110
4.3 Results and Discussion	111
4.3.1. PART A: Evaluation of TMC-PEGDMA-MAA Microparticulate System using Insulin, EPO and INF- $\beta$ as Optimized Protein Delivery Systems	111
4.3.1.1. Protein-loading evaluation for each protein microgel formulation	111
4.3.1.2. <i>In vitro</i> release analysis on design and optimized formulations	112
4.3.2. Concluding Remarks	117
4.3.2. PART B: Evaluation of CHT-PEGDMA-MAA Microgel System using Insulin, EPO and INF- $\beta$ as Optimized Protein Delivery Systems	118
4.3.2.1. Protein-loading evaluation for each protein microgel formulation	118
4.3.2.2. <i>In vitro</i> protein release analysis on design and optimized formulations	119
4.3.3. Concluding Remarks	124
	125

## CHAPTER 5

### EVALUATION OF THE *IN VIVO* RELEASE POTENTIAL OF THE ORAL INSULIN, INF- $\beta$ AND EPO-LOADED TMC-PEGDMA-MAA MICROPARTICULATE AND CHT-PEGDMA-MAA MICROGEL SYSTEMS IN A RABBIT MODEL 125

5.1. Introduction 125

5.2. Materials and Methods 126

5.2.1. Materials 126

5.2.2. Animal study protocol for dosing and blood sampling 127

5.2.3. Histopathological tissue evaluation postdosing 130

5.2.4. Pharmacokinetic modeling employing compartmental and non-compartmental algorithms 130

5.3 Results and Discussion 130

5.3.1. Part A: Evaluation of TMC-PEGDMA-MAA-Loaded Copolymeric Delivery System for *In Vivo* Evaluation

5.3.1.1. Quantitative *in vivo* release analysis 131

5.3.1.2. Histopathological evaluation 136

5.4. Part B: Evaluation of CHT-PEGDMA-MAA Protein-Loaded Copolymeric Delivery System for *In Vivo* Evaluation 138

5.4.1 Quantitative *in vivo* release analysis 138

5.4.2 Histopathological evaluation 140

5.5. Comparative pharmacokinetic analysis of the INF- $\beta$ -loaded TMC-PEGDMA-MAA microparticles and CHT-PEGDMA-MAA microgel formulations. 142

5.5.1. INF- $\beta$  non-compartmental and compartmental analysis 142

5.6. Concluding Remarks 146

## CHAPTER 6

### CONCLUSION AND RECOMMENDATIONS

6.1. Conclusion 147

6.2. Future Outlook and Recommendations 147

7. REFERENCES 151

8. APPENDICES	174
8.1. Animal Ethics Clearance Certificate	174
8.2. Research Paper 1	175
8.3. Research Output Presentation	176

## LIST OF FIGURES

- Figure 1.1:** Schematic representing PEG- INF- $\beta$  conjugate 3
- Figure 1.2:** Schematic illustrating how the pH sensitive, biostable particles shrink in gastric pH (pH 1.2), in comparison to their swelling abilities in the basic pH of the small intestine (pH 6.8). Being mucoadhesive in nature they will adhere to the mucus lining and release the protein, which will further enter into the blood stream via paracellular pathways 7
- Figure 2.1:** Illustration of axonal damage, in which myelin is perceived as a foreign intruder and mounts an immune response to attack and destroy myelin sheaths. This causes deterioration of nerve conduction and impulses. Scarring normally starts forming if the condition is not controlled, thereby forming plaques as material is deposited into the scar formation. In this specific axonal transaction and Immune-mediated demyelination, a great degree of ovoids were identified from a MS tissue (a), red identifies stain for myelin protein and green for axons. The arrowheads depict demyelination, in which microglia and hematogenous monocytes are believed to mediate the degenerative process. The large green swelling of the axonal bulb,(b and c) is a typical response of axonal transaction, due to the immune-mediated demyelination process. Once transaction occurs, the distal end of the axon substantially degenerates, in relation to the proximal end connected to the neuronal cell body that sustains itself without undergoing degeneration, allowing transported organelles to locate itself at the site of transaction, thus forming an ovoid (arrows) (Figure reproduced with permission from Elsevier Ltd.: Dutta *et al*, 2011) 15
- Figure 2.2:** Schematic representing the main symptoms associated with MS as a result of not seeking treatment (van den Noort., 2005., Poser *et al.*, 2001) 16
- Figure 2.3 (a)** RRMS is the most common form of MS with 65-80% of patients starting in this stage. This stage comprises of acute attacks (exacerbations), and if not treated leads to serious loss of function. Symptoms may resolve, until another attack occurs (relapse) **(b)** PPMS comprises of a uniform steady increase in deterioration, with no occurring relapses and remissions. This form of MS is more predominant in people over the age of 40 and prevalent in approximately 15% of people with MS **(c)** SPMS 17

starts with RRMS, which later develops into progressive disease. Statistics indicate that 50% of patients develop SPMS after acquiring RRMS within a 10 year gap period **(d)** this stage of MS (PRMS) is characterized by steady progression of disability with acute attacks which may or may not follow recovery. This is one of the least prevalent stages of MS, and usually appears as PPMS. (Figure adapted with permission from Elsevier Ltd.: Davis., 2010)

**Figure 2.4:** Schematic depiction of axonal injury, due to inflammation caused by demyelination in an active MS lesion. Glial and immune cells cause damage to the tissue, as well as axonal transection. Degeneration occurs at sites distal to the site of transection. Myelin forms empty tubes that later develop into degenerated ovoids. White matter may seem normal on standard MRI images. (Figure reproduced with permission from Elsevier Ltd.: Bjartmar *et al*, 2003) 20

**Figure 2.5:** Depiction of a relatively common MS model in mice, illustrating systemic and local disease process points of interest and analysis. As part of the active immunization process, antigens are injected at the toe pad of the animal, since this is a highly effective systemic immune response due to highly responsive lymphatic draining nodes at the site for the autoimmune procedure to be induced efficiently. (Figure reproduced with permission from Elsevier Ltd.: Mix *et al*, 2010) (AT-EAE, adoptive transfer EAE; CFA, complete Freund's adjuvant; i.p., intraperitoneal; i.v., intravenous; LN, lymph node; MOG, myelin oligodendrocyte glycoprotein; PB, peripheral blood; PLP, proteolipid protein; s.c., subcutaneous; SP, spleen, Th1 cells, T helper type 1 cells.) 23

**Figure 2.6:** A viral autoimmune model of sequential molecular mimicry and epitope spreading. The black straight lines (not broken up) depict the acute viral infection, where APC or macrophages present antigens of viral peptides to specific viral epitope CD4 T cells located at the periphery(1a), or directly to the CNS (1b). These activated cells at the periphery, cross the BBB, thereby releasing a range of proinflammatory chemokines and cytokines, increasing the inflammatory process (2) this causes a great deal of tissue destruction further amplified by activating and attracting a greater number of monocytes, macrophages and other inflammatory mediators (3) the virus and self antigens, induces self-peptide processing to occur (4) cross reaction 25

(molecular mimicry) also occurs between self-peptides (galactocerebroside, GALC) as well as viral peptides (VP1) (5). The red dashed lines depict a time response of a persistent viral infection, the epitope spreading model (1) the antigen is then processed by APC's (2) this is then presented to virus epitope-specific CD4 T cells, which can be in the peripheral or crossing the BBB to nervous tissue (3) proinflammatory cytokines and chemokines are thus activated, attracting a greater number of monocytes and macrophages (4) this results in self-tissue destruction (5) leading to greater inflammatory reactions and processing of self-antigens (6) activation of virus-specific and self-epitope CD4 T cells (7), thus resulting in a prolonged immune-mediated disease state model.(Figure reproduced with permission from Elsevier Ltd.: Mecha *et al*, 2013)

**Figure 2.7:** Various stages of MS and the implementation of disease modifying drugs (DMD) in relation to the increasing state of neurodegeneration (MTR-magnetization transfer ratio; DTI-diffusion tensor imaging; OCT-optical coherence tomography,;EP-evoked potential; fMRI-functional magnetic resonance imaging; DTI-diffusion tensor imaging ; MRS- magnetic resonance spectroscopy; CSF-cerebrospinal fluid;). (Figure reproduced with permission from Elsevier Ltd.: Ziemann *et al*, 2011) 27

**Figure 2.8:** Treatment procedures for relapsing–remitting multiple sclerosis. (Figure adapted with permission from Elsevier Ltd.: Sorensen., 2011) 32

**Figure 2.9:** Mode of action of IFN- $\beta$ . (Figure adapted with permission from Elsevier Ltd.: Rudicka *et al*, 2011) 36

**Figure 3.1:** Phase shift illustrated using the Theorem of Pythagoras in relation to complex modulus ( $G^*$ ), storage modulus ( $G'$ ) and loss modulus ( $G''$ ). 60

**Figure 3.2:** Residual and surface plots of (a) average particle size, (b) fractional release in gastric medium at 2 hours and (c) fractional release in intestinal medium at 2 hours. 62

**Figure 3.3:** Optimization plot for the response optimization of the copolymeric formulation 63

**Figure 3.4:** FTIR spectra of (a) TMC-PEGDMA-MAA, (b) CHT, (c) MAA, (d) TMC, (e) PEGDMA 64

**Figure 3.5:** Schematic depicting (a) the types of isotherms at different relative pressure, (b) the types of hysteresis loops according to the IUPAC classification system (adapted from Sing et al., 1985). 66

69

**Figure 3.6:** Isotherm Linear plots (a) gastric medium and (b) intestinal medium

**Figure 3.7:** Scanning electron micrographs of copolymeric particles at 10 000X magnification (a) in gastric medium (pH 1.2) (b) in intestinal medium (pH 6.8). 70

**Figure 3.8:** Percentage crosslinking of prepared copolymeric particulate system to mucous 71

**Figure 3.9:** DSC thermogram of a) TMC, b) PEGDMA and c) TMC-PEGDMA-MAA d) PMAA 74

**Figure 3.10:** TGA profile of (a) PEGDMA, (b) TMC and (c) TMC-PEGDMA-MAA 76

**Figure 3.11:** Evaluation of mechanical properties of copolymeric particles a): Matrix Hardness (MH) (N/mm); b) Matrix Resilience (MR) (Kg/sec) 76

**Figure 3.12:** Oscillation curves representing storage modulus ( $G'$  in red) and loss ( $G''$  in green), using a 0.1% constant strain in a) gastric medium and b) intestinal medium 79

**Figure 3.13:** Diffractogram Representing the intensity of crystalline nature of PEGDMA (red), PMAA (blue), TMC (green), TMC-PEGDMA-MAA (yellow) 81

**Figure 3.14:**  $^{13}\text{C}$  solid state NMR spectra of a) chitosan, b) TMC, c) MAA, and d) TMC-PEGDMA-MAA spinning side band CO peak 83

**Figure 3.15:** Reaction mechanism involving each reactant in the free radical polymerization reaction to form the copolymeric crosslinked microparticulate system. 84

- Figure 3.16:** Representation of residual and surface plots of the formulations, with regard to average particle size, fractional release at 2 hours in gastric medium and fractional release at 2 hours in intestinal medium. 87
- Figure 3.17:** Program specifications for obtaining an optimal desirability index of 93% for the copolymeric insulin delivery system 88
- Figure 3.18:** FTIR spectra of (a) CHT-PEGDMA-MAA, (b) CHT, (c) MAA, (d) PEGDMA 89
- Figure 3.19:** Isotherm Linear plots (a) gastric medium and (b) intestinal medium. 93
- Figure 3.20:** SEM images of copolymeric microgel at 10 000X magnification (a) in gastric medium (pH 1.2) (b) in intestinal medium (pH 6.8). 94
- Figure 3.21:** Percentage crosslinking of prepared copolymeric microgel system to mucous 95
- Figure 3.22:** DSC thermograms for copolymeric microgel a) CHT-PEGDMA-MAA, and polymers b) PEGDMA, c) CHT, d) PMAA 98
- Figure 3.23:** TGA profile representation of a) CHT, b) PEGDMA and c) CHT-PEGDMA-MAA 100
- Figure 3.24:** a) MH (N/mm) Grad net fd =80.016, Area Fd =0.009 b) MR (Kg/sec) = 30% 101
- Figure 3.25:** Dynamic oscillation curves depicting storage modulus (G' in red) and loss (G'' in green) under constant strain of 0.1% a) in gastric medium pH 1.2 and b) in intestinal medium pH 6.8 103
- Figure 3.26:** Diffractogram representing each polymer CHT(green), PEGDMA(red), PMAA(blue) and copolymer CHT-PEGDMA-MAA(yellow). 104

<b>Figure 3.27:</b> $^{13}\text{C}$ solid state NMR spectra of a) chitosan b) MAA, and c) CHT-PEGDMA-MAA	106
<b>Figure 3.28:</b> Reaction mechanism of the crosslinked copolymer with proposed structure for the microgel system.	106
<b>Figure 4.1:</b> Fractional release of insulin in gastric medium: a) formulations 1-7, b) formulations 8-13.	114
<b>Figure 4.2:</b> Fractional release of insulin in intestinal medium: a) formulations 1-7, b) formulations 8-13.	115
<b>Figure 4.3:</b> (a) Fractional release of Proteins in gastric medium, (b) Fractional release of proteins in intestinal medium.	116
<b>Figure 4.4a-b:</b> Demonstrates the drug release properties of the Box Behnken series of formulations in gastric medium over 2.5 hour duration.	121
<b>Figure 4.5a-b:</b> Demonstrates the drug release properties of the Box Behnken series of formulations in intestinal medium over 8 hour duration.	122
<b>Figure 4.6:</b> (a) Fractional release profiles of insulin, INF- $\beta$ and EPO in gastric medium (b) Fractional release profiles of insulin, INF- $\beta$ and EPO in intestinal medium.	123
<b>Figure 5.1:</b> Summarised flow-chart of the animal study undertaken for <i>in vivo</i> evaluation of all protein-loaded formulations of the microgel and microparticulate systems.	129
<b>Figure 5.2:</b> One-compartmental model representing the pharmacokinetic distribution of protein released from the microparticulate and microgel systems.	130
<b>Fig.5.3:</b> Mechanism of action depicting the mucoadhesive characteristic of the protein-loaded microparticulate system adhering to the gastric linings of the stomach, forming a site specific directed passage for protein to enter the blood stream.	132

**Fig.5.4a:** *In vivo* release of INF- $\beta$  from the optimized oral microparticles compared to the commercial subcutaneous dose administration. 134

**Figure 5.4b:** Blood glucose response to insulin-loaded microparticles, commercial SC formulation and placebo dose. 135

**Figure 5.4c:** EPO-loaded microparticles, commercial SC formulation and placebo *in vivo* studies. 136

**Figure 5.5:** Histological evaluation of tissue samples from rabbits in the experimental oral microparticles. a) Intestinal mucosal crypts confirm normal intestinal mucosa (X10), b) Intestinal mucosa which shows normal epithelium (X10), c) Fundic portion of the stomach which shows normal fundic glands (X10) d) Severe loss of cellularity and necrosis of the islet cells in the islet of Langerhans (X20). 137

**Figure 5.6:** *In vivo* analysis of the oral protein-loaded microgel system in a rabbit model a) INF- $\beta$ , b) Insulin c) EPO 140

**Figure 5.7:** Histological evaluation of the GIT from rabbits dosed with the protein-loaded microgel formulation. a) Intestinal mucosa showing normal intestinal villi (10X), b) normal fundic mucosa of the stomach (10X), c) duodenal mucosa showing normal glands and intestinal crypts (X10), d) normal intestinal mucosa with gutter cells among epithelial cells (X10) 141

**Figure 5.8:** (a) Concentration-time profiles demonstrating the predicted and observed concentration values from the release profiles of INF- $\beta$  microparticulate system over 24 hours for one compartmental analysis with lag, (b) demonstrating the predicted and observed concentration values from the release profiles of INF- $\beta$  of the microparticulate system over 24 hours for noncompartmental analysis, demonstrating a significant maintenance of slow release behavior of the INF- $\beta$  loaded copolymeric delivery system. 144

**Figure 5.9:** (a) Predicted and observed concentration values from the release profiles 145

of INF- $\beta$  over 24 hours for noncompartmental analysis (b) Predicted and observed concentration values from the release profiles of INF- $\beta$  over 24 hours for one compartmental analysis with lag.

**Figure 5.10:** (a) Predicted and observed concentration values from the release profiles of INF- $\beta$  over 24 hours for noncompartmental analysis (b) Predicted and observed concentration values from the release profiles of INF- $\beta$  over 24 hours for one compartmental analysis with lag. 147

## LIST OF TABLES

<b>Table 2.1:</b> Treatment options and mechanism of action of the drugs in MS therapy	46
<b>Table 3.1:</b> Variables in Box-Behnken design	53
<b>Table 3.2:</b> Formulations generated by Box-Behnken design for CHT-PEGDMA-MAA microgel formulations.	53
<b>Table 3.3:</b> Formulations generated by Box-Behnken design for TMC-PEGDMA-MAA microparticulate formulations.	54
<b>Table 3.4:</b> Evacuation and Heating Phase Parameters for Porositometric Analysis	56
<b>Table 3.5:</b> Parameter settings for determining MR and MH	58
<b>Table 3.6:</b> Parameters employed for rheological evaluation	59
<b>Table 3.7:</b> Experimental design formulation analysis of average particle size according to specifications of the design in gastric and intestinal fluid	65
<b>Table 3.8:</b> Porosity analysis of optimized copolymeric delivery system at different pH ranges of gastric and intestinal medium	68
<b>Table 3.9:</b> Experimental design formulation in gastric and intestinal fluid for evaluation of average particle size	91
<b>Table 3.10:</b> Porosity analysis of optimized copolymeric delivery system at different pH ranges of gastric and intestinal medium	92
<b>Table 3.11:</b> TGA analysis of polymers and copolymeric microgel	100
<b>Table 4.1:</b> Experimental design formulation analysis for protein loading efficiency and release	113

**Table 4.2:** Experimental design formulation analysis for protein loading efficiency and release 119

**Table 5.1:** Doses of drugs administered to rabbits during *in vivo* study. 127

**Table 5.2:** Dosages for protein-loaded microparticulate, microgel and comparator subcutaneous formulations. 127

## LIST OF COMMONLY-USED ABBREVIATIONS

4-AP- 4-aminopyridine

AIBN- Azobisisobutyronitrile

ATR-FTIR- Attenuated Total Reflectance-Fourier Transform Infrared

BBB- Blood Brain Barrier

BET- Brunauer–Emmett–Teller

CHT- PEGDMA-MAA-Chitosan-polyethylene glycol dimethacrylate-methacrylic acid

DMT- Disease Modifying Treatments

DSC- Differential Scanning Calorimetry

EAE- Experimental autoimmune encephalomyelitis

EPO- Erythropoietin

GA- Glatiramer Acetate

INF- $\beta$ - Interferon beta

MAA- Methacrylic acid

mAbs- Monoclonal antibodies

MH- Matrix hardness

MR- Matrix resilience

MS- Multiple sclerosis

$M_w$  - Molecular Weight

NMR- Nuclear Magnetic Resonance

PDI- Polydispersity Index

PEGDA- Polyethylene Glycol Diacrylate

PEGDMA- Poly(ethylene glycol) dimethacrylate

SEM- Scanning Electron Microscopy

$T_g$ - Glass Transition

TGA- Thermogravimetric analysis

$T_m$ - Melting Point

TMC- PEGDMA-MAA- Trimethyl chitosan polyethylene glycol dimethacrylate-methacrylic acid

XRD- X-Ray Diffraction

# CHAPTER 1

## INTRODUCTION

### 1.1. Background into Protein Therapeutics

The field of advanced drug delivery has contributed significantly to the entire world, with its dynamic innovative therapeutic means of administration and significant polymer engineering which enables drugs which were previously not known to be absorbed in a certain way, a new dimensional insight into the dynamics of absorption and distribution of the chemical entity. Drug delivery uses various routes for drug administration which commonly include transdermal, intranasal, intravenous, intramuscular, subcutaneous and oral (Katzung 2007). The manner in which the desired formulation has to be absorbed, depends significantly on the formulation synthesis, as well as the pre-formulation studies undertaken to determine success of the desired formulation. Many drugs are relatively simple to absorb via the oral route however, the oral absorption of macromolecules like proteins and peptides, require significant polymeric properties for stability in the gastric and intestinal conditions, also taking into consideration the mucoadhesive properties of the system, since this can also have significant drawbacks if the protein is unable to pass through the mucus layers in its intact form (Tomar *et al.*, 2011).

The development of peptide and protein oral formulations has become an increasingly demanding form of drug delivery, and remains an attractive alternative to parenteral formulations, consequently possessing various challenges in delivery development (Morishita and Peppas *et al.*, 2006). Interferon- $\beta$  (INF- $\beta$ ), a peptide, is the most effective and widely used peptide drug for the treatment of multiple sclerosis (Jongen *et al.*, 2011). Multiple sclerosis (MS) is a chronic neurodegenerative disease that is characterized by its central nervous system effects commonly manifesting as tremors, dizziness, visual disturbances, limb weakness, muscle spasms, loss of sensation, speech impediment and depression, as detailed in Chapter 2 of the thesis (Fischer and Heesen *et al.*, 2011, Stuart *et al.*, 2011). Currently, INF- $\beta$  is effectively being used to treat MS subcutaneously or as intramuscular injections. This form of administration has commonly been associated with multiple problems of pain, allergic reactions, poor patient compliance and chances of infection (Chiu *et al.*, 2007). Interferons exist naturally as a globular protein comprising of 5 helices. It has a  $M_w$  of 20 kDa, although it often runs on SDS-PAGE gels with an apparent  $M_w$  closer to 25 kDa due to glycosylation (Arduini *et al.*,

1999). The coding region encodes a predicted protein amino acid count of 197 amino acids, consisting of a signal sequence of 32 amino acids and a mature INF- $\beta$  of 165 amino acids (Iwata *et al.*, 1996). The fundamental effect of INF- $\beta$  in the treatment of MS is based on reducing the immune response that is directed against central nervous system myelin, i.e. the fatty sheath that surrounds and protects nerve fibers. Damage of nerve fibers, resulting in demyelination, consequently causes nerve impulses to be slowed or halted, thus producing symptoms of MS (Jongen *et al.*, 2011).

Insulin and erythropoietin oral therapeutics, among other widely researched peptide drugs, constitute a significant platform of demand for delivering these via the oral route (Cefalu, 2004). Currently these macromolecular peptides have been effectively used subcutaneously or as intramuscular injections. Regular injection therapy of INF- $\beta$  has various disadvantages. This form of administration has commonly been associated with multiple problems of pain, allergic reactions, poor patient compliance and chances of infection (Chiu *et al.*, 2007). To overcome these problems, researchers are investigating alternative ways to enhance formulations, such as increasing the retention time of the formulation, or by adopting other modes of delivery routes such as nasal, pulmonary and oral routes out of which oral can be the most beneficial mode of delivery, provided it is protected against all forms of degradation. Administering these proteins orally may be the most convenient and beneficial route of administration, hence achieving better patient compliance. According to Veronese *et al.* (2005) PEGylation of INF- $\beta$  was investigated to have many advantages. The stability of INF- $\beta$  by PEGylation increases the retention time, which is one of the most beneficial advantages for absorption through the GIT. Figure 1.1 below represents a polymer-protein conjugate. The polymer, polyethylene-glycol (PEG), shields the protein surface from degrading agents by steric hindrance, in addition, the increased size of the conjugate is the basis of the decreased kidney clearance of the PEGylated INF- $\beta$  (Veronese *et al.*, 2005).

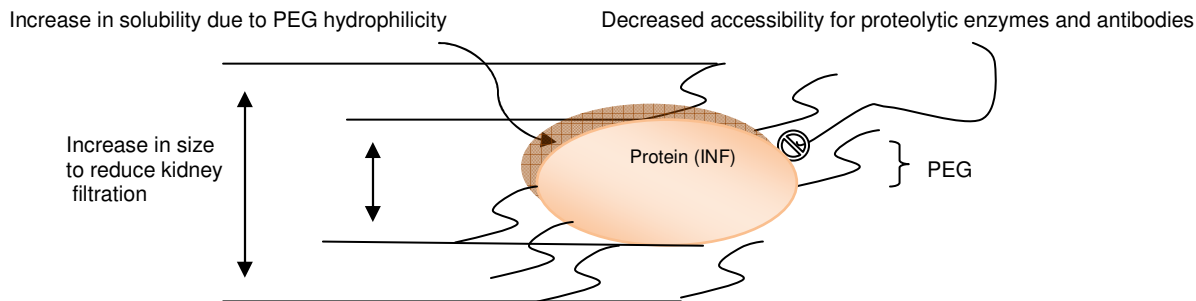


**Figure 1.1:** Schematic representing PEG- INF- $\beta$  conjugate

Various challenges associated with the oral route of peptide delivery include highly acidic pH of the stomach, presystemic enzymatic degradation of peptide, and its poor permeation through the intestinal membrane (Morishita and Peppas *et al.*, 2006). Research in this field which aims to deliver peptides successfully through the oral route are under investigation. Many strategies such as the use of enteric-coated dry emulsions, microspheres, liposomes and nanoparticles for encapsulation of peptides are being critically evaluated (Shaji and Patole, 2008).

Of pertinent interest is the design of an effective carrier system for oral delivery of these essential proteins that surpasses the various challenges of the GIT. According to Kumar *et al.*, (2008) biostable polymers crosslinking poly(ethylene glycol) dimethacrylate (PEGDMA) and methacrylic acid (MAA) based micro and nanoparticles were prepared to evaluate a carrier system for oral delivery of a highly unstable peptide. Studies have proven that polymers containing carboxylic acid groups have the ability to protect peptides from the protease enzymes such as trypsin and chymotrypsin. These polymers were proposed to react by binding of divalent cations (calcium and zinc) to exhibit their enzyme inhibitory effects (Sajesh *et al.*, 2006). Another study undertaken by Bowman and Leong (2006) demonstrated administration of a biodegradable oral formulation, chitosan-insulin nanoparticles, to diabetic rats. Incubation of Caco-2 cells with chitosan-insulin nanoparticles resulted in greater cell binding and uptake compared with chitosan-insulin micoparticles. A significant quantity of fluorescently labeled nanoparticles were contained inside the cells after 2 hour incubation, principally near the apical surface. Results revealed administration of these chitosan-insulin nanoparticles to diabetic rats led to prolonged reduction in serum glucose levels (Bowman and Leong, 2006).

Based on a study performed by Kumari *et al.*, 2010, another approach for delivering peptides is based on its incorporation with biodegradable polymers. Poly-caprolactone (PCL) along with polycationic non-biodegradable acrylic polymers have been used successfully in the study of

delivering oral insulin to rats. The use of chitosan nanoparticles for encapsulation of insulin markedly enhanced intestinal absorption of insulin following oral administration. It is thus essential to look into biostable mediums for oral delivery of INF- $\beta$ .

*In vitro* and *ex vivo* evaluations of the developed novel drug delivery systems may provide valid information regarding the drug release characteristics, but they cannot completely simulate *in vivo* conditions. Therefore, *in vivo* studies are essential to obtain salient pharmacokinetic data. For undertaking insulin studies, healthy rabbits were used during this experiment, since this animal model was induced with diabetes by administering Alloxan<sup>®</sup> (50mg/kg) in order to destroy the pancreatic cells of the rabbit in an attempt to measure blood glucose level reduction due to the effect of the oral insulin formulation rather than from endogenous insulin produced from the animal itself, in which these conditions cannot be fully simulated by cell cultures or other *in vitro* systems (Lenzen, 2008). After 24 hours of the study, the animals were euthanized so as to prevent any further unforeseen difficulty the animals may be experiencing. The group of rabbits given the oral interferon- $\beta$  formulation was not induced with any condition and were euthanized at completion of the study. The release profile of the *in vivo* study were compared to the *in vitro* release studies undertaken. Additionally these are novel orally administered drug delivery systems which require exposure to the animal's physiological environment to operate effectively. In the design of a novel versatile oral protein pH-responsive polymeric drug delivery system, the properties of its composite nature were exclusively evaluated and characterized.

## **1.2. Rational and Motivation of Study**

According to the National Institute of Neurological Disorders and Stroke, research claims that approximately 200 new cases of MS are diagnosed each week in the United States. People diagnosed with MS endure life-long chronic disease, primarily in young adults who have a virtually normal life expectancy. Consequently, the economic, social, and medical costs associated with the disease are significant. Estimates place the annual cost of MS in the United States in the billions of dollars. According to the New York Times health guide, 2010, MS is currently being treated with a variety of drugs, most popularly being Interferon injections. Other medication used are fingolimod, methotrexate, azathioprine, intravenous immunoglobulin (IVIg) and cyclophosphamide ([www.health.nytimes.com](http://www.health.nytimes.com)). IV administration of INF- $\beta$  has commonly been associated with multiple problems of pain, allergic reactions, Flu-like symptoms, injection-

site skin reaction, blood count and liver test abnormalities, poor patient compliance and chances of infection (Chiu *et al.*, 2007).

Diabetes, when uncontrolled, leading to renal failure and severe anemia, on the other hand has a greater impact in the world, than MS. There are endless causes of these diseases and patients have significant factors that worsen the condition due to the lack of patient compliance with insulin injections (Tomar *et al.*, 2011). The need for an oral insulin and erythropoietin formulation has long passed its time, in comparison to the significant number of people affected with diabetes and renal failure that are unable to meet the daily requirements of administering the injection.

Erythropoietin (EPO) has primarily been used to treat anemia for chronic conditions of kidney disease and cancer chemotherapy for nearly 20 years in injectable forms. The interaction of EPO with its receptor (EPO-R) has significant cytoprotective cellular responses, including mitogenesis, angiogenesis, inhibition of apoptosis and promotion of vascular repair through mobilization of endothelial progenitor cells from the bone marrow. EPO was also shown to display substantial renoprotection in experimental ischaemic and toxic acute renal failure, in which studies proved suppressed tubular epithelial apoptosis, enhanced tubular epithelial proliferation and hastened functional recovery (Johnson *et al.*, 2006).

In the design of an oral biostable proteomatrix polymeric delivery system, many crosslinked polymers, shown to be highly efficient in encapsulating the 3 different proteins under study in separate oral formulations, were strategically designed to overcome harsh gastric and intestinal conditions, which provide a poor environment for absorption of peptides. These polymers, exclusively selected and strategically crosslinked, are capable of intelligently reaching their site of absorption, through a pH responsive biostable mechanism of action.

Copolymeric chitosan-polyethylene glycol dimethacrylate-methacrylic acid (CHT-PEGDMA-MAA) and trimethyl chitosan polyethylene glycol dimethacrylate-methacrylic acid (TMC-PEGDMA-MAA) were prepared by free radical suspension polymerization technique with the intention of loading INF- $\beta$  for specifically combating MS thus, implementing the system as a versatile platform for efficient macromolecular peptide delivery. A Box-Behnken design was completed for acquiring the optimized formulations, with responses most desired for the polymeric systems. The manipulation of chain conformation due to its pH-responsive nature is considered the primary mechanism by which drug is released by the exceptional swelling

behavior in basic pH, and its contrary reaction in acidic pH, shrinking and protecting its contents in a uniquely responsive way. The excellent mucoadhesive and antimicrobial properties of CHT and TMC provides an intact crosslinked network beneficial for absorption through the gastrointestinal membrane. The purpose of developing this composite molecule network is to obtain the highest degree of loading efficiency in the formulation, a minimum percentage of drug being released in acidic medium according to its intelligent pH responsive nature and obtaining maximum release profiles in basic intestinal medium. To obtain optimum characteristics of this polymer, crosslinking specialized components to yield these results were the focus of successful oral drug delivery. The physiological mechanism of oral protein delivery after being absorbed from the intestine is that it passes through the liver via the hepatic portal circulation, similar to the endogenous route of proteins. The oral route is thus the most preferential, since complications of subcutaneous injections and long term complications do not arise. Figure 1.2 depicts an overview of the process of drug release that the polymeric systems demonstrate as they move from the gastric to the intestinal medium.

The comparisons between the proteomatrix copolymeric delivery systems were critically evaluated and correlations were determined according to *in vitro* and *in vivo* studies. Acquired information from these comparisons increases the novelty of the research, in addition *in silico* analysis of the mucoadhesive behaviors were used to evaluate the novelty of polymers that assist in attaining enhanced *in vivo* relevant mechanisms.

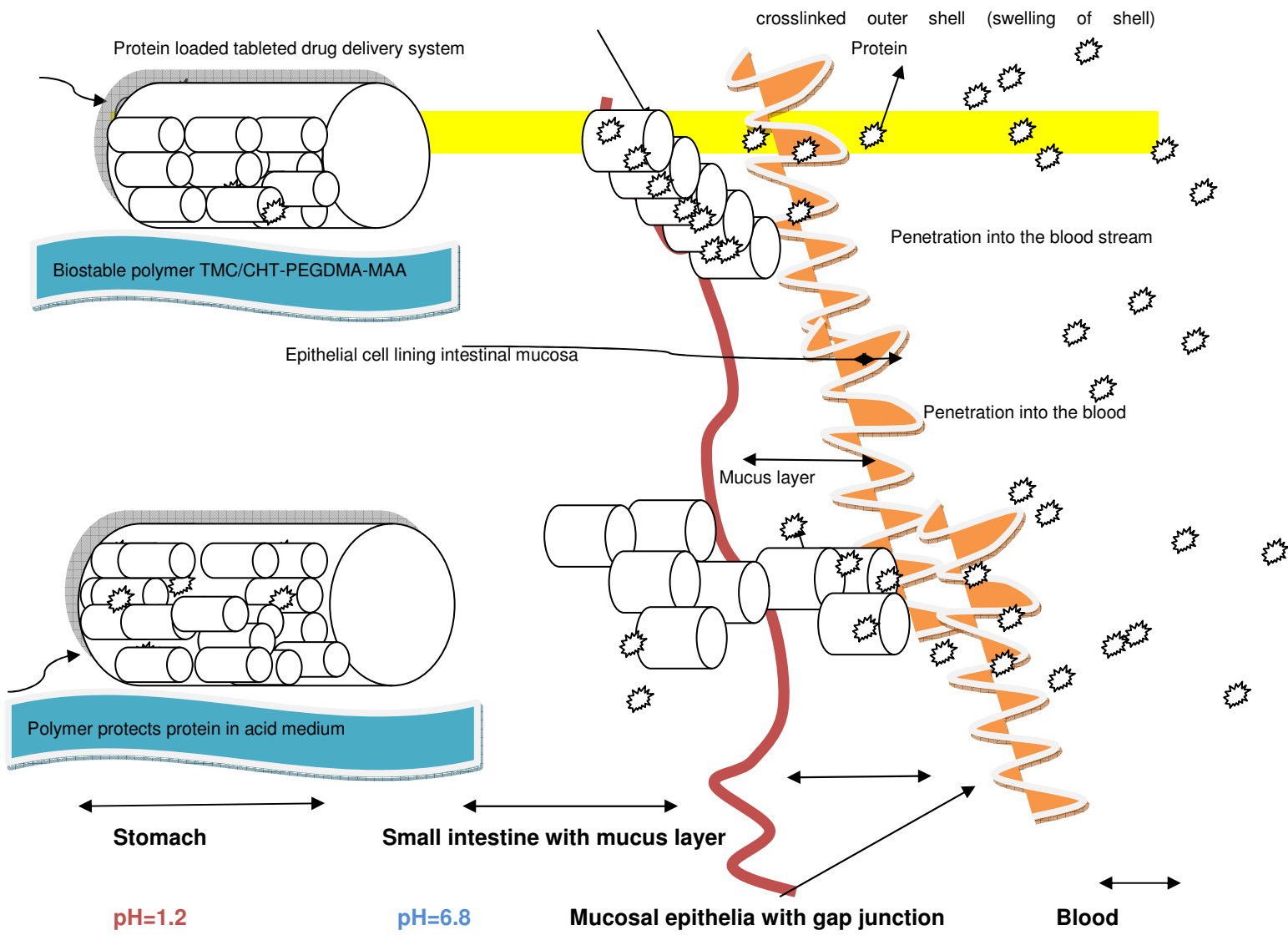


**Figure 1.2:** Schematic illustrating the pH sensitive shrinking of the biostable particles in gastric pH (pH 1.2), in comparison to their swelling abilities in the basic pH of the small intestine (pH 6.8). Being mucoadhesive in nature they will adhere to the mucus lining and release the protein, which will further enter into the blood stream via paracellular pathways.

### **1.3. Possible Therapeutic Agent Application of the Delivery System**

This unique oral copolymeric drug delivery system was analyzed for its application in delivery in 3 protein therapeutics. The first being interferon beta, the next investigated of the most demanding proteins being insulin, and the third protein analyzed was erythropoietin for achieving high statistical scientific validity. Interferon beta, insulin and erythropoietin were analyzed using 2 modified optimized formulations, in total giving a complete number of 6 optimized formulations for *in vitro* and *in vivo* studies, pronouncing the delivery system as a truly versatile proteomatrix oral copolymeric delivery system, due to possessing exceptional scientific *in vitro* and *in vivo* results, even though all these protein systems have completely different physicochemical characteristics and varying specific chemical structure activity relationships. All physicochemical and physiomechanical studies were conducted on all the systems developed, as well as exposing the systems to a rabbit model to prove success on a physiological scale. All formulations with different proteins were compared on a kinetic statistical approach, producing data in the most reliable form *in vitro* as well as *in vivo*, to finally conclude success of the copolymeric system.

### **1.4. Aim and Objectives**

The aim of the research project was to develop a novel formulation using pH sensitive (bio-stable or biodegradable) polymeric nano/micro particles with high loading efficiency for effective delivery of a range of proteins, using a variety of 3 different polypeptides as the basis for achieving a successful pH sensitive oral proteomatrix copolymeric delivery system. Interferon beta, insulin and erythropoietin were delivered in separate formulations as an oral dosage form for effective oral protein delivery in two different optimized copolymeric systems.

The following objectives were defined for the study:

1. Development of a novel pH sensitive oral proteomatrix formulation, incorporating crosslinking of polymers to produce 2 optimized copolymeric delivery systems and providing a study between each *in vitro* and *in vivo* analysis for 3 different oral proteomatrix systems.
2. All formulations were evaluated on a physicochemical and physiomechanical basis, for determination of the stability of the formulations and their characteristic profiles. Texture Analysis, Porosity, Scanning Electron Microscopy (SEM), Attenuated Total Reflectance-

Fourier Transform Infrared (ATR-FTIR), Thermogravimetric Analysis (TGA), Nuclear Magnetic Resonance (NMR), particle size, zeta potential, rheology and *in vitro* drug release were some of the many characterization studies undertaken.

3. Mucoadhesive studies were undertaken on all formulations to demonstrate the great mucoadhesion of each system, due to its essential requirement for successful adsorption in the small intestine.
4. All formulations were uncoated, for determination of efficacy of the polymer and its pH responsive nature, thereby proving complete stability of the oral copolymeric delivery system being exposed to all harmful gastric, intestinal, mucosal as well as enzymatic threats of oral protein deliveries.
5. *In vivo* analysis was carried out on each oral proteomatrix system, using a rabbit model, and detecting the concentration of protein in blood samples extracted.
6. Further histology studies were conducted on all formulations, to prove non toxicity of the system, and determine other effects the protein may have on specific organs/tissues.
7. Inducement of diabetes in the rabbit model was undertaken for insulin studies, for precise determination of the hypoglycemic effects resulting from the formulation, detecting endogenous insulin produced by the rabbit itself.
8. A direct comparison study was undertaken for *in vitro* studies in relation to its *in vivo* studies across all formulations, to determine the correlation and precision between the formulations.

### **1.5. Novelty of the delivery systems**

This unique free radical polymerization and crosslinking approach provides conjugation between 1) two extremely mucoadhesive polymers (CHT/TMC and poly-MAA); 2) a synthetic (poly-MAA) and natural polymer (TMC); 3) and two pH responsive polymers (poly-MAA and CHT/TMC), forming a semisynthetic mucoadhesive-pH responsive conjugated polymeric system capable of encapsulating proteins and peptides due to the presence of –COOH moieties; protecting the peptide from harsh gastric environment; and retaining the microparticulate system in close vicinity of intestinal wall for a prolonged period. Additionally, the CHT/PEGDMA-MAA or TMC/PEGDMA-MAA polymeric architecture is characterized by three-in-one matrix types: 1) a semi-interpenetrating polymer network consisting of CHT or TMC and PEGDMA crosslinked MAA wherein one polymer is crosslinked in the presence of another polymer; 2) a polyelectrolyte complex formed between the -COOH functionalities of PEGDMA crosslinked

MAA<sup>+</sup> and -NH<sub>3</sub><sup>+</sup> functionality of CHT or TMC; and 3) PEGDMA crosslinked MAA conjugated to CHT or TMC forming CHT-PEGDMA-MAA. Furthermore the high resilience acrylate polymer (PEGDA crosslinked MAA) on the TMC backbone provided for a long side-chain molecular conformation capable of entrapping higher amount of peptide. This entrapment was further enhanced by the use of a long chain crosslinker (PEGDA) providing an inter- and intra-chain crosslinked network. The retention of this conjugate polymer in “tethered” intestinal mucosa was mediated via two different mechanisms: 1) the entangling of PEGDA crosslinked MAA side chains into the mucus lining and 2) the charged electrostatic interaction provided by the cationic polyquaternium chitosan backbone. Additionally, the unique mechanical properties provided by high molecular weight chitosan and PEGDA crosslinked MAA aided the prolonged retention in the intestine via a unique hard-to-soft swollen hydrogel architecture. The ability of the conjugated system to accommodate various chitosan derivatives (in terms of molecular weight) and crosslinkers and monomers with varying chain length can provide the flexibility required for the extent and rate of protein and peptide release from the microparticulate matrix.

## 1.6. Overview of the Thesis

This thesis covers all aspects of the research from preformulation design studies to *in vitro* and *in vivo* critical evaluation of the drug delivery system.

**Chapter 1** entails a comprehensive overview of the rationale and motivation for undertaking this research, thereby explaining the mechanism of action of the delivery system, and research undertaken previously in this field. Evaluations of the various preformulation studies are summed up, indicating the novelty of the research on hand. The proposal of dosing the oral delivery system without a protective coating is also a significant property of the oral matrix. The aims and objectives of the study are clearly explained, ensuring clarity and analytical sequence throughout the study.

**Chapter 2** discusses in detail critical evaluation of therapeutic MS interventions: diagnosis and treatment options. This covers all treatment options and research undertaken in many clinical trials and provides insight into various mechanisms of action of the therapeutics used in MS. A significant proportion of interest of this thesis deals with the criteria of the different stages of MS, and the therapy required for stabilizing the condition. Overviews of the current route of administration of these therapeutics are essential, therefore indicating a contrast between the newly formulated research and the current therapy on hand.

**Chapter 3** entails the design and optimization of the copolymeric microgel and microparticulate system. A complete design evaluation was conducted on the microgel and particulate system, formulating a pH responsive copolymeric microgel of chitosan-poly(ethylene glycol) dimethacrylate-methacrylic acid (CHT-PEGDMA-MAA) and copolymeric microparticles trimethyl chitosan-poly(ethylene glycol) dimethacrylate-methacrylic acid (TMC-PEGDMA-MAA). Using a Box-Behnken experimental design, a series of formulations were synthesized and evaluated using insulin as a prototype peptide for drug loading and *in vitro* behavior, which are extensively discussed in Chapter 4. Due to the high cost implications associated with extensive experimental use of INF- $\beta$  and EPO, these prototype experimental studies were conducted. A series of formulations were designed and analyzed for conclusive determination of the optimized formulation. The optimized formulation was synthesized according to the responses from the design formulations on insulin and further evaluated for INF- $\beta$  and EPO.

Characterization studies on the copolymeric systems were conducted for determination of chemical, physical and thermal sensitive properties. Mucoadhesive studies were extensively conducted on all design and optimized formulations, significantly determining the ability for percentage crosslinking interaction with the copolymeric system and the mucus. This chapter therefore provides a platform for the development, characterization and responsive nature of the copolymeric systems.

**Chapter 4** expounds on the *in vitro* behavior of the copolymeric drug delivery systems. Drug loading and release studies were undertaken for determination of the capacity of drug available for delivery, thereby providing a site specific dose for absorption across epithelial membranes. Drug loading and release analysis was carried out on all Box Behnken formulations of TMC-PEGDMA-MAA and CHT-PEGDMA-MAA. Insulin was selected for all design formulations due to the great cost implications incurred for such a vast range of analysis undertaken in triplicate. Determination of concentration released over various time periods were analyzed using High Performance Liquid Chromatography (HPLC), thereby determining the amount of insulin loaded and released over a specific range of time. All samples were analyzed for 2.5 hours in gastric medium and 24 hours in intestinal medium. Physiological sink conditions were maintained throughout the study, thereby providing a basis for mimicking *in vivo* properties.

**Chapter 5** critically discusses *in vivo* studies conducted on all groups of rabbits from the respective protein studies. All rabbits were tested in triplicates, composed of 3 groups, namely

the control, the experimental and the commercially tested product. Diabetes was induced in all rabbits of the insulin study, thereby providing a definite model for determining the effects of the insulin loaded copolymeric delivery system. INF- $\beta$  and EPO were dosed without inducing any pathological condition in the rabbit, thereby significantly determining the concentration of the protein in the serum. All rabbits after completion of the respective studies were euthanized and histological GIT samples of pertinence were analyzed for any effects of toxicity due to inflammatory responses or necrosis in the observed tissue samples. Kinetic modeling was undertaken on results obtained from *in vitro* and *in vivo* analysis, thereby conceptualizing a compartmental and non-compartmental analysis of the study.

**Chapter 6** summarizes the entire study as a concludry chapter and takes into account all results obtained from the study.

### **1.7. Concluding Remarks**

This chapter introduces the purpose of the novel research undertaken and the significance of conducting this research. The unique behavior of the copolymeric delivery system provides a mechanism for reacting according to pH stimuli, delivering proteins in the most intact viable form for effective optimized delivery *in vivo*. This thesis is therefore a foundation into a revolutionary platform of protein therapeutics, looking at the most convenient non-invasive route of administration, providing patients with a simple hope of maintaining a healthy lifestyle with absolute control of the their pathological condition, by providing a novel unique system, able to load a variety of protein therapeutics for optimum drug delivery, resulting in an enormous impact to scientific research of revolutionary standards.

## CHAPTER 2

### CRITICAL EVALUATION OF THERAPEUTIC MULTIPLE SCLEROSIS INTERVENTIONS: DIAGNOSIS AND TREATMENT OPTIONS

#### 2.1. Introduction

Neurodegenerative diseases remained a condition of uncertain evaluation until three and a half decades ago, where immense research in this category of neuroscience yielded the confirmation of abnormalities in the processing of proteins, causing the accumulation of one or more specific neuronal proteins (Prusiner, 2001). Neurodegenerative diseases are classified based on their progressive dysfunction of neurons and consequent death of the neural networks. Disorders pertaining to a degenerative nature manifest as either cognitive disabilities or disturbances in sense and movement abilities, in some instances it can procure a combination of both. Movement disorders manifest as akinetic and rigid forms of hyperkinetic deregulation. Temporal and parietal degenerations consequently results in dementia marked by memory disturbances with precipitating forms of depression due to parietal lobe dysfunctioning (Vajda, 2002). These degenerative diseases retard the functional abilities of specialized areas of the brain, spinal cord, or peripheral nerves, with the end stage neural death of the dysfunctional region. Many neurodegenerative diseases can also be classified according to age groups in which they appear more predominantly, and express their symptoms as either disorders of the brain, nerves, or myelin degeneration, such as conditions pertaining to Parkinson's disease, Alzheimer's disease and Multiple Sclerosis respectively.

It has become ever increasingly evident how Multiple sclerosis (MS) affects young adults of the average age 30 years with the statistical value of 1.3 in 1000 people affected in developed world countries (Henriksen *et al.*, 2010). Autoimmunity is considered to be primarily responsible for this disorder in which T lymphocytes are autoreactive against myelin proteins in particular, however other immunopathological mechanisms such as oligodendrocyte apoptosis and B cell autoimmunity initiated/activated in response to such a state, encompasses a vital role in progression of MS (Ziemann *et al.*, 2011). There is however, a high degree of correlation between inflammation and axonal injury in all possible stages of MS with axonal and neuronal degenerative lesions in active demyelinating neuronal tissue (Frischer *et al.*, 2009). The majority of patients experience waxing and waning as a primary start to the disease, later

progressing to relapsing remitting MS, characterized by episodes of acute attacks, in which there is partial or complete recovery between two relapses experienced, but in many circumstances of poor management at this stage, a secondary progressive disease state steps in (Compston *et al.*, 2008).

This condition however has not seen a noteworthy cure to date, rather it is treated by various disease modifying agents, to prevent further axonal degeneration and inflammation of myelin, which would otherwise cause irreversible disability. Magnetic resonance imaging (MRI) evidence for inflammatory response is a fundamental factor to diagnose the severity and progression of MS, thereby treating the condition as early as inflammation is detected in neural tissue. Initiating treatment instantly through correct disease modifying agents is instrumental in preventing the progression and irreversible damage (Katrych *et al.*, 2009).

## **2.2. Multiple Sclerosis Symptoms and Prognosis**

MS is part of a neurodegenerative disease in which myelinated axons in the central nervous system (CNS) are destroyed by an immune-mediated inflammatory disorder which aggressively targets the myelin and axons to considerable degrees. The disease follows a relapsing-remitting pattern, with short-durations of neurologic despondency that resolves entirely or to a certain degree. The exact cause of MS is not fully understood, and remains a topic for much research to be conducted. Genetic predisposition and a non genetic trigger factor, such as viral conditions as well as low vitamin D levels, substantially results in an autoimmune condition, leading to recurrent immunological attacks on the CNS. Many physicians diagnose acute MS once they detect myelin degeneration in a patient. This perception however is regarded as a huge mistake by many researchers, since there are various other neuroinflammatory conditions that could be implicated by these responses (Bruce *et al.*, 2008). Since the regulatory mechanisms are not functional in MS, the immune system recognizes neural cells as the pathogen, rather than part of its own composite nature (Goodnow *et al.*, 2005).

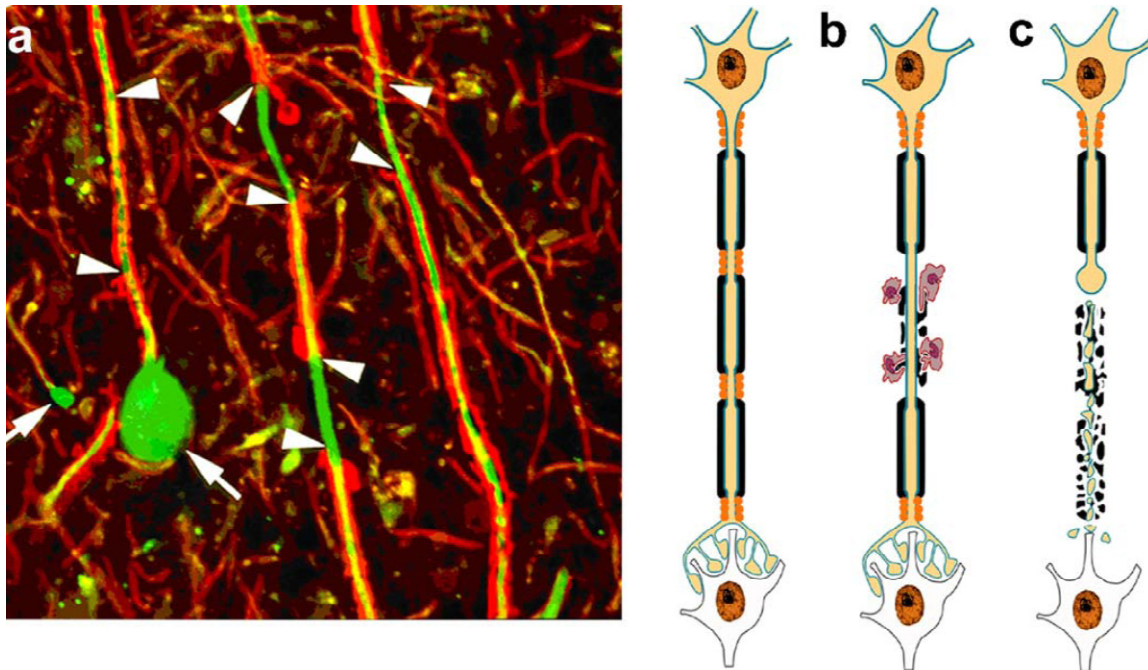


**Figure 2.1:** Illustration of axonal damage, in which myelin is perceived as a foreign intruder and mounts an immune response to attack and destroy myelin sheaths. This causes deterioration of nerve conduction and impulses. Scarring normally starts forming if the condition is not controlled, thereby forming plaques as material is deposited into the scar formation. In this specific axonal transaction and Immune-mediated demyelination, a great degree of ovoids were identified from a MS tissue (a), red identifies stain for myelin protein and green for axons. The arrowheads depict demyelination, in which microglia and hematogenous monocytes are believed to mediate the degenerative process. The large green swelling of the axonal bulb,(b and c) is a typical response of axonal transaction, due to the immune-mediated demyelination process. Once transaction occurs, the distal end of the axon substantially degenerates, in relation to the proximal end connected to the neuronal cell body that sustains itself without undergoing degeneration, allowing transported organelles to locate itself at the site of transaction, thus forming an ovoid (arrows) ( Figure reproduced with permission from Elsevier Ltd.: Dutta *et al*, 2011)

A model of nerve fibers compared to an insulated wire is illustrated in Figure 2.1, where specific axonal transaction and Immune-mediated demyelination is depicted, is used to enhance the understanding of this condition. Myelin represents the insulated covering of this electrical wire, thus preventing any “short-circuits” and diversion in electrical signaling from occurring. If myelin is being destroyed resulting in fiber scarring, due to attempts of continuous demyelination and remyelination, transmission of neural impulses are interfered which could cause possible progressive disability including cognitive and physical aspects concurrently or independently

(Frohman *et al.*, 2006). Figure 2.2 depicts the following physical symptoms that patients frequently undergo as a result of untreated or incorrect diagnosis.

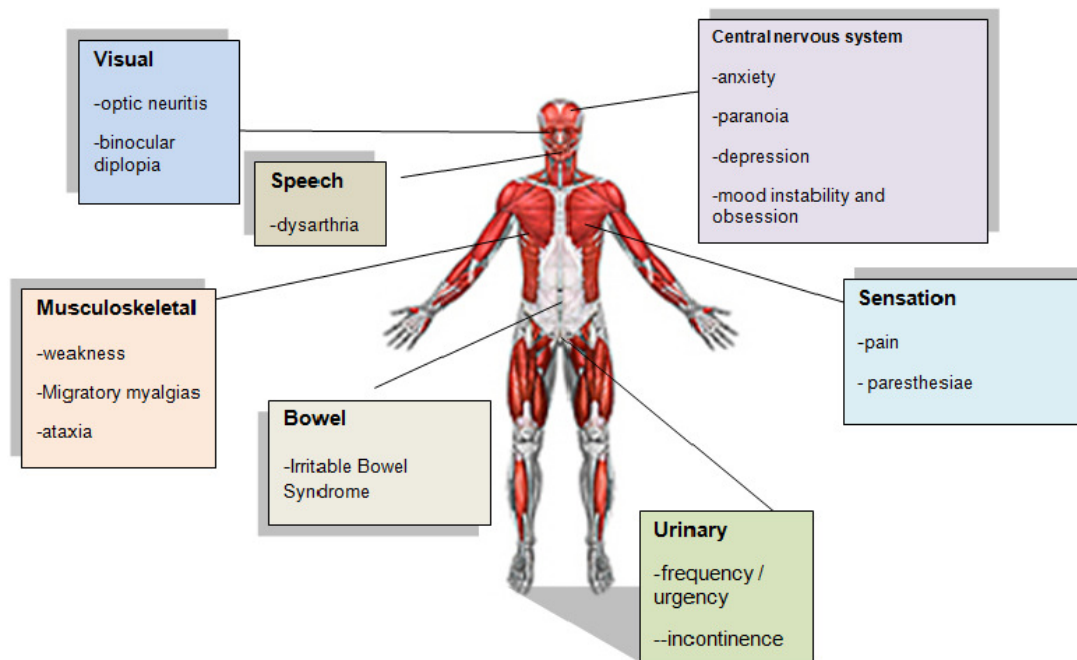


**Figure 2.2:** Schematic representation of the main symptoms associated with MS as a result of not seeking treatment (van den Noort., 2005., Poser *et al.*, 2001)

MS, based on critical clinical presentation and long term progression, has been classified mainly into four subtypes as depicted and represented in different phases and progressions in Figure 2.3: Relapsing Remitting, Secondary Progressive, Primary Progressive, and Progressive Relapsing. The most common being, Relapsing Remitting MS (RRMS) is found in approximately 85% patients being diagnosed with MS. There are events characterized by unpredictable durations of symptoms, followed by a space of remission with no disease activity detectable. These symptoms either resolve suddenly or leave with no apparent stimulus (Bergamaschi *et al.*, 2001). The next stage is Secondary Progressive MS (SPMS), in which the duration of onset from RRMS to SPMS is approximately 19 years (Lassmann, 2004).

From the stage of RRMS, patients who begin to show progressive neurological decline, with no apparent signs of definitive durations of remission between acute attacks, fall into this category, slowly possessing further degenerative neurological evidence. The next category is Primary Progressive MS (PPMS), in which patients show no improvement and remission of disability,

progressing to further decline in disability with no signs of improvement in the condition. There are approximately 10-15% of MS-affected patients in this category (Ingle *et al.*, 2005). The last stage of MS, which is also the least common subtype, is Progressive Relapsing MS (PRMS). This category of patients show a steady decline in neurological abilities, concurrently suffering from superimposed attacks, and further complete disabilities. This is the rarest subtype of MS, since most patients' do not deteriorate to this stage due to medication compliance in earlier stages of diagnosis (Andersson *et al.*, 1999).

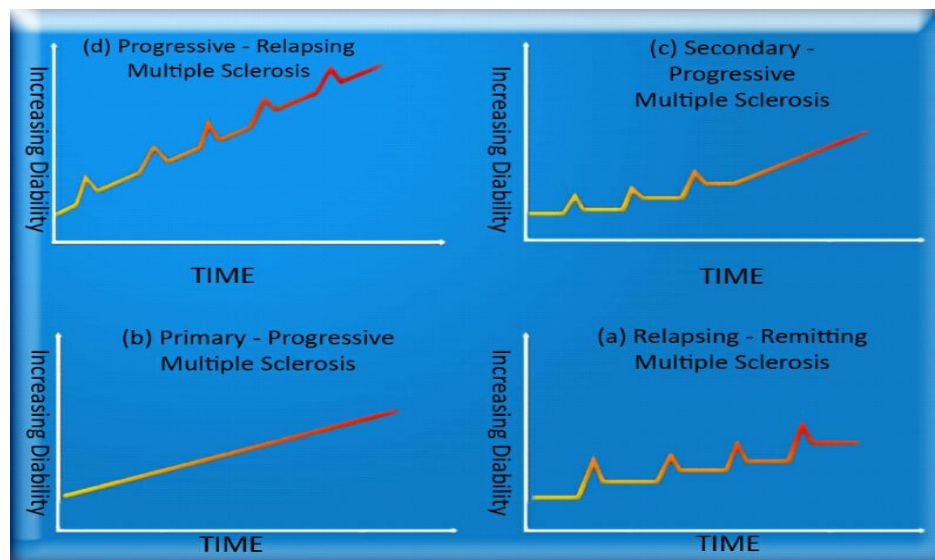


**Figure 2.3** (a) RRMS is the most common form of MS with 65-80% of patients starting in this stage. This stage comprises of acute attacks (exacerbations), and if not treated leads to serious loss of function. Symptoms may resolve, until another attack occurs (relapse) (b) PPMS comprises of a uniform steady increase in deterioration, with no occurring relapses and remissions. This form of MS is more predominant in people over the age of 40 and prevalent in approximately 15% of people with MS (c) SPMS starts with RRMS, which later develops into progressive disease. Statistics indicate that 50% of patients develop SPMS after acquiring RRMS within a 10 year gap period (d) this stage of MS (PRMS) is characterized by steady progression of disability with acute attacks which may or may not follow recovery. This is one of the least prevalent stages of MS, and usually appears as PPMS. (Figure adapted with permission from Elsevier Ltd.: Davis, 2010)

### 2.3. Advances in Diagnosis

MS is an age long neurological disease, much of which was hardly known when neurologists first became intrigued with this condition (Finger, 1998). Charcot first described the condition as 'La sclerose en plaques disseminees' in 1868 and proposed a non-specific criteria for the disease (Gafson *et al.*, 2012). It was much later that it came to be known as neurological

disorder called MS. The symptoms as observed by Charcot, in his patients, were not clearly differentiated from those of syphilis patients or any form of cerebellar lesions, and primarily comprised of nystagmus, intention tremor and scanning speech. After a substantial period of 68 years, an Australian neurologist Marburg, proposed another set of criteria, comprising signs of Uhthoff and that of pyramidal tract with the absence of abdominal reflexes (Gafson *et al.*, 2012). Not long after this publication was released, Allison and Millar acknowledged the lack of detail from the previous researchers and in 1954, categorized the condition as 'early', 'probable' and 'possible'. In early disseminated sclerosis, patients showed no significant physical illnesses, but had a history of various remitting symptoms. Patients falling in the 'probable' category were evaluated by physical examinations for signs of multiple lesions. Patients of the 'possible' category possessed a history of symptoms that were progressive, but had inadequate indication of scattered lesions. This form of criteria was more intuitive rather than covering a specific set of guidelines (Allison *et al.*, 1954). During this interim, Broman modified the criteria, adding a significant evaluation oligoclonal bands (OCB) from cerebrospinal fluid (CSF), identifying immunoglobulins present in CSF (Broman *et al.*, 1965). His model consisted of age of onset, multiplicity of lesions, recurrence of attacks, as well as incorporating electrophoretic evaluation of CSF protein. His criteria became the foundation for subsequent characterizations to follow, which lead to the principles of dissemination in time and in space, that has significance for diagnosis of MS even up till today (Poser *et al.*, 2004).

According to Schumacher *et al.* 1965, MS patients were characterized or diagnosed with two or more parts of white matter of the CNS affected by the disease, occurring in two or more episodes separated by a time period of 1 month or even longer, or with progression over 6 months and each episode lasting more than 24hrs (Schumacher *et al.*,1965). Later, McAlpine and coworkers made efforts to modernize the Allison and Millar criteria. To differentiate the 'probable' and 'possible' fields of diagnosis, the patient had to have a certain degree of lesions at different levels of the neuraxis, with a combination of definite clinical signs and a degree of remission pertaining to the specified category (McAlpine *et al.*,1972). Rose *et al.*, attempted to clarify 'possible' and 'probable' categories further for better understanding of MS. According to Rose, 'probable' MS could involve a single encounter with signs of prevalent disease, or two episodes with signs at a single site. 'Possible' MS was regarded as two episodes with no or very few symptoms (Rose *et al.*, 1976).

Charles Poser and team decided to investigate CSF as one of the crucial markings for the disease and tried defining the condition with an onset of an 'attack' and age of onset as 59. CT, MRI scans and cerebrospinal fluid analysis were carried out/investigated thereby concluding that remission had to persist at least 1 month as was earlier defined in the case in the Schumacher criteria (Poser *et al.*, 1983).

Emerging from the 20<sup>th</sup> century, McDonald revealed a series of diagnostic criteria, much of which became more accessible with widespread availability of MRI. If a patient suffered an attack, MRI studies could be undertaken to evaluate new lesions over various areas of the CNS. If a patient presented with 2 or more lesions, and had one attack, evidence had to be confirmed with MRI. On the other hand, if a patient presented with '2 or more attacks and evidence of 2 or more lesions', MRI was not necessary to complete the diagnosis, of which clinical examination would prove sufficient (McDonald *et al.*, 2001). In 2005, McDonald revised the criteria, and declared that abnormal CSF was not required to make the diagnosis of primary progressive MS. In May 2010, the McDonald criteria was reviewed for the 3<sup>rd</sup> time, under the supervision of Chris Polman. Information from the European Magnetic Imaging in MS (MAG- NIMS) research team was incorporated. The Barkhoff/Tintore guidelines for dissemination in space (DIS) was admitted to be difficult to apply and adhere to, thus simpler specific DIS criteria was devised (Polman *et al.*, 2011). MCMS 2005, for dissemination in time (DIT) required confirmation of MRI of a new T2 lesion, in comparison to previous MRI scans at least 30 days ago. The panel proposed that a single scan be carried out if there were asymptomatic gadolinium-enhancing and non-enhancing lesions in areas pertaining to guidelines for DIS. The MRI requirements have been reevaluated for the guideline criteria for 2010, but still remains an intricate process for many clinicians, of which much history and clinical examinations are also required (Gafson *et al.*, 2012).

### **2.3.1. Pathophysiology of MS**

Under microscopic examination, pathological specimens of demyelinated neural tissue of MS appear as plaques (indurated areas) thus classified as sclerosis. Astrogliosis and profound damage to oligodendrocytes as well as substantial destruction to axons are clearly visible as illustrated in Figure 2.4 (Bruce *et al.*, 2008). A large percentage of studies have correlated axonal damage to the severity of inflammation in MS cerebral lesions (Bjartmar *et al.*, 2003). According to Ferguson *et al.*, buildup of axonal amyloid precursor protein (APP), which is a marker of axonal damage in progressive active lesions also manifest on the edge of chronic lesions (Ferguson *et al.*, 1997). Numerous APP, the immunoreactive structures bear a

resemblance to axonal ovoids - transected axons - which was confirmed using confocal microscopy. Terminal ends of transected axons were viewed for non-phosphorylated neurofilaments. An average number of 11,236 terminal ends per  $\text{mm}^3$  were established in areas of the active lesions, 3138/ $\text{mm}^3$  were viewed at the edge of chronic active lesions, and 875/ $\text{mm}^3$  were established in the core of chronic active lesions. Much to the contrary, in the control research, white matter contained less than one transected axon per  $\text{mm}^3$  (Bjartmar *et al.*, 2003). According to Kornek *et al.*, comparable associations between MS lesions and concentration of APP-positive axons were deduced. Terminal ends detected in spaces of active lesions, found relatively in those with early disease states, confirms axonal transection from the diagnosis of MS. Correlations with these profound lesions, maintains the idea of inflammatory mediators produced by glial or immune cells (Kornek *et al.*, 2000). Percentage loss of axons over long periods of time can prove detrimental to all patients with chronic active MS. A study was undertaken on chronic paralyzed MS patients, and found that the degree of disability was proportional to the percentage of axonal loss (Lovas *et al.*, 2000). Thus it is conclusive that axonal damage starts from the onset of the disease and its pathological impact due to axonal loss has a collective nature, leading to permanent disability in patients suffering from MS (Bjartmar *et al.*, 2003).

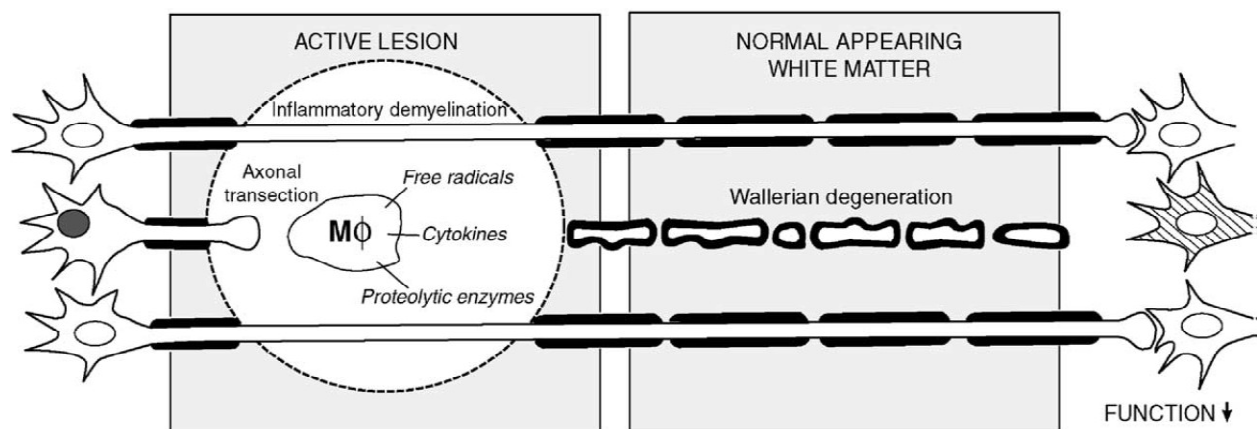


**Figure 2.4:** Schematic depiction of axonal injury, due to inflammation caused by demyelination in an active MS lesion. Glial and immune cells cause damage to the tissue, as well as axonal transection. Degeneration occurs at sites distal to the site of transection. Myelin forms empty tubes that later develop into degenerated ovoids. White matter may seem normal on standard MRI images. (Figure reproduced with permission from Elsevier Ltd.: Bjartmar *et al.*, 2003)

### **2.3.2. Immunological studies**

Studies on white matter plaque tissue shows high levels of IL-12, which is responsible for much inflammation, and is expressed in high concentrations at lesions found in patients from the early diagnosis of MS. Another molecule B7-1, which is responsible for stimulating lymphocytes to release proinflammatory cytokines, is also expressed in high concentrations from the early phases of MS. Found in patients with relapsing-remitting MS, are activated myelin-reactive T-cell clones, in comparison with patients with progressive MS, in which high levels of IL-12 and Immunoglobulins (Igs) were found (Bruce *et al.*, 2008). This has been one of the most earliest and crucial evidence, confirming the role for B-cells and antibodies in the pathology of MS. Humeral response also has an involvement in benign MS, since the presence of increased CSF Ig and the absence of OCB was quite evident in these patients. B cells normally cannot cross the blood brain barrier (BBB), but due to the initiation of inflammation, there are a wide range of antibodies, B cells, and complement passing through the CNS. Increased Igs were found in the CSF of patients however, serum did not possess Igs, indicating local production at the sites of the lesions. B cell activation occurs due to, 'stimulation with antigen from self or foreign proteins, via a random bystander effect during inflammation, or by superantigen stimulation' (Sospedra *et al.*, 2005). Being implicated in MS, is the low functioning of T-lymphocytes with its regulatory role (Tregs). The Tregs, which are CD4<sup>+</sup> CD25<sup>+</sup> T cells, are confirmed by a transcription factor known as Foxp3 (Huan *et al.*, 2005). Cells are shown to follow a pathogenic phenotype in autoimmune diseases, especially MS, due to the cytokine IL-23. CD4<sup>+</sup> T cells act to oppose Treg function, and can be determined by proinflammatory cytokine IL-17, which are referred to as T<sub>H</sub> 17 cells (Tesmer *et al.*, 2008). These cells (Tregs and T<sub>H</sub> 17) are apart of the many other cells in the pathogenesis of MS. Other cells such as natural killer (NK) cells, microglia and dendritic cells have also been associated with the process of CNS inflammation (Minagar *et al.*, 2001).

### **2.3.3. Genetic predisposing factors**

According to statistics of international rating, 1.3 in 1000 individuals are diagnosed with MS, of which young individuals peaking at an age of 30 are mostly affected (Bergamaschi *et al.*, 2001). According to Compston and co-workers from Cambridge University, a study was conducted in which genomes of people with MS were scanned to differentiate DNA in over 17,000 healthy people. The research revealed a total number of 57 genetic faults linked with the disease. A new technique using genome-wide scanning, which analyses the entire length of a patient's DNA for anomalies that do not normally exist in healthy individuals, confirmed a strong genetic

predisposition to MS, in relation to healthy individuals carrying none of these altered genetic components(<http://www.independent.co.uk/news/science/multiple-sclerosis-study-identifies-genetic-causes-2335615.html>, 2011). According to Nielsen *et al.*, 20-35% of monozygotic twins showed these genetic predisposing factors. Other factors such as non-Mendelian (ie, epigenetic modification in 1 twin), as well as environmental effects play a fundamental aspect in the development of the disease. In first degree family, the risk of developing the disorder is sevenfold higher in comparison to individuals with no genetic predisposing factors (Nielsen *et al.*, 2005). Polymorphism of genes lead to a variety of cellular expressions and therefore the pattern of proteins they encode. In patients with MS, polymorphism within the promoter region of a gene, mounts an accelerated response, i.e. increased expression of proinflammatory genes, in response to a specific antigen, resulting in uncoordinated proliferation and an autoimmune state. HLA-DRB1 is the only chromosomal locus which persists to be associated with the susceptibility of MS. Various other contributor genes are linked to MS, but none are as highly susceptible to MS as the HLA locus (Nischwitz *et al.*, 2011). Current research in the field of genetics have been critically evaluating aspects to determine protection against MS, concluding that the major histocompatibility complex (MHC) region, *HLA-C\*05* allele in particular accounts for protection against MS (Yeo *et al.*, 2007).

#### **2.3.4. Experimental autoimmune encephalomyelitis (EAE) and viral animal modeling for multiple sclerosis**

Autoimmune encephalomyelitis is considered an appropriate model in understanding how brain inflammation and immune mediated CNS damage are brought about, and to investigate ways in which therapeutic treatments are worthy in the approach of combating this disease. The first model of EAE was undertaken on primates in 1933 by Rivers. In the 1950s, experimental research revealed that rats and guinea pigs were more sensitive with CNS tissue. From then, this model has been induced in a variety of rodents and primate models that reproduce conditions specific to human pathological conditions. This model modulates a system of immune mediated response on myelin sheaths of the CNS, resulting in intensive demyelination and consequent depletion of oligodendrocytes (Ingwersen *et al.*, 2012). This neuroinflammatory process results in substantial collateral damage, such as destruction of axons, astrogliosis and loss of neuronal tissue. The results from these models can be difficult to interpret and sometimes limited to the study being undertaken. However, this animal model serves as a useful tool in the clinical evaluation of new therapeutic agents, and offers a reasonably in-depth mechanism of areas of neuroinflammatory processes, such as primary lesion formation, the

behavior of dendritic cells in the monitoring of BBB permeability, as well as evaluating collateral damage of neurons (Ransohoff., 2006). Early clinical signs were observed within 9-12 days of sensitization. EAE induction in the animal results in progressive degrees of ascending paralysis. The consequential paralysis is debilitating. Figure 2.5 relates to a typical procedure of induction in a mice model, where active immunization process, antigens are injected at the toe pad of the animal, since this is a highly effective systemic immune response due to highly responsive lymphatic draining nodes at the site for the autoimmune procedure to be induced efficiently. Paralysis usually commences with a weakened tail, gradually proceeding to hind limb paralysis, and seldom paralysis of the front limb in the animal model. Myelin antigens are part of the CNS and PNS myelin, thus inducing a great variety of peripheral involvement as noted in spinal roots of Lewis rats that were immunized with MBP (myelin basic protein) (Gold *et al.*, 2006). The ability to induce this pathology is not confined to ‘myelin-antigen-specific T-cell lines’, since the disease also has specific targets for astrocytes and neuronal antigens (Sospedra *et al.*, 2005). We can thus deduce that there is no one specific model that covers the complexities of this human disease, rather a combination of various approaches aid in understanding the complexities of this condition (Gold *et al.*, 2006).

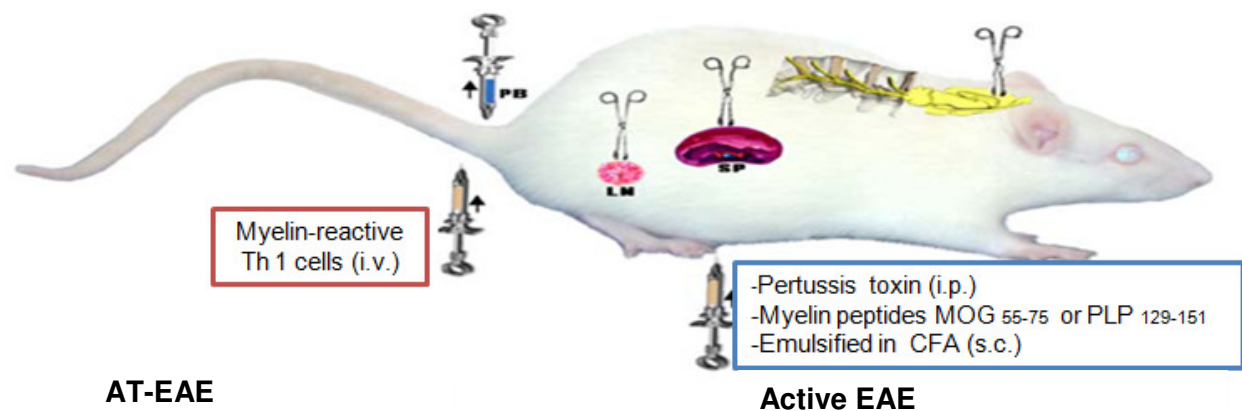


**Figure 2.5:** Depiction of a relatively common MS model in mice, illustrating systemic and local disease process points of interest and analysis. As part of the active immunization process, antigens are injected at the toe pad of the animal, since this is a highly effective systemic immune response due to highly responsive lymphatic draining nodes at the site for the autoimmune procedure to be induced efficiently. (Figure reproduced with permission from Elsevier Ltd.: Mix *et al.*, 2010) (AT-EAE, adoptive transfer EAE; CFA, complete Freund’s adjuvant; i.p., intraperitoneal; i.v., intravenous; LN, lymph node; MOG, myelin oligodendrocyte glycoprotein; PB, peripheral blood; PLP, proteolipid protein; s.c., subcutaneous; SP, spleen, Th1 cells, T helper type 1 cells.)

Studies have also been undertaken on viral models, as explained in Figure 2.6, in which inoculating an animal model, using mice with different strains of viruses such as Epstein–Barr virus, human herpes virus type 6 and various other types of viruses closely related with causing debilitation, proposed a molecular mimicry reaction, involving a sequence of trigger autoimmunity events, in which self-epitopes and foreign pathological epitopes develop cross reactivity, resulting in viral autoimmunity. (Virtanen *et al.*, 2011; Tzartos *et al.*, 2012). There are three hypotheses, namely, ‘bystander activation’, ‘epitope spreading’ and ‘molecular mimicry’, by which infection with a viral strain induces an immune response as seen in Figure 2.6. Bystander activation, involves a non specific reaction, occurring at sites of inflammation, increasing damage to tissues by a response of activated lymphocytes to secrete a variety of inflammatory mediators. Tissue injury, due to a sequence of cytotoxic inflammatory molecules from autoreactive T cells, possessing Vb receptors, or indirectly due to APC’s activated via Toll-like receptors (TLRs) or other patterns recognition receptors (PRRs). As a result of bystander activation, epitope spreading is the next direct effect, leading to greater tissue destruction and a prolonged anti-viral-immune response, releasing cryptic self-epitopes, which are consequently engulfed and presented to T lymphocytes via APC’s, thus developing a range of autoreactive T cells. The final stage involves molecular mimicry, therefore allowing a trigger autoimmunity reaction by the viral strain, resulting in cross reactivity between epitopes of the pathogen and self-epitopes (Mecha *et al.*, 2013).

## MOLECULAR MIMICRY EPITOPE SPREADING

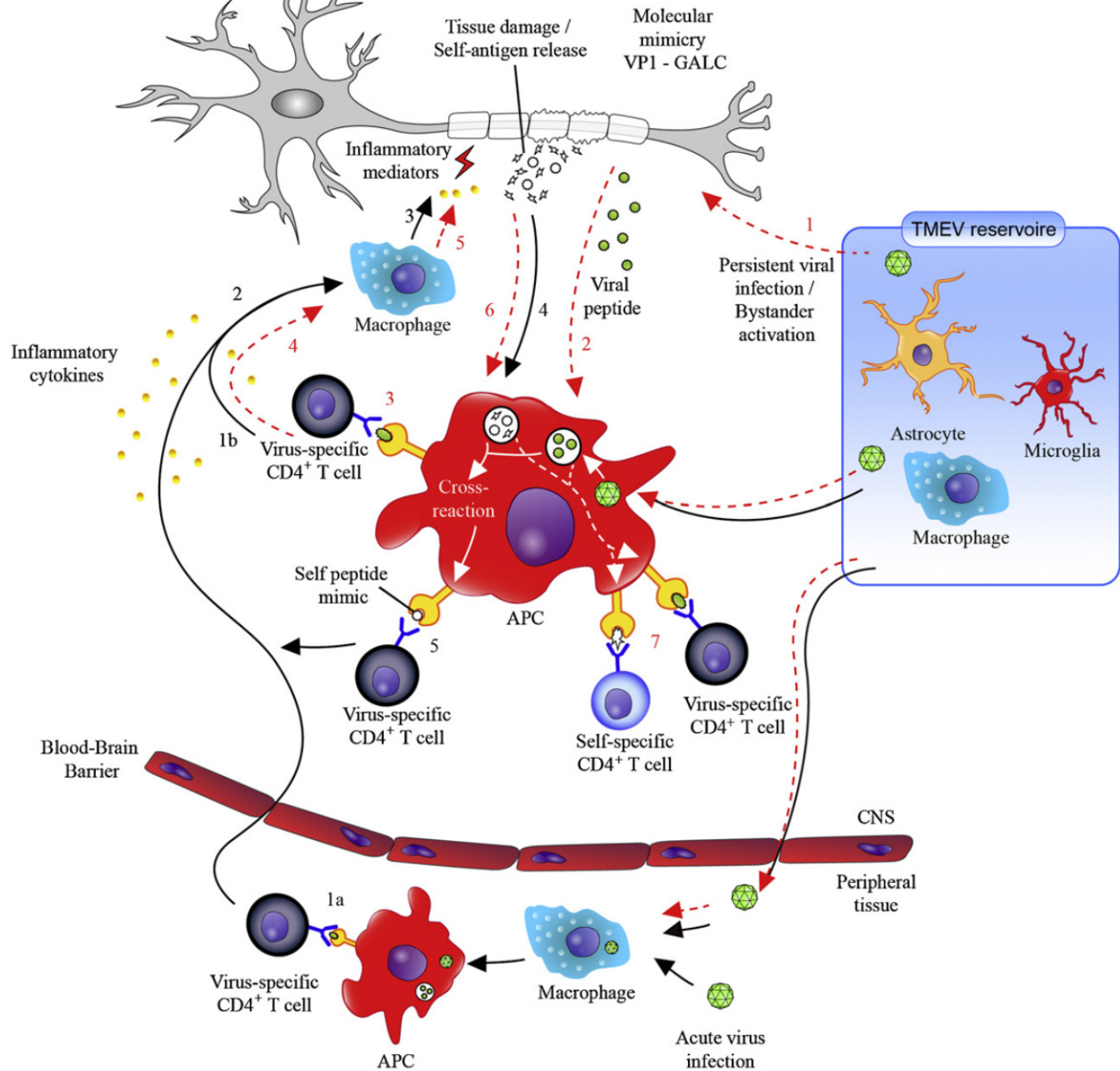


**Figure 2.6:** A viral autoimmune model of sequential molecular mimicry and epitope spreading. The black straight lines (not broken up) depict the acute viral infection, where APC or macrophages present antigens of viral peptides to specific viral epitope CD4 T cells located at the periphery(1a), or directly to the CNS (1b). These activated cells at the periphery, cross the BBB, thereby releasing a range of proinflammatory chemokines and cytokines, increasing the inflammatory process (2) this causes a great deal of tissue destruction further amplified by activating and attracting a greater number of monocytes, macrophages and other inflammatory mediators (3) the virus and self antigens, induces self-peptide processing to occur (4) cross reaction (molecular mimicry) also occurs between self-peptides (galactocerebroside, GALC) as well as viral peptides (VP1) (5). The red dashed lines depict a time response of a persistent viral

infection, the epitope spreading model (1) the antigen is then processed by APC's (2) this is then presented to virus epitope-specific CD4 T cells, which can be in the peripheral or crossing the BBB to nervous tissue (3) proinflammatory cytokines and chemokines are thus activated, attracting a greater number of monocytes and macrophages (4) this results in self-tissue destruction (5) leading to greater inflammatory reactions and processing of self-antigens (6) activation of virus-specific and self-epitope CD4 T cells (7), thus resulting in a prolonged immune-mediated disease state model.(Figure reproduced with permission from Elsevier Ltd: Mecha *et al.*, 2013)

## **2.4. Current Line of Treatment**

According to literature, there has not been a formulation for the cure of MS to date. Various therapeutic regimens are available to treat MS, according to the stage of severity. Therapy introduced slows the progression of the disease by controlling the symptoms and helping affected individuals maintain a healthy life with minimum recurrent attacks. Medication used in treatment of MS includes anti-CD20 antibodies, disease modifying treatments (DMTs), and Vitamin D therapy, which are discussed in detail later in the paper. Intravenous corticosteroids such as methylprednisolone, are used during symptomatic attacks but has no value in long term control of the condition (Sospedra *et al.*, 2005).

Patients with RRMS had no formal treatment for the disorder, approximately 20 years back. With the advancement in pharmaceutical developments, several treatment options are now available which, if initiated early as a response to early disease diagnosis, can prevent many detrimental progressive disease states. In patients with clinically isolated syndrome (CIS), DMTs are used to prevent any further disease progression. As depicted in Figure 2.7, disease modifying drugs are essential at early stages due to the exponential rate of neurodegeneration, resulting in different combinations of drugs used as well as increasing the dosage as the condition deteriorates. A substantial amount of phase 3 clinical trials, have yielded crucial results, that DMTs decrease the conversion to clinically definite multiple sclerosis (CDMS) in CIS patients. The implementation of DMTs in early diagnosis has also been incorporated into the McDonald diagnostic criteria (McDonald *et al.*, 2001). Through the use of highly sophisticated technology of MRI, it is easy to diagnose CIS in patients who have experienced a single clinical attack. This allows early diagnoses and treatments, which was not possible decades ago (Elovaara *et al.*, 2011). According to Montalban, 2010, evidence for dissemination in time and space might be easily diagnosed from single MRI scans with patients presenting with CIS (Montalban *et al.*, 2010). Early stage diagnosis reflects CIS, of which RRMS becomes the next level of concern, associated with recurrent, unpredictable attacks. RRMS is believed to

be treated as early as possible, since its immunopathology can lead to severe disability. MRI visualizations, indicate tissue damage, hence the degree of severity can be easily deduced (Compston *et al.*, 2008).

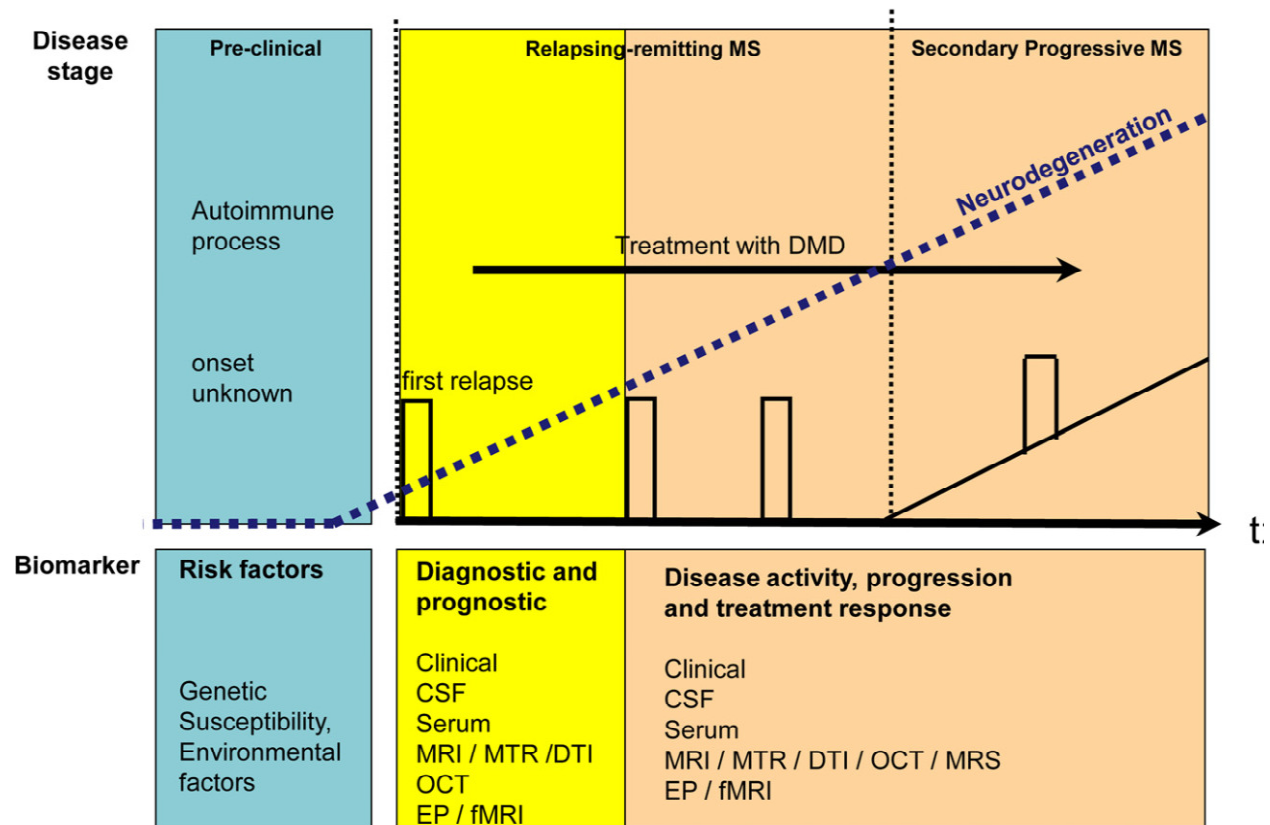


**Figure 2.7:** Various stages of MS and the implementation of disease modifying drugs (DMD) in relation to the increasing state of neurodegeneration (MTR-magnetization transfer ratio; DTI-diffusion tensor imaging; OCT-optical coherence tomography; EP- evoked potential; fMRI-functional magnetic resonance imaging; DTI-diffusion tensor imaging ; MRS- magnetic resonance spectroscopy; CSF-cerebrospinal fluid;). (Figure reproduced with permission from Elsevier Ltd.: Ziemann *et al.*, 2011)

In view of Elovaara *et al.*, 2011, despite all these advances in diagnostic tools, there is no set standard in which physicians treat patients with MS. Of debatable nature, is the decision of who the most appropriate candidate for early clinical intervention is, in relation to the risks and benefit of early treatment. Some patients may be exposed to a benign course, and not experience an attack for years, hence the neurologist in some cases may prefer to wait and monitor patients progress before initiating demanding therapy. Some neurologists believe that it is crucial to allow patients a certain amount of time to come to terms with their newly diagnosed

condition and make a choice of how they would prefer their treatment. Factors such as side effects, inconvenience of self injection and cost of treatment are many variables to consider when initiating treatment in patients. Contrary to this believe, other neurologists initiate treatment as soon as the early diagnosis is confirmed, since 'time is brain lost, and brain tissue cannot be regained' (Elovaara *et al.*, 2011). The various strategies for MS treatment are as discussed below.

#### **2.4.1. Anti-CD20 antibodies**

Monoclonal antibodies (mAbs) targeting CD20 have become a topic of great interest in targeting B cells of those diagnosed with MS. Many clinical trials, undertaken over the past few years, have been focusing on whether B cell depletion considerably aids in therapeutic efficacy in MS. CD20 transmembrane protein molecules cover a broad spectrum of B cell activity, ranging from pre-B cells, including naïve and memory B cells, however is not a part of differentiated plasma cells, stem cells or pro B cells. CD20 has many hydrophobic regions and possess properties of calcium channels, which assist in B cell differentiation and B cell activation (Barun *et al.*, 2012).

A genetically advanced anti CD20 monoclonal antibody (anti CD20 mAb) formulation known as Rituximab has been produced with the purpose to demolish circulating CD20+ B cells to treat non-Hodgkin's B-cell lymphomas (Maloney *et al.*, 1994). The important aspect/feature of this CD20 molecule, which makes it a suitable target includes its expression in high concentrations on B cells, thus the ability for interaction with antibody and not being internalized, thus remaining on the surface of the cell, and the lack of CD20 in the blood stream, thus not competing with anti-CD20 mAb binding. AntiCD20 mAbs deplete CD20 cells by mechanisms of: 'complement dependent cytotoxicity' (CDC); 'antibody dependent cellular cytotoxicity' (ADCC); and a process of 'induction of B cell apoptosis' (Barun *et al.*, 2012). Rituximab has multiple mechanisms of action by which it induces killing of CD20+ cells. ADCC and CDC are the direct properties that rituximab possess. Apoptosis, structural changes as well as sensitization to cancer cells are other ways in which rituximab plays a role in anti CD20 activity (Shim., 2011). The rituximab associated side effects include flushing, fever, rigors, hypotension and chills, as well as infusion related reactions. One of the important concern raised with the use of rituximab is that of progressive multifocal leukoencephalopathy (PML), observed in few patients diagnosed with lymphoma, rheumatoid arthritis (RA) or systemic lupus erythematosus (SLE), who also receive other immunosuppressive agents along with rituximab (Paues *et al.*, 2010).

Clinical trials for rituximab therapy in MS has been carried out in 4 categories, to date: i) phase 1, open label study, re-treatment trial in RRMS (Bar-Or *et al.*, 2008; Barun *et al.*, 2012), ii) RRMS affected patients with deteriorating conditions regardless of them continuing their normal regimen (Naismith *et al.*, 2010; Barun *et al.*, 2012), iii) phase 2, randomized placebo-controlled trial in RRMS (Hauser *et al.*, 2008; Barun *et al.*, 2012), iv) phase 2/3 randomized placebo controlled trial in PPMS (Hawker *et al.*, 2009; Barun *et al.*, 2012). In the first study, open label, re-treatment trial in RRMS, 26 patients were evaluated on the safety and tolerability of rituximab infusions of 1000 mg each, on the 1<sup>st</sup> and 15<sup>th</sup> day, thereafter a following dose 6 months from the first dose (2 doses of 1000 mg at weeks 24 and 26), and thereafter proceeded for a total of 72 weeks. 1000 mg acetaminophen and 50 mg diphenhydramine HCl were administered 30-60 minutes before commencing rituximab infusion. Results obtained over the 72 weeks revealed fewer new gadolinium-enhancing (Gdenhancing) or T2 hyper-intense brain MRI lesions, in addition to much less relapses in comparison to previous years of treatment. At week 48, no subjects tested positive for serum Human Anti-Chimeric Antibody (HACA), however, on the 72<sup>nd</sup> week, only 6 of 21 subjects reacted positive to HACA. No noted side effects were concluded (Bar-Or *et al.*, 2008, Barun *et al.*, 2012). In the second study, RRMS affected patients with deteriorating conditions regardless of them continuing their normal regimen were administered with Rituximab to 30 patients, who were also on the treatment with injectable disease modifying agents. These patients received 4 doses of 375 mg/m weekly. The team revealed decreased MRI disease activity: 74% of the post-treatment MRI scans having no traces of Gd-enhancing lesions and 26% at baseline (pb 0.0001). Gd-enhancing lesions median number was decreased from '1.0 to 0, and the mean number was decreased from 2.81 per month to 0.33 after treatment', showing an 88% reduction. Expanded Disability Status Scale (EDSS) remained stable and no severe side effects were reported (Naismith *et al.*, 2010; Barun *et al.*, 2012). In the 3<sup>rd</sup> study, 69 out of 104 subjects were randomized to administer 1000mg rituximab stat on the 1<sup>st</sup> and 15<sup>th</sup> day (administered intravenously), whereas the other 35 patients were administered placebos. Patients administered rituximab revealed considerable decreased total new Gd-enhancing lesions, at weeks 12, 16, 20, and 24, remaining stable over 48 weeks. No severe side effects were distinguished during this clinical trial (Hauser *et al.*, 2008; Barun *et al.*, 2012). In the 4<sup>th</sup> study, phase 2-3 randomized placebo controlled trial in PPMS, patients were randomized (2:1) out of a total number of 439, receiving 2 doses of 1,000 mg each of rituximab, with an interim of 14 days, or placebo infusions, every 24 weeks up to the 96<sup>th</sup> week. Results proved that 24.5% of subjects possessed Gd-enhancing MRI lesions. EDSS was elevated for a

period of 12 weeks, in which the primary end point was a ratio of 'time to confirmed disease progression (time to CDP). There were no marked variations in observations of 'time to CDP' in comparison to rituximab- and placebo subjects after a period of 96 weeks of the trial. Variations in brain volume were comparable in both groups ( $p= 0.62$ ), however patients administered with rituximab displayed a minor raise in T2 lesion volume ( $p<0.001$ ) (Hawker *et al.*, 2009; Barun *et al.*, 2012).

To sum up this study, it is quite evident that anti-CD20 mAbs, remarkably inhibit new brain lesions, as well as reduce the relapse rate in patients with RRMS and PPMS. Infusion therapy is generally well received, with little or minor side effects, becoming less sensitive with every exposure. Positive MRI outcomes in patients administered with rituximab additionally confirms that B cells play a crucial role in the development of MS. Among other commercially available anti-CD20 mAbs is Ofatumumab and Obinutuzumab (GA101) which is being investigated in collaboration with Biogen Idec.

Among all relevant questions pertaining to mAbs targeting CD20, the focus in research has evolved significantly from the understanding of whether B cells contribute to MS, shifting paradigms to target how they contribute biologically based on concepts that lead to decreases in pathogenic CNS-autoreactive antibodies due to depletion of B cells for therapeutic efficacy as discussed above.

#### **2.4.2. Disease Modifying Treatments**

RRMS is a widely researched condition of MS, yet it remains a disease with no significant therapeutic cure (Goodin *et al.*, 2002). The only form of aid that therapy provides for this condition, is inhibit further disease progression, thus preventing onset of major disability as outlined in the treatment stages according to the severity of the disease states as depicted in Figure 2.8 (Goodin *et al.*, 2008). Reducing the relapsing frequency as well as new lesion formation, and providing symptomatic improvement, is the primary goals of existing therapies. The most significant amount of neuronal damage takes place during early stages of the disease, thus early therapy has maximum benefit when commences in early phases of the disease condition, thereby preserving maximum neuronal tissue from degradation. Patients suffering with acute relapses are generally treated with corticosteroids, but these have no beneficial results in long term therapy. DMTs instead are used for long term management of patients suffering from multiple attacks and RRMS (Stuart., 2004).

DMT therapy so far covers six drug formulations that are FDA approved for treating RRMS. These include glatiramer acetate (GA) - a polymer consisting of 4 amino acids found in the myelin sheath and interferon beta (IFN- $\beta$ ) – IFN $\beta$ -1a and IFN $\beta$ -1b. Two forms of infusion therapies include Mitoxantrone and Natalizumab, the former is an antineoplastic anthracenedione used in SPMS, PRMS, or worsening RRMS and the later is a recombinant monoclonal antibody instituted for the treatment of RRMS in late 2006. These infusion therapies are second line therapies for most patients because of the associated side effects. Fingolimod is an oral formulation, which traps immune cells in lymph nodes, hence reducing attacks of MS thus preventing short-term disability(<http://www.mayoclinic.com/health/multiple-sclerosis>., 2012).

The first line therapies are IFN- $\beta$  and glatiramer acetate, which have no major concerns in terms of safety profile, and possess good levels of efficacy. A second line therapy such as natalizumab, has greater degree of side effects, but at the same time has better levels of efficacy. Two oral formulations, cladribine and fingolimod, were initially marketed based on their success of phase 3 clinical programmes where both appeared relatively effective and safe, until events of severe adverse reactions (malignancies and fatal infections) were noted with the use of cladribine, resulting in it being withdrawn from the market. Therapies causing adverse side effects are considered applicable only for patients who cannot be treated or who do not respond to the first line therapy and in most cases should not be used in average RRMS or in CIS patients (Sorensen., 2011).

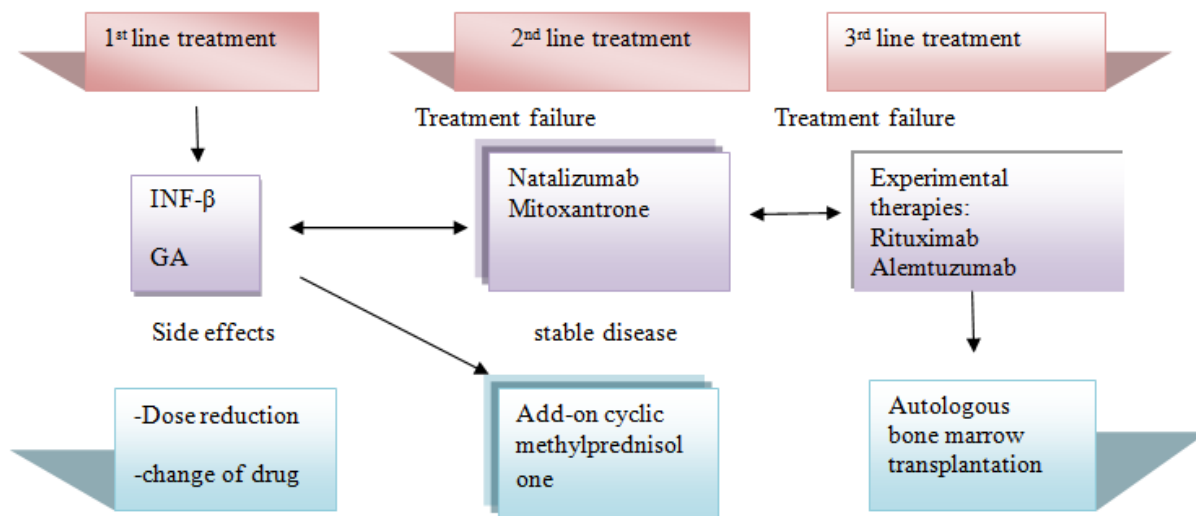


**Figure 2.8:** Treatment procedures for relapsing–remitting multiple sclerosis. (Figure adapted with permission from Elsevier Ltd.: Sorensen., 2011)

#### 2.4.2.1. Glatiramer acetate (GA)

The polymerization product of 4 amino acids: ‘L-Glutamic acid, L-Lysine, L-Alanine, and L-Tyrosine, previously known as copolymer 1’, is now clinically referred to as Glatiramer acetate (Teitelbaum *et al.*, 1997). GA has been used for the treatment of RRMS since 1996, and has significantly shown to reduce the activity of RRMS (Johnson *et al.*, 1995; Johnson *et al.*, 1998; Johnson *et al.*, 2001).

According to Filippi and coworkers, a study conducted on 239 RRMS patients, revealed that new lesions were inhibited from progressing into permanent tissue disruption (black holes appearance), when GA was clinically administered to these patients (Filippi *et al.*, 2001). Much research has been undertaken to understand the mode of action of GA; it is believed to competitively inhibit myelin antigens through MHC blockade, but its pharmacology still appears to be not fully understood. Its inhibition of myelin antigens occurs quite effectively *in vitro*, in relation to it being significantly degraded to oligopeptides at the site of injection. GA is also responsible for the conversion of TH1 to TH2 cells (T suppressors cells), which is not possible in MS immunology (Teitelbaum *et al.*, 1997; Sherki *et al.*, 2003).

GA administered IV, travels through the BBB to areas of the CNS, in which myelin antigens are stimulated, releasing anti-inflammatory cytokines (Neuhaus *et al.*, 2001). GA has shown many neuroprotective characteristics, such as in acute and chronic motor neuron disease, evident in

optic nerve injury and glutamate toxicity (Angelov *et al.*, 2003). These activated GA reactive T-cells, produced large concentrations of brain derived neurotrophic factor (BDNF), a neurotransmitter which has crucial properties for neuronal sustenance (Ziemssen *et al.*, 2002). Sherki *et al.*, 2003, conducted studies on GA which was tested in mice induced with chronic EAE, which showed reduction in clinical and pathological symptoms. These mice revealed minimum focal inflammation, axonal disruption as well as demyelination compared to their controls. Thus, it was proved that axonal damage is substantially reduced in the treatment with GA (Sherki *et al.*, 2003). Herrmann *et al.*, 2010 tested GA in animal models with varying degrees of central nervous system degenerative and inflammatory diseases. It was profoundly noted that GA-induced T cells cross the BBB, secreting high concentrations of anti-inflammatory cytokines and neurotrophins, consequently reducing neuronal damage and promoting neurogenesis. It was also proposed that GA, under the conditions of inflammatory-mediated neurodegeneration, permeates through the impaired BBB, eliciting reactions/responses protecting neurons under these detrimental conditions (Herrmann *et al.*, 2010).

*In vitro* Immunological studies pertaining to the adaptive immune system, revealed the binding of GA to MHC class II molecules on surface of APC receptors. Binding of GA to MHC class II showed inhibition of T cells specifically for the myelin basic protein, concluding the possibility that GA might compete with myelin antigens with affinity for binding to MHC class II molecules (Lalivie *et al.*, 2011).

Further studies revealed that GA attracts a range of CD4+ GA reactive TH2 cells in the peripheral nervous system (Wiesemann *et al.*, 2001; Dhib-Jalbut., 2002). According to Neuhaus *et al.*, 'GA reactive TH2 cells may be reactivated within the CNS by cross-recognition of myelin', following the release of anti inflammatory cytokines via 'bystander suppression' (Neuhaus *et al.*, 2000). CD4+, CD25+ and Foxp3+, known as T regulatory cells (Treg) function in the preservation of immunological tolerance as a result of decreasing the effects of self-reactive lymphocytes (Hori *et al.*, 2003). Foxp3, considered as the key transcription factor in response to controlling T regulatory cells therefore aids in controlling expression of critical suppression-mediated molecules. In MS patients, Treg were found in low concentrations in patients with MS. Research studies confirmed that GA increased Treg activity, converting CD4+CD25- to CD4+CD25+, thus increasing the expression of CD4+ Tcells via an increase in Foxp3. In GA reactive CD4+CD25+ T-cell lines, a correlation of high levels of Foxp3 showed increased levels of T regulation (Hong *et al.*, 2005). Animal studies in demyelinated diseases, revealed that GA

promoted myelin repair, indicating positive response towards antibodies, instead of it being recognized as a harmful antigen (Ure *et al.*, 2002).

GA has significant reactions on the innate immune system, manifesting as an early step related to the immunological cascade (Jung *et al.*, 2004; Sanna *et al.*, 2006). *In vitro*, GA inhibited lipopolysaccharide expression of several markers on isolated human monocytes, such as CD150 signaling lymphocytic activation molecule (SLAM), CD25 and CD69, and showed major reduction of proinflammatory TNF and IL-12' (Weber *et al.*, 2004). Kim *et al* reported that IL2 were reduced in significant concentrations, in comparison to IL10, which was present in considerably high concentrations (Kim *et al.*, 2004).

In light of the immunomodulatory effect this copolymer has in MS, it is evident that much research of this polymeric drug has expanded its views from understanding the influence on Th2 cells due to its behavioral properties similar to that of a peptide ligand, to further exploring its properties on antigen-presenting cells, monocytes and dendritic cells, thus providing an explanation for a shift in Th2 cells. It can thus be considered that a better understanding of GA has promising potential in future development of new immunomodulatory agents, specifically pertaining to MS.

#### **2.4.2.2. Beta-interferon treatment**

Interferon  $\beta$ -1b was first approved in 1993 by the US FDA, after 15 years of research, using natural type 1 IFN (Rudicka., 2011). It was earlier thought that MS was caused by a viral infection; hence the anti inflammatory characteristics were the logic for using IFN. A number of trials were carried out using IFN- $\alpha$  and IFN- $\gamma$ . Unfortunately, too many side effects were found associated with IFN- $\alpha$  and studies with IFN- $\gamma$  (type II IFN) showed severe, frequent relapses in MS patients (Panitch *et al.*, 1987). After the first phase of safety studies, it was decided that IFN- $\beta$  might be clinically effective in reducing the course of the disease. Formulations for intramuscular as well as subcutaneous administration were tested, which proved to reduce the relapse rate by 30% and new lesion activity by 65%. Results of worsening disability and whole brain atrophy, was remarkably reduced with patients on IFN $\beta$ -1a therapy (Rudick *et al.*, 1999).

There is wide use of IFN-  $\beta$  as first line treatments in RRMS, and its effectiveness varies in a small percentage of patients, however it still maintains a good safety profile in long term administration (Rudick *et al.*, 2005; Ebers *et al.*, 2010).

On a molecular level, as depicted in Figure 2.9, IFN I and IFN II are composed of single chains of polypeptides, with alpha helices and beta pleated chains and the size range from 15 to 25kDa. These IFN(I and II), bind specifically to their heterodimeric receptors, signaling discrete JAK/STAT phosphorylation cascades, with the final phase of transcription regulation of their genes (van Boxel-Dezaire *et al.*, 2006). IFN- $\beta$  has no polymorphism, having a single gene with no introns encoded, whereas, IFN- $\alpha$  possess at least 12 different functional subtypes. IFN- $\beta$  was earlier called fibroblast IFN, since the *in vitro* induction of fibroblasts could produce IFN- $\beta$ . Other cells that could produce IFN- $\beta$  are endothelial cells, various leukocytes and epithelial cell. Unlike IFN- $\alpha$ , where a subtype of dendritic cells appear to produce a good quantity of IFN- $\alpha$  *in vivo*, a physiological source of IFN- $\beta$  has not been discovered and is not easily detectable endogenously in humans (Taniguchi *et al.*, 2002). The natural form of IFN- $\beta$ , found in humans is glycosylated at one portion with N-linked complex carbohydrates. This composition is essential for monomer stability, also providing a basis of considerate solubility and biodistribution, however the carbohydrate moiety is not vital for receptor binding (Rudicka *et al.*, 2011). Stone *et al.*, reported on numerous clinical tests, proving that IFN- $\beta$  has a mechanism of action that temporarily inhibits the opening of the BBB (Stone *et al.*, 1995). A signaling chain IFNAR1, and a binding chain, IFNAR2, are the 2 composite units of IFN- $\beta$  which are expressed on cells at their surface. IFN- $\beta$  can easily bind to IFNAR2 alone, but binding to IFNAR1 can only take place in the presence of IFNAR2, however the strength of binding is much greater when both subunits are available (Uze *et al.*, 2007). According to Prajean *et al.*, (91), there are five series of events that lead to the biological activity of IFN- $\beta$ . 1) IFN attaches and binds to the external surface of the cell, being the IFNAR2. 2) IFNAR1 receptors then attach with to the IFN- $\beta$ -IFNAR2 complex, allowing the protein interaction with the high affinity receptor-ligand complex. 3) JAK1 (associated with IFNAR2) and Tyk2 (associated with IFNAR1) interaction, produces a cascade series of phosphorylation, thereby implementing STATS to be activated. 4) These activated STATS, form a composite with cytoplasmic proteins, allowing translocation to the site of the nucleus, binding to Interferon Sensitive Response Elements (ISRE) 5) As a result of ISRE binding, transcriptional regulation (induction and inhibition) occur in more than 1000 genes (Prejean *et al.*, 2000).

In essence, the exact biological response to IFN- $\beta$  remains highly non-specific to its mechanism of action due to its variation in therapeutics among various patients. It can therefore be concluded that more intense research is greatly required and biomarkers for IFN- $\beta$  is definitely a link that is missing, requiring more strategic research for its development. Future advancement

of IFN- $\beta$  formulations, with the possibility of increasing the half-life of the drug, remains an area of substantial demand, by which patients will be using injections less frequently, thus resulting in a decrease of side effects and higher patient compliance. Strategies employing pegylation has known effects of decreasing metabolism of the drug, and are under research at present. Other endeavors of providing oral IFN- $\beta$  remain highly favorable in comparison to the injectable form. This long-term management will be highly beneficial, thus reducing inconveniences and discomfort from injectables.

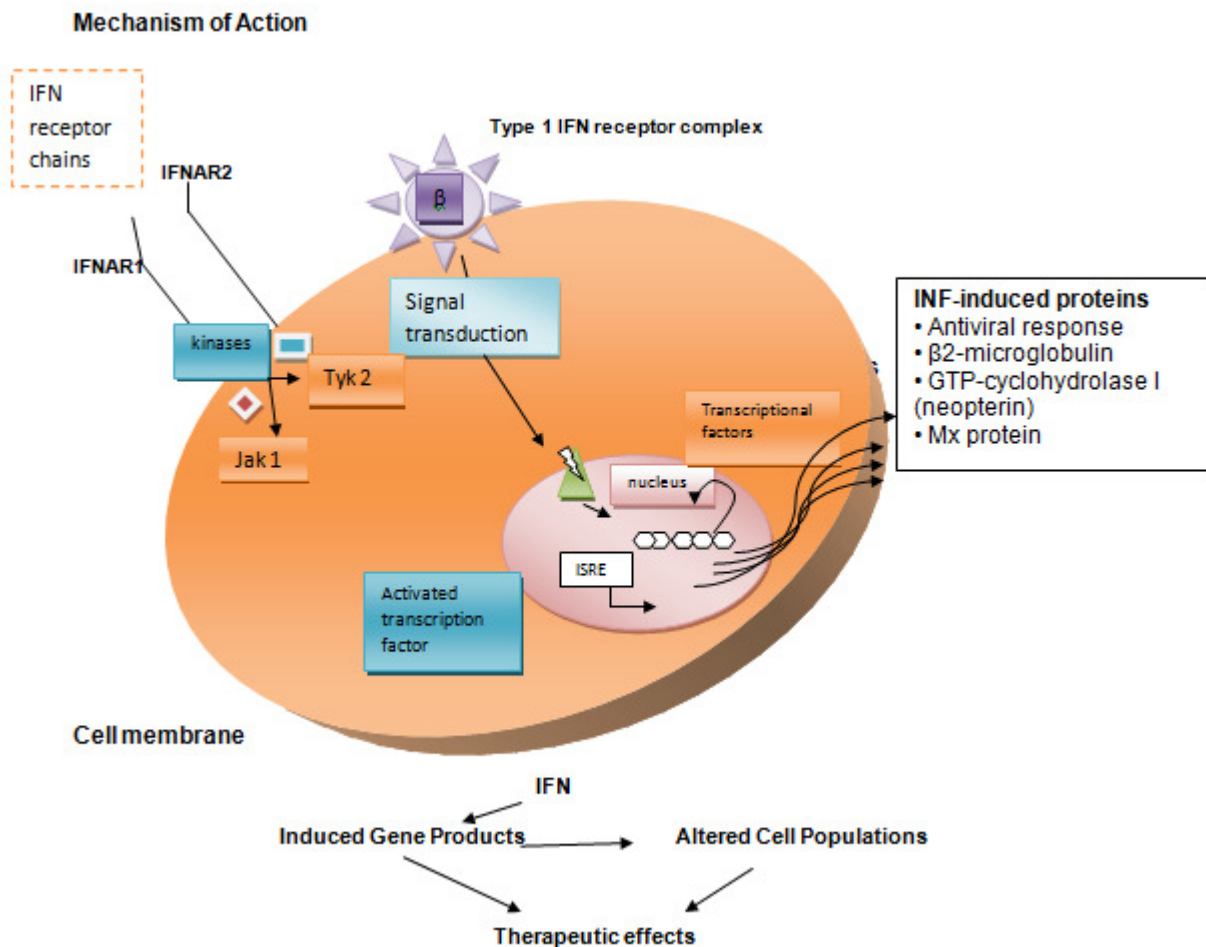


**Figure 2.9:** Mode of action of IFN- $\beta$ . (Figure adapted with permission from Elsevier Ltd.: Rudicka *et al.*, 2011)

### 2.4.2.3. Natalizumab treatment

Natalizumab is characterized as a humanized monoclonal antibody, binding specifically to the  $\alpha$ -chain of  $\alpha$ 4-integrins, thus inhibiting the binding of leukocytes to vascular cell adhesion

molecule-1 (VCAM-1). It is used as a 2<sup>nd</sup> line treatment of active RRMS. This drug is only prescribed to patients who fail to respond to 1<sup>st</sup> line treatment, or for those who have a very active form of the disease (Kappos *et al.*, 2011). In 2005, Natalizumab was suspended from the market based on 3 adverse reports, as a consequence of drugs' use: progressive multifocal leukoencephalopathy (PML), onset of diseases with much fatality, inflammation and damage to white matter of the CNS. This was, however, reviewed in 2006, when the USA and the European Union (EU) reintroduced this drug, claiming that no identifiable incidents of PML were previously seen in patients using this drug under specific conditions (Yousry *et al.*, 2006). In 2011, another study was initiated to evaluate safety profiles and determine the efficacy of Natalizumab. Approximately 83,300 patients worldwide participated in this study, exposing themselves to natalizumab (representing 148,000 patient-years of exposure). Results revealed positive outcomes, such that, 'low annual relapse rates and stable EDSS scores were evident during a 120 week treatment period' (O'Connor *et al.*, 2011; Kappos *et al.*, 2011). Natalizumab has been extensively researched by various groups and tested in animals as well as humans for its efficacy, which showed profound reduction in RRMS and positive MRI activity (Miller *et al.*, 2003).

According to Coisne *et al.*, intravital microscopy of mice with acute EAE demonstrated that natalizumab inhibits firm adhesion of T cells, 'but not the capture of human T-cells on the inflated BBB'. It was deduced that the effectiveness of natalizumab in blocking T cell adhesion to the inflated BBB, were more pronounced in EAE models in relation to acute systemic TNF- $\alpha$  induced inflammations. Data generated from this study strongly concluded that  $\alpha$ 4 integrin-mediated adhesion of human T cells (in EAE models), on the inflated BBB, is efficiently blocked by natalizumab, providing substantial proof *in vivo* of this concept in MS (Coisne *et al.*, 2009).

In a clinical study undertaken to determine mean saturation of  $\alpha$ 4-integrin, MS patients administered with 3mg/kg and 6mg/kg IV natalizumab, 'achieved approximately 80% and 90% mean saturation of  $\alpha$ 4-integrin, respectively'. Phase 2 trials recommended that, 'a stat fixed dose of 300 mg would sustain optimal  $\alpha$ 4-integrin saturation for over 4 weeks'. 300 mg of the dose administered every 4<sup>th</sup> week in Phase 3 trials revealed a mean saturation level of  $\geq$ 70%  $\alpha$ 4-integrin (Hutchinson., 2007). Rudick, *et al.*, adopted a new approach of combining the therapy of IFN $\beta$ -1a with natalizumab to a standard regimen. Such a treatment showed significant, 'decrease in annual relapse rate by 55%', 'sustained developmental progression by 24%', and an 83-89% reduction of new lesions, in relation to just a single IFN- $\beta$ 1a single

regimen (Rudick *et al.*, 2006). Natalizumab therapy in those who do not respond positively to IFN- $\beta$  or GA should be considered especially if their functional processes have deteriorated substantially and have possibly reduced treatment options available (Miller *et al.*, 2007).

Thus it can be concluded that, this type of treatment requires special evaluation strategies in patients who are likely to respond to the treatment and demonstrate no fatal side-effects. This treatment is considered appropriate as a first-line regimen to those not responding to IFN- $\beta$  and GA in patients with more functional loss and greater neurodegenerative severity states as discussed above.

#### **2.4.2.4. Mitoxantrone treatment**

Mitoxantrone is a potent IV immunosuppressant, inhibiting the differentiation of T cells, B cells and macrophages. Much of its effects focus on, 'reducing neurologic disability and relapse frequency, in patients suffering from SPMS, PRMS, or severe stages of RRMS' (Fox., 2006). Mitoxantrone falls in the category of chemotherapeutic related anthracenedione derivatives, falling in the category of anthracyclins doxorubicin and daunorubicin. It is a water-soluble drug and therefore does not normally cross the BBB under normal conditions. The drug penetrates into DNA molecule via hydrogen bonding thus causing cross linking and breakup of strands. Interruption of RNA and inhibition of topoisomerase II, which is significantly involved in aiding repair to damaged DNA and promoting uncoiling, are significantly compromised. *In vitro* studies confirm the activity of this drug having inhibitory effects on inflammatory mediators; B cells, T cells, and macrophages (Watson *et al.*, 1991). It is clinically used against various tumors conditions such as breast, leukemia and colon cancers. Studies have proved an increase in life expectancy in rodents glioma tumor model when administered with mitoxantrone. Formulations available are intratumoral mitoxantrone which has been clinically administered to patients to successfully improve survival of recurrent gliomas (Joshi *et al.*, 2011). Another study was undertaken with animals exposed to experimental allergic encephalomyelitis (EAE), with the aim of mimicking symptoms of MS. These animals under mitoxantrone treatment revealed substantial decrease in immunological responses, suppressing myelin-directed T and B-cell activity by 3- 9-fold (Mustafa *et al.*, 1993). The drug shows high affinity for suppression towards certain immunoglobulin subtypes, such as Ig M, which were suppressed, mainly due to macrophage-mediated B-cell inhibition. Mitoxantrone, after infusion demonstrated extensive tissue distribution, reaching a steady-state volume of distribution of  $>1000 \text{ /m}^2$ . It was apparent that drug concentration in the tissue, far exceeded those in the blood stream during phases of terminal elimination. This extended tissue sequestration and delayed release of mitoxantrone

into the blood stream allows cellular tissue to be exposed to high drug concentrations for at least 1 month, hence acting as a long half-life immunosuppressive formulation (Fox., 2006).

The treatment duration for mitoxantrone has been proposed to be used for no longer than 2 to 3 years or 140 mg/m<sup>2</sup> of a cumulative dose, due to negative cardiotoxic adverse reactions that allows a short duration for chronic treatment (Ghalie *et al.*, 2002). A study was undertaken *in vitro* to analyze immunological effects of mitoxantrone in MS. It was deduced that apart from possessing the ability to suppress B and T cells, the prominent target of mitoxantrone action is the antigen presenting cell (APC) which is promoted to undergo apoptosis (Neuhaus (a) *et al.*, 2005). Additionally, the drug was noticed to inhibit dendritic cells by Neuhaus and group. A dose dependant inhibitory effect on the surface MHC (major histocompatibility complex) of dendritic cells was observed, at various concentrations starting from 2ng/ml. However at a concentration of 2000ng/ml, a high proportion of necrotic cells were observed, indicating its toxic properties at very high concentrations (Neuhaus (b) *et al.*, 2005).

It is thus essential for patients to have careful monitoring for possible side-effects after initiating therapy with mitoxantrone, specifically relating to cardiotoxicity and toxic leukemias. It is therefore mandatory for research in this area to evaluate other anthracyclines that have lower toxicity profiles but have similar/enhanced therapeutic benefits.

## **2.5. Fingolimod Therapy**

The drug commonly termed FTY720 is chemically isolated from myriocin (ISP-1), a metabolic product from fungus *Isaria sinclairii*, which was derived from ancient Chinese therapy, believed to have immunosuppressive effects on the body. This drug belongs to the sphingosine-1-phosphate receptor modulators, a new class of drugs used to treat CNS inflammatory conditions, because of their phenomenal effects on the immunological and neurobiological systems (Ingwersen *et al.*, 2012). An important aspect of fingolimod is the way in which it produces its anti-inflammatory effects, unlike other typical cascades of anti inflammatory formulations. Fingolimod does not impair or suppress the action of immune cells, instead selectively regulates the lymphocyte activity among lymphoid tissues. The hydrophobic nature of the drug allows it to cross the BBB, entering the CNS more effectively (Schwab *et al.*, 2007). Data from number of researchers suggests the fingolimod to have specific action on glial cells for reducing neuroinflammation (Kim *et al.*, 2011). Inactive FTY720 is converted via hepatic conversion of sphingosine kinase 2 (SphK2), to its active phosphorylated form, FTY720-P.

FTY720-P, being activated, binds to 4 subtypes, which are S1P1, S1P3, S1P4, and S1P5 (Ingwersen *et al.*, 2012).

Animal models, reflecting on histopathological studies on the expression of S1P (lipid signaling molecule) receptors in animals being induced with EAE, showed remarkable impact of fingolimod therapy in EAE models (Brinkmann *et al.*, 2002). The efficacy of orally administered fingolimod was tested using monophasic EAE Lewis rats. The results obtained showed a reduction in T cell infiltration in CNS tissue, and a substantial decrease in the expression of proinflammatory cytokines. Promising neuroprotective results were obtained in mice, when myelin-reactive lymphocytes that were administered FTY720, could not be induced with EAE following initiation of this treatment. It was also noted that the drug demonstrated substantial therapeutic efficacy regardless of being administered after noticeable first stages of the disease progression (Kataoka *et al.*, 2005). Of critical observation, it was profound that fingolimod reversed neuronal conduction impairment, and prevented further axonal degeneration. In addition, it was able to control lymphocyte migration, and prevent further BBB dysfunction, even at lower concentrations (Foster *et al.*, 2009).

Contrary to the success of this drug, the evaluation of adverse effects was seriously noted; specifically pertaining to cardiologically related symptoms of bradycardia after the first dose of fingolimod is taken. Instances where deaths were also reported are still under serious investigation in an effort to deduce the relationship if any with this drug. According to the European Medicines Agency, an alert of close monitoring of patients after their first dose was highly advised and long term monitoring of patients are essential for maintenance of good health (Yadav *et al.*, 2012). To sum up this study on fingolimod, it is of great benefit that an oral therapeutic agent is available for MS; however, due to its recent approval on the market, cautions in terms of unexpected safety and tolerability profiles should be carefully monitored in all patients undergoing this therapy. It is not apparent that all long term adverse effects reported in clinical trials are the only issues to consider; hence a comprehensive approach in evaluating this therapy should be based on the overall safety, efficacy and tolerability of this newly marketed oral delivery system for MS.

## **2.6. 4-aminopyridine (4-AP) (Fampridine-SR) and 3, 4-diaminopyridine**

The fundamental of MS, as detailed through this review explains the sequence of events leading to demyelination and to a minimum extent a degree of axonopathy. In patients suffering from spinal chord injuries (SCI), myelinopathy constitutes the principal neurological deficit, initiated by

trauma-induced axonopathy, hence these above pathologies, fundamentally display central conduction deficits, due to demyelination (Hayes., 2007). In an endeavor to improve motor neuron function and improve conduction amongst demyelinated axons, 4-aminopyridine (4-AP) and 3,4-diaminopyridine which fall into the category of  $K^+$  channel-blocking agents have been critically evaluated and implemented (Totoiu *et al.*, 2005; Krishnan (a) *et al.*, 2012). Patients suffering from MS and SCI display minimum neurological conduction, hence 4-AP and 3, 4-diaminopyridine are used to inhibit this aspect of neurological malfunction thereby initiating movement in these less mobile individuals (Hayes., 2007). Fampridine-SR (Acorda Therapeutics, Inc., Hawthorne, NY, USA) is an oral tablet formulation of 4-AP, designed as a sustained-release formulation, targeting neuromuscular disability in which the demand has met the region of 400,000 Americans and much greater than a million MS patients globally (Hayes., 2007).

The mechanism by which Fampridine-SR delivers its effect is by; primarily targeting malfunctioning ion channels, which further affects axonal degeneration in MS. MS results in substantial neurological inflammation, which causes a complex rearrangement of voltage-gated  $Na^+$  channels, resulting in increased numbers of  $Na^+$  channel isoforms such as Nav 1.2. Conduction failure is also exemplified by the increasing levels of  $K^+$  channels expression. This up-regulation may sustain neural conduction, however substantial expression of elevated  $Na^+$  conductance's significantly compromise  $Na^+/K^+$  pump functioning, thereby elevating axonal degeneration in MS. (Smith., 2007).

According to Goodman and co-workers a randomized, double-blind, placebo-controlled, dose-ranging study was undertaken to monitor optimum doses and evaluate any shortcomings from Fampridine-SR using MS functional composite, lower extremity manual muscle testing as well as subjective assessment of fatigue in patients suffering from walking impairments and ambulatory functioning which is a serious consequence in MS patients. A variation in doses of Fampridine-SR were evaluated starting from 10mg twice daily and increasing by 5mg at weekly intervals, reaching a maximum of 40mg twice daily. Less serious side effects reported include insomnia, paraesthesiae and asthenia, in comparison to more serious side effects of increasing the potential of seizures, where it occurred exclusively at doses greater than 25mg twice daily. Little benefit was seen in patients who were given higher dosages, thus reporting that these adverse effects in higher dosages may outweigh any significant benefits. Finally the study approved the efficacy of Fampridine SR and its association with greater mobility and strength in

lower extremity muscles (Goodman *et al.*, 2007). In comparison to this study, a subsequent evaluation was undertaken in 206 MS subjects where they were randomly distributed to four dose specific categories, 10mg, 15mg, 20mg and placebo doses of Fampridine SR, all given twice daily, in a pursuit to analyze the effects on walking speeds on the timed 25-foot walk test. The results proved that, '35% of patients receiving fampridine experienced a sustained response to treatment and improved walking speeds on the timed 25-foot walk test', in comparison to the placebo formulation, drawing a conclusion between the direct relationship in deterioration in walking speed and life expectance quality (Krishnan (b) *et al.*, 2012).

These studies have demonstrated the high level of significance of Fampridine-SR as a potent ion channel regulator, thus implementing a primary therapeutic strategy in MS. Studies are still under development in other domains such as cognition and balance as well as upper limb function (Hayes., 2007), thus creating a possibility for enhancement of clinical research and future development in this field.

## **2.7. Teriflunomide**

Teriflunomide, a metabolite of leflunomide, previously administered to patients with rheumatoid arthritis, preventing pyrimidine synthesis and T-lymphocyte proliferation by inhibiting mitochondrial enzyme dihydroorotate dehydrogenase. Due to the drug inducing a small degree of lymphocytopenia, these mechanisms to a certain extent are responsible for its effects (Killestein *et al.*,2011). Teriflunomide phase 2 trials undertaken on patients with relapsing stage of MS, demonstrated a decrease in MRI brain active lesions (O'Connor *et al.*, 2006).

A study of Phase 3 trials presented in 2011, comprising of a 2 year randomized control of 1088 patients with RRMS, dosed with either placebo, 7mg or 14mg of a once only dose of teriflunomide, revealed both doses of teriflunomide decreasing the annual relapse rate (ARR) and relative risk, in comparison to the placebo. Results revealed a 31.2% for the lower dose and 31.5% for the higher dose, in comparison to the placebo. A 12 week expanded disability status scale (EDSS) evaluation was decreased by 29.8% with the higher dose of teriflunomide. Several MRI studies also revealed greater impact in reduction of new lesion formation, with a 39% reduction on the lower dose, compared to a 67% reduction on the 14mg. Both doses were well tolerated with satisfaction on safety profile reports (Miller *et al.*, 2011). Side effects that were reported due to teriflunomide ranged from abnormal liver enzymes, diarrhea and nausea.

A concern of this drug in clinical practice was the aspect of safety profiles, since rare cases of fatal liver failure and a case of progressive multifocal leukoencephalopathy in a systemic lupus erythematosus patient was reported. Another concern is the teratogenic effects of leflunomide in women of child bearing age diagnosed with MS (Killestein *et al.*, 2011, Claussen *et al.*, 2012).

## **2.8. Dimethyl fumarate**

This oral drug, also referred to as BG-12, metabolized to monomethyl fumarate, activates the factor E2-related factor-2 pathway, which is responsible for protection against stress related oxidative neuronal death and damage to myelin. The expression of phase 2 detoxification enzymes in microglial and astroglial cells, as well as greater anti-inflammatory profiles with induction of Th2-type cytokines and expression of adhesion molecules, have been attributed to significant neuroprotection of the drug (Kappos *et al.*, 2008, Fontoura *et al.*, 2010, Linker *et al.*, 2011).

A pilot study of RRMS patients administered with an oral formulation of fumaric acid (Fumaderm, Biogen Idec, Ismaning, Germany), approved for application in psoriasis patients, showed a significant decreased GdE lesions in brain MRI scans (Moharreggh-Khiabani *et al.*, 2009).

A phase 2b study DEFINE (determination of the efficacy and safety of oral fumarate in relapsing-remitting MS) was undertaken in 257 patients with RRMS, using 3 doses of BG-12. Results concluded a 69% decrease in GdE lesions from duration of week 12-24, at a dose of 240mg three times a day in comparison to the placebo. There were also a decrease in new T2-hyperintense and T1-hypointense lesions (Kappos *et al.*, 2008). A phase 3 trial of  $\pm 1200$  patients deduced that 240mg of BG-12, twice a day, revealed a 49% reduction in the amount of patients who relapsed compared to the placebo, with a 53% decrease of ARR, 90% reduction of GdE lesions and 85% decrease in new/enlarging T2 lesions. A 38% reduction in EDSS worsening for cumulative probability of 3 month was also observed. No safety issues were reported during the study (Killestein *et al.*, 2011). Some of the commonly experienced side effects are headaches, GIT symptoms, mild infections, slight increase in liver enzymes as well as facial flushing (Kappos *et al.*, 2008).

Another global, placebo-controlled clinical trial called CONFIRM (comparator and an oral fumarate in relapsing-remitting MS), consisting of approximately 1200 patients assigned to 4

groups, BG-12 240mg twice a day, BG-12 240mg thrice a day, 20mg SC daily glatiramer acetate (GA), or placebo. Results obtained showed a 44% reduced ARR for twice daily dosage of BG-12 and a 51% reduction in thrice daily dosing, in comparison to the placebo over 2 years study. GA showed a 29% reduction in ARR compared to the placebo over 2 years. BG-12 secondary relapse endpoint was determined as significantly reducing the amount of patients who relapsed at 2 years. Twice daily BG-12 showed a 34% reduction, compared to 45% for the thrice daily dosing, in comparison to the placebo. GA showed a 29% reduction in patients who relapsed over the 2 year duration. Significant reductions in new brain lesions were definite within the first year of study and sustained during the duration of the study. BG-12 demonstrated a reduced number of new enlarging T2-hyperintense lesions (secondary endpoint) by 71% in twice daily dosage, 73% for thrice daily dosage and 54% reduction for GA. The reduction in number of new non-enhancing T1-hypointense lesions (secondary endpoint) was 57% for twice daily dose of BG-12, 65% for thrice daily dose and 41% reduction for GA. The probability of acquiring greater gadolinium-enhancing (Gd+) lesions (tertiary endpoint) was reduced by 74% in twice daily dose, 65% in thrice daily dose and 61% reduction in GA patients, compared to the placebo. Results for the BG-12 reduced risk of 12 week confirmed disability progression as accounted by the EDSS, showed 21% for twice daily dose, 24% for the thrice daily dose and 7% for GA, compared to the 2 year duration with the placebo. It can therefore be affirmed that BG-12 has significant therapeutic efficacy and will definitely improve the status of disability in patients with RRMS ([www.biogenidec.com](http://www.biogenidec.com)).

## **2.9. Vitamin D therapy**

Since the early days of identification of MS, it was thought that vitamin D deficiency was the cause for MS development. It was only after much extensive research, it was clarified that many years of Vit D deficiency, actually precedes the onset of MS (Munger *et al.*, 2006). The exact cascade of how Vit D reacts to elucidate an effect on MS is still being analyzed. Research that has been carried out, involves the regulation of the expression of HLA (human leukocyte antigen) susceptible allele - HLA-DRB1\*1501. This regulation is conferred through the Vit D receptor (VDR)-binding, that leads to a conserved vitamin D response element (VDRE), via VDR-binding in close proximity to other non-HLA susceptible genes (Ramagopalan *et al.*, 2010). It was further highlighted that functional interaction between HLADRB1\* 1501 alleles and VDR SNPs (single nucleotide polymorphism), play an important role in MS susceptibility (Handel *et al.*, 2012), in addition to VDR rs2228570 genotypes, which offers protective properties that are

dependent on Vit D levels, implicating that the interaction between HLA and VDR, increases the contact between Vit D and MS implicated genes. Environmental risk factors associated with SNP, increases the susceptibility to MS, thus implicating that genetic predisposition to MS may have a degree of modifiable nature (Islam *et al.*, 2006). This form of therapy is only an adjunctive to the main regimens and remains an area of complicated evaluation in isolation to other M.S related therapies.

## **2.10. Fatigue in MS**

Fatigue is a major aspect of MS that many individuals experience on daily basis. The pathophysiology of MS fatigue can be attributed to individual or combinatory effect of: discontinuation of cortico-subcortical circuits, in which there are deviations in neurotransmitter levels having various interactions on this pathway, pro-inflammatory cytokines and dysfunction of neuroendocrine axis. The management of this condition includes non pharmacological as well as pharmacological factors which aid to relieve fatigue (Pozzilli *et al.*, 2006).

Non pharmacological factors are considered to majorly impact the physical fitness of an individual, and relieve mental exhaustion which causes many neurological complications. Aerobic exercise in moderation can positively enhance energy levels and aid in general physical fitness (Romberg *et al.*, 2004). Practicing yoga as a regular discipline has shown to be effective in comparison to the control studies conducted in randomized MS patients (Oken *et al.*, 2004). Simple alterations in lifestyle, such as consuming higher energy release foods and lighter loads of occupational tasks carried out during the day, can greatly alter energy patterns leading to greater levels of energy conservation (Pozzilli *et al.*, 2006). Other measures undertaken to maintain a comparatively lower body temperature, such as by consuming cool beverages regularly or using cool clothing, have been shown to decrease the symptoms associated with acute and chronic fatigue (Beenakker *et al.*, 2001).

Pharmacological factors related to management of fatigue include: antivirals, potassium-channel blockers, cyclooxygenase and prostaglandin E2 inhibitors as well as acetyl esters of carnitine (ALCAR). Amantadine is one such antiviral drug but its mechanism of action is still not fully understood. This tricyclic amine is believed to have an indirect dopaminomimetic effect. It is primarily prescribed as a first line treatment for MS-related fatigue, due to supporting evidence from randomized control trials showing a 20-40% success in combating MS related fatigue (Krupp *et al.*, 1995). According to Taus *et al.*, (2003) studies indicate a conclusive success rate for amantidine, however it possesses various side effects such as insomnia, constipation,

nausea, headaches and irritability (Taus *et al.*, 2003). Potassium-channel blockers such as 3-4-aminopyridine (3-4-AP) and 4-aminopyridine (4AP) increases muscle tension by enhancing synaptic transmission (Mainero *et al.*, 2004). During a study conducted on a randomized double-blind, significant effects on fatigue were observed in patients who had taken the drug in comparison to the placebo (Rossini *et al.*, 2001). Aspirin irreversibly inhibits cyclooxygenase and prostaglandin E2 production, which is believed to affect the hypothalamic neuroendocrine response. It is possible that cytokine induced mechanisms are closely related to MS fatigue, hence aspirin or other non steroidal anti inflammatory agents are very useful in this regard. A randomized placebo controlled trial undertaken for aspirin, revealed positive outcomes for MS related fatigue with the use of 1300mg of aspirin daily (Wingerchuck *et al.*, 2005). A randomised, double-blind, cross-over study showed ALCAR to have significant effects on the energy metabolism of individuals by either, 'increasing the levels of stimulating neurotransmitters in the CNS, or exerting cholinomimetic activity on striatum and prefrontal areas'. Patients suffering with exhaustive MS related fatigue reported a marked increase in energy levels under ALCAR treatment (Kuratsune *et al.*, 2002).

**Table 2.1: Treatment options and mechanism of action of the drugs in MS therapy**

Category	Drug used clinically	Mechanism of action
Anti-CD20 Mab	Rituximab	Antibody-dependent cell-mediated cytotoxicity and complement-mediated cytotoxicity are the direct properties of rituximab against CD20+ cells. Apoptosis, structural changes as well as sensitization to cells are other ways in which rituximab plays a role in anti CD20 activity (Shim., 2011).
DMT	Glatiramer acetate(GA)	It competitively inhibits myelin antigens, through MHC blockade. GA is also responsible for the conversion of TH1 to TH2 cells (specific suppressors T cells), which are not possible in MS immunology (Sherki <i>et al.</i> , 2003; Teitelbaum <i>et al.</i> , 1997). GA has proven many neuroprotective characteristics, such as in acute and chronic motor neuron disease, evident in optic nerve injury and glutamate toxicity (Angelov <i>et al.</i> , 2003). These activated GA reactive T-cells, produce large concentrations of brain derived neurotrophic factor (BDNF), a neurotransmitter which has crucial properties for neuronal sustenance (Ziemssen <i>et al.</i> , 2002).
	Interferon $\beta$ -1b	IFN- $\beta$ attaches and binds to the external surface of the cell through IFNAR2. IFNAR1 receptors then attach to the IFN $\beta$ -IFNAR2 complex, allowing the protein interaction with the high affinity receptor-ligand complex. JAK1 and Tyk2 interaction thereupon, produces a cascade of phosphorylation, leading to activation of STATS. These activated STATS, complex with cytoplasmic proteins, which translocate into the nucleus, binding to Interferon Sensitive Response Elements (ISRE). Through this ISRE binding, transcriptional regulation (both induction and inhibition) >1000 genes occur (Prejean <i>et al.</i> , 2000).
	Natalizumab	Humanized monoclonal antibody, binding specifically to the $\alpha$ -chain of $\alpha$ 4-integrins, thus inhibiting the binding of leukocytes to VCAM-1 (Vascular cell adhesion molecule-1). Natalizumab acts by

inhibiting and blocking T-cell adhesion molecules on the inflated BBB through  $\alpha 4$  integrin (Kappos *et al.*, 2011).

	Mitoxantrone	Mitoxantrone, is a potent IV immunosuppressant, inhibiting the differentiation of T cells, B cells and macrophages (Fox <i>et al.</i> , 2006). Mitoxantrone penetrates into DNA via hydrogen bonding thus causing cross linking and breakup of strands. Interruption of RNA and inhibition of topoisomerase II, an enzyme responsible for uncoiling and repairing damaged DNA, are significantly compromised. In vitro studies confirm the inhibition of inflammatory cells being B cells, T cells, and macrophages (Watson <i>et al.</i> , 1991).
sphingosine 1-phosphate receptor modulator	Fingolimod	Fingolimod might have a specific action on glial cells in reducing neuroinflammation (Kim <i>et al.</i> , 2011). Fingolimod was shown to reverse neuronal conduction impairment, and prevented further axonal degeneration. It was also able to control lymphocyte migration, and prevent further BBB dysfunction, even at lowered concentrations (Foster <i>et al.</i> , 2009).
Pyrimidine synthesis inhibitor	Teriflunomide	Teriflunomide, a metabolite of leflunomide, previously administered to patients with rheumatoid arthritis, preventing pyrimidine synthesis and T-lymphocyte proliferation by inhibiting mitochondrial enzyme dihydroorotate dehydrogenase (Killestein <i>et al.</i> , 2011).
Nrf2 activator	Dimethyl fumarate	Dimethyl fumarate, also referred to as BG-12, metabolized to monomethyl fumarate, activates the factor E2-related factor-2 pathway, which is responsible for protection against stress related oxidative neuronal death and damage to myelin (Kappos <i>et al.</i> , 2008).
Vitamins	Vit D	Vit D involves the regulation of expression of HLA (human leukocyte antigen), susceptibility allele, HLA-DRB1*1501, through the process of Vit D receptor (VDR)-binding (Ramagopalan <i>et al.</i> , 2010). It was further highlighted that functional interaction between HLADRB1* 1501 alleles and VDR SNPs (single nucleotide polymorphism), play important factors for MS susceptibility. Evidence also suggests that VDR rs2228570 genotypes, offer protective properties that are dependent on Vit D levels (Handel <i>et al.</i> , 2012).
Potassium-channel blockers for MS related fatigue	3-4-Aminopyridine (3-4-AP) and 4-aminopyridine (4AP) (Fampridine-SR)	Potassium-channel blockers such as 3-4-Aminopyridine (3-4-AP) and 4-aminopyridine (4AP) increase muscle tension by enhancing synaptic transmission (Mainero <i>et al.</i> , 2004), in which significant effects on fatigue and lower limb mobility were observed on patients who had taken the drug in comparison to the placebo (Rossini <i>et al.</i> , 2001). This up-regulation of primitive Na <sup>+</sup> channel isoforms such as Nav 1.2 in M.S may sustain neural conduction, however substantial expression of elevated Na <sup>+</sup> conductance's significantly compromise Na <sup>+</sup> /K <sup>+</sup> pump functioning, thereby elevating axonal degeneration in MS. Conduction failure is also exemplified by the increasing levels of K <sup>+</sup> channels expression (Smith, 2007).
Antiviral drug tricyclic amine for MS related fatigue	Amantadine	Amantadine is an antiviral drug of which the mechanism of action is still not fully understood. This tricyclic amine is believed to have an indirect dopaminomimetic effect. It is primarily prescribed as a first line treatment for MS-related fatigue, due to supporting evidence from randomized control trials showing a 20-40% success in combating MS related fatigue (Krupp <i>et al.</i> , 1995).
Anti-inflammatory agent for MS related fatigue	Aspirin	Aspirin irreversibly inhibits cyclooxygenase and prostaglandin E2 production, which is believed to affect the hypothalamic neuroendocrine response. It is possible that cytokine induced mechanisms are closely related to MS fatigue, hence aspirin or other non steroidal anti inflammatory agents are very useful in this regard (Wingerchuck <i>et al.</i> , 2005).

Amino acid for MS related fatigue      Acetyl-L-carnitine

Acetyl-L-carnitine is an amino acid which is naturally produced in the body. It affects the metabolism of energy, either by increasing levels of stimulating neurotransmitters in the CNS, or by exerting cholinomimetic activity on striatum and prefrontal areas (Kuratsune *et al.*, 2002).

---

## 2.11. Concluding Remarks

MS is fundamentally associated with disability if it is not treated according to the correct regimens available. Various biomarkers for neurodegeneration provide an indication for axonal degeneration and neural inflammation, thus playing a key role in the prevention of progression to advanced stages of disability. Through the highly technical available MRI scans, it is easy to diagnose in a patient who has CIS, and has experienced a single clinical attack. This allows early diagnoses and treatment, which was not possible decades ago, due to the lack of highly sophisticated technology. DMTs are used for long term management of patients suffering from multiple attacks and RRMS. The current intramuscular disease modifying treatment options available include glatiramer acetate, beta-interferon, natalizumab, and mitoxantrone. Other oral treatments include fingolimod and fampridine. The first line therapies constitute interferon- $\beta$  and glatiramer acetate, which have no major concerns in terms of safety profile, and possess good levels of efficacy. A second line therapy, such as natalizumab, has a greater level of side effects, but has better levels of efficacy. An oral formulation, fingolimod, was marketed on its success of phase 3 clinical programs, appearing relatively effective and safe.  $K^+$  channel-blocking agents, such as fampridine has been critically evaluated and implemented in an endeavor to improve motor neuron function and improve conduction amongst demyelinated axons. Anti-CD20 antibodies have become a topic of great interest in targeting B cells in MS patients. Many clinical trials undertaken over the past few years constitute a great area of concern as to whether B cell depletion considerably aids in therapeutic efficacy in MS. Dynamic research in this field consists of various strategies to improve diagnosis, as well as treatment formulations, to attain a uniquely novel, modified approach in the treatment of MS. This thesis therefore discusses the platform for successful oral protein delivery, of which the synthesis and characterization are elaborated in the following chapter.

## CHAPTER 3

### CRITICAL EVALUATION OF PHYSICOCHEMICAL AND PHYSICOMECHANICAL PROPERTIES OF NOVEL MICROGEL AND MICROPARTICULATE SYSTEMS

#### 3.1. Introduction

Interferon- $\beta$  (INF- $\beta$ ) is the most effective and widely used peptide for the treatment of MS (Jongen *et al.*, 2011). Interferons exist naturally as a globular protein comprising of 5 helices and a molecular weight ( $M_w$ ) of 20kDa (Arduini *et al.*, 1999). The fundamental effect of INF- $\beta$  in the treatment of MS is based on reducing the immune response that is directed against the myelin of the CNS, i.e. the fatty sheath that surrounds and protects nerve fibers. Damage of nerve fibers, resulting in demyelination, consequently causes nerve impulses to be slowed or halted, thus producing symptoms of MS. (Jongen *et al.*, 2011). Presently INF- $\beta$  dose is administered via the parenteral route. This injection therapy (subcutaneously or as intramuscular injection) of INF- $\beta$  has various disadvantages associated with challenges such as pain, allergic reactions, poor patient compliance and risk of infection (Chiu *et al.*, 2007). To overcome these challenges, researchers are investigating alternative routes of delivery such as oral or pulmonary which may increase patient compliance and relieve side-effects. (Shaji *et al.*, 2008).

The development of peptide and protein oral formulations has become an increasingly demanding form of drug delivery, and remains an attractive alternative to parenteral formulations. However, there are challenges associated with the oral route of peptide delivery which include presystemic enzymatic degradation of the peptide and its poor permeation through the intestinal membrane (Morishita and Peppas *et al.*, 2006). Absorption is the primary concern of the therapeutic in which the small intestine is the targeted area for this to occur, provided the dosage form reaches this site intact without being degraded. Translocation through the mucus layer is also an essential component, since this can severely hinder the absorption if the polymer system does not adhere to the mucus layer and release the peptide concurrently (Mustata *et al.*, 2005).

Research in this field aims to successfully deliver peptides orally and is currently under investigation. Many strategies such as the use of enteric-coated dry emulsions, microspheres, liposomes and nanoparticles for encapsulation of peptides are being critically evaluated (Shaji and Patole, 2008). According to Veronese and co-workers, PEGylation of proteins was

investigated to have many advantages such as, the stability of the protein by PEGylation increases the retention time, which is one of the most beneficial advantages for absorption through the GIT. The polymer, polyethylene-glycol (PEG), shields the protein surface from degrading agents by steric hindrance in addition; the increased size of conjugate is the basis of the decreased kidney clearance of PEGylated protein (Veronese *et al.*, 2005). Studies have proved that polymers containing carboxylic acid groups have the ability to protect peptides from protease enzymes such as trypsin and chymotrypsin. These polymers were proposed to react by binding of divalent cations (calcium and zinc) to exhibit their enzyme inhibitory effects (Sajesh *et al.*, 2006).

In this study a pH responsive copolymeric microgel of chitosan-poly(ethylene glycol) dimethacrylate-methacrylic acid (CHT-PEGDMA-MAA) and copolymeric microparticles trimethyl chitosan-poly(ethylene glycol) dimethacrylate-methacrylic acid (TMC-PEGDMA-MAA) were successfully prepared for loading of the respective proteins (insulin, INF- $\beta$  and EPO) in separate formulations. Using a Box-Behnken experimental design, a series of formulations were synthesized and evaluated using insulin as a prototype peptide for loading and release studies, due to the high cost implications associated with extensive experimental use of INF- $\beta$  and EPO. The optimized formulation was determined according to the responses from the design formulations on insulin and further evaluated for INF- $\beta$  and EPO. Part A of this thesis focuses on the results and discussion of TMC-PEGDMA-MAA and Part B on CHT-PEGDMA-MAA for all 3 protein-loaded therapeutics.

## **3.2. Materials and Methods**

### **3.2.1. Materials**

Chitosan (CHT) (medium  $M_w=450kDa$ ), PEG ( $M_w=4000g/mol$ ), MAA, methyl iodide, polyethylene glycol diacrylate (PEGDA), sulfonic acid, mucin (type 2) from porcine stomach and azobisisobutyronitrile (AIBN) were purchased from Sigma-Aldrich (St. Louis, MO, USA). Human insulin-R (Actrapid<sup>®</sup>, r-DNA origin) of 100I.U./mL was purchased from Eli Lilly and Company (USA). INF- $\beta$  1a (Rebif<sup>®</sup>), and *N*-methyl-2-pyrrolidone was procured from Merck (Pty) Ltd, Estate South, Modderfontein, Gauteng, South Africa, at reagent grade and was used without further purification. Erythropoietin beta was obtained from Roche Pharmaceuticals (Recormon<sup>®</sup>).

### 3.2.2. Synthesis of TMC for microparticulate formation

TMC was synthesized in a three stage procedure. In the first stage, 80mL of N-methyl pyrrolidone was heated at 60°C in a water bath incubating for 30 minutes, thereafter 2g of CHT, 4.8g of sodium iodide and 10mL of 20%w/v sodium hydroxide solution were added. This reaction mixture was incubated in a water bath for a further 30 minutes at 60°C. Methyl iodide (12mL) was then added immediately after extracting the reaction mixture from a water bath and then inserted into a direct reflux apparatus using a Liebig condenser, under constant magnetic stirring of 300rpm, for 90 minutes, also maintained at a temperature of 60°C. During this phase, a thick bright yellow homogenous mixture was formed, which was precipitated using 250mL of diethyl ether and 250mL ethanol. The precipitate was then filtered and dried under vacuum at 60±0.5°C for 48 hours. The dried polymer was finely reduced to grains and used for the next stage reaction. The second stage replicated the first, however, no CHT was used in the reaction, instead the polymer from the first stage was substituted. For the final stage of reaction where ion exchange of iodide ions for chloride ions occur, 80mL of 5%<sup>w/v</sup> sodium chloride was prepared and the ground polymer from the previous stage was added to the solution, with continuous magnetic stirring for 30 minutes. The reaction mixture was then added to 250mL of diethyl ether and 250mL of ethanol, as used previously, for precipitation. After filtering the mixture, the precipitate was once again dried in the vacuum oven for 48 hours at 60°C and stored for further use.

### 3.2.3. Synthesis of PEG(dimethacrylate) (PEGDMA)

High molecular weight PEG4000 and MAA were employed in a molar ratio of 1:2 for esterification reaction, using sulphonic acid as a catalyst and hydroquinine as a radical inhibitor, taken 1.5%<sup>w/w</sup> and 0.01%<sup>w/w</sup> respectively, of the monomers. The reaction was carried out in a round bottom flask, maintaining a temperature of 80-90°C throughout in an oil bath for a period of 7 hours at 40rpm under constant magnetic stirring. Water was removed during the reaction using toluene, and neutralized by 5%<sup>w/v</sup> sodium bicarbonate solution. Ice hexane was added to precipitate the polymer PEGDMA from the solution and dried at 60°C under vacuum conditions of 0.6kPa for 24 hour duration (Cruise *et al.*, 1998).

#### **3.2.4. Preparation of CHT-PEGDMA-MAA/TMC-PEGDMA-MAA copolymeric particles**

pH-sensitive copolymeric particles were prepared by free radical suspension polymerization technique. PEGDMA and MAA were taken in molar feed ratios of 1:2 while CHT/TMC and crosslinker PEGDA proportions were varied as 0.05-0.5g and 3-8%<sup>w/w</sup> (of monomer concentration), respectively as specified in the Box-Behnken design discussed in Chapter 3, section 3.2.5. Free radical initiator AIBN was used as 0.6%<sup>w/w</sup> of monomer concentration. The polymerization reaction was carried out at controlled temperature of 75°C, under constant purging of nitrogen gas, at 400rpm for 6 hours. The copolymeric particles thus prepared were repeatedly washed with deionized water to remove any unreacted monomers, and pH was adjusted to 7.4. The particles were finally lyophilized for further application (Tomar *et al.*, 2011). TMC and CHT were reacted in the same molar ratios in their respective design formulations for synthesis of separate microparticulate and microgel copolymers respectively.

#### **3.2.5. Box-Behnken Design of copolymeric particles**

For designing an optimum formulation, a 2-factor, Box-Behnken experimental design was generated using Minitab<sup>®</sup> V15 statistical software (Minitab<sup>®</sup> Inc., PA, USA). The variables employed in the experimental design were CHT/TMC concentration (0.05-0.5g/mL) and crosslinker amount (3-8%<sup>w/w</sup> of the monomer). The formulation variables were evaluated for their effect on drug release in gastric (pH 1.2), intestinal (pH 6.8) simulated USP buffer and average particle size. The series of independent variables and dependant responses are listed in Table 3.1. Fractional release responses were evaluated at a 2 hour time point in both pH mediums, with insulin taken as model peptide drug in the experimental design formulations. The design template generated 13 formulations for each copolymeric system of CHT-PEGDMA-MAA and TMC-PEGDMA-MAA as indicated in Tables 3.2 and 3.3, respectively.

**Table 3.1:** Variables in Box-Behnken design

<b>Independent Variables</b>	<b>Levels</b>		
	Low (-1)	Medium (0)	High (+1)
Crosslinker (%w/w of monomer)	3	5.5	8
CHT/TMC concentration (g/100mL)	0.05	0.25	0.5
<b>Dependent Variables</b>	<b>Gastric media</b>	<b>Intestinal media</b>	
Fractional drug release	Minimum	Maximum	
Particle size analysis	Minimum	Maximum	

**Table 3.2:** Formulations generated by Box-Behnken design for CHT-PEGDMA-MAA microgel formulations.

<b>Formulation</b>	<b>CHT* (g/100mL)</b>	<b>Crosslinker (%w/w of monomer)</b>
1	0.05	8
2	0.275	5.5
3	0.05	3
4	0.275	5.5
5	0.275	8
6	0.5	5.5
7	0.275	3
8	0.275	5.5
9	0.5	3
10	0.05	5.5
11	0.5	8
12	0.275	5.5
13	0.275	5.5

\*Chitosan

**Table 3.3:** Formulations generated by Box-Behnken design for TMC-PEGDMA-MAA microparticulate formulations.

<b>Formulation</b>	<b>TMC* (g/100mL)</b>	<b>Crosslinker (%w/w of monomer)</b>
1	0.5	5.5
2	0.275	3
3	0.5	8
4	0.275	5.5
5	0.275	5.5
6	0.275	5.5
7	0.5	3
8	0.05	8
9	0.275	5.5
10	0.05	5.5
11	0.275	5.5
12	0.275	8
13	0.05	3

\*Trimethylchitosan

### **3.2.6. Attenuated Total Reflectance-Fourier Transform Infrared (ATR-FTIR) spectroscopy**

ATR-FTIR spectra were recorded for monomers, participating polymers and the resultant copolymeric systems for characteristic crosslinking determination using a Perkin Elmer Spectrum 2000 FTIR spectrometer, employing a single-reflection diamond MIRTGS detector, (PerkinElmer Spectrum 100, Llantrisant, Wales, UK). All samples were analyzed by universal ATR polarization accessory for the FTIR spectrum series at a resolution of  $4\text{cm}^{-1}$ . Samples were placed on a diamond crystal running each sample 100 times in order to reduce the signal to noise ratio to a minimum of 10, in the range of  $4000\text{-}600\text{cm}^{-1}$  using a constant pressure of 120psi.

### **3.2.7. Particle size and zeta potential analysis of copolymeric systems**

All Box-Behnken copolymeric formulations, after lyophilization, were separately added (5mg) to 12mL gastric and intestinal USP buffer of pH 1.2 and 6.8, respectively. For a maximum response to different pH conditions, the copolymeric microparticles were left in the respective medium for 2 hours. The particles were thoroughly dispersed before adding a 2mL of the sample into a cuvette, for zeta size and zeta potential analysis, using a ZetaSizer Nano ZS instrument (Malvern Instruments Ltd. UK).

### 3.2.8. Mucoadhesion studies

Mucoadhesion studies were performed on all Box-Behnken design formulations to deduce the effect of the change in variable concentration on the degree of mucoadhesion of the polymer. For this study a 0.1%<sup>w/v</sup> mucin solution prepared in USP intestinal fluid (pH 6.8) was incubated with copolymeric particles in an orbital shaker maintained at 37°C and 50rpm. Concentration of free mucin in the solution, after 6 hour duration, was determined by a UV spectrophotometer, at wavelength 201nm (IMPLEN Nanophotometer<sup>TM</sup>, Implen GmbH, München Germany), using a 10 times dilution factor of pathlength 0.1mm. The difference in the concentration of the mucin solution before and after incubation, was the indication of the amount crosslinked with the copolymeric particles as seen in Equation 3.1, indicating the interaction between particles and mucin (Ping *et al.*, 1998).

$$\% \text{ mucoadhesion} = \frac{\text{Concentration of mucin before adding polymer} - \text{concentration of mucin after adding polymer}}{\text{Concentration of mucin before adding polymer}} \times 100$$

(Equation 3.1)

### 3.2.9. Porositometric analysis

The lyophilized copolymeric systems were kept in gastric and intestinal USP buffers for 2 hours, for the polymer to respond to the respective pH, thereafter, lyophilizing once again to remove moisture from the polymer. For porositometric analysis, 4mm diameter tablets were prepared taking 120mg of the lyophilized samples of the respective pH medium and compressing at 0.6MPa using a tablet compressor. A Porositometric Analyzer (Micrometritics ASAP 2020, Norcross, GA, USA), was employed, which encompassed 2 stages of analysis, first following a degassing stage, thereafter an absorption and desorption cumulative phase for accurate analysis of surface area, pore volume, pore size and various other isotherms were analyzed using BJH and BET profiles. The evacuation and heating phase parameters are listed in Table 3.4. The degassing procedure is essential for removing impurities and excess moisture in the sample, and was undertaken in a sample tube (I.D=9.53 mm), inserting a glass filler rod in the tube, to increase the capacity of the vacuum pressure, and reducing the free volume in the tube. The heating and evacuation phases of the degassing procedure were completed in 12 hours, and the analysis step was carried out thereafter.

The enthalpy of absorption, from a linear form of a monolayer capacity determination, using the BET gas absorption method, can be related to Equation 3.2 for accurate determination of surface area of the tablet.

$$p/n^a (p-p) = 1/n_m^a \times C + (C-1)p/n_m^a Cp^0 \quad (\text{Equation 3.2})$$

Where  $n^a$  is the amount of nitrogen gas absorbed at the relative pressure  $P/P^0$  and  $n_m^a$  is the monolayer capacity, and  $C$  was directly related exponentially to enthalpy in the first absorption layer. Applying values from the molecular crosssectional area, Equations 3.3 and 3.4 were implemented for BET surface area determination.

$$A_s(\text{BET}) = n_m^a \times L \times a_m \quad (\text{Equation 3.3})$$

$$a_s(\text{BET}) = A_s(\text{BET})/m \quad (\text{Equation 3.4})$$

Where  $A_s$  (BET) and  $a_s$  (BET) are the total and specific surface areas, respectively, of the adsorbent (of mass  $m$ ) and  $L$  is the Avogadro constant.

**Table 3.4:** Evacuation and Heating Phase parameters for porositometric analysis

Parameter	Rate/target
<b>Evacuation phase</b>	
Temperature ramp rate	10 °C/min
Target temperature	40 °C
Evacuation rate	50.0 mmHg/s
Unrestricted evacuation from	30 mmHg/s
Vacuum set point	500 µmHg
Evacuation time	60 min
<b>Heating phase</b>	
Temperature ramp rate	10 °C/min
Hold temperature	30 °C

### **3.2.10. Morphological Characteristics of the Particles using Scanning Electron Microscopy (SEM)**

The lyophilized copolymeric particles were dispersed in gastric and intestinal USP buffers for 2 hours, and lyophilized once again for determining the morphological characteristics of the particles at the respective pH. The samples were sputter coated using gold compound, being mounted on an aluminum spud, using an EPI sputter coater (SPI Module TM sputter-coater and control unit, West Chester, Pennsylvania USA). After coating the samples for 60 seconds, under helium gas conditions, the samples were analyzed using a FEI ESEM Quanta 400F (FEI™, Hillsboro, OR, USA) electron microscope, employing an electron acceleration charge of 20kV, to produce high resolution images of the microgel networks/particles.

### **3.2.11. Thermal Properties of the Monomers, Polymers and Copolymeric Systems using Differential Scanning Calorimetry (DSC) analysis**

The thermal properties of the monomers, polymers and copolymeric systems were evaluated on the basis of their characteristic melting points and crystallization behavior using a Mettler Toledo DSC-1 STAR<sup>®</sup> system. Samples of 15mg were accurately weighed and sealed in a 40 $\mu$ L aluminum crucible pan, in which a tiny hole of 0.2mm was punctured on the lid of the pan, before sealing the contents. All samples were run twice, the first for removing extra water in the polymer at a temperature range of 25-110 $^{\circ}$ C at 10 $^{\circ}$ C/min, and the second run from 25 $^{\circ}$ C-250 $^{\circ}$ C at 10 $^{\circ}$ C/min, to achieve optimum results with least deviations (Guinesi *et al.*, 2006). Inert atmospheric conditions were maintained throughout the analysis with a flow rate of 50mL/min of N<sub>2</sub> gas.

### **3.2.12. Thermogravimetric analysis (TGA)**

A TGA 4000 thermogravimetric analyzer (PerkinElmer Inc, Massachusetts, USA), set from 50-500 $^{\circ}$ C, at a ramping rate of 10 $^{\circ}$ Cmin<sup>-1</sup>, under inert nitrogen conditions, was used to analyze polymers and copolymeric systems for specific thermal degradation. 15mg of polymer was loaded in a ceramic pan, generating thermograms and their 1<sup>st</sup> derivatives, to determine the amount of moisture liberated from the sample and the percentage of degradation of the polymer.

### 3.2.13. Matrix hardness (MH) and Matrix resilience (MR)

After lyophilizing the polymer, a cylindrical tablet with a 4mm diameter having a mass of 120mg was compressed at 0.6MPa, for evaluation of the mechanical properties of the polymeric tablet. A well calibrated textual analyzer (TA.XT*plus*, Stable Microsystems, Surrey, UK), under standard conditions of 25°C, 1atm pressure, using a steel cylindrical probe of 50mm diameter for MR, and a steel flat tip probe of diameter 2mm for MH was employed respectively. The force-time graph obtained from MR evaluations yielded the percentage MR of the polymer. The force-distance graph obtained from MH evaluations yielded the maximum force required for deformation of the tablet. Table 3.5 indicates the various parameters for MR and MH evaluations. A pre-test speed, test speed and post test speed of 1mm/s, 0.5mm/s and 10mm/s were employed respectively. A trigger force of 0.05N with a load cell weight of 5Kg was implemented for all MH and MR evaluations.

**Table 3.5:** Parameter settings for determining MR and MH

<b>Parameters</b>	<b>MR<sup>a</sup>(%)</b>	<b>MH<sup>b</sup>(N/mm)</b>
Pre-test speed	1 mm/s	1mm/s
Test speed	0.5 mm/s	0.5mm/s
Post-test speed	10 mm/s	10mm/s
Trigger type	Auto	Auto
Trigger force	0.05 N	0.05 N
Load cell	5 Kg	5 Kg
Compression strain	Variable	N/A
Target mode	Strain (5%)	Distance

<sup>a</sup>Matrix resilience; <sup>b</sup>Matrix Hardness

### 3.2.14. Rheological evaluation

The viscoelastic behavior of the copolymeric particles was determined using a 0.1%<sup>w/v</sup> formulation in gastric (pH1.2) and intestinal (pH 6.8) fluid respectively incubated for 2 hour duration. The strains employed were in the linear viscoelastic (LVE) region, where G' (dynamic storage modulus) and G'' (loss modulus) which were evaluated using a Modular Advanced Rheometer (ThermoHaake MARS Modular Advanced Rheometer, Thermo Electron, Karlsruhe, Germany), comprising of a C35/1<sup>+</sup> Ti sensor. Rheological measurements were employed under

parameters as shown in Table 3.6. A sample volume of 0.5mL was analyzed over a fine range of 0-1.0 Hz, falling within the shear independent plateau of the strain amplitude sweep test.

**Table 3.6:** Parameters employed for rheological evaluation

<b>Parameters</b>	<b>Value</b>
Cone and plate gap	0.0051m
Driver version	0.29
Inertia	1.721 X 10 <sup>-6</sup> kg m <sup>2</sup>
A-factor	89051.00 Pa
M-factor	57.010 rad/s
Temperature	37 °C
Damping	30.00

The study of Dynamic oscillation involves the aspect of complex modulus ( $G^*$ ), indicating the total resistance in relation to the applied strain, resulting from the amplitude of stress ( $T_\theta$ ) and deformation ( $y_\theta$ ), as depicted in Equation 3.5.

$$G^* = T_\theta / y_\theta \quad (\text{Equation 3.5})$$

After subjecting a material to sinusoidal oscillation, the resulting effects of elastic energy (storage modulus or  $G'$ ), viscous energy (loss modulus or  $G''$ ) or a resultant of both properties can be observed.  $G'$  relates to the stress energy, conserved in a transient mode, for the duration of oscillatory evaluation, upon completion of testing, possessing the ability of recovery of said energy. Conversely,  $G''$  is the amount of energy used to induce a flow of the material, thereby impacting on the irreversible degree of deformation and heat produced on the sample (Schramm *et al.*, 2004; Ramazani-Harandi *et al.*, 2006).

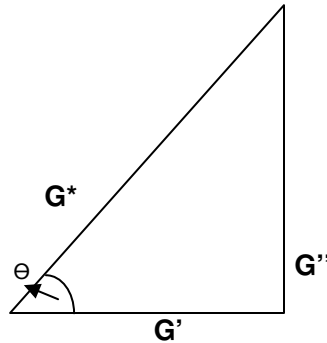


**Figure 3.1:** Phase shift illustrated using the Theorem of Pythagoras in relation to complex modulus ( $G^*$ ), storage modulus ( $G'$ ) and loss modulus ( $G''$ ).

$$G' = G^* \cos \theta \quad (\text{Equation 3.6})$$

$$G'' = G^* \sin \theta \quad (\text{Equation 3.7})$$

Both these energy transitional states are dependent upon phase shift and  $G^*$ . Implementing the Theorem of Pythagoras (Figure 3.1), storage and loss moduli can be expressed in Equation 3.6 and 3.7 (Schramm *et al.*, 2004).

### 3.2.15. X-Ray Diffraction (XRD) analysis

Individual polymers and copolymeric systems were analyzed using a Rigaku MiniFlex600 Benchtop X-ray Diffractometer (Rigaku Corporation, Tokyo, Japan), using a 600W (40Kv-15mA) X-ray generator, a counter monochromator to cut X-rays besides Cu  $K\alpha$  X-rays, implementing a D/tex Ultra high speed 1D detector. Samples were evaluated on the basis of operating the software Rigaku MiniFlex Guidance version 1.2.0, and analyzed on Rigaku PDXL Basis software, for calculations of degree of crystallinity in each sample. Parameters for the measurement of samples were selected as a divergence slit (DS) of  $1.25^\circ$ , 0.3mm receiving slit (RS), Goniometer radius of 150mm and a Scattering slit (SS) of  $1.25^\circ$ . Samples were scanned at  $0-100^\circ/\text{min}$ , using an angle diffraction range of  $3^\circ-60^\circ 2\theta$ .

### **3.2.16. Nuclear Magnetic Resonance (NMR) Evaluation**

Solid state NMR (ssNMR)-1D<sup>13</sup>C cross-polarization (CP) solid-state NMR magic angle spinning (MAS) spectra was collected on a 600MHz Avance III Bruker spectrometer (Bruker BioSpin, Germany) with spinal 64 decoupling equipped with a 4mm MAS probe, calibrated with glycine, with a spin rate of 10kHz. The powder sample was packed into 4mm Bruker MAS rotor. The MAS spinning rate was maintained at 10kHz and all samples were run for a 4.5 hour duration. Functional groups and the transition of signal peaks were analyzed, resulting in a proposed structural design of the crosslinked copolymeric formulation. This technique was further used to confirm the crosslinking occurrence, thereby confirming successful organic synthesis of the copolymer.

## **3.3. Results and Discussion**

### **3.3.1 PART A: Evaluation of TMC-PEGDMA-MAA copolymeric microparticulate system**

#### **3.3.1.1. Box-Behnken optimization evaluation of the copolymeric microparticulate system**

The design generated responses from the results of each formulation for determining the greatest correlation for the optimized formulation. Residuals were used for evaluating differences in observed values and predicted responses, thereby correlating results according to the design desired outcome (Stewardson and Whitfield, 2004).

The ideal histograms represent bell shaped curves for the responses (Stewardson and Whitfield, 2004), however slight variations are evident in the responses obtained due to the unique behavior of the polymers in different pH states. Variations of the proposed behavior of the polymer can be attributed to alterations in particle sizes and % drug-loading as well as release rates in different pH states, in some instances, releasing greater in gastric than in intestinal medium at the 2 hour duration, due to the significant constriction of the particles in gastric medium and their release of insulin while undergoing this change. Figure 3.2 represents residual and surface plots of the formulations, with regard to average particle size, fractional release at 2 hours in gastric medium and fractional release at 2 hours in intestinal medium.

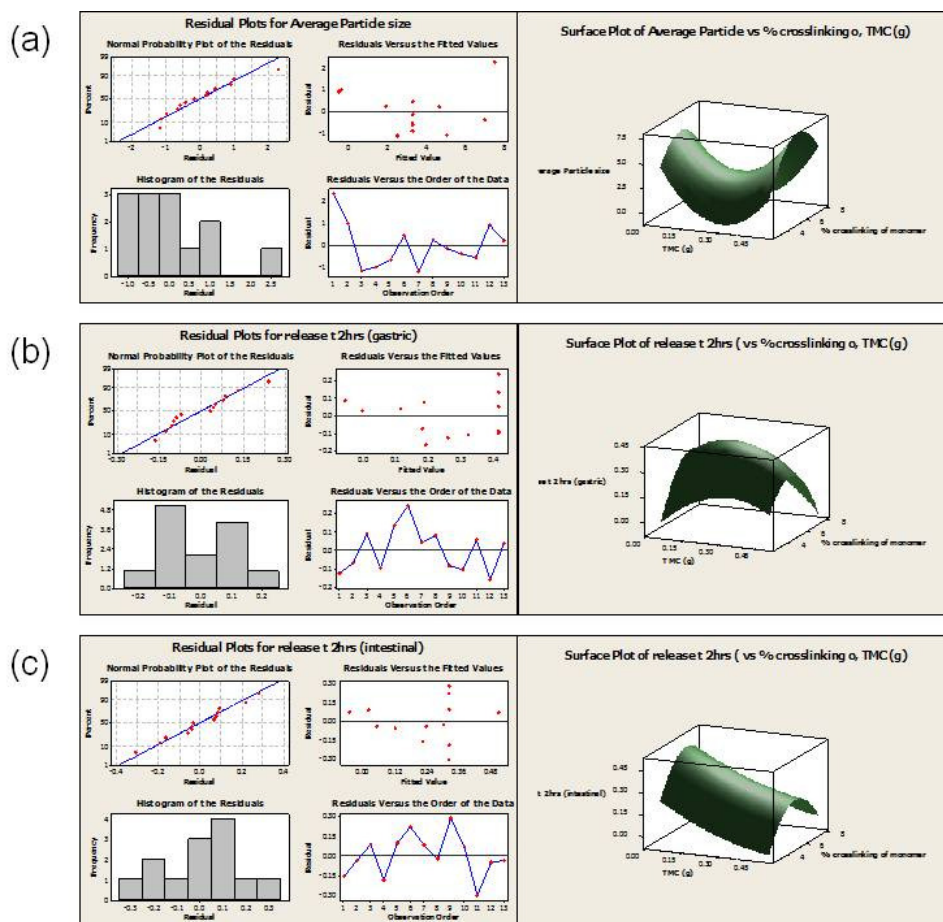


**Figure 3.2:** Residual and surface plots of (a) average particle size, (b) fractional release in gastric medium at 2 hours and (c) fractional release in intestinal medium at 2 hours.

MINITAB<sup>®</sup>, V15 (Minitab<sup>®</sup>, PA, USA) statistical software, for producing optimal responses for particle size and drug release behavior, using a multiparticulate system as seen in Figure 3.2, where high, low and optimal factors were generated yielding a desirability value of 1, to produce optimal factor levels for most desirable response behavior as outlined in Table 3.1. This evaluation yielded responses for the optimized formulation, inputting average particle size, fractional release in gastric and intestinal conditions at 2 hours into the Box-Behnken design, for an optimum formulation of desirability of 93.01%. This formulation comprised of having concentrations of 0.5g/100mL of TMC composition, and 3% of crosslinker. Figure 3.3 indicates the program specifications with graphs generated for the optimized formulation, taking into consideration the average minimum size of the particles, possessing greater release rates in intestinal conditions and minimum release rates in gastric conditions which is further discussed in subsequent sections.

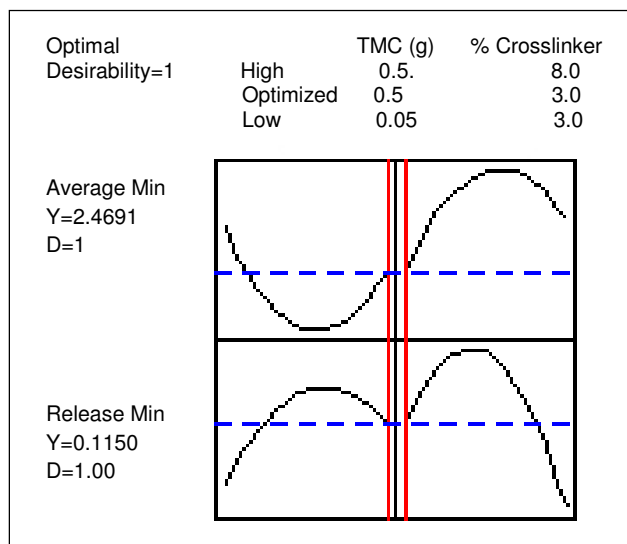


**Figure 3.3:** Optimization plot for the response optimization of the copolymeric formulation.

### 3.3.1.2. ATR-FTIR Spectroscopy of monomers and copolymeric microgel formulation

FTIR spectra of TMC, PEGDMA, MAA, CHT and copolymeric particles TMC-PEGDMA-MAA is shown in Figure 3.4. MAA displayed peaks for carbonyl groups and vinyl groups at  $1635\text{cm}^{-1}$  and  $1697\text{cm}^{-1}$  respectively. A wide stretch from  $3000\text{--}3450\text{cm}^{-1}$  corresponds to hydroxyl groups of carboxylic acid in MAA (Kumar *et al.*, 2006). In TMC spectra the two peaks observed at  $1475\text{cm}^{-1}$  and  $1559\text{cm}^{-1}$ , which are not found in CHT, and absence of peak at  $1577\text{cm}^{-1}$ , which is characteristic of CHT, confirms the successful synthesis of TMC from CHT (Mourya *et al.*, 2009). Asymmetrical angular deformation with reference to methyl groups of C-H bonds, characterized by peak at  $1475\text{cm}^{-1}$ , indicates that these methyl groups are covalently bonded to the amino groups on the chitosan structure, since this peak does not exist for chitosan polymer. N-methylation gives a peak at  $1555\text{cm}^{-1}$ , due to angular deformation of N-H bond as well as bending of the amino groups. Peaks in the range of  $1415\text{--}1430\text{cm}^{-1}$  are characteristic of N-CH<sub>3</sub> absorption (Domard, A., *et al.*, 1986). PEGDMA<sub>4000</sub>, gave characteristic spectra that shows broad band at  $1639\text{cm}^{-1}$  characteristic of an interaction between carbonyl and vinyl groups. CH stretching and bending in the polymer is clearly identified by peaks at  $2882\text{cm}^{-1}$  and  $1466\text{cm}^{-1}$  (Tomar *et al.*, 2011). TMC-PEGDMA-MAA spectra shows a peak for the strong interactive carboxylic acid groups at  $1654\text{cm}^{-1}$ , supporting the strong hydrophilic, pH sensitive nature of the polymer. The peak at  $1545\text{cm}^{-1}$  also indicates the presence of N-H bending, due to the strong interaction of methyl groups with amino groups. The characteristic peak of TMC at  $1475\text{cm}^{-1}$  has shifted to  $1466\text{cm}^{-1}$ , indicating the crosslinking in the copolymer.

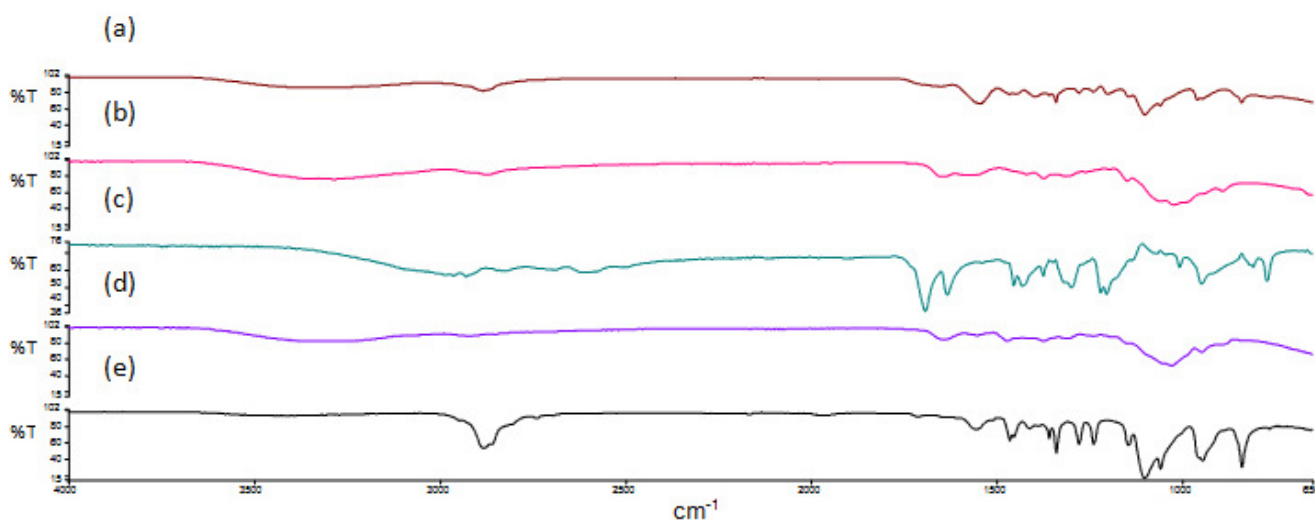


**Figure 3.4:** FTIR spectra of (a) TMC-PEGDMA-MAA, (b) CHT, (c) MAA, (d) TMC, (e) PEGDMA.

### 3.3.1.3 Particle size and zeta potential analysis

Particle size is an important factor for drug-loading efficiency and targeted drug delivery to the small intestine. Particle size was evaluated for all 13 experimental design formulations, with varying concentrations of TMC and crosslinker. The formulations were evaluated after standing in respective pH conditions, gastric and intestinal USP buffers, to exemplify the pH responsive nature of the particles, and the size transition the particles undergo in the respective mediums. The particles were not filtered during particle size evaluation, as this would have significantly altered the size. Results presented in Table 3.7 indicate an increase in particle size as the concentration of TMC and crosslinker increased. A lower concentration of crosslinker, such as 3%, noticeably yielded a lower particle size at both pH values as seen in formulations 1, 3 and 7. Theoretically, at low pH values, carboxylic groups interact with ether functional groups of PEG, therefore forming strong hydrogen bonding between the particles that would result in smaller particles at gastric pH. After evaluation, it was distinctly clear that larger particles were obtained at low pH of gastric medium in comparison to intestinal medium (pH 6.8). This is attributed to the aggregation properties of the particles at low pH resulting in particles clumping together forming larger masses and therefore displaying greater particle size.

Much to the contrary, lower particle size was observed in intestinal medium, on account of particles being dispersed as more or less distinct identities because of the breaking of hydrogen bonding and ionization of carboxylic groups. The polydispersity index (PDI) of the particles in

gastric medium displayed much greater values, than in intestinal medium as seen in Table 3.7. The optimal PDI values, indicating stability and uniformity of the particles, are in ranges of less than 0.5. Therefore, a clear analysis reflects the instability of particles in gastric medium due to clumping, and greater uniformity of particles in intestinal conditions. This confirms the particle aggregation in gastric pH, and its dispersion in intestinal pH, since particles will display less order of arrangement in their aggregation state, and will remain much more uniform in their dispersed state (Tomar *et al.*, 2011). As shown in Table 3.7, the Box Behnken design generated formulations 4, 5, 6, 9 and 11 of the same composition and could therefore relate to the reproducibility of the formulation responses. Inputting responses from the design formulations, the Box-Behnken design identified Formulation 7 (F7) with the ideal range of properties for an optimum copolymeric system based on particle size and drug release behavior. The zeta potential of the optimized formulation was recorded to be 9.58 and 21.5 in gastric and intestinal conditions, respectively. These values correlate with the pH sensitive nature of the particles, since the electro repulsive charges on the particles are much greater in basic medium due to their disruption of hydrogen bonding and ionization of carboxylic groups, which opposes its characteristic nature in gastric medium by aggregation of particles due to interparticle hydrogen bonding.

**Table 3.7:** Experimental design formulation analysis of average particle size according to specifications of the design in gastric and intestinal fluid

Formulation	TMC* (g/100mL)	Crosslinker (%w/w of momomer)	Av size ( $\mu$ m) (pH 1.2)	PDI**	Av size ( $\mu$ m) (pH 6.8)	PDI**
1	0.5	5.5	4.2	0.41	2.57	0.25
2	0.275	3	2.2	0.67	1.8	0.27
3	0.5	8	6.2	0.72	2.4	0.35
4	0.275	5.5	5.7	0.52	3.7	0.42
5	0.275	5.5	5.4	0.68	2.6	0.36
6	0.275	5.5	5.2	0.49	2.4	0.53
7	0.5	3	4.7	0.68	1.2	0.61
8	0.05	8	6.3	0.77	2.9	0.52
9	0.275	5.5	6.6	0.62	3.3	0.41
10	0.05	5.5	6.6	0.45	2.3	0.62
11	0.275	5.5	5.2	0.56	3.0	0.38
12	0.275	8	6.7	0.69	3.4	0.46
13	0.05	3	3.6	0.51	2.8	0.63

\*Trimethylchitosan; \*\*Polydispersity index, Ave= average

### 3.3.1.4. Porosity analysis of optimized copolymeric delivery system

The optimized copolymeric particles dispersed in different pH medium were lyophilized and then compressed into tablets, were subjected to porosimetric evaluation. Brunauer–Emmett–Teller (BET) adsorption and desorption profiles were evaluated for both conditions, in an endeavor to relate drug release profiles and SEM images to the porosity of the samples. Analysis of pore size characteristics determined by a technique of physical gas adsorption, which was employed over a wide range of relative pressures ( $P/P_0$ ) and Nitrogen adsorption isotherms, provided significant insight regarding pore size distribution. The sample demonstrated a type IV isotherm in basic medium with a type H1 hysteresis loop as depicted in Figure 3.5. Figure 3.5 illustrates the different types of isotherms and hysteresis loops that are produced according to differences in the amount of gas adsorbed onto a particular material in relation to its relative pressure. From the hysteresis loop, a number of primary magnetic properties of a material can be determined, including - retentivity, residual magnetism or residual flux, coercive force, permeability and reluctance (Sing *et al.*, 1985).

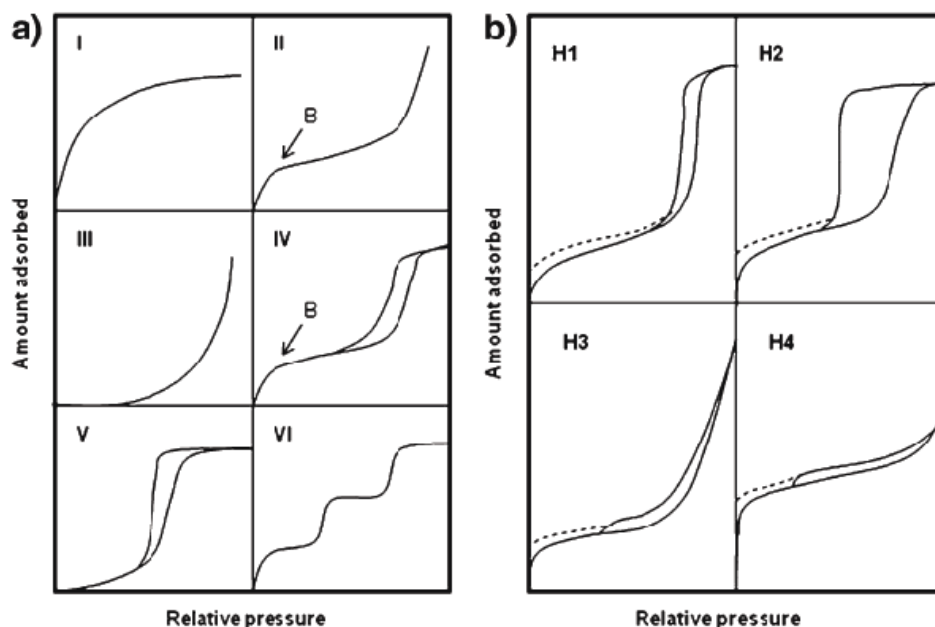


**Figure 3.5:** Schematic depicting (a) the types of isotherms at different relative pressure, (b) the types of hysteresis loops according to the IUPAC classification system (adapted from Sing *et al.*, 1985).

The type IV adsorption isotherm explains formation of a multilayer material. The saturation level reaches a pressure below the saturation vapor pressure. This can be explained on the basis of

a possibility of gases getting condensed in the tiny capillary pores of adsorbent at pressure below the saturation pressure (PS) of the gas. According to a type II and type IV isotherm, the point marked 'B' depicted on Figure. 3.5a isotherms, refers to the point at which adsorption was complete and was visible at the beginning of the almost linear mid-section of the isotherm. Table 3.8 indicates the differences in properties of the delivery system with a change in pH conditions. It is evident that the polymeric delivery system possesses greater pore size and surface area in intestinal medium, as seen in Table 3.8. The isotherm for the sample tablets in gastric medium did not produced any results for pore volume and pore size, due to the pores being too small to measure, due to the strong hydrogen bonds and aggregation behavior of the polymer in gastric pH. Isotherms recorded for copolymeric system, depicted in Fig. 3.6b, confirms the swelling ability in intestinal medium whereas, lower values observed in gastric medium (Figure 3.6a), confirms its shrinkage/aggregation in such medium.

**Table 3.8:** Porosity analysis of optimized copolymeric delivery system at different pH ranges of gastric and intestinal medium

<b>Parameter</b>	<b>Gastric pH (1.2)</b>	<b>Intestinal pH (6.8)</b>
<b>Surface Area</b>		
Single point surface area (m <sup>2</sup> /g)	0.1913	0.9952
BET Surface Area (m <sup>2</sup> /g)	0.2092	0.1172
BJH Adsorption cumulative surface area of pores between 17.000 Å and 3000.000 Å diameter (m <sup>2</sup> /g)	-	3.986
BJH Desorption cumulative surface area of pores between 17.000 Å and 3000.000 Å diameter (m <sup>2</sup> /g)	-	4.4645
<b>Pore Volume</b>		
Single point adsorption total pore volume of pores less than 796.892 Å diameter (cm <sup>3</sup> /g)	-	0.004900
BJH Adsorption cumulative volume of pores between 17.000 Å and 3000.000 Å diameter (cm <sup>3</sup> /g)	-	0.005245
BJH Desorption cumulative volume of pores between 17.000 Å and 3000.000 Å diameter (cm <sup>3</sup> /g)	-	0.004725
<b>Pore Size</b>		
Adsorption average pore width (4V/A by BET) (Å)	-	1672.1311
BJH Adsorption average pore diameter (4V/A) (Å)	-	52.632
BJH Desorption average pore diameter (4V/A) (Å)	-	42.334

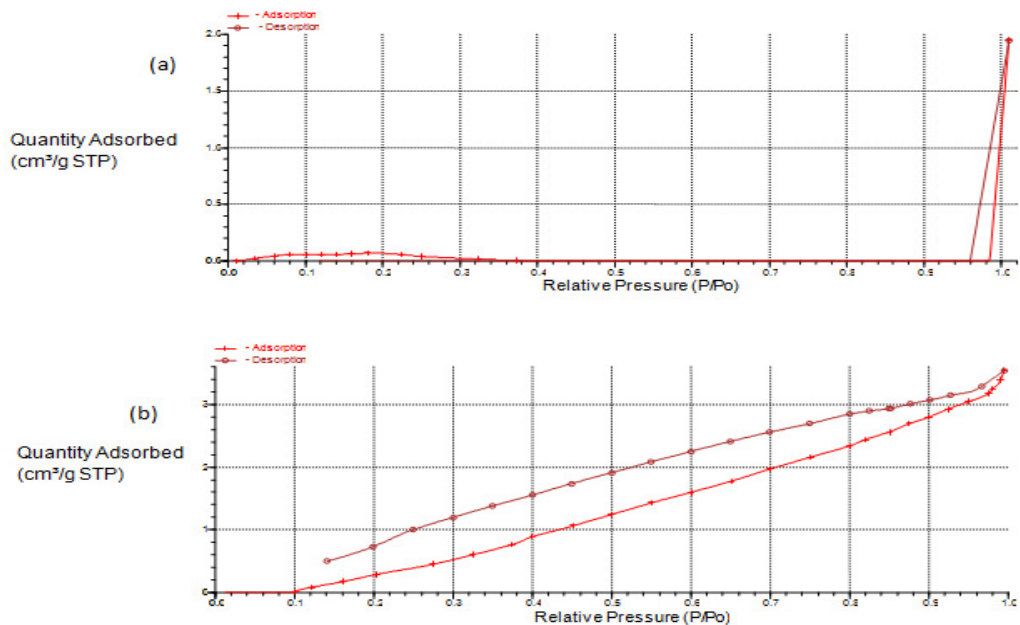


**Figure 3.6:** Isotherm Linear plots of microparticles in (a) gastric medium and (b) intestinal medium.

### 3.3.1.5. Morphological characteristic determination using SEM techniques

The morphological characteristics of lyophilized copolymeric particles were analyzed at pH 1.2 and 6.8 as seen in Figure 3.7a and 3.7b, respectively. At pH 1.2, the particles appeared to be tightly clumped in large masses of oval to longitudinal shape with little or no pores visible between the particles. This clumping of the copolymeric particles is due to the strong hydrogen bonds formed between carboxylic acid groups of MAA with etheric groups of PEG at gastric pH (Sajesh *et al.*, 2006). A reverse observation was made at pH 6.8 (Fig. 3.7b), where particles practically explode in their morphology, showing massive swelling and dispersion due to the ionization of carboxylic groups and disruption of hydrogen bonding between the particles. These studies thus indicate the spontaneous pH sensitive nature of the copolymeric system and hydrophilic properties. The morphology of the particles further support results obtained from porosity analysis and is highly correlated to drug release studies which follow through subsequent chapter.

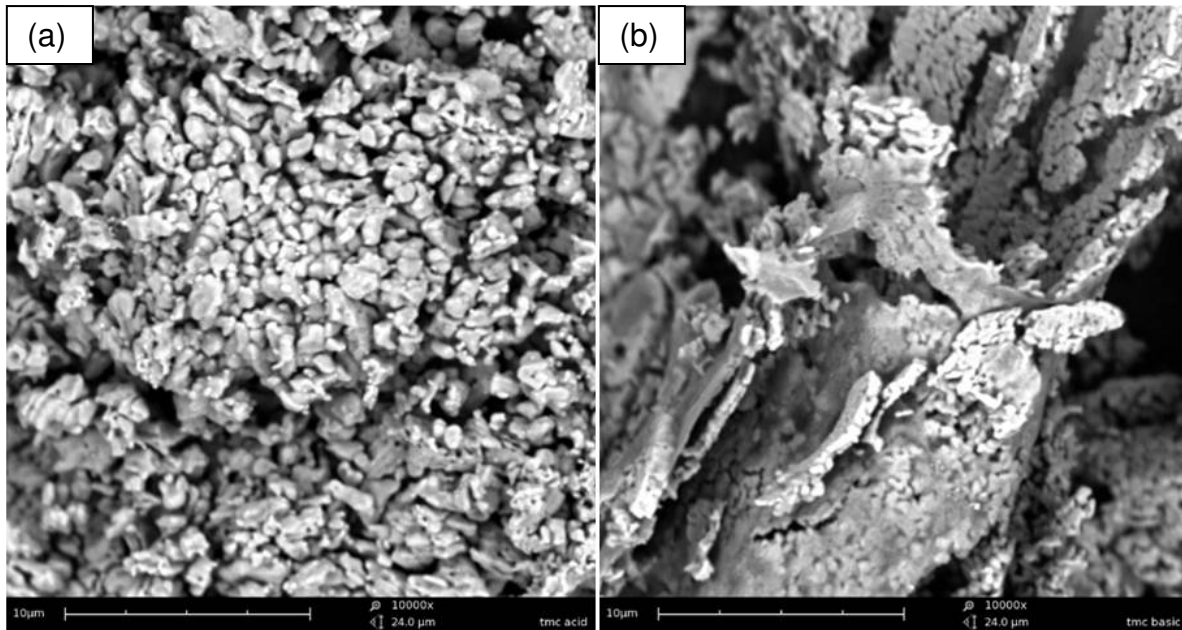


**Figure 3.7:** Scanning electron micrographs of copolymeric particles at 10 000X magnification (a) in gastric medium (pH 1.2) (b) in intestinal medium (pH 6.8).

### **3.3.1.6. Mucoadhesive properties of optimized copolymeric delivery system**

Mucoadhesive properties of the formulation designs were evaluated to screen for their ability to adhere to the intestinal surface lining to increase the retention time and enhance the absorption of the peptide through the mucosal lining of the small intestine. Figure 3.8 summarizes the mucoadhesion results of all the 13 formulations, yielding average percentage crosslinking values of the formulation to mucus solution. It was clearly evident that as the concentration of TMC increased, mucoadhesion was proportionally elevated, allowing greater interaction between the copolymeric particles and mucous. Results obtained also demonstrate the inverse relationship between the percentage of crosslinker used and the amount of mucoadhesion to the polymer. At high concentrations of crosslinker, the bonds in the copolymeric system were too strong for the polymer to expand and share charges with the mucous solution, however, at low concentrations of crosslinking agent, the polymer was able to share bond charges and adhere to the surrounding mucous solution.

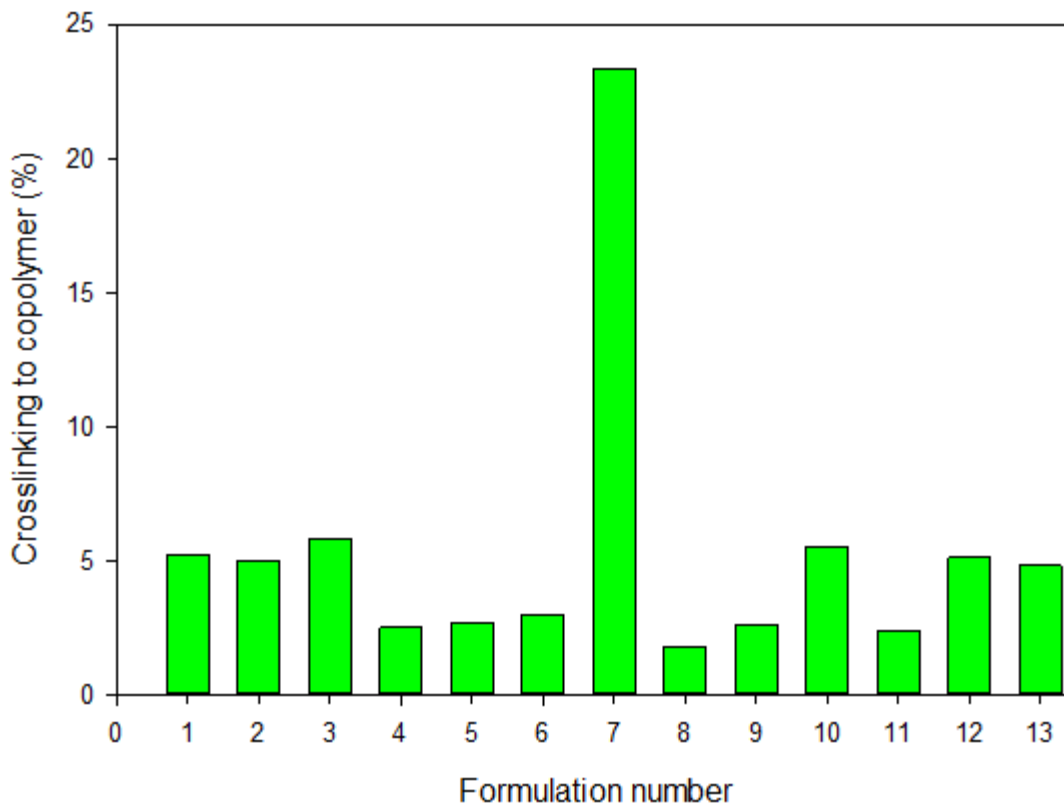
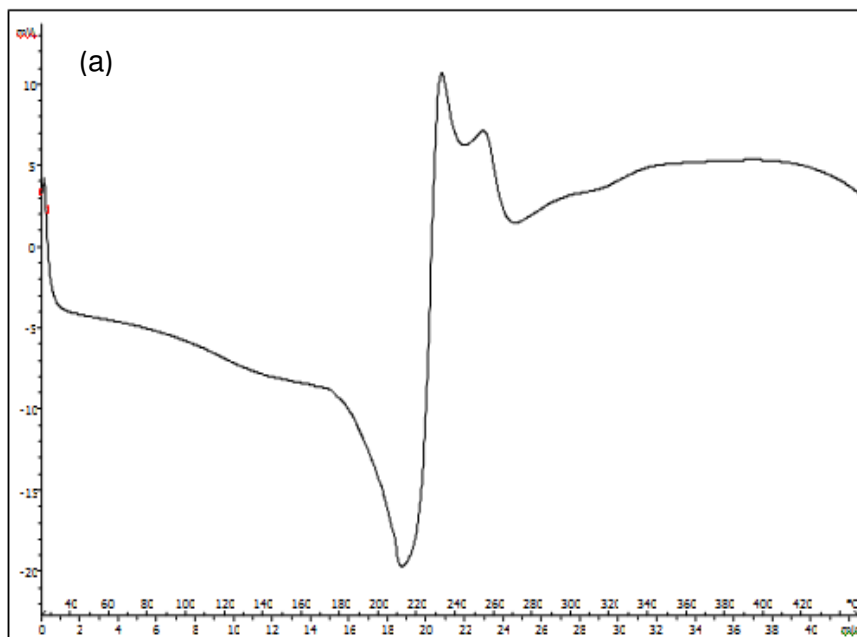


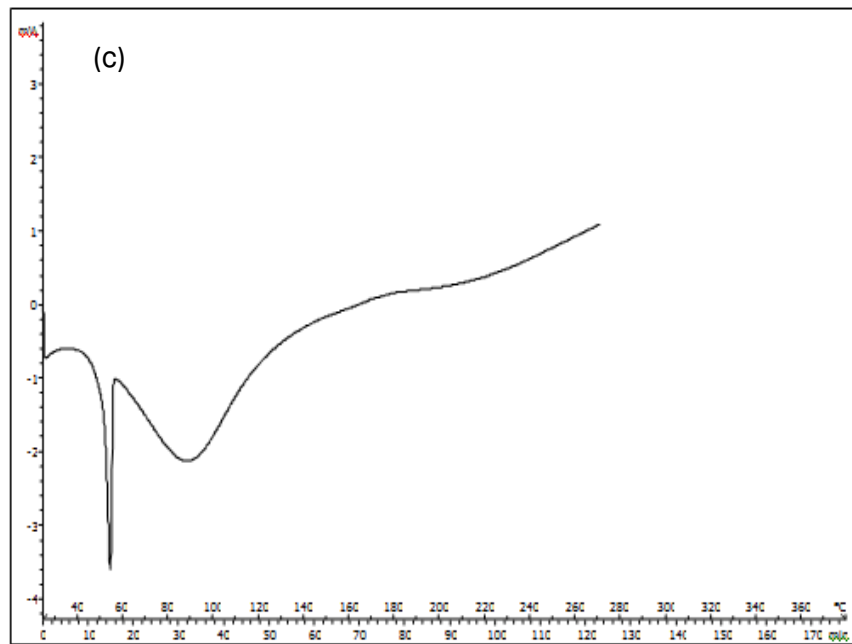
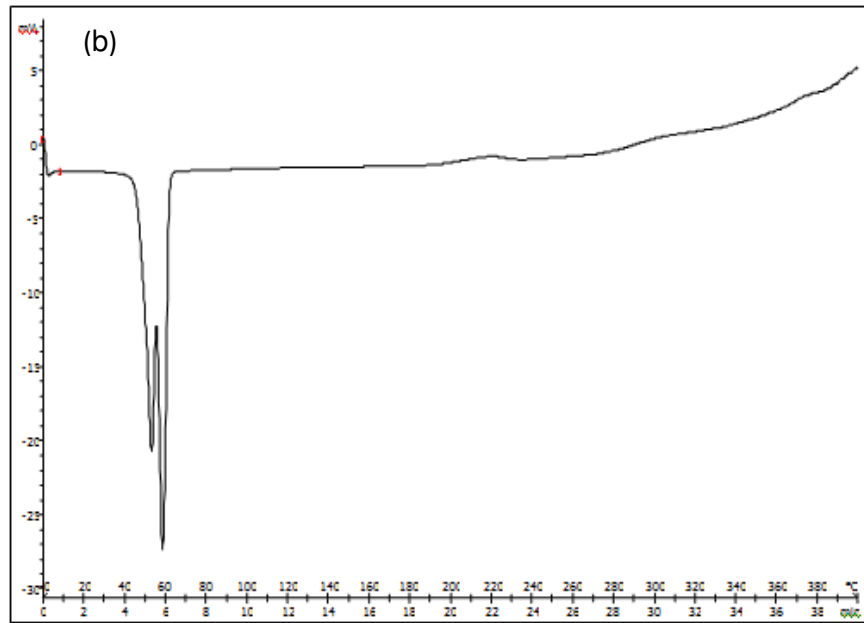
**Figure 3.8:** Percentage crosslinking of prepared copolymeric particulate system to simulated mucous solution

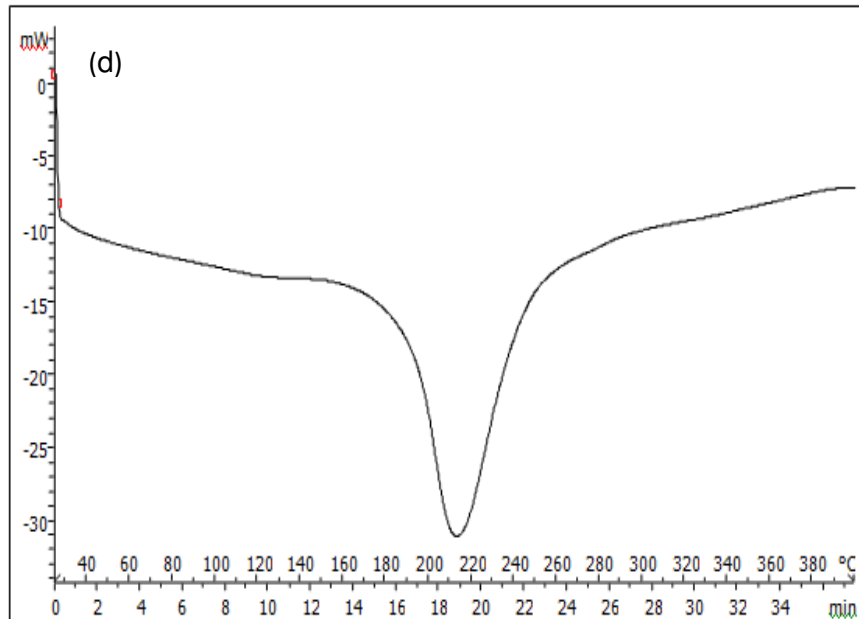
TMC is the main polymer component responsible for the mucoadhesive properties of the prepared copolymeric microparticulate system, due to its considerate degree of strong electrostatic interactions with mucus and the charged mucosal surface, because of the cationic polyelectrolyte nature of TMC. The density of charges is due to its quaternization having significant effects on the absorption enhancing properties. During the synthesis of TMC, it is well noted that many positive charges on the polymer are expanded in solution, due to repelling forces between functional groups and is therefore able to transport numerous hydrophilic compounds easily across the mucosal epithelia by providing easy opening of tight junctions on mucosal linings (le Dung *et al.*, 1994; Hemant *et al.*, 2010). Additionally, it has a well defined structural arrangement with improved solubility compared to its parent polymer, chitosan. It can therefore be concluded that the optimized formulation displays significant mucoadhesive properties, thereby enhancing the penetration and absorption of the peptide through the intestinal mucosa.

### 3.3.1.7. Thermal evaluation using Differential Scanning Calorimetry (DSC) analysis

The analytical technique of DSC can be explained as the measurement of change of the difference in the rate of heat flow to a reference sample and a sample while they are exposed to a controlled thermal program (Celej, *et al.*, 2006). DSC thermograms were evaluated for thermal properties of the copolymeric particles, thereby determining the melting and crystallization points of the polymers and copolymeric particles as shown in Figure 3.9. TMC displayed an endothermic peak at 214 °C, and an exothermic peak at 256 °C and 300 °C. TMC displayed decomposition of amine functionalities approaching crystallinity of the polymer (Kittur *et al.*, 2002). PMAA indicated a distinctive endothermic melting peak at 211 °C. PEGDMA gave double melting points at 52.61 and 57.91 °C. The copolymeric particles TMC-PEGDMA-MAA gave a single melting peak at 54.59 °C, indicating that crosslinking was evident due to the modification of the melting peaks from the original polymers.



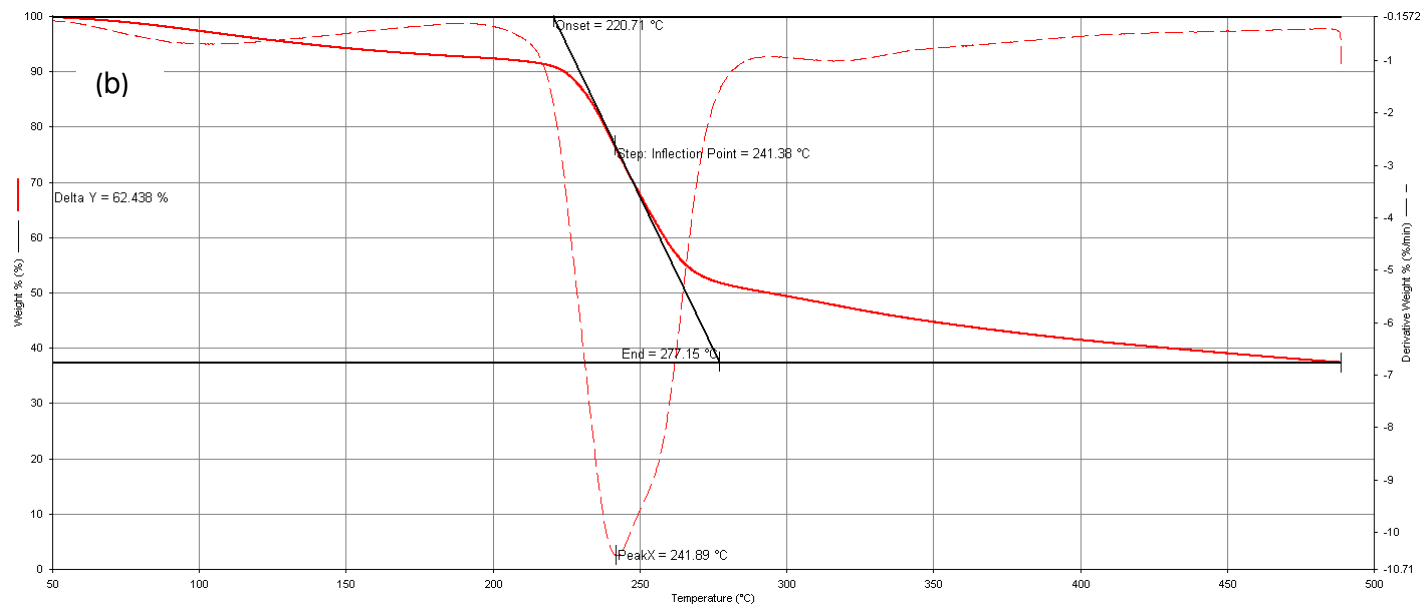
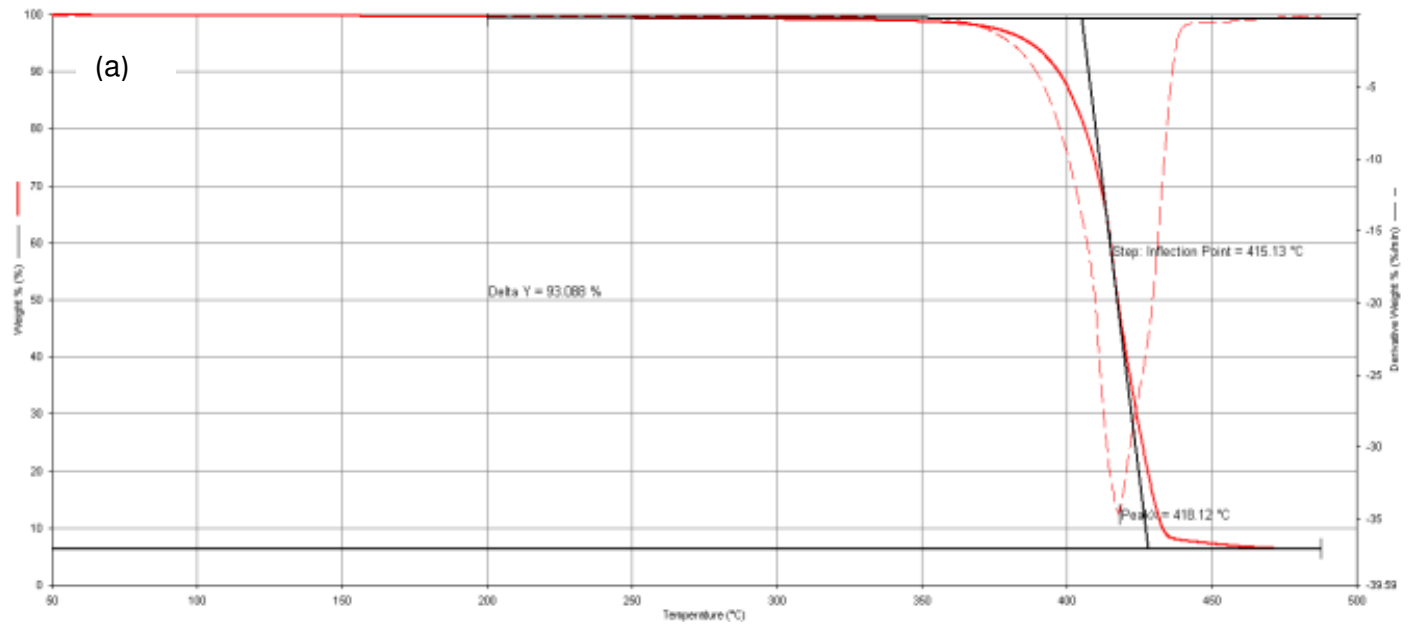




**Figure 3.9:** DSC thermogram of a) TMC, b) PEGDMA and c) TMC-PEGDMA-MAA d) PMAA

### 3.3.1.8. Thermogravimetric analysis (TGA)

Thermal characteristics of the polymers TMC, PEGDMA and copolymeric particles TMC-PEGDMA-MAA were analyzed for determination of degradation and moisture content. TMC displayed 3.37% of water content emitted at 110°C and 23.34% of degradation at 241°C. PEGDMA showed negligible liberation of moisture content at 110°C, however at 415°C, 40% of the polymer showed thermal degradation. Evaluation of TMC-PEGDMA-MAA liberated 14.5% of water at 110°C and at 407°C, 50% of the polymer showed thermal degradation. As seen in Figure 3.10a-c, the evaluation of thermal graphs obtained were undertaken using first derivative principles (red dotted lines), which calculates the amount of moisture loss from 50-110°C and polymer degradation at much higher temperatures. The percentage moisture content of the copolymeric particles is significantly due to the hydrophilic nature of the copolymer. The copolymeric particles also demonstrated great sensitivity to degradation, thereby requiring less energy to yield thermal decomposition. At this stage of the reaction, it can be explained that decarboxylation occurs in the copolymeric particles, during which functional groups no longer sustain their intact structures (Tomar *et al.*, 2011).



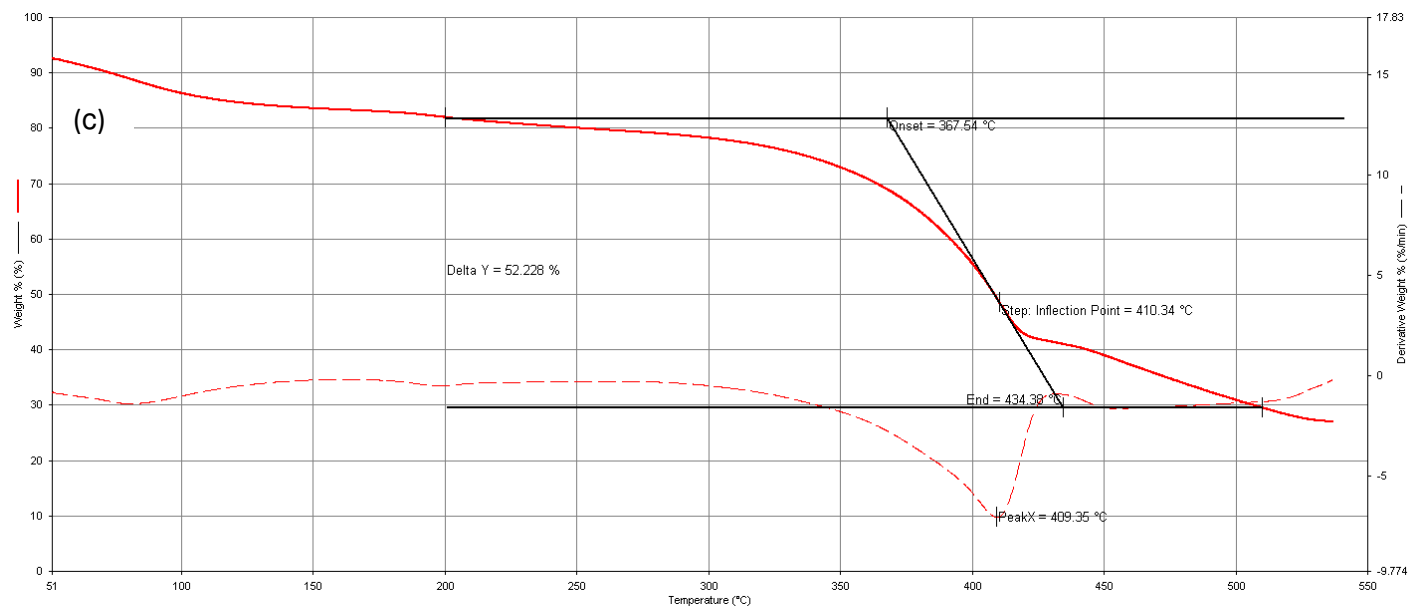


**Figure 3.10:** TGA profile of (a) PEGDMA, (b) TMC and (c) TMC-PEGDMA-MAA

### 3.3.1.9. Matrix hardness (MH) and Matrix resilience (MR)

The optimized copolymeric particles in tableted form were evaluated for properties of MH and MR. Figure 3.11a was generated from the evaluation of properties for MH, with a force-distance ratio,  $Fd=0.011$  and a Gradient net  $Fd=95.37$ , which can be interpreted as having significantly strong bonds between the particles, thus maintaining an intact mini-tablet structure.

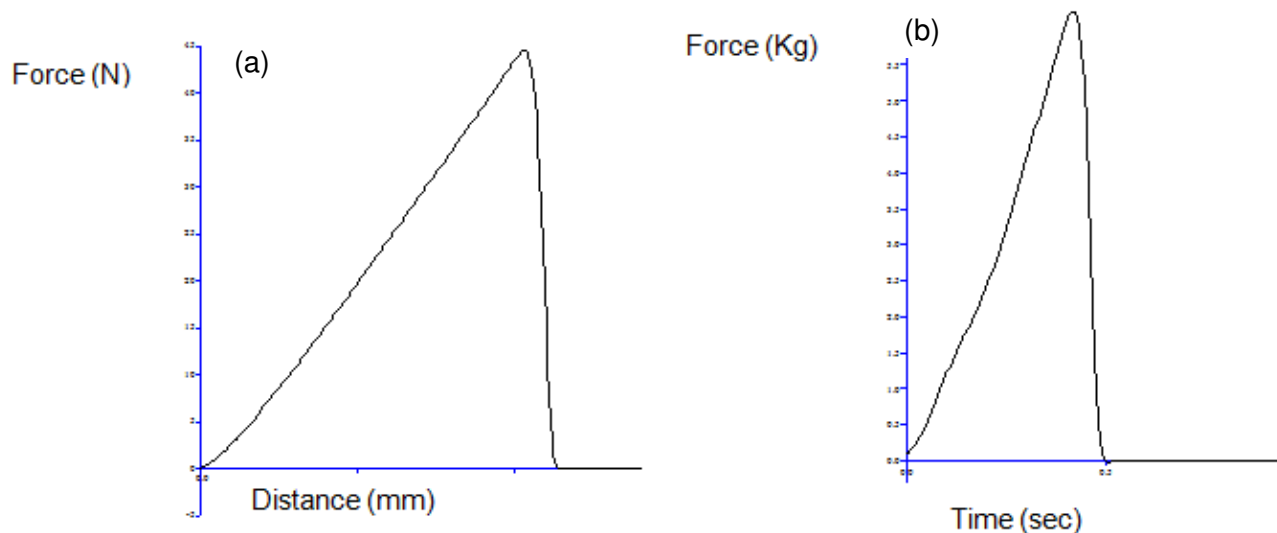


**Figure 3.11:** Evaluation of mechanical properties of copolymeric particles a): Matrix Hardness (MH) (N/mm); b) Matrix Resilience (MR) (Kg/sec)

Figure 3.11b represents a Force-Time profile for MR, with a ratio of the area under the curve (AUC), from peak to baseline, after removing the Force initiated ( $AUC_{2-3}$ ), over the baseline to peak, before removing force ( $AUC_{1-2}$ ), yielding a percentage of 22.27% MR, indicating a firm, minimally elastic property of the tablet. Physical properties of MH of the copolymeric particles were evaluated to determine the intensity of force required per millimeter of distance to induce an indentation on the tablet. The gradient of the curve represents the flexibility of the tablet, whilst the AUC is the amount of deformation energy of the tablet. The stability of the tablet in terms of its biomechanical properties are essential for maintaining appropriate drug release kinetics, in which the time taken for the tablet to dissociate into its powder form will yield proportional amounts of drug release (Ellison *et al.*, 2008). MH demonstrated a significant value of 0.011N/mm, depicting the copolymeric tablet as a significantly strong matrix system, which was further proved by porositometric and SEM analysis, showing characteristic mini pore particulate formation. This property is essential for a tableted system due to mechanical protocol undertaken during manufacture and packaging.

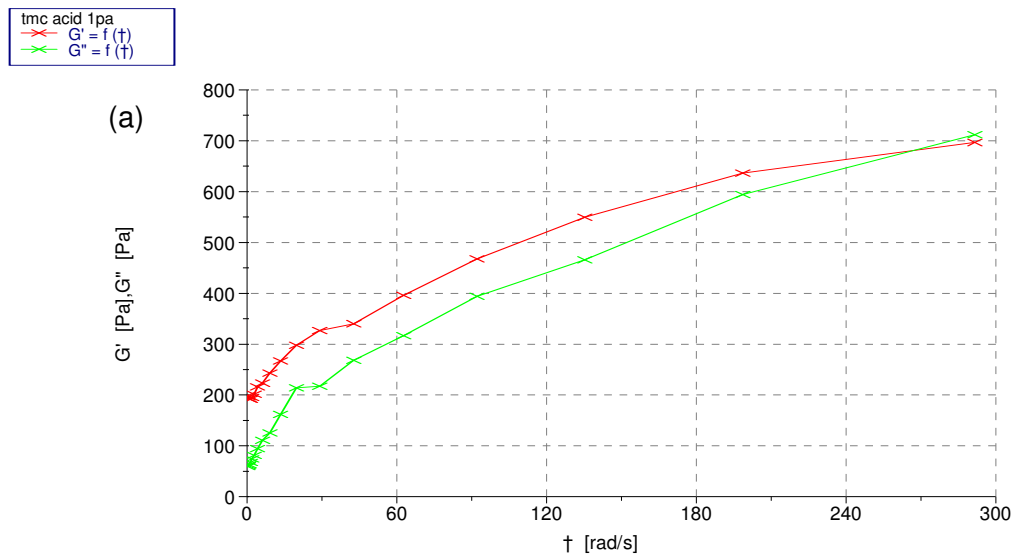
MR of is the ability of a given substance to deform elastically, but revert to its original state, once the force is removed. Many polymers do not possess high resilience since the interfacing surfaces from the interparticulate granules have minimum voids within the matrix structure, which are reduced in the process of compressing the tablet. The greater the void volume capacity, the greater the ability of the tablet to return to its original form to a certain extent after compression, until the interfacing surfaces collapse to a state where elastic deformation is replaced with placticity deformation, i.e, permanent alteration in shape/structure of the tablet. As the number of interfacing particle surfaces (physical interaction) or a higher strength of interfacing particle surfaces (chemical interaction) increase in the copolymeric particles, the compression induced will not create elastic deformation in the structure, allowing a proportional relationship between the intermolecular bonds stretch and the resilience properties of the tablet (van der Voort Maarschalk *et al.*, 1996).

A 22.27% MR indicated that the tablet possesses minor elastic properties, representing strong particle bonding with least amount of air spaces between the particles, despite the minimum amount of force of 0.6MPa used to compress the copolymeric particles. This is also an essential aspect for consideration when packaging of tablets, as well as more physiological parameters of force to withstand swallowing and delayed release disintegration parameters for desired drug

release. The results obtained thus display sufficient evidence that the copolymeric particles possess superior mechanical properties for oral drug delivery.

### 3.3.1.10. Rheological Evaluation

The viscoelastic nature of the copolymeric particles was determined in the respective gastric and intestinal pH medium, evaluating the degree of characteristic responses of the particles due to change in pH.  $G'$  is a measure of deformation energy stored in the particles, indicating the elastic solid phase property of the particles and  $G''$ , measures the viscous behavior and deformation energy used and lost in the particles during application of applied strain. As observed in Figure 3.12a, particles in gastric medium display distinctive solid phase characteristics, with great elastic properties, since  $G'$  dominates above  $G''$ . Towards the end of the graph, where the frequency is substantially high, the viscous behavior exceeds the elastic property of the particles, displaying greater flow characteristics with greater strain applied. Figure 3.12b illustrates particles in intestinal medium, demonstrating greater viscous behavior than elastic behavior of the particles during the initial stage, with dynamically shifting phases of solid and viscous properties during progression of the applied strain. The viscous nature however still remains significantly lower than the solid phase property of the particles, indicating greater elasticity of the particles as the strain increases.



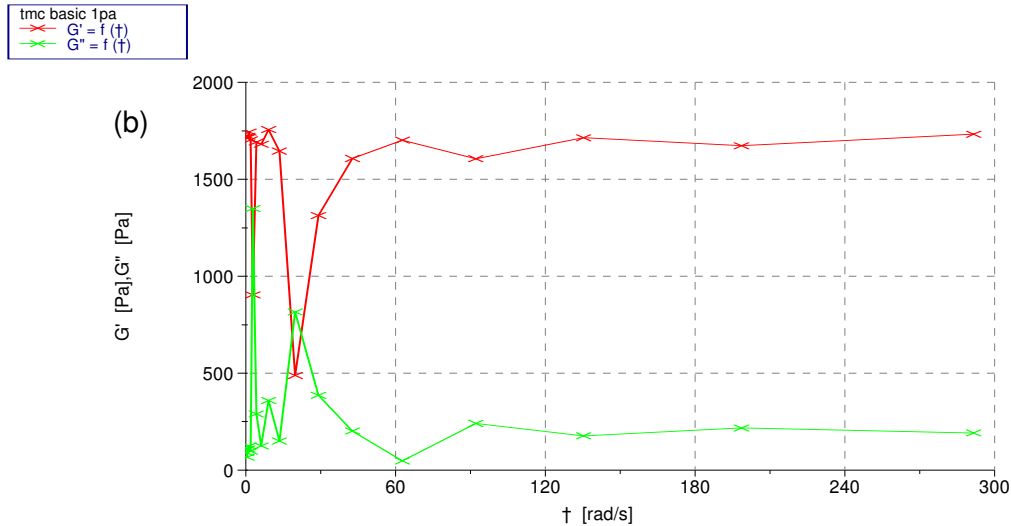


**Figure 3.12:** Oscillation curves representing storage modulus ( $G'$  in red) and loss ( $G''$  in green), using a 0.1% constant strain in a) gastric medium and b) intestinal medium

Yield stress ( $T$ ) is a measure of minimum force necessary to cause deformation or flow, dependant on time. Below the yield stress, the degree of deformation that occurs is a linear manner, increasing in shear stress, thus categorizing the sample as a solid phase behavior. Above this critical yield value, the sample displays deformation and flows in nature, displaying a greater liquid phase property (Herh et al., 1998). The test undertaken oscillates the cone at a fixed frequency sinusoidal time basis, producing a sinusoidal shear strain in a non destructive manner as given in Equation 3.8.

$$T = T_{\theta} \sin(\dot{\omega}.t) \quad (\text{Equation 3.8})$$

In which  $T_{\theta}$  is the stress amplitude,  $\dot{\omega}$  is angular velocity, and  $t$  is time. Data points are derived from the phase angle of the applied stress and the amplitude of the stress. As the sample is being analyzed, deformation occurs due to the stress imposed on the sample. The amplitude of deformation is not achieved in conjunction with the stress amplitude, due to the variations of vicious and solid phase elastic properties of the particles. The resultant phase shift occurs between the deformation and the stress applied, thus referred to as  $\theta$  or phase shift angle. Samples that are completely elastic in nature, possesses a phase shift of  $0^{\circ}$ , unlike samples that are pure viscous, displaying a  $90^{\circ}$  phase shift. Equation 3.9 indicates these properties of the viscoelastic sample.

$$T = T_{\theta} \sin(\dot{\omega}.t + \alpha) \quad (\text{Equation 3.9})$$

T is the stress,  $T_e$  is stress amplitude,  $\omega$  is angular velocity, t is time and  $\alpha$  is phase shift ( $\omega=2\pi.f$ ; f is the oscillation frequency) (Schramm *et al.*, 2004). It can clearly be seen that the particles in gastric medium display greatest elastic behavior, due to the clumping of particles and formation of hydrogen bonding, to protect the loaded protein in the particles, further confirmed by  $G'$  being greater than  $G''$ . Particles in intestinal medium clearly show a transition of viscous and elastic properties,  $G''$  and  $G'$  interchange, since particles are swelling in nature, absorbing a significant amount of water, thereafter predominantly behaving as solid elastic phase particles.

#### **3.3.1.11. X-Ray Diffraction (XRD) analysis on copolymeric microparticles**

X-ray diffraction was carried out on all polymers and copolymeric microparticles. The percentage crystallinity of each sample was calculated, indicating the impact crosslinking has on the state of the copolymer. TMC and PMAA showed less than 0.1% crystallinity, while PEGDMA and TMC-PEGDMA-MAA showed a 15.42% and 37% crystallinity respectively. Figure 3.13 demonstrates the intensity of the crystalline nature of the polymers, proportional to the area of the peaks. It is clearly evident that crosslinking of the polymers substantially increased the crystalline nature of the copolymeric particles, allowing greater order in the structural arrangement of the particles.

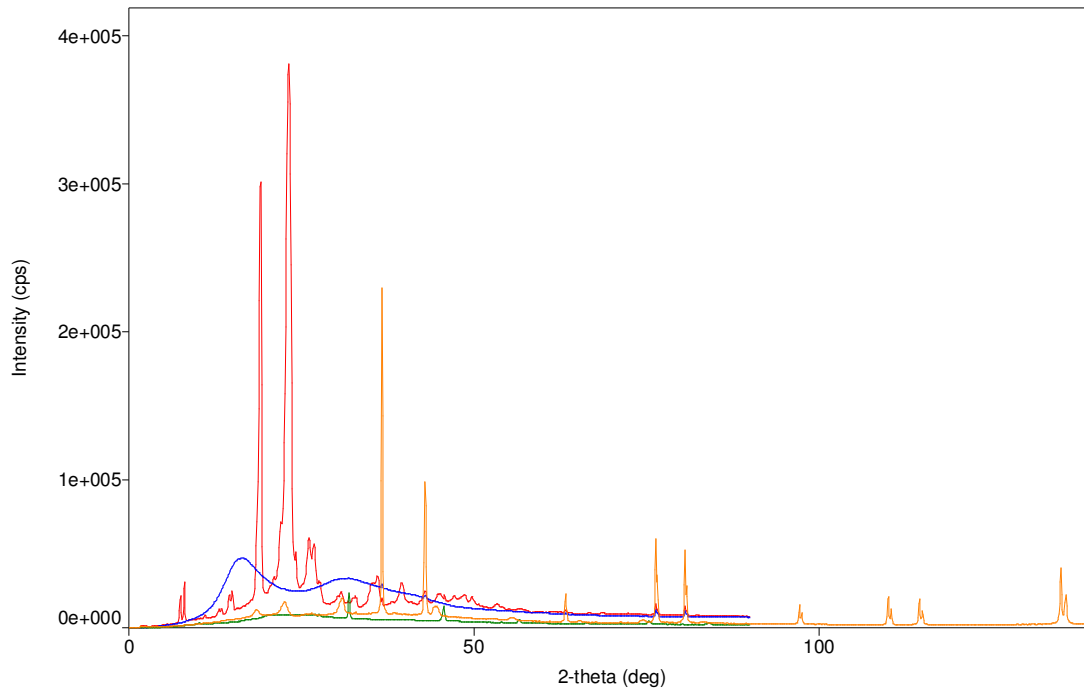


**Figure 3.13:** Diffractogram Representing the intensity of crystalline nature of PEGDMA (red), PMAA (blue), TMC (green), TMC-PEGDMA-MAA (yellow)

This technique was employed for determination of degree of phases present in a sample, using a non destructive technique, for analysis of polymers and copolymeric particles. Using Braggs law, as seen in Equation 3.10, each ring diffraction is correlated to a lattice vector in the crystalline sample. The scattering angle is the angle between the beam axis and the ring. Analysis of the polymers thus produce a diffractogram, representing the intensity of diffraction to the scattering angle. The greater the crystalline nature of the sample, the narrower the peaks produced. The lower the crystalline nature, the greater the peak broadening.

$$n \gamma = 2d \sin \theta \quad \text{(Equation 3.10)}$$

$n$  is the integer,  $\gamma$  is wavelength of x-ray beam,  $d$  is the distance of lattice planes and  $\theta$  is Braggs angle.

It is clearly evident that polymers PEGDMA and copolymer TMC-PEGDMA-MAA are significantly crystalline in nature, thereby enhancing the order of the molecules in the crystal lattice. Due to crosslinking of the polymers, the resultant copolymer displays the most crystalline nature, since a higher order of the particles are significantly achieved. Since the degree of

crystallinity is dependent on factors of chain length, chain branching and interchain bonding, crosslinking of polymers increase these properties, resulting in greater order of the crystal lattice ([www.chemistry.msu.com](http://www.chemistry.msu.com)).

### 3.3.1.12. NMR analysis

NMR analysis was conducted on the polymers and copolymeric microparticles as depicted in Figure 3.14. Peaks at 25ppm and 175ppm are indicative of the presence of acetyl functional groups in TMC. Similar peaks were observed in CHT, since CHT is the precursor to synthesis of TMC. The peak represented at 55ppm is diagnostic of the quarternisation of  $\text{NH}_2$  to  $\text{N}(\text{CH}_3)_3$  as an appearance of a trimethylated signal. The signal for  $\text{C}_6$  and  $\text{C}_2$  are now slightly downfield, depicting a change in the structural arrangement of the carbons. Looking at the crosslinked copolymeric microparticles, there is an additional CO,  $\text{CH}_3$  bond in the spectrum, indicating the presence of the crosslinking to PEGDMA. The peak for MAA is also evident in the spectrum in the region of 48ppm, illustrating the  $\text{OCH}_3$  functionalities in the crosslinked copolymeric system. The peak at 55ppm is thus indicative of trimethylation of the amine moiety. This peak is not observed for the spectra of chitosan. For the spectrum of chitosan, we observe a doublet diagnostic of  $\text{CH}_2\text{-NH}_2$  and  $\text{CH}_2\text{-OH}$  (only protons bonded to an alcohol and amine), and these chemical shifts were also comparable to those values reported in literature.

There is a broadened set of signals in the region of 185ppm which can be assigned to  $\text{C=O}$  and this is indicative of the crosslinked PEGDMA-MAA. The functional groups on TMC and PEGDMA are similar in nature, ie there have  $\text{CH}_3$ ,  $\text{CH}_2$ ,  $\text{CH}$  and  $\text{C-O}$ . With the exception for  $\text{C=O}$ , we observed these carbons signals but could not be easily assigned directly to TMC or PEGDMA respectively, however we observe different carbon signals confirming that the integrity of the structure was maintained with most peaks collectively appearing at same chemical shifts respectively for the hybridization of the carbon.

It was also found in powder XRD diffractogram of TMC-PEGDMA-MAA that the degree of crystallinity was greater than TMC and PEGDMA. This could possibly account for the fact that in the solid state spectrum of TMC-PEGDMA-MAA, there is a greater occurrence of chemically equivalent signals possibly due to fewer structural conformation that would lead to chemical inequivalence, hence more signals. This is a desired goal in the rational design of the optimized copolymer, as this leads to controlled drug release. Therefore SS NMR has great potential for use as a complementary tool for the full characterization of novel copolymers such as TMC-

PEGDMA-MAA microparticulate formulation, thereby proving the crosslinking due to the free-radical polymerization reaction. As depicted in Figure 3.15, the structure of the crosslinked copolymeric polymer was proposed according to the specification criteria confirming the structural arrangement. This structural arrangement thus concludes the primary link for confirming successful free radical polymerization reaction.

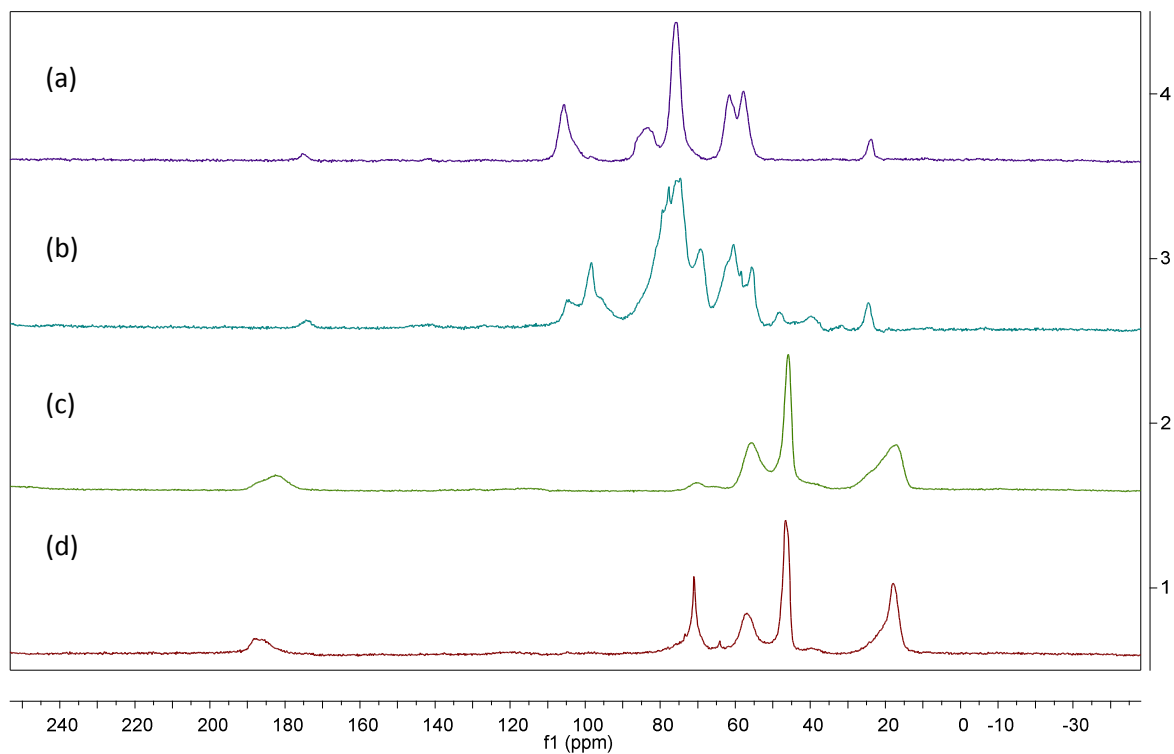


**Figure 3.14:**  $^{13}\text{C}$  solid state NMR spectra of a) chitosan, b) TMC, c) MAA, and d) TMC-PEGDMA-MAA spinning side band CO peak

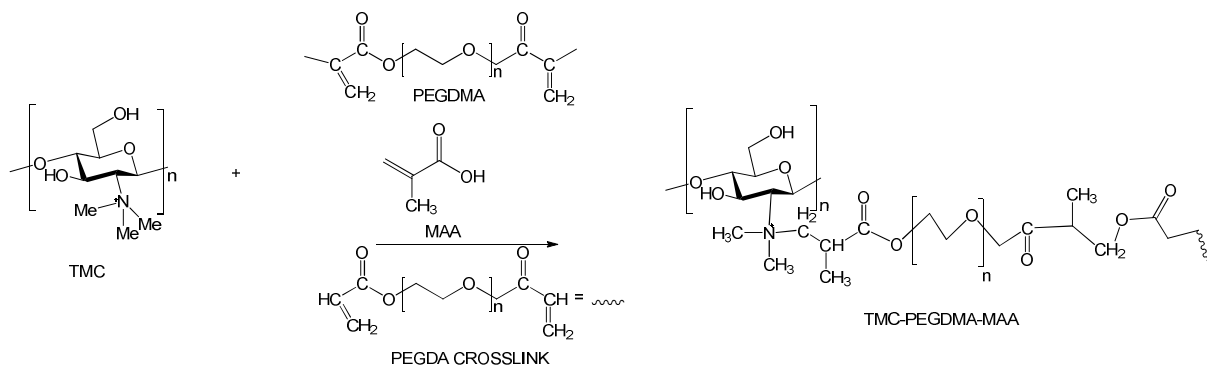


**Figure 3.15:** Reaction mechanism involving each reactant in the free radical polymerization reaction to form the copolymeric crosslinked microparticulate system.

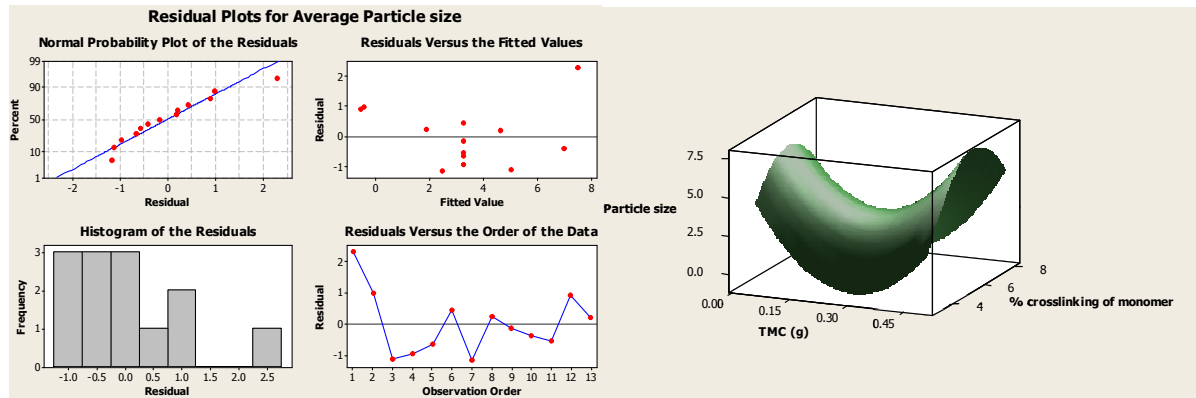
### 3.3.1.13. Concluding Remarks

A copolymeric particulate system of TMC-PEGDMA-MAA was prepared by free radical suspension polymerization method and established to possess pH-sensitive, mucoadhesive, hydrophilic properties. A Box-Behnken experimental design was used for formulation optimization. Out of 13 experimental design formulations generated for selected variables (TMC and crosslinker), formulation 7 with 0.5g/100mL TMC and 3% crosslinker was deemed optimum based on response generated for the dependent variables. TMC-PEGDMA-MAA spectra demonstrated the nature of crosslinking with strong interactive carboxylic acid groups backing the strong hydrophilic, pH sensitive nature of the polymer. Particle size analysis demonstrated significant differences in gastric and intestinal pH, due to the clumping and dispersed nature of the particles respectively, which were clearly demonstrated by SEM images. Mucoadhesive studies demonstrated substantial adhesion of the particles to mucus, thereby confirming the ability of the particles to interact with mucus solution, which is essential for absorption of the protein *in vivo*. Thermal evaluation was undertaken on the polymers and copolymeric microparticles, demonstrating the melting point and percentage water emission. The physical durability of the compressed copolymeric particles was tested for matrix hardness and resilience, demonstrating significant strength and mechanical interparticulate bonding. The flow properties of the particles were also determined, differentiating its behavior in gastric and intestinal medium. Particles demonstrated significant solid phase characteristics with elastic properties in gastric medium and in intestinal medium displaying greater viscous than elastic behavior in the initial applied force, thereafter demonstrating a shift in the elastic and viscous properties due to progression of the applied strain. XRD analysis demonstrated high percentage crystallinity in the copolymeric particles, with the most crystalline arrangement found in the crosslinked copolymeric particles, in comparison to the individual polymeric substituents. NMR analysis was undertaken for evaluation of chemical shifts in the copolymeric formulation, thereby confirming successful crosslinking in microparticulate formulation.

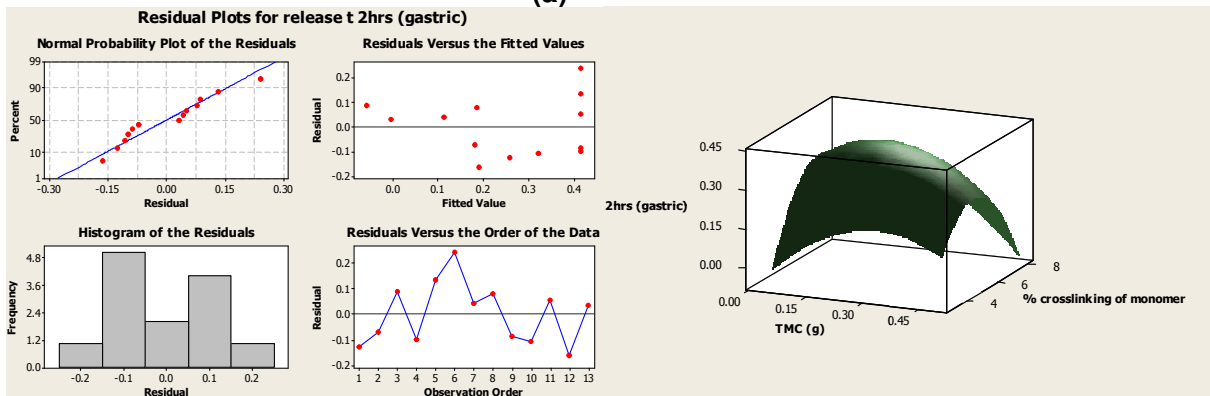
### **3.3.2 PART B: Evaluation of CHT-PEGDMA-MAA Copolymeric Microgel System**

#### **3.3.2.1. Box-Behnken optimization analysis**

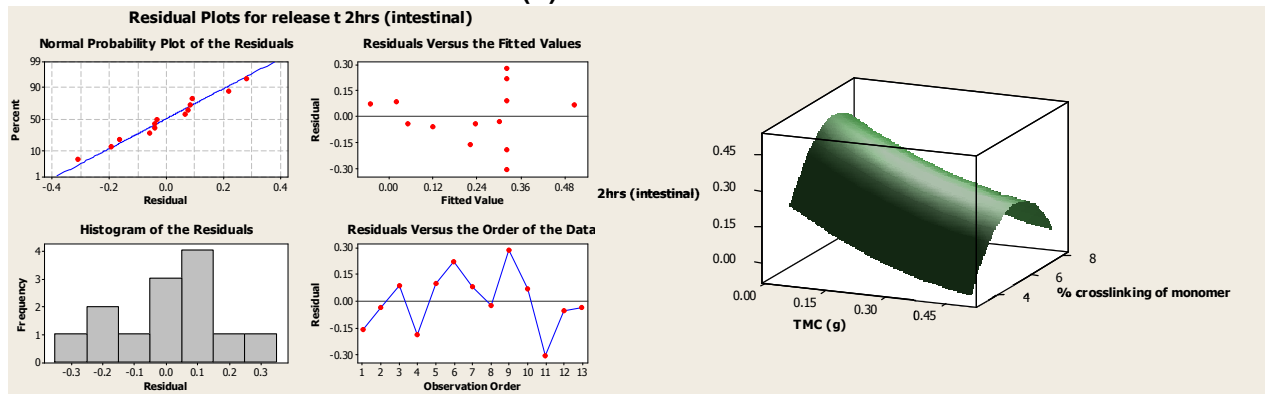
The Box-Behnken generated a series of formulations, where the responses were evaluated using residual and surface plots as observed in Figure 3.16, for variables of CHT and % crosslinking concentration for identification of an optimized microgel formulation. Particle size and drug release results were correlated to obtain an optimized formulation. The ideal representation of data generated from the software, generates histograms with bell shaped curves for the responses, however slight deviation in response elements were due to the instantaneous pH responsive nature of the particles. In some formulations, greater concentrations of drug were released over 2 hour duration than in intestinal conditions, due to the immediate sensitivity of the microgel to the gastric environment, releasing insulin in the process of constricting and aggregating to protect the contents of the loaded microgel.



(a)



(b)



(c)

**Figure 3.16:** Representation of residual and surface plots of the microgel formulations, with regard to average particle size, fractional release at 2 hours in gastric medium and fractional release at 2 hours in intestinal medium.

Optimal		CHT (g)	% Crosslinker
Desirability= 0.93	High	0.5	8.0
	Optimized	0.5	3.0
	Low	0.05	3.0

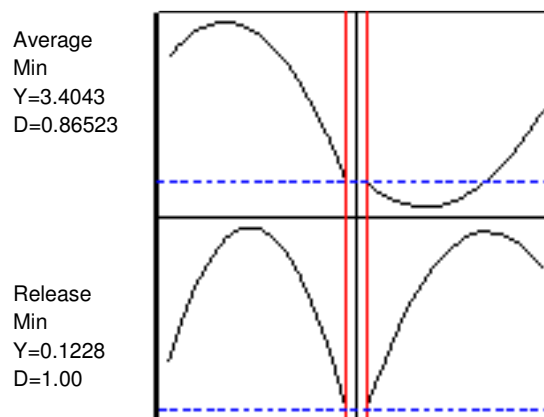


**Figure 3.17:** Design specifications for obtaining an optimal desirability index of 93% for the copolymeric insulin delivery system

Optimization of the copolymeric microgel yielded a desirability of 93%, as seen in Figure 3.17. MINITAB®, V15, PA, USA statistical software was employed to evaluate all variables inputting all responses of particle size, fractional release of insulin in gastric and intestinal condition at 2 hours, producing a delivery system for greatest drug release in intestinal conditions, least insulin release in gastric conditions and smallest particle size possible. F9 as set out in Table 3.9 was thus calculated as the optimized formulation for further *in vivo* and characterization studies.

### 3.3.2.2. ATR-FTIR Spectroscopy of monomers and copolymeric microgel formulation

ATR-FTIR analysis was undertaken on monomers and copolymers involved in the synthesis of the copolymeric microgel as seen in Figure 3.18. MAA displayed characteristic vinyl and carbonyl groups at  $1697\text{cm}^{-1}$  and  $1635\text{cm}^{-1}$  respectively. Wide stretching of hydroxyl and carboxyl groups were observed in regions  $3000\text{-}3450\text{cm}^{-1}$  (Kumar *et al.*, 2006). PEGDMA<sub>4000</sub> was observed to have characteristic CH stretching at  $2882\text{cm}^{-1}$  and CH bending at  $1466\text{cm}^{-1}$ . Broad band spectra in regions of  $1639\text{cm}^{-1}$ , due to interactions between vinyl and carbonyl functionalities were also observed.

For CHT-PEGDMA-MAA copolymeric microgel, carbonyl group at  $1695\text{cm}^{-1}$  was clearly distinguished, due to the strong interactive carboxylic acid groups of PEGDMA and MAA. This bonding provides a hydrophilic as well as a pH sensitive nature of the copolymeric microgel (Kumar *et al.*, 2006). Chitosan has a characteristic peak at  $1577\text{cm}^{-1}$  (Mourya *et al.*, 2009), which

can be seen to have shifted in the crosslinked copolymeric microgel to  $1553\text{cm}^{-1}$  due to angular deformation of N-H bond of amino groups during the crosslinking reaction, however the intensity of peak  $1553\text{cm}^{-1}$  in the copolymeric microgel is reduced in comparison to the peak  $1577\text{cm}^{-1}$  due to N-methylation occurring. The peak of  $1553\text{cm}^{-1}$  in the copolymeric microgel also explains the presence of N-H bending, in addition to the range of peaks from  $1415\text{-}1430\text{cm}^{-1}$  which is characteristic for N-CH<sub>3</sub> absorption (Domard *et al.*, 1986).

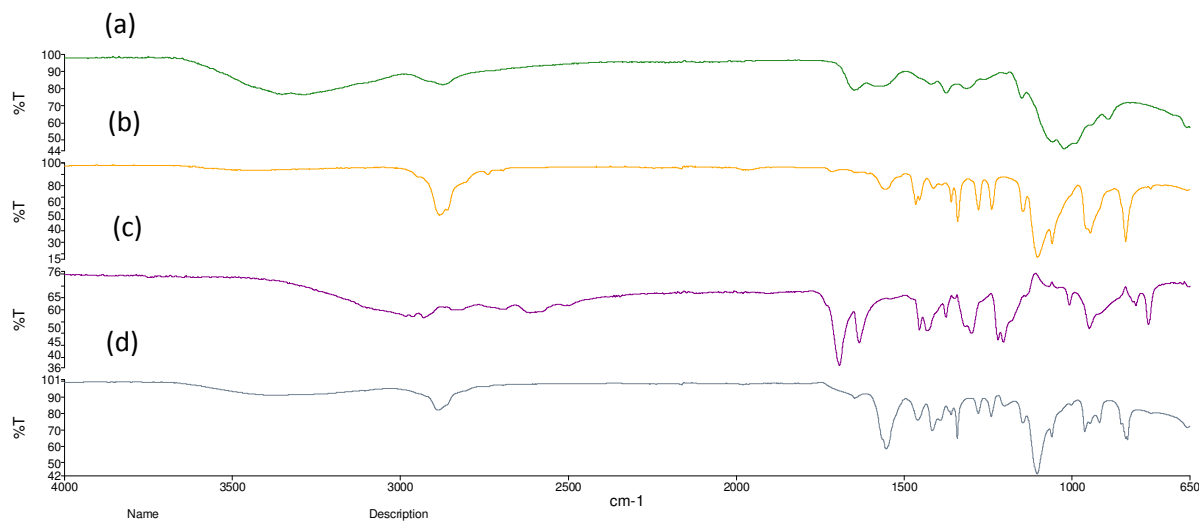


**Figure 3.18:** FTIR spectra of (a) CHT (b) PEGDMA (c) MAA (d) CHT-PEGDMA-MAA

### 3.3.2.3. Particle size and zeta potential analysis

All design formulations were evaluated for particle size in gastric and intestinal condition due to the pH sensitive nature of the particles, to determine the effect the variables have on the physical properties of the copolymeric particles. No filtration was carried out during evaluation, since this would propose false representations of the particle characteristics. Results observed in Table 3.9, indicates a proportional relationship with respect to concentration of CHT and % crosslinker in the formulations. At high concentrations of CHT and % crosslinker, microgel particles showed greatest size in both pH mediums, while at 3% crosslinker concentration, smaller particle size was observed. Evaluating the chemistry of the particles, at low pH, there is strong interaction of carboxylic groups with ether functional groups of PEG, thus creating strong hydrogen bonding between the particles. This also explains the increase in size of the microgel in gastric medium, due to the ability of microgel to aggregate and clump, forming networks of large masses of microgel thereby conserving the ability to release the loaded protein from the

particles. Results in intestinal conditions showed microgel to possess a smaller particle size, even though the microgel is observed to swell in intestinal medium. The reason for a smaller particle size range is due to the dispersion of the microgel particles to release drug in intestinal medium, due to breaking of hydrogen bonds and ionization of carboxylic functionalities.

The polydispersity index (PDI) of the formulations revealed a greater value in gastric medium than intestinal medium. Microgel particles demonstrating a PDI less than 0.5 are considered optimal in their uniformity and particle size distribution. It can therefore be affirmed that the microgel clumps in large non uniform masses in gastric pH, conserving and protecting the loaded protein in the copolymeric particles, whereas particles are more uniform and well distributed in intestinal medium, releasing drug as they swell and disperse in nature. As displayed in Table 3.9, F2, F4, F8, F12 and F13 were designed with the same composition, thereby determining the degree of consistency in the responses obtained. Using the software specifications as outlined above, F9 was determined as the optimal formulation for oral protein delivery.

Zeta potential analysis of the optimized formulation demonstrated a value of 9.51 and 21.6 in gastric and intestinal conditions, respectively. These results correlate precisely to the behavior of the particles, since in gastric medium, the microgel particles clump in nature due to strong hydrogen bonds, giving a low zeta potential, as opposed to the particles dispersed in intestinal conditions resulting in the ionization of carboxylic groups, yielding a higher zeta potential of the copolymeric particles.

**Table 3.9:** Experimental design formulation in gastric and intestinal fluid for evaluation of average particle size.

Formulation	CHT* (g/100mL)	Crosslinker (%w/w of momomer)	Av size (µm) (pH 1.2)	PDI**	Av size (µm) (pH 6.8)	PDI**
1	0.05	8	7.2	0.83	4.5	0.46
2	0.275	5.5	11.8	0.78	7.3	0.37
3	0.05	3	5.4	0.68	4.2	0.22
4	0.275	5.5	10.4	0.8	8.8	0.42
5	0.275	8	8.7	0.53	4.6	0.24
6	0.5	5.5	8.7	0.51	6.7	0.52
7	0.275	3	8.5	0.63	6.1	0.62
8	0.275	5.5	10.2	0.66	8.2	0.47
9	0.5	3	5.5	0.35	3.5	0.22
10	0.05	5.5	5.6	0.54	3.3	0.46
11	0.5	8	16.3	0.74	8.2	0.61
12	0.275	5.5	9.6	0.79	6.7	0.35
13	0.275	5.5	8.8	0.66	5.9	0.54

\*Chitosan \*\*Polydispersity index

#### 3.3.2.4. Porosity analysis of optimized copolymeric delivery system

The optimized copolymeric microgel was evaluated in gastric and intestinal pH, evaluating Brunauer–Emmett–Teller (BET) desorption and adsorption profiles as well as nitrogen isotherms generated from the porosimetric analysis. As differentiated in Table 3.10, it is clearly evident that there are less intermolecular spaces present between the microgel in gastric medium, as opposed to those present in intestinal medium. This further reaffirms the basic properties of the microgel in the respective mediums, demonstrating their pH sensitive nature in relation to surface area, pore volume and pore size. The copolymeric microgel demonstrated a type IV isotherm, with a type H1 hysteresis loop. This property explains the multilayer composition of the material, in which the saturation level reaches a pressure below the saturation vapor pressure, more clearly defined as gases getting condensed into the tiny pores at pressure below the saturation pressure of the gas (Sing *et al.*, 1985). As seen in Figure 3.19, the beginning of the linear mid section of the isotherm demonstrates a point of completion for adsorption of the copolymeric particles. It was clearly evident that the microgel in gastric medium maintained their aggregation properties, due to the smaller pore size and volume, responsible for their strong hydrogen bonds between the particles, as opposed to results in

intestinal medium, in which microgel is observed to be dispersed and possess many intermolecular spaces between them. Values not recorded in the table are due to the limitation of the instrument to detect extensive values, thereby unable to calculate specific parameters relating to porositometric analysis.

**Table 3.10:** Porosity analysis of optimized copolymeric delivery system at different pH ranges of gastric and intestinal medium

<b>Parameter</b>	<b>Acidic pH</b>	<b>Basic pH</b>
<b>Surface Area</b>		
Single point surface area (m <sup>2</sup> /g)	1.0973	2.1416
BET Surface Area (m <sup>2</sup> /g)	5.0316	-
BJH Adsorption cumulative surface area of pores between 17.000 Å and 3000.000 Å diameter (m <sup>2</sup> /g)	1.731	3.4400
BJH Desorption cumulative surface area of pores between 17.000 Å and 3000.000 Å diameter (m <sup>2</sup> /g)	2.0094	3.4400
<b>Pore Volume</b>		
Single point adsorption total pore volume of pores less than 817.293 Å diameter (cm <sup>3</sup> /g)	0.002068	0.004173
BJH Adsorption cumulative volume of pores between 17.000 Å and 3000.000 Å diameter (cm <sup>3</sup> /g)	0.002379	0.004504
BJH Desorption cumulative volume of pores between 17.000 Å and 3000.000 Å diameter (cm <sup>3</sup> /g)	0.002414	0.004565
<b>Pore Size</b>		
Adsorption average pore width (4V/A by BET) (Å)	16.4411	-
BJH Adsorption average pore diameter (4V/A) (Å)	54.975	56.834
BJH Desorption average pore diameter (4V/A) (Å)	48.052	53.087

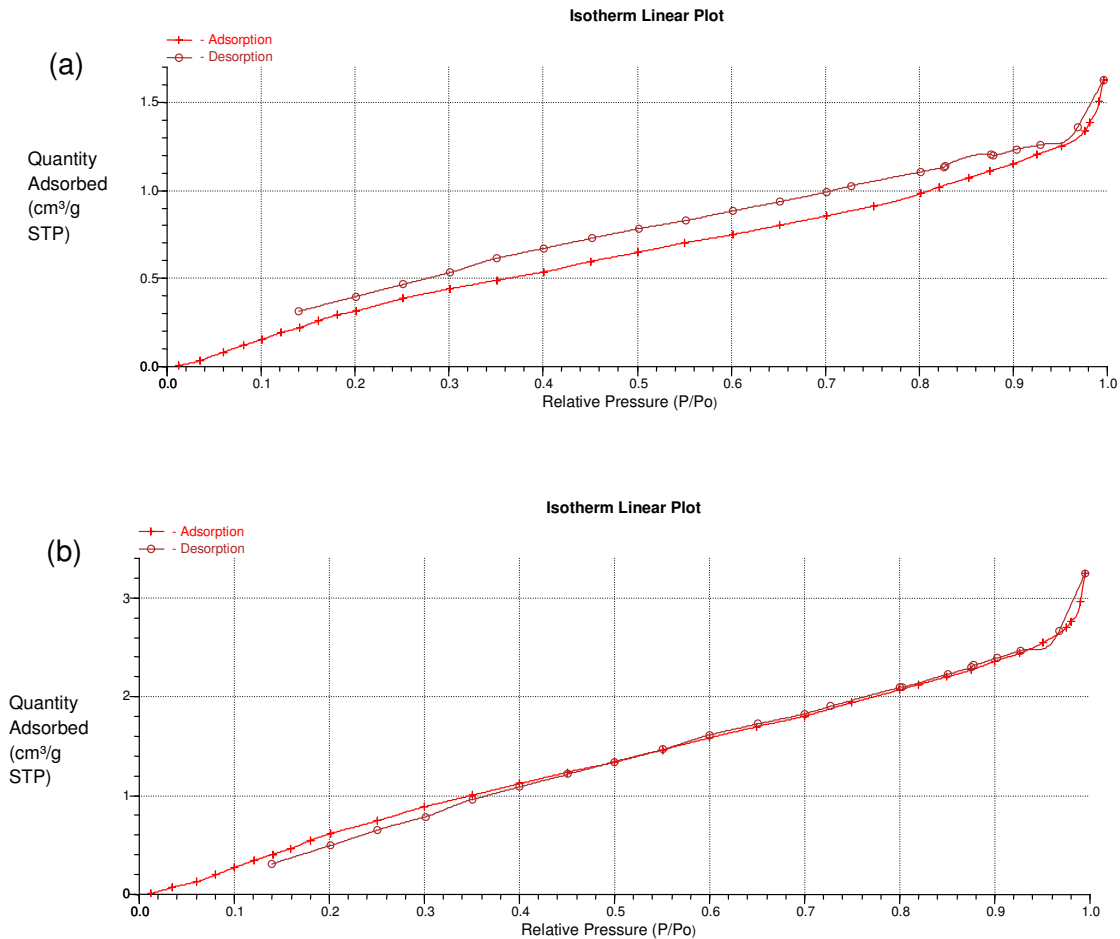


**Figure 3.19:** Isotherm Linear plots (a) gastric medium and (b) intestinal medium.

### 3.3.2.5. Scanning Electron Microscopy (SEM) of the microgel formulation

Microgel surface morphology analysis was undertaken in gastric and intestinal conditions, as demonstrated in Figure 3.20a-b. In gastric pH, microgel appear as tightly clumped and aggregated in nature, with minimum spaces between microgel network as opposed to microgel in intestinal medium, which show greatly swelled microgel network of particles with many spaces between them. The strong hydrogen bonds in gastric medium, between carboxylic and etheric groups of MAA and PEG respectively, clearly form tight networks of particles as opposed to dispersed particles in intestinal medium, which are greatly swollen in nature due to the ionization of the carboxylic groups of the particles. These studies further affirm the significant pH responsive nature of the particles, and their hydrophilic properties allowing them to constrict and swell accordingly. The tight network of particles in the microgel system clearly demonstrates their ability to adhere and form a composite trapping system for the loading of protein,

encapsulating the maximum capacity possible. Comparing the microgel system in basic medium, it evident that exponential swelling occurs giving rise to drug release and disintegration of the particle network.

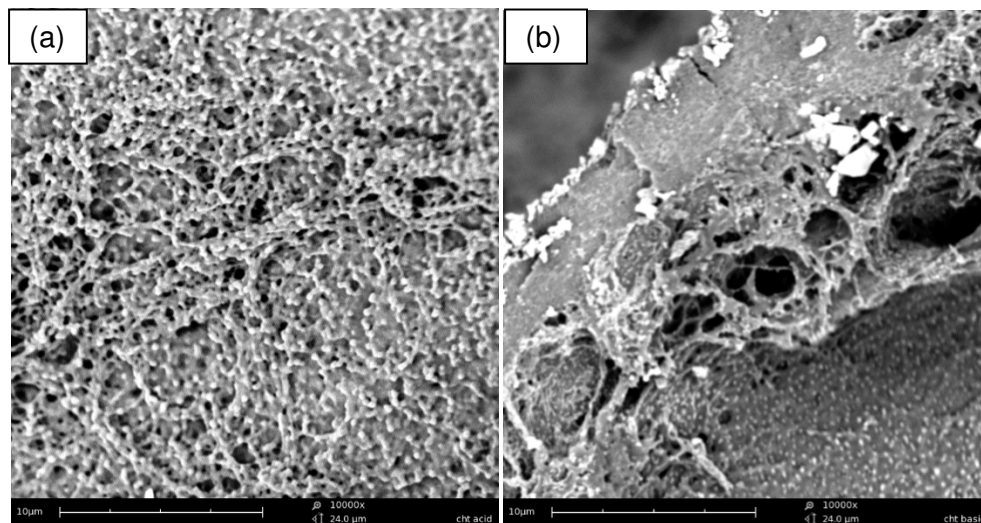


**Figure 3.20:** SEM images of copolymeric microgel at 10 000X magnification (a) in gastric medium (pH 1.2) (b) in intestinal medium (pH 6.8).

### 3.3.2.6. Mucoadhesive properties of the optimized copolymeric delivery system

Mucoadhesive studies were evaluated as a fundamental aspect for successful protein absorption across the intestinal epithelium, since the greater the mucoadhesivity of the microgel, the greater the retention time for adherence and drug release. Figure 3.21 demonstrates the percentage crosslinking of mucin to the copolymeric microgel for all the design formulations. It was clearly evident that the optimized formulation demonstrated the best mucoadhesive properties. Results obtained clearly showed an inverse relationship between the percentage crosslinker and the degree of mucoadhesion of the copolymeric particles. There was however the opposite effect seen with the concentration of CHT used, which was found to be proportional to the mucoadhesion. It can be explained that, as the percentage crosslinker in the formulation increases, the bonds in the copolymeric microgel are too strong for the polymer to swell and share charges with mucin, therefore at lower concentration, the copolymeric microgel has greater ability to share charges and adhere to mucin. CHT is the essential polymer, contributing its mucoadhesive properties to the copolymeric particles, possessing a considerable degree of electrostatic interactions with mucin, due to its cationic polyelectrolyte

nature, which allows significant absorption of peptide across the epithelial membranes (Sonia *et al.*, 2011).

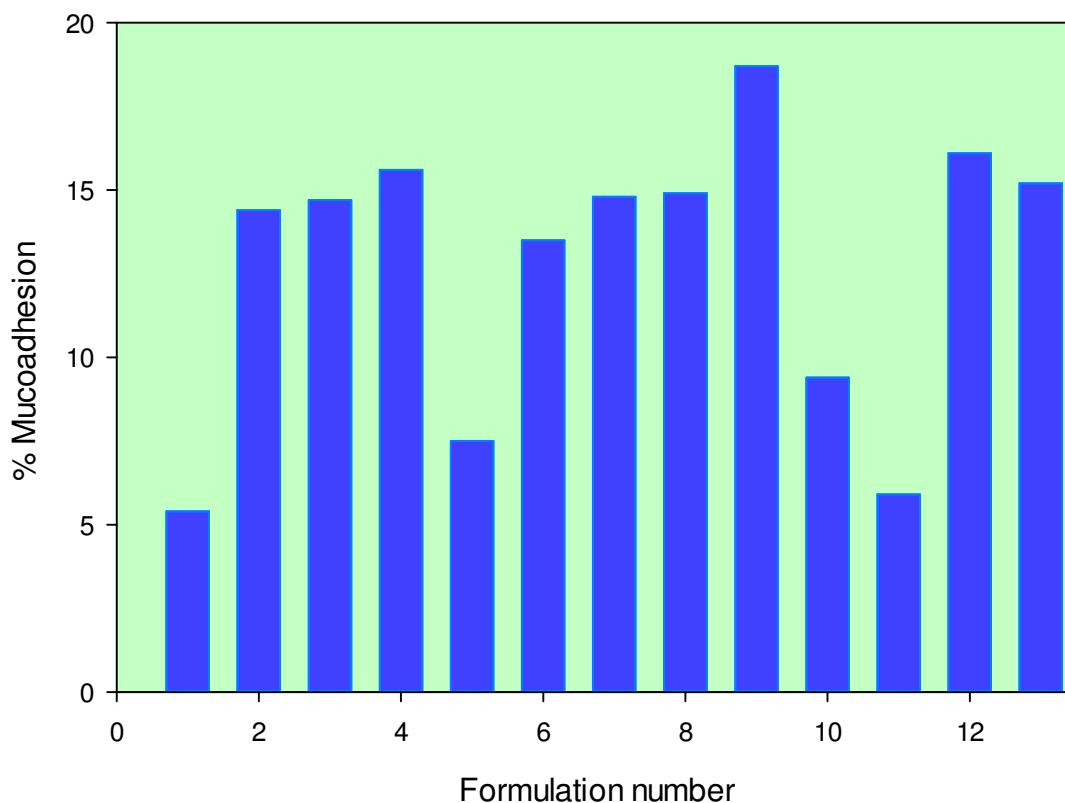


**Figure 3.21:** Percentage mucoadhesion crosslinking of prepared copolymeric microgel system to mucous

### 3.3.2.7. Differential Scanning Calorimetry (DSC) analysis of monomers and copolymeric microgel formulation

Thermal characterization was evaluated on polymers and the copolymeric micogel, to determine changes in endothermic/exothermic behavior. Calorimetry is the study of heat measurement, which is unique for all polymers and copolymeric formulations. In order for measurement of heat flow to be determined, an exchange of heat must occur within the instrument and the material analyzed. DSC thus measures the heat/heat flow of the sample as well as the rate of the heat flow. Thermal transitions can be evaluated in terms of its glass transition ( $T_g$ ), melting point

( $T_m$ ) as well as point of crystallisation ( $T_c$ ) due to chemical reactions that occur during heat flow measurements. Therefore DSC measures the change of the differentiation of the rate of heat flow to the reference sample and sample being analyzed, whilst being exposed to a controlled thermal parameter (Celej *et al.*, 2006). The reference sample used in the study comprised of a blank 40 $\mu$ L aluminium crucible. Heat capacity ( $C_p$ ) is the quantity of heat required to elucidate a temperature increase, requiring a certain amount of energy to elevate the temperature of 1g of sample by 1 K under constant pressure (Mettler Toledo Usercom 7, 1998; Xua *et al.*, 2000). During transitions such as  $T_m$  and  $T_c$ , heat flow is generally not measured due to the value being substantially great. Therefore the heat capacity of the system can be measured by the heat supplied divided by the resultant increase/change in temperature. It can thus be understood that heat capacity (HF) can be measured in terms of heat flow over the rate heating (HR) as shown in Equation 3.11.

$$C_p = HF/HR \quad \text{(Equation 3.11)}$$

As heating is undertaken on the polymers above the value of  $C_p$ , a significant adjustment of the thermogram would be noted, thus occurring once the polymer has reached the  $T_g$  value. This physical change transition is sometimes very subtle and cannot be detected in many polymers under standard heat ramping procedures (Fujimori *et al.*, 2005). The behavior of polymers below  $T_g$  appear hard/brittle in nature, however above this state, polymers exhibit elastic flow properties, possessing a higher heat capacity above the  $T_g$  value, than below it.  $T_g$  is taken from the midpoint of the curve, since the change in heat capacity occurs over a range of temperatures and not at a given point of a thermal event. In order for  $T_g$  to occur, a certain degree of disorder is required in the molecular structure of the polymer due to molecular interactions which are dependent on the degree of crosslinking in the sample (Maes *et al.*, 2005). Upon evaluation of the thermograms generated,  $T_g$  does not appear as a peak or trough as this is neither an endothermic or exothermic event, since heat is not given off or absorbed during this phase. This is called a second order transition, since there is a change in heat capacity, but as discussed no heat is absorbed or given off, unlike  $T_m$  and  $T_c$ , which are first order transitions. At temperatures above the  $T_g$ , the molecules exhibit a highly mobile sequence of activity, thereby aligning themselves in an ordered form of crystals, resulting in an exothermic event, thereby releasing a substantial amount of heat, depicted as a peak on the thermogram. The area within the peak, is indicative of the latent energy of the crystals, however the peak

represented in the thermogram indicates that the polymer has reached the stage of crystallization due to heat transition.

At the stage of  $T_m$ , the crystals of the polymeric structure break apart from the uniform order, thus reaching the stage of melting point of the polymer, absorbing significant amount of heat and appearing as a trough as depicted on the thermogram as an endothermic thermal event (Mettler Toledo Usercom 11, 1998).

After removing all moisture from the polymers, running samples from 25-110 °C, temperature settings from 25-350 °C was evaluated for all samples at 10 °C/min. Figure 3.22 depicts thermograms for polymers and the copolymeric microgel, evaluating thermal events observed from each sample. CHT displayed characteristic melting peak at 121 °C, thereafter reaching events of crystallization at 306 °C. Due to the sensitivity of  $T_g$ , this event could not be detected in the sample. PEGDMA displayed 2 melting peaks at 52.61 °C and 57.91 °C, due the crosslinked nature of the polymer. At 221 °C, the polymer displays a crystalline peak, thereby indicating an alteration in stability of the polymer. At 211 °C, PMAA displayed a melting peak with a greater area depicted from the thermogram. The copolymeric microgel displayed a single melting peak at 56.28 °C, indicating successful crosslinking of the polymers. After reaching 180 °C, the copolymeric system displays great crystalline nature, thereby indicating loss in stability and functionality of the formulation.

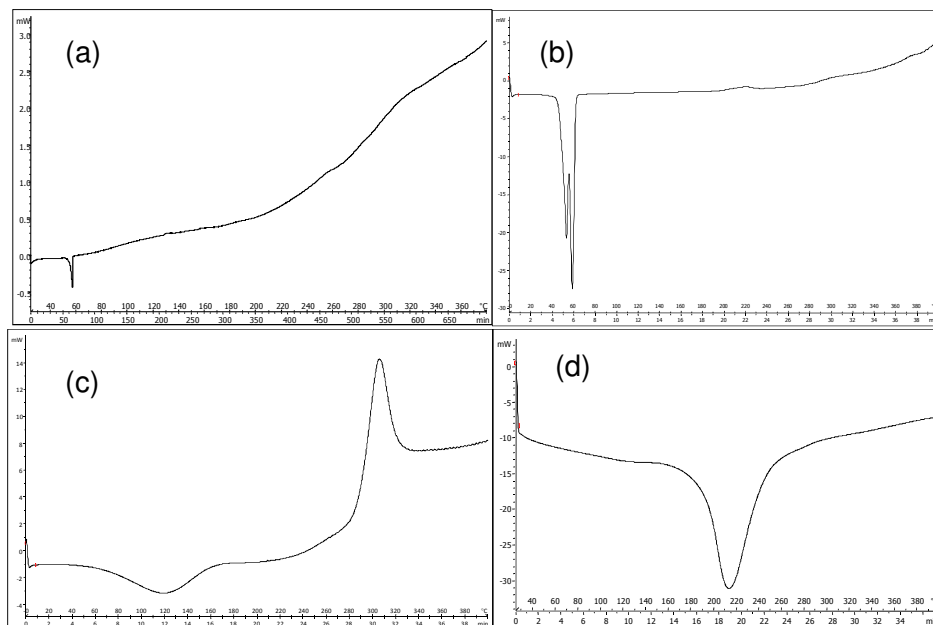


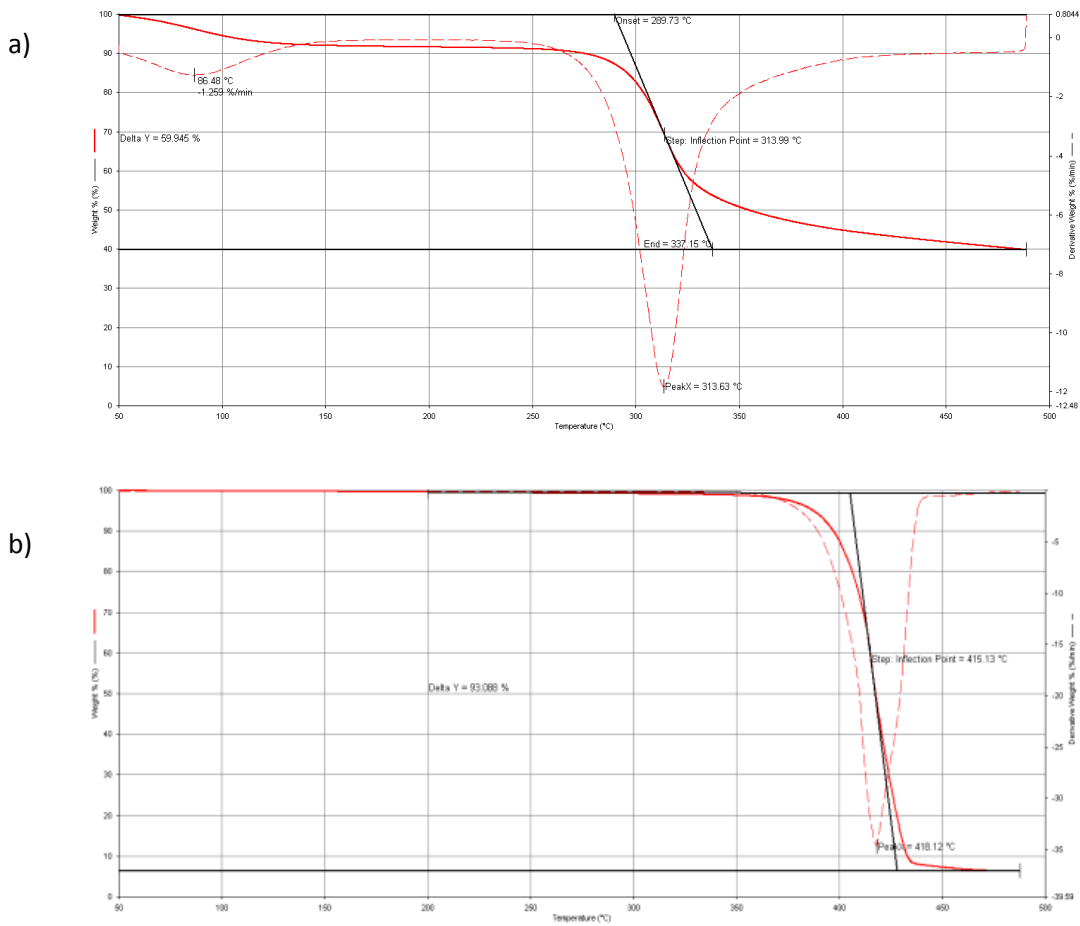
**Figure 3.22:** DSC thermograms for copolymeric microgel a) CHT-PEGDMA-MAA, and polymers b) PEGDMA, c) CHT, d) PMAA

### 3.3.2.8. Thermogravimetric analysis (TGA)

Thermogravimetric analysis is the study of determining the mass of a substance over a function of controlled temperature and time under standard atmospheric conditions. This technique analyses the change in weight of the sample as heat is passed at a constant rate. A TGA thermal curve is evaluated from left to right, as the downward dip in the curve represents weight loss in the sample. Samples were evaluated in triplicates for reproducibility of data. Variation in experimental data is an indication of a lack in reproducibility of sample preparation, temperature range, temperature scanning rate, calibration of the instrument, furnace cleanliness as well as sample atmosphere. Therefore, in order to attain reliability of results, all these factors have to be kept constant (www.perkinelmer.com, 2010).

Samples evaluated were analyzed from 50-550°C at a rate of 10°C/min, for determination of % degradation and liberation of moisture from the sample. CHT showed an initial loss of moisture of 1.26% at 86.48°C and a significant step of degradation of 59.94% at 313.61°C. PEGDMA showed no significant initial liberation of moisture content, however at 418.12°C, 93.1% of the polymer showed thermal degradation. Evaluation of CHT-PEGDMA-MAA copolymeric microgel

liberated 3.5% of water at 76°C and at 403.58°C, 44.66% of the polymer showed thermal degradation as depicted in Table 3.11. These characteristic degradation values were obtained from 1<sup>st</sup> derivate principles, calculating points of significant changes in % weight of the samples. This degradation point can be explained as the decarboxylation reaction that occurs in the copolymeric mirogel (Tomar *et al.*, 2011). It can also be confirmed that crosslinking occurred in the copolymeric microgel, since no separate degradation points were present in the optimized formulation. The copolymeric microgel demonstrates less water retention than CHT polymer after crosslinking occurred, thereby making the formulation more stable. Figure 3.23 demonstrates the changes in thermal events of the polymers and copolymeric microgel system, showing distinct variations in the thermal behavior of each sample.



c)

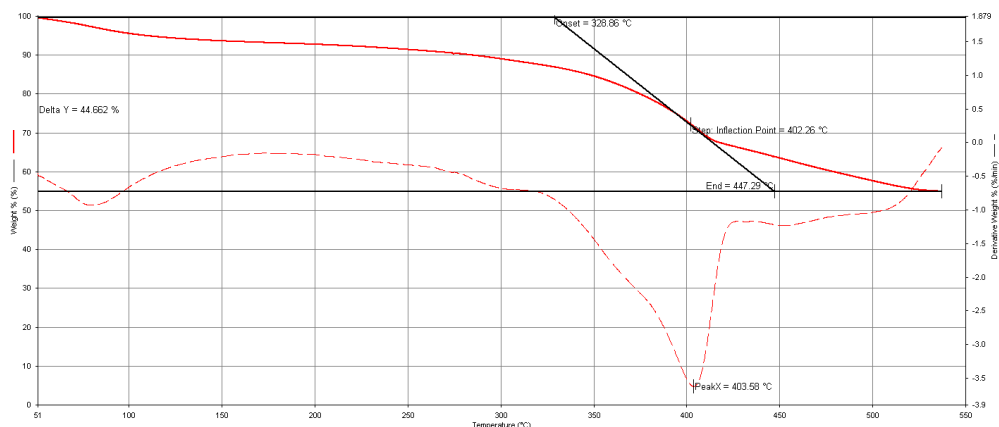


**Figure 3.23:** TGA profile representation of a) CHT, b) PEGDMA and c) CHT-PEGDMA-MAA

**Table 3.11:** TGA analysis of polymers and copolymeric microgel

Parameter	CHT	PEGDMA	CHT-PEGDMA-MAA
Maximum degradation temperature (°C)	314	418.12	403.5
Water loss at maximum temperature (°C)	86.48	Negligible	76
Percentage of water loss at maximal degradation temperature (%)	1.25	Negligible	3.5
Percentage of weight loss at maximal degradation temperature (%)	59.95	93.08	44.66
Weight remaining at 500 °C (%)	40.05	6.92	55.34

### 3.3.2.9. Mechanical evaluation of the copolymeric microgel tablet

MH and MR were conducted on the copolymeric microgel tablet, generating a force-distance and force-time graph respectively as depicted in Figure 3.24. Interpreting textural analysis, the area under the curve represents amount of deformation energy of the sample, whereas the gradient represents the flexibility of the sample. The MH was evaluated, using a 2mm diameter cylindrical stainless steel probe, where an indentation on the tablet, generated a regression curve, measuring the intensity of the intermolecular bond forces latent in the tablet amongst the interparticulate microparticles, thus measuring the amount of force required per millimeter of distance to induce an indentation on the tablet. This biomechanical property of the tablet is an important parameter in maintaining the stability of the tablet for appropriate drug release kinetics, since reverting back to the powder form will express a greater amount of drug released per given time (Ellison *et al.*, 2008). MR, as depicted in Figure 3.24(b) was determined as a

percentage of the ratio of the area under the curve (AUC), from peak to baseline, after removing the force initiated ( $AUC_{2-3}$ ), over the baseline to peak, before removing force ( $AUC_{1-2}$ ), on a force-time axis. MH as depicted in Figure 3.24(a) was calculated on the basis of the gradient generated from the curve of the initial force and maximum force derived on a force time axis (N/mm).

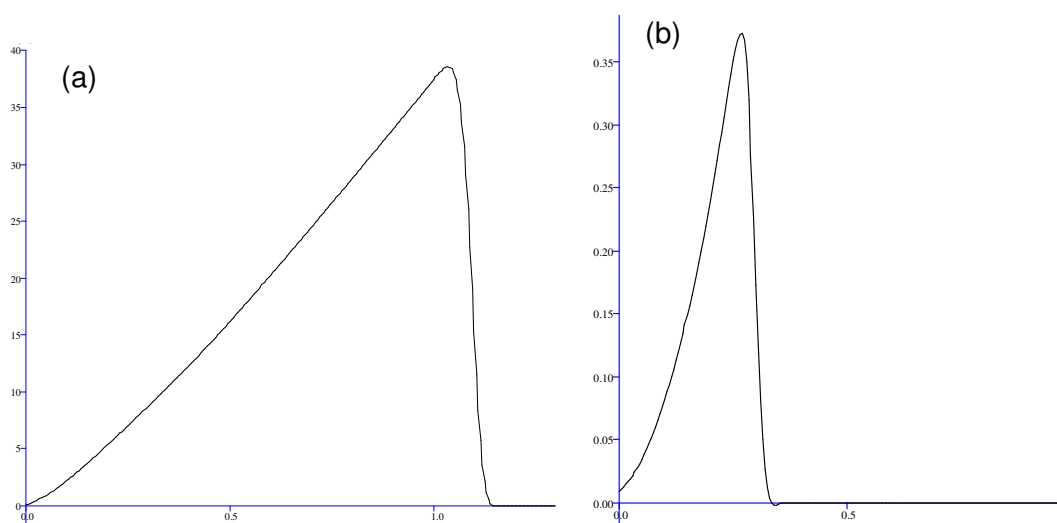


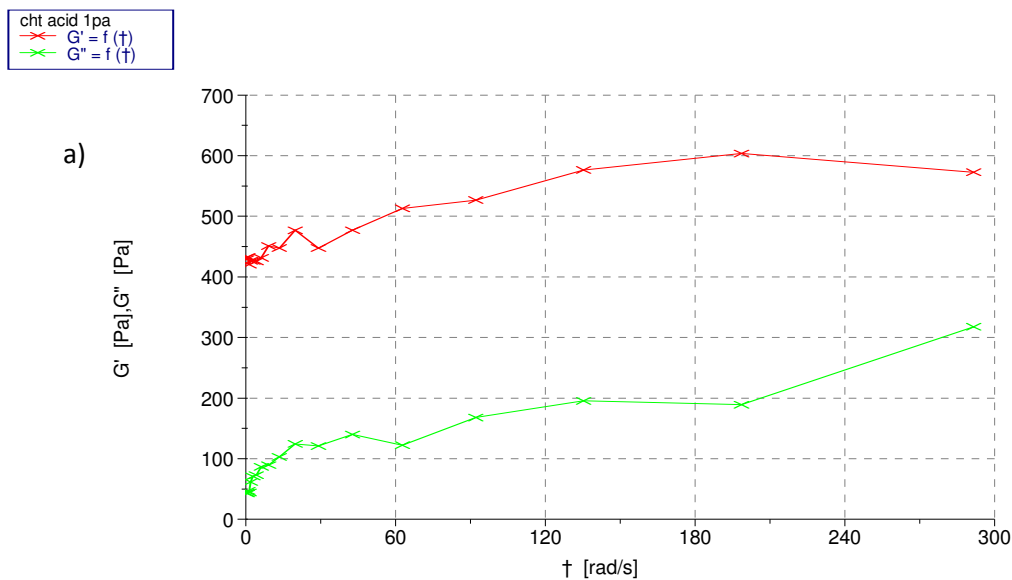
**Figure 3.24:** a) MH (N/mm) Grad net fd =80.016, Area Fd =0.009 b) MR (Kg/sec) = 30%

MH results obtained in Figure 3.24(a) indicated a gradient value of 0.009, representing a tight formation of bonding in the polymer matrix, even though a small compression force of 0.6MPa was used to compress the microgel. This MH value characteristic is essential due to storage/packaging parameters, as well as more physiological parameters of force to withstand swallowing and delayed release disintegration properties for desired outcomes. MR is an indication of the ability of a given substance to deform elastically, but revert to its original state, once the force is removed. The copolymeric microgel formulation demonstrated a 30% MR value, due to the viscoelastic nature of the copolymer and the degree of crosslinking of the microgel. Most compressed polymers don't share a great resilience profile, since the interparticulate particles have interfacing surfaces which have voids within the matrix structure, created during compression of the tablet process. As the void volume of the tablet has a greater capacity, the greater will be the ability of the tablet to return to its original form to a certain extent after compression, until the intermolecular forces between the interfacing surfaces collapse to a state where elastic deformation is replaced with plasticity deformation, i.e., permanent alteration in shape/structure of the tablet. Some highly durable polymers possess a greater number of

interfacing particle surfaces (physical interaction) or a high strength of interfacing particle surfaces (chemical interaction), in which case, the compression induced will not create elastic deformation in the structure. Therefore, as the intermolecular bonds stretch in the tablet, the greater the resilience properties of the tablet. It can therefore be concluded that the copolymeric microgel tablet formulation has good properties of mechanical nature, even at low pressures of compression, particles form good physical interaction, thus maintaining a good MH and MR profiles.

### 3.3.2.10. Rheological evaluation of the microgel formulation

The microgel copolymeric system was incubated in gastric and intestinal USP buffer of pH 1.2 and 6.8 respectively, to determine the pH sensitive behavior of the microgel in relation to its viscoelastic nature. A frequency sweep test was undertaken, in which  $G'$  is the measure of deformation energy latent in the microgel, during the shearing procedure.  $G'$  thus represents a measure of elastic behavior (solid phase) in the microgel and  $G''$  is a measure of viscous behavior (liquid phase), evaluating the deformation energy used in the microgel throughout the shearing duration and lost to the microgel thereafter. Figure 3.25 represents rheological analysis for the microgel in the different pH medium, using the same analytical parameters.



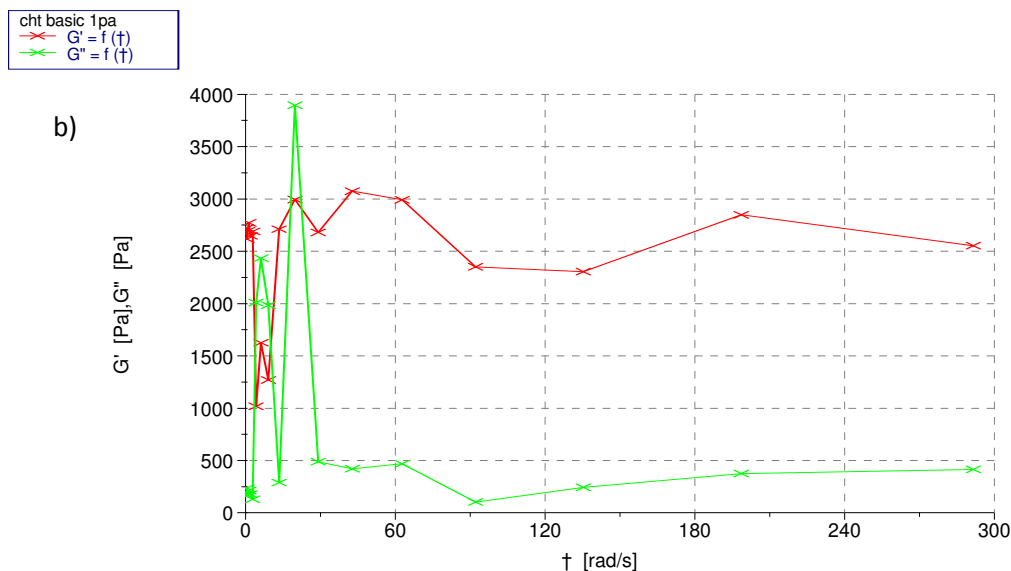


**Figure 3.25:** Dynamic oscillation curves depicting storage modulus ( $G'$  in red) and loss ( $G''$  in green) under constant strain of 0.1% a) in gastric medium pH 1.2 and b) in intestinal medium pH 6.8

As observed in gastric medium, the microgel maintains its solid state elastic behavior, since  $G'$  is greater than  $G''$ , and at no time does the viscous property of the microgel exceed the elastic nature. This exemplifies the solid, elastic property of the microgel under gastric conditions, with no  $G'/G''$  crossover. On examination of the molecular science of the microgel, hydrogen bonds are formed with carboxylic acid functionalities of MAA and etheric groups of PEG. This results in the clumping behavior, forming a greater composite mass of micronetworks, thus entrapping and preserving protein from enzymatic degradation. Using the same evaluation parameters, a variation in behavior was observed in intestinal medium. A crossover of  $G'$  and  $G''$  was observed, with  $G''$  exceeding  $G'$  during the early phase, demonstrating greater viscous behavior initially and switching to its solid elastic property as the frequency range increases. In intestinal medium, massive swelling of the microgel is observed and breaking of micronetworks due to ionization of carboxylic groups and interference of hydrogen bonding (Tomar *et al.*, 2011). This evaluation thus confirms the pH sensitive nature of the microgel, as a more viscous/mobile characteristic promoted greater disintegration and drug release from the microgel formulation, allowing successful delivery of the protein for site specific absorption. This increased rigidity in gastric medium allows greater mechanical strength in the microgel network, thus constricting in nature but clumping together forming a greater mass, allowing greater shielding and the least release of protein from the microgel.

### 3.3.2.11. X-Ray Diffraction (XRD) analysis of the microgel formulation

The technique of X-ray diffraction is a non-destructive characterization, determining the phase properties of various polymers and copolymeric formulations, thereby determining the amorphous or crystalline nature of the sample. During evaluation, X-ray beams are directed on the sample, monitoring the intensities of reflections (counts per second), in relation to the angle of scattering (Zhou *et al.*, 2009). As variations in the density of the electrons are observed, constructive interference and diffraction rings around the beam axis are produced. Every diffraction ring is correlated to a reciprocal lattice vector, produced from the crystal, as referred to from Bragg's law. The scattering angle is a result of the angle between the ring and the beam axis. Evaluation of highly crystalline samples, produce a diffractogram with distinctive peaks which are narrow and sharp in nature. The intensities as well as the positions of the peaks, subsequent to lattice spacing, display a specific phase and material, resulting in a fingerprint analysis of the sample. As the crystallinity of the sample is decreased, broadening of the peaks are observed, generating a lower sensitivity to detect crystallinity. The samples thus analyzed represent a diffractogram, relating the diffracted intensity to the observed scattering angle (Leuner *et al.*, 2000., Lifshin *et al.*, 1999., Zhou *et al.*, 2009).

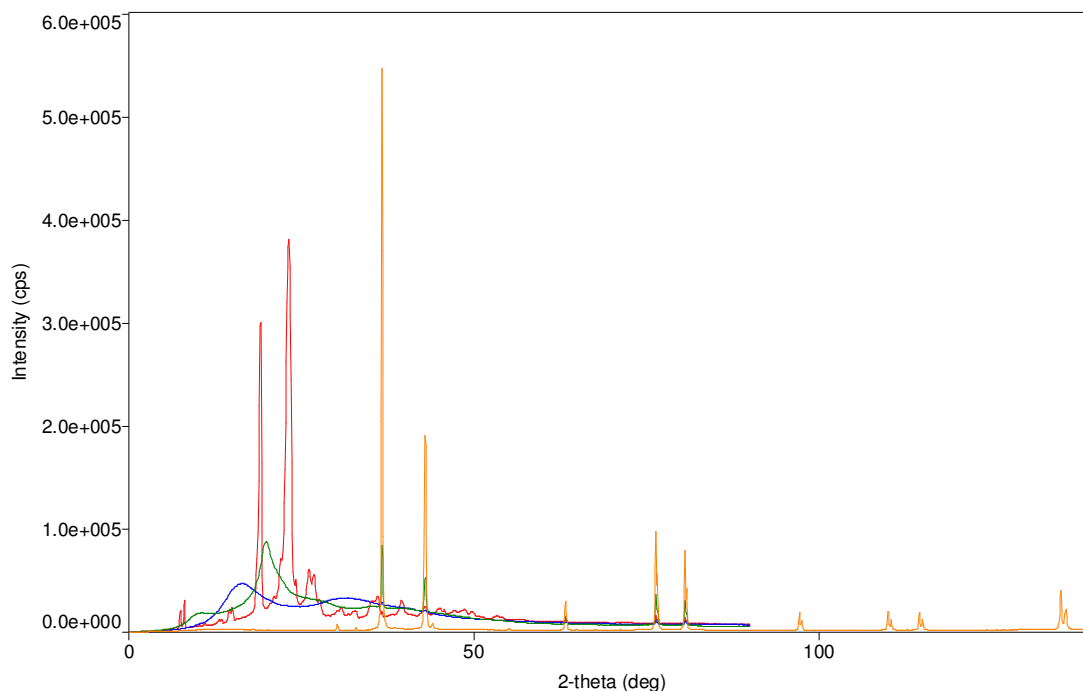


**Figure 3.26:** Diffractogram representing each polymer CHT(green), PEGDMA(red), PMAA(blue) and copolymer CHT-PEGDMA-MAA(yellow).

XRD analysis was undertaken on polymers CHT, PMAA, PEGDMA and copolymeric microgel CHT-PEGDMA-MAA. The degree of crystallinity was evaluated on each polymer, determining the effects of crosslinking on the copolymer, thereby increasing the rate of dissolution as the % of crystallinity is proportional to the rate of drug release. CHT showed 1.58% crystallinity, while PMAA showing less than 0.1% of crystalline nature. The polymer with the highest crystalline nature was PEGDMA, producing a 15.42% crystalline nature. After successful copolymerization, the microgel showed 20.9% crystallinity. Figure 3.26 represents the degree of intensity each polymer displays, thereby demonstrating low crystallinity as the area of the peaks are decreased. Since copolymerization increased the degree of crystallinity, a greater order in the structure of the copolymer network can thus be deduced.

### 3.3.2.12. NMR analysis

Chitosan is a well characterised backbone in literature (Saito *et al.*, 1987), however limited data is presented using Solid state (SS) NMR. To this end, we investigated the use of SS NMR as a recently used characterization method. The samples that were dry due to lyophilization and gave relative powder particles were analyzed and the spectrum presented below (Figure 3.27). Some samples that did not afford a dry powder and were not suitable for analysis. CHT displayed a clear acetyl moiety residue of  $\text{CH}_3$  ( $\alpha$ )  $\text{CO}$  ( $\beta$ ), in regions of  $\delta$  24 and 175ppm respectively. Evaluating spectrums of the polymers and copolymeric formulation, it was evident that functional groups were clearly shifted in the crosslinked copolymeric formulation. This can be attributed to the presence of the PEGDMA chain and crosslinked MAA. The peak represented at 46ppm in the crosslinked polymer represents  $\text{OCH}_3$  groups, clearly showing the functionalities of MAA in the crosslinked polymer. In the SS spectrum of MAA and PEGDMA,  $\text{C}=\text{O}$  is conjugated with  $\text{C}=\text{C}$ , this results in a further downfield chemical shift in  $\text{C}=\text{O}$ . However, in the spectrum of CHT-PEGDMA-MAA, there is a slight upward chemical shift for the many  $\text{C}=\text{O}$  functional groups. This is diagnostic that after successful free radical polymerization at  $\text{C}=\text{C}$ , we now have  $\text{R}-\text{C}=\text{O}$ . Additionally, in the spectra of MAA, the signal around 55ppm assigned to  $\text{H}_2\text{C}=\text{}$  and 70ppm assigned to  $=\text{C}$  is no longer present in the spectrum of CHT-PEGDMA-MAA. These reduced carbons however could not be assigned due to their peaks overlapped with carbons on chitosan backbone. Therefore SS NMR has great potential as a significant diagnostic tool to assay the success for the synthesis of novel chitosan crosslinked formulations. Figure 3.28 represents the copolymeric crosslinked polymer, being confirmed with

specifications from SS NMR, thereby indicating a conformational proposed structure for the resulting microgel system.

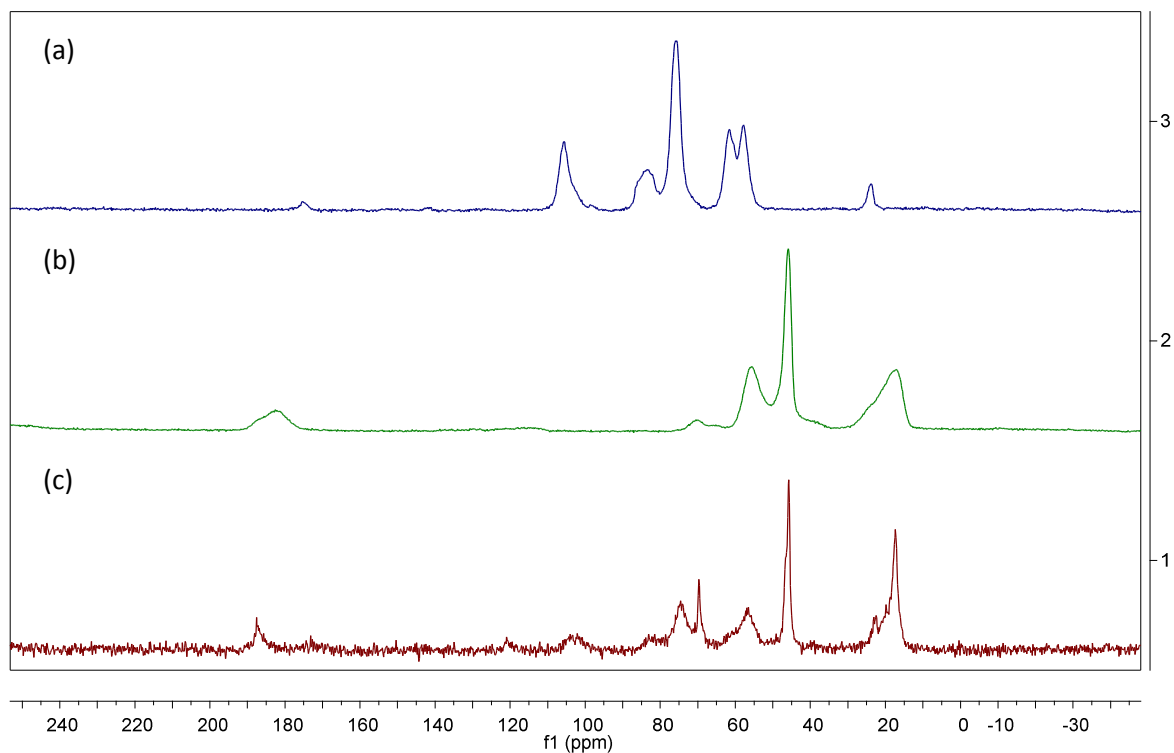


**Figure 3.27:**  $^{13}\text{C}$  solid state NMR spectra of a) chitosan b) MAA, and c) CHT-PEGDMA-MAA

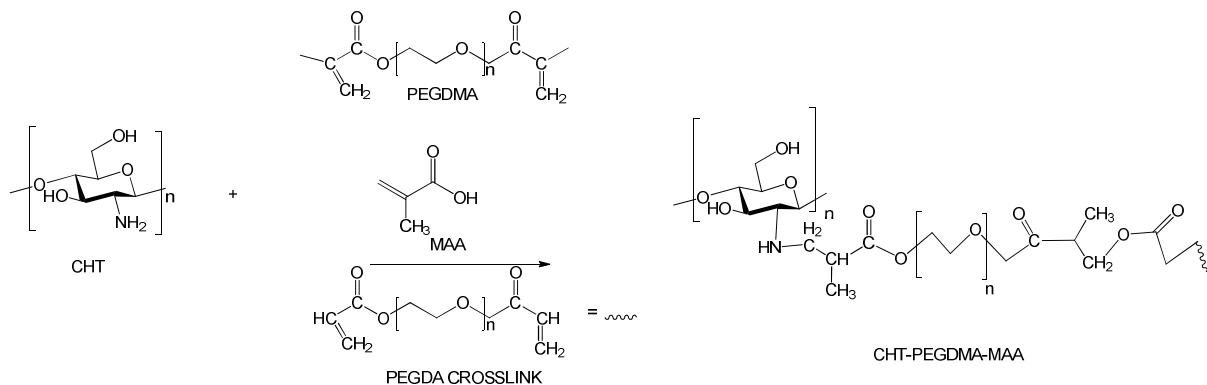


**Figure 3.28:** Reaction mechanism of the crosslinked copolymer with proposed structure for the microgel system.

### 3.3.3. Concluding Remarks

The optimized microgel tablet formulation was determined to constitute 0.5% CHT polymer concentration and 3% crosslinking agent, as calculated from results from the series of formulations derived from the Box Behnken design. FTIR analysis confirmed crosslinking of the copolymerized microgel formulation, further explaining angular deformation of N-H bonding of amino groups during the crosslinking reaction. The behavior of the microgel demonstrates clumps in large non-uniform masses in gastric pH due to strong hydrogen bonds, protecting and conserving the loaded protein. The microgel thus displayed more uniform distribution in intestinal medium, swelling and releasing loaded protein accordingly due to ionization of carboxylic groups. Porosity analysis was clearly correlated with SEM profiles, demonstrating greater pore sizes in intestinal medium as opposed to the minute pore size in gastric medium. Mucoadhesive studies demonstrated highest mucoadhesion in the optimized formulation possessing a considerable degree of electrostatic interactions with mucin, due to its cationic polyelectrolyte nature, thereby providing significant absorption across the GIT membranes. Thermographic representation indicates crosslinking of the copolymeric microgel, with a great amount of water released during the initial stage of heating. The mechanical properties of the compressed system further confirmed the tight formation of bonding in the polymer matrix with the smallest possible compression force of 0.6MPa for formation of a complete durable tablet to withstand swallowing and delayed release disintegration properties for desired outcomes. Rheological studies demonstrated the solid state elastic behavior in gastric medium and in intestinal medium demonstrating greater viscous behavior initially, thereafter switching to its solid elastic behavior as the frequency range increases. XRD analysis confirmed successful increase in crystallinity after crosslinking of the copolymeric microgel, compared to individual polymers, thus creating a greater network of stable copolymeric microgel delivery system. NMR analysis further confirmed the crosslinking of the copolymeric microgel, demonstrating the shifts occurring in relation to the polymers and resultant copolymeric system. The next step in the evaluation of the microparticulate and microgel formulations are the degree of drug loading and drug release, which are extensively discussed in the next chapter, correlating the physiochemical and biomechanical properties to the *in vitro* behavior of these formulations.

## CHAPTER 4

### PROTEIN LOADING AND *IN VITRO* RELEASE ANALYSIS OF THE ORAL MICROPARTICULATE AND MICROGEL DRUG DELIVERY PLATFORMS

#### 4.1. Introduction

*In vitro* protein-loading studies are essential for determination of the capacity of drug release, thereby providing a site specific dose for absorption across epithelial membranes. Protein-loading and release analysis was carried out on all Box-Behnken formulations of TMC-PEGDMA-MAA and CHT-PEGDMA-MAA. As a prototype model protein, insulin was selected for all design formulations due to the cost implications incurred for such a vast range of analysis in triplicate for INF- $\beta$  and EPO. Insulin drug-loading and release of the formulations were tested using HPLC analysis as this was found to be highly reliable and precise for drug concentration determination. Insulin, INF- $\beta$  and EPO were evaluated on the optimized formulations in the respective gastric and intestinal medium. All samples were analyzed for 2.5 hours in gastric medium and 24 hours in intestinal medium. All physiological conditions were maintained during drug release studies, thereby promoting most significant data available for analysis. Evaluating the loading capacity of the microgel/copolymeric particulate system, it can be explained that neutral PEG chains interacted with carboxylic groups which were negatively charged, thus shielding the protein from surrounding charges (Foss *et al.*, 2004). It is well documented that PEG has a high affinity for protein molecules, and is also one of the reasons why PEG is so essential in the stability of the loaded protein (Lowman *et al.*, 2000; Veronese *et al.*, 2005).

In gastric medium, the microgel and microparticulate system constricts and clumps in nature, protecting its protein loaded contents. At low pH values, carboxylic groups interact with ether functional groups of PEG, therefore forming strong hydrogen bonding between the particles that would result in smaller particles at gastric pH. In intestinal medium, a converse behavior of the particles is observed. Massive explosion/swelling of these systems are clearly noted allowing the release of the loaded protein, thereby expressing its pH sensitive nature of the crosslinked copolymeric systems. Particles appear dispersed as more or less distinct identities because of the breaking of hydrogen bonding and ionization of carboxylic groups.

This chapter entails a detailed study of the pH sensitive nature of the microgel and microparticulate systems in relation to their drug loading capacity and release profiles. Part A of

this chapter will discuss the microparticulate formulation and Part B will discuss the microgel formulation.

## 4.2. Materials and Methods

### 4.2.1. Materials

PEG ( $M_w=4000\text{g/mol}$ ), MAA, methyl iodide, polyethylene glycol diacrylate (PEGDA), Chitosan (CHT) (medium  $M_w=450\text{kDa}$ ), sulfonic acid and azobisisobutyronitrile (AIBN) were obtained from Sigma-Aldrich (St. Louis, MO, USA). Erythropoietin beta (Recormon<sup>®</sup>), Roche Ltd, Basel, Switzerland. Humuinsulin-R (Actrapid<sup>®</sup>, r-DNA origin) of 100I.U./mL was purchased from Eli Lilly and Company (USA). INF- $\beta$  1a (Rebif<sup>®</sup>) and *N*-methyl-2-pyrrolidone was procured from Merck (Merck (Pty) Ltd, Estate South, Modderfontein, Gauteng, South Africa) at reagent grade and was used without further purification. Verikine<sup>™</sup> Human INF- $\beta$  ELISA kit was obtained from PBL Interferon Source, Piscataway, USA. Erythropoietin Human ELISA Kit was purchased from Abcam<sup>®</sup>, Cambridge, USA. All other reagents were of analytical grade and used as received.

### 4.2.2. Protein-loading in copolymeric microgel and microparticulate systems

Insulin-loading was carried out by dispersing 1g of copolymeric particles in 5mL solution of insulin (pH 7.4) for a time period of 8 hours, to attain maximum loading. Thereafter pH of the solution was gradually lowered to 2.5 by adding 1N HCL solution to allow entrapment of insulin in the particles. The particles were then filtered and lyophilized using a Freezone 12 freeze drier (Lanconco, Kansas City, USA), during which a 2 hour condensation phase at  $-60^\circ\text{C}$  was followed by a 24 hour sublimation phase at 25mm Torr. Concentration of left over insulin in the filtrate was evaluated by HPLC and Equation 4.1 was used to determine the entrapment efficiency of the protein in the particles (Tomar *et al.*, 2011).

*% Entrapment Efficiency =*

$$\frac{\text{theoretical amount of protein loaded} - \text{amount of protein measured from filtrate}}{\text{theoretical amount of protein loaded}} \times 100$$

(Equation. 4.1)

The optimized formulations were used for INF- $\beta$  and EPO loading according to the same procedure, as undertaken for insulin loading and subsequent lyophilization. The concentration of INF- $\beta$  in the filtrate was analyzed by using Verikine<sup>™</sup> Human INF- $\beta$  ELISA kit, at 450nm wavelength using a VICTOR X3 Multilabel Reader (PerkinElmer, Waltham, MA, USA) and EPO

was analyzed using Abcam® Erythropoietin Human ELISA Kit at same wavelength settings as INF-  $\beta$ .

Insulin concentration was determined by employing C<sub>18</sub> silica phase Symmetry 300 column of particle size 5 $\mu$ m with a Waters 1525 Binary Pump with 2489 UV/visible detector and an auto-sampler attachment for multiple sample queue analysis. The absorbance was recorded at a wavelength was 214nm and a constant column temperature of 25°C was maintained throughout the analysis. The mobile phase comprising of a mixture of solvent A and solvent B in a ratio of 24:76 had a flow rate of 1.0mL/min. Solvent A was pure acetonitrile (99.98%) of UPLC grade and solvent B was sodium sulfate buffer (pH 2.3).

#### **4.2.3. Protein release studies undertaken on all Box-Behnken design and optimized formulations**

*In vitro* protein release studies were performed with all the Box-Behnken experimental design formulations at both gastric and intestinal pH conditions for both microparticulate and microgel formulations. For conducting these studies, lyophilized insulin, INF- $\beta$  and EPO loaded particles were accurately weighed individually and placed on a punch and dye apparatus for preparing a tablet of 4mm diameter, using a hydraulic pressure of 0.6MPa. The punched tablets (2 tablets with 100I.U each of insulin) were placed in 50mL of simulated gastric (pH 1.2) and intestinal (pH 6.8) USP buffer for duration of 2.5 hour and 24 hour, respectively. An Orbit shaker incubator (LM-530-2, MRC Laboratory Instruments Ltd, Hahistadrut, Holon, Israel) at 37 $\pm$ 0.5°C and 50rpm was used to incubate all samples during the release duration.

At every time point 0.5mL of sample withdrawn for analysis was replaced with the same volume of fresh buffer, in order to maintain physiological sink conditions during the complete release studies. Samples were withdrawn from simulated gastric release buffer every half an hour for 2.5 hour duration, and at an hourly interval from the intestinal release buffer for 24 hours. All samples extracted were filtered using a 22 $\mu$ m Millipore Millex filter (Billerica, MA, USA), into HPLC vials and stored at 4-8°C. To prevent degradation of protein release samples, they were evaluated by HPLC within 3 hours of sampling. The concentration of the samples were evaluated from the area under the curve and calculated using the standard curve to deduce the concentration of insulin present. INF- $\beta$  drug release studies from the prepared particles were similarly undertaken in both the mediums (1 tablet of 14.6 $\mu$ g of INF- $\beta$ ) as elucidated for insulin release studies and the samples were analyzed using a Verikine™ Human Interferon beta ELISA kit, at a wavelength of 450nm, with the use of a VICTOR X3 Multilabel Reader

(PerkinElmer, Waltham, MA, USA). EPO tablets contained a loaded dose of 100IU, using 2 tablets for each release study medium. EPO concentration was calculated using an ELSIA kit detected at wavelength 450nm (Abcam<sup>®</sup> Human EPO ELISA kit).

## **4.3 Results and Discussion**

### **4.3.1. PART A: Evaluation of TMC-PEGDMA-MAA Microparticulate System using Insulin, EPO and INF- $\beta$ as Optimized Protein Delivery Systems**

#### **4.3.1.1. Protein-loading evaluation for each protein microgel formulation**

The mechanism of insulin, INF- $\beta$  and EPO loading can be simply analyzed with respect to the pH at which loading is accomplished. The copolymeric particulate carrier system significantly swells at pH 7.4, expanding large enough to allow the protein to diffuse into the particles. The strong ionization of MAA due to carboxylic functional groups significantly allowed higher absorption level of these proteins into the particles. Further, upon reducing the pH of the encapsulating medium to 2.5, carboxylic groups get complexed with etheric groups of PEG, decreasing the size of the polymeric network due to strong hydrogen bonding occurring between the particles, thus entrapping the absorbed protein within the particulate system. After 8 hours of incubating the protein at pH 7.4 and thereafter changing the pH to 2.5, it can be explained that neutral PEG chains interacted with carboxylic groups which were negatively charged, thus shielding the protein from surrounding charges (Foss *et al.*, 2004). It is well documented that PEG has a high affinity for protein molecules, and is also one of the reasons why PEG is so essential in the stability of the loaded protein (Veronese *et al.*, 2005; Lowman *et al.*, 2000).

The result of insulin entrapment efficiency of the respective experimental design formulations is documented in Table 4.1. Relating this to the particle size presented in previous chapter, it could be distinguished that particles with greater sizes, demonstrated higher loading. Some formulations however displayed lower encapsulation values, possibly due to a high degree of carboxylic functional groups on the surface of the particles as noticed in FTIR analysis, maintaining its high acid value. It is evident from Table 4.1, that the degree of drug loading in comparison to particle size in the swelled state correlate significantly, thus a proportional relationship can be deduced between particle size and drug loading efficiency. It is also noted that, as the percentage of crosslinker and TMC concentrations were increased in the formulation, the protein loading increased substantially.

All proteins were loaded using a transitional pH encapsulation method, to obtain maximum drug loading efficiency. Insulin showed 58.78% drug entrapment, in comparison to INF- $\beta$  and EPO, which showed a lower entrapment of 53.25% and 44.2%, respectively. It was significantly noted that as the size of the protein molecule increased from insulin to INF- $\beta$  and greatest in EPO, the loading capacity decreased in the copolymeric particles due to the significant size transitions of the proteins.

#### **4.3.1.2. *In vitro* release analysis on design and optimized formulations**

*In vitro* insulin release was carried out in gastric and intestinal USP buffer medium, simulating GIT conditions. Table 4.1 summarizes the fractional release (FR) data at a 2 hour time point in both mediums and maximum at pH 6.8 over the duration of studies. Each formulation was intended for minimum drug release in gastric conditions and maximum release in intestinal condition. The maximum drug release in the intestinal medium was observed to be in the middle region of both variable limits. The accountability of greater drug release in gastric medium than intestinal medium at a 2 hour duration point is due to the further constriction of the polymer at a lower pH, thereby releasing drug at a faster pace, however not beyond certain degree which itself did not ever exceeded the amount released in the total duration of intestinal conditions in a sustained slow release manner. Formulations having high percentage crosslinker, such as F12, regardless of having the highest drug entrapment, resulted in the lowest amount of drug released, due to the strong interparticulate crosslinking preventing protein release from particulate system. On the other extreme, the lowest percentage of crosslinker in the formulation, as seen in F7, showed a minimum amount of drug released in gastric environment, and above 80% release in intestinal conditions. It can therefore be concluded that the percentage of crosslinker used has a significant impact on the amount of drug released in both gastric and intestinal conditions. The optimized formulation for effective peptide delivery was therefore selected by the Box-Behnken design as F7. Its shrinkage in gastric environment, rendering minimum release, was most desirable, protecting the peptide to the maximum capacity possible and releasing drug to a substantial amount in intestinal environment. Figure 4.1a-b represents insulin release rates in gastric medium and Figure 4.2a-b represents insulin release rates in intestinal medium for all experimental design formulations.

The optimized formulation, in accordance to the Box-Behnken experimental design, was finally evaluated as a versatile delivery system for all the above proteins. After a maximum of 2.5 hour

duration in gastric simulated fluid, insulin showed a fractional release of 3.2% in comparison to intestinal fluid, in which a maximum of 83% of insulin was released. INF- $\beta$  released a similar 3% in gastric medium after 2.5 hours, and a maximum of 74% in intestinal conditions. EPO drug release studies showed a 9.7% in gastric medium, and 81.3% drug release in intestinal conditions. Figure 4.3a depicts fractional release of proteins in gastric medium over 2.5 hour duration. Figure 4.3b depicts fractional release of proteins in intestinal medium, in which maximum drug release occurred over 8 hour duration. These diverse characteristic release rates at gastric and intestinal pH conditions further exemplifies minimum loss of the peptide drug in gastric environment and maximum release at the intestinal site of absorption.

**Table 4.1:** Experimental design formulation analysis for protein loading efficiency and release

<b>Formulation</b>	<b>TMC* (g/100mL) %<sup>w</sup>/<sub>v</sub></b>	<b>Crosslinker (%<sup>w</sup>/<sub>w</sub> of momomer)</b>	<b>% entrapment efficiency</b>	<b>% FR** (pH 1.2) at 2 hours</b>	<b>% FR** (pH 6.8) at 2 hours</b>	<b>Maximum % FR (pH 6.8) at 8 hours</b>
1	0.5	5.5	45.5	15.2	6.2	97.2
2	0.275	3	59.4	12.5	11.0	95.0
3	0.5	8	71.18	3.07	18.5	43.0
4	0.275	5.5	60.93	52.3	12.9	86.3
5	0.275	5.5	74.69	54.8	41.4	83.0
6	0.275	5.5	72.13	65.6	54.3	84.0
7	0.5	3	58.78	3.2	16.3	83.0
8	0.05	8	51.26	26.3	27.3	96.6
9	0.275	5.5	71.97	42.1	60.4	74.00
10	0.05	5.5	16.72	21.2	57.5	66.4
11	0.275	5.5	63.41	46	10.0	84.0
12	0.275	8	99.4	9	6.3	22.9
13	0.05	3	34.204	2.8	20	43.4

\*Trimethyl chitosan, \*\* Fractional release

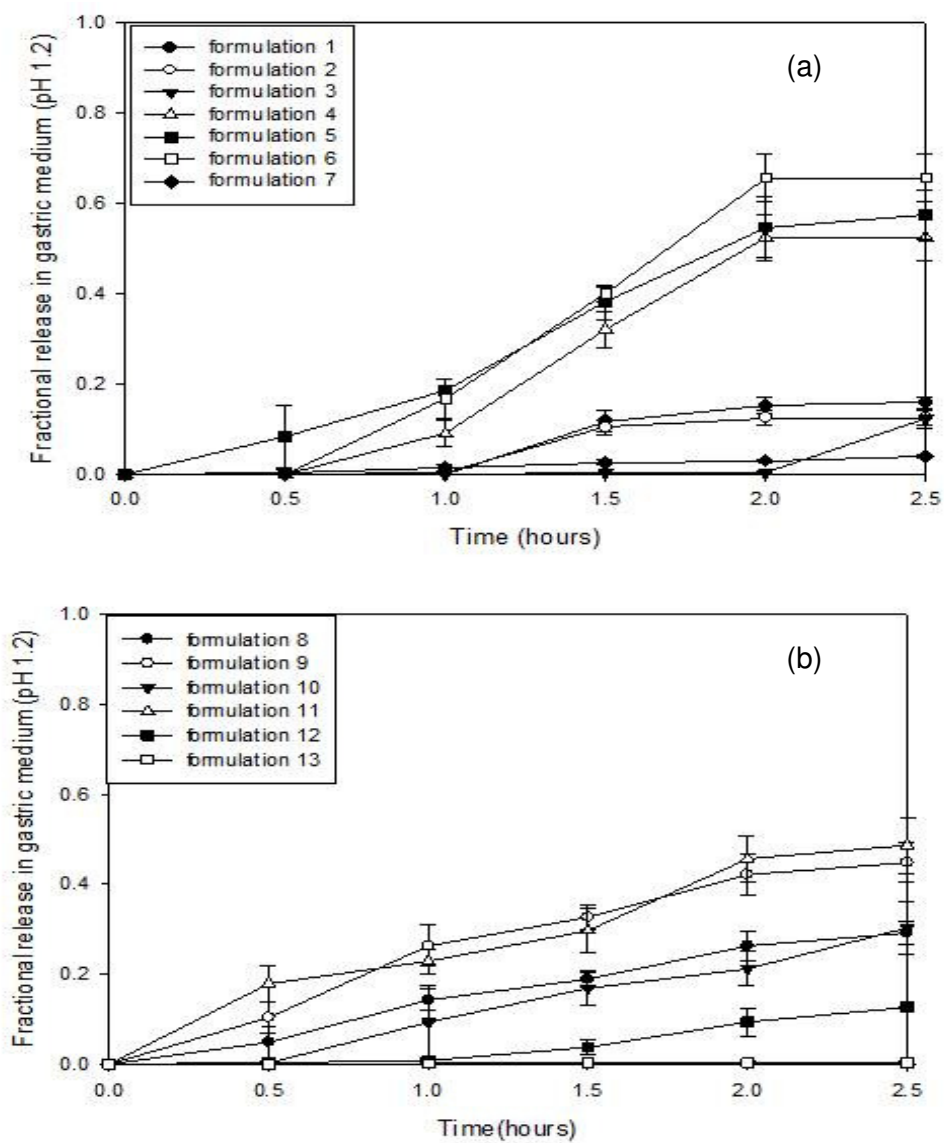


**Figure 4.1:** Fractional release of from TMC-PEGDMA-MAA insulin in gastric medium: a) F1-7, b) F8-13.

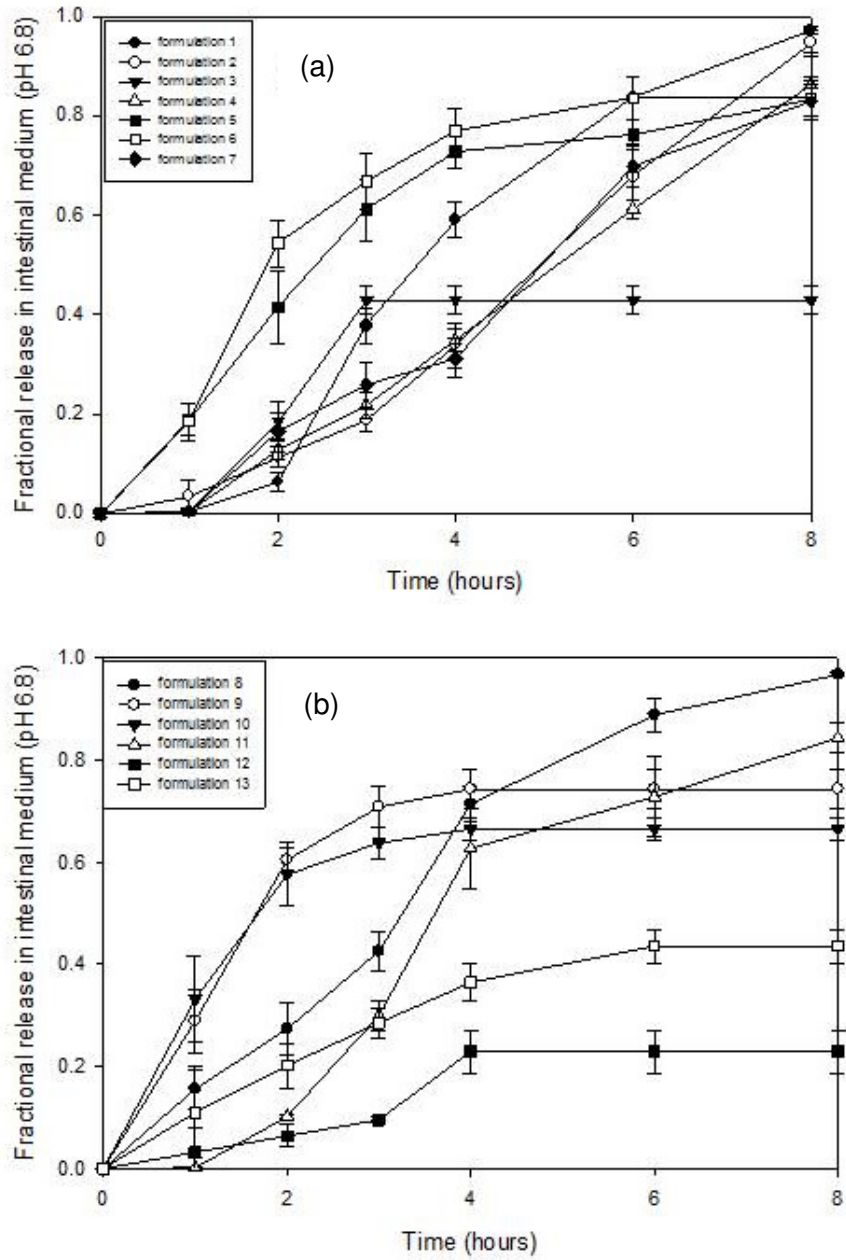


**Figure 4.2:** Fractional release of insulin from TMC-PEGDMA-MAA in intestinal medium: a) F1-7, b) F8-13.

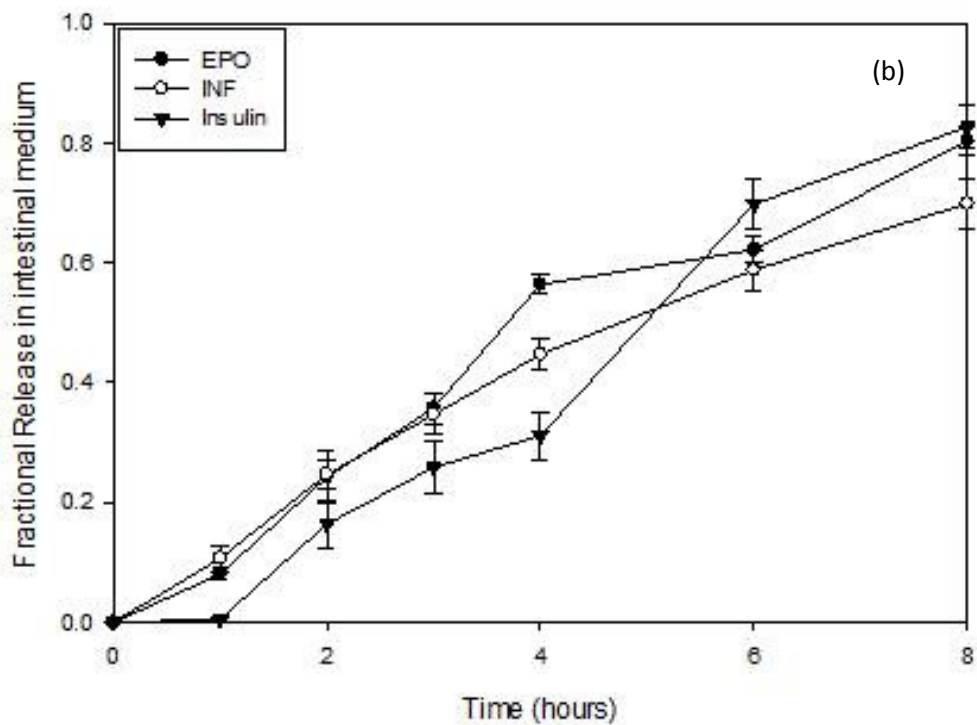
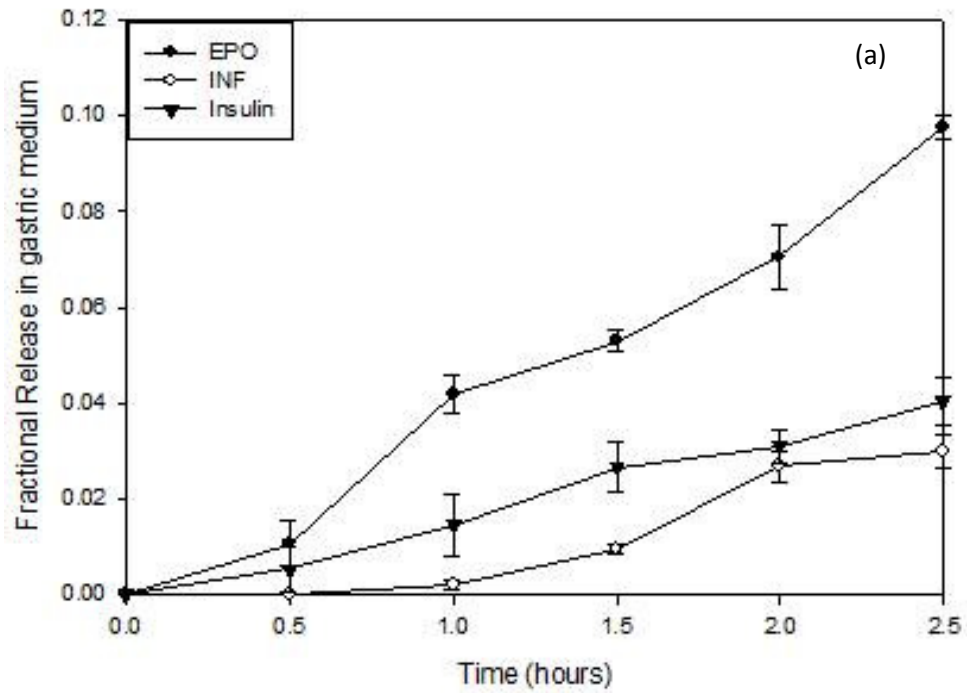


**Figure 4.3:** (a) Fractional release of proteins in gastric medium, (b) Fractional release of proteins in intestinal medium

### 4.3.2. Concluding Remarks

Protein-loading analysis was undertaken on all designed formulations. It was clearly evident that particles with greater sizes, demonstrated higher loading efficiencies. Formulations with low encapsulation can be attributed to high degree of carboxylic functional groups, maintaining a high level of acidity, thereby decreasing the degree of swelling in the microgel formulation. A conclusive finding was observed in which loading efficiency in comparison to particle size in the swelled state demonstrated significant correlation. The percentage of crosslinker and TMC concentrations were proportional in nature to the protein loading. Insulin demonstrated 58.78% drug entrapment, in relation to INF- $\beta$  and EPO, which showed a lower entrapment of 53.25% and 44.2% respectively. Results clearly demonstrated an increase in the size of the protein molecule, from insulin to INF- $\beta$  and greatest in EPO, demonstrating a decrease in the loading capacity of the copolymeric particles in the same order respectively. Protein release studies demonstrated substantial release kinetics in both mediums observed in the middle region of both variable limits. Formulations possessing a high percentage crosslinker demonstrated the lowest amount of protein released over time, due to the strong interparticulate crosslinking thereby preventing protein release. Formulations with the lowest percentage of crosslinker in the formulation showed a minimum amount of drug release in gastric environment, and greater than 80% release in intestinal medium. The optimized formulation of insulin demonstrated a 3.2% in gastric medium as compared to intestinal medium in which a maximum of 83% was released. INF- $\beta$  delivered 3% in gastric and a maximum of 74% in intestinal medium. EPO studies released a maximum of 9.7% in gastric medium and 81.3% protein release in intestinal conditions. It can therefore be concluded that the percentage of crosslinker used has a significant impact on the amount of protein released in both gastric and intestinal conditions, due to the degree of interparticulate bonding observed.

## **4.3.2. PART B: Evaluation of CHT-PEGDMA-MAA Microgel System using Insulin, EPO and INF- $\beta$ as Optimized Protein Delivery Systems**

### **4.3.2.1. Protein-loading evaluation for each protein microgel formulation**

Due to the significant pH responsive properties of the copolymeric particles, a substantial ability of the microgel to absorb and entrap protein allows for a protective platform for the loaded peptide. Due to strong ionization of carboxylic functionalities due to MAA, a great amount of protein is able to be absorbed into the particles. When the pH of microgel is reduced to 2.5, the carboxylic groups complex with etheric groups of PEG, thus constricting and entrapping maximum peptide in the particles. PEG has a great affinity for peptide molecules, therefore increasing the stability and entrapment of the protein loaded copolymeric microgel (Veronese *et al.*, 2005). As discussed in Chapter 4, section 4.3.1.1, protein loading efficiency demonstrated a proportional relationship with the size of the copolymeric particles. Microgel which demonstrated a lower loading efficiency can be attributed to the high degree of carboxylic functionalities in the formulation, therefore maintaining a low pH nature, allowing less absorption of protein into the particles. It was also observed that, as the concentration of CHT and percentage crosslinker increased in the formulation, the loading also increased accordingly as seen in Table 4.2.

Protein-loading studies demonstrated a 25.3% loading efficiency for EPO, 31.5% for INF- $\beta$  and 38.01% for insulin. An inverse relationship was observed with the size of the protein molecule and the percentage drug loading efficiency. Due to smallest size of insulin, greater amount was encapsulated into the particles, as opposed to EPO, which has the highest molecular weight from the 3 proteins, therefore observing the least percentage encapsulation.

**Table 4.2:** Experimental design formulation analysis for protein-loading efficiency and release

Formulation	CHT* (g/100mL)	Crosslinker (%w/w monomer)	% entrapment of efficiency	% FR** (pH 1.2) at 2 hours	% FR** (pH 6.8) at 2 hours	Maximum % FR (pH 6.8) at 8 hours
1	0.05	8	18.1	0.26	0.438	0.98
2	0.275	5.5	58.6	0.385	0.499	0.82
3	0.05	3	33.35	0.177	0.520	0.86
4	0.275	5.5	60.82	0.68	0.550	0.84
5	0.275	8	33.81	0.503	0.191	0.95
6	0.5	5.5	47.73	0.268	0.142	0.57
7	0.275	3	58.26	0.298	0.058	0.86
8	0.275	5.5	64.1	0.541	0.429	0.79
9	0.5	3	38.01	0.162	0.240	0.81
10	0.05	5.5	49.72	0.391	0.455	0.53
11	0.5	8	56.56	0.292	0.132	0.64
12	0.275	5.5	60.19	0.670	0.640	0.84
13	0.275	5.5	63.49	0.588	0.633	0.86

\*Chitosan ,\*\* Fractional release

#### 4.3.2.2. *In vitro* protein release analysis on design and optimized formulations

All Box-Behnken formulations were evaluated in the respective gastric and intestinal simulated buffer. Each formulation was intended for least insulin release in gastric medium, and maximum release in intestinal medium as discussed in Part A. It was evident that formulations with a high percentage crosslinker and low CHT concentration, demonstrated the greatest drug release over 8 hour duration in both gastric and intestinal conditions as seen in Table 4.2. Some formulations released a greater concentration of insulin over 2 duration in gastric than intestinal medium. This is attributed to the instant transitional stage of the particles, constricting and resulting in a massive release of insulin. However, this release does not exceed the total amount of insulin released gradually in intestinal medium over the 8 hour duration. Microgel with lower percentage crosslinker also demonstrated lower insulin loading efficiencies with least insulin release in gastric medium and above 80% release in intestinal medium. It is therefore conclusive that the percentage of crosslinker used in the formulations has a significant impact on protein loading and drug release in gastric and intestinal medium. Figure 4.4a-b, demonstrates the drug release properties of the Box-Behnken series of formulations in gastric

medium over 2.5 hour duration using insulin as the prototype for the design of the optimized formulation. Figure 4.5a-b, demonstrates the drug release properties of the Box Behnken series of formulations in intestinal medium over 8 hour duration.

The pH responsive nature of the microgel was evaluated for all protein loaded copolymers, evaluating the release behavior in gastric and intestinal conditions. In gastric medium, insulin showed the most release of 23.3% as opposed to EPO and INF- $\beta$ , demonstrating a 12.9% and 10.1% respectively as illustrated in Figure 4.6a. It can further be explained that, since insulin is the smallest protein molecule of the 3, there is a greater ability of the loaded microgel to release more protein due to the greater surface area the insulin loaded particle possesses. Protein release behavior in intestinal medium demonstrates that 80.6% of insulin was released, as compared to 59.6% and 61.8% of EPO and INF- $\beta$  respectively as illustrated in Figure 4.6b . The ionization of the bonds in intestinal medium, allow maximum swelling of the microgel, thereby releasing the loaded protein. EPO was observed to show the least drug release as well as the lowest drug loading, due to the greatest size of the protein molecule, compared to insulin and INF- $\beta$ . These studies therefore demonstrate that the size of the protein molecule is essential for drug loading and release, which are clearly illustrated in Figure 4.6 from release profiles in gastric and intestinal conditions respectively.

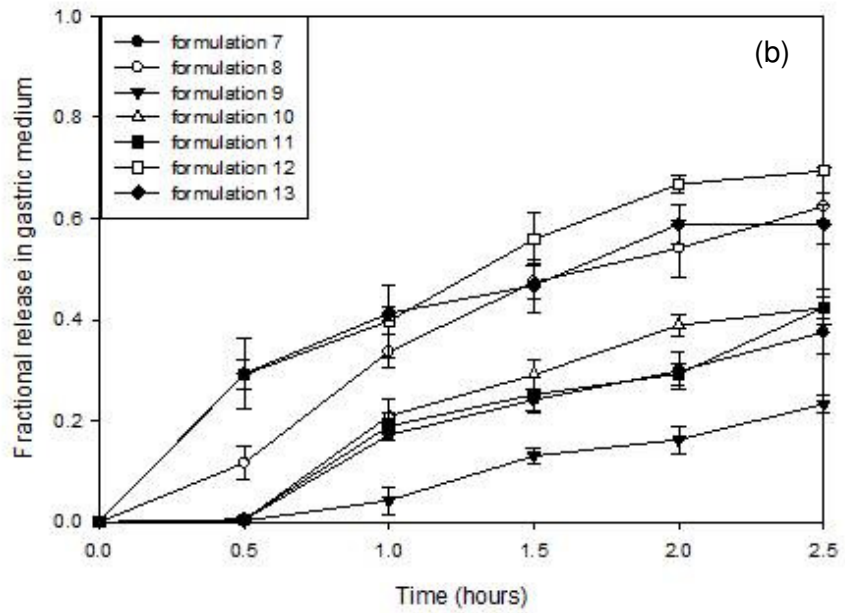
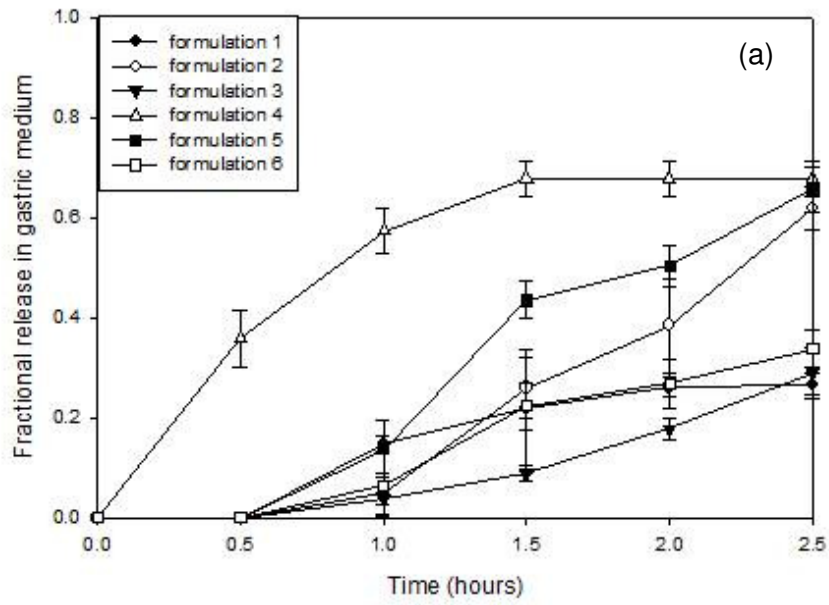


**Figure 4.4a-b:** Fractional release of insulin from CHT-PEGDMA-MAA in gastric medium a) F1-7, b) F8-13.

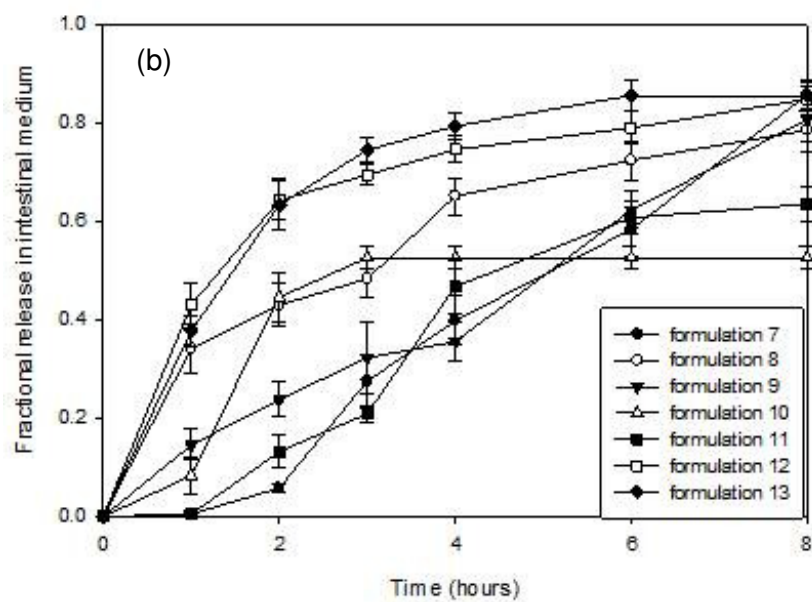
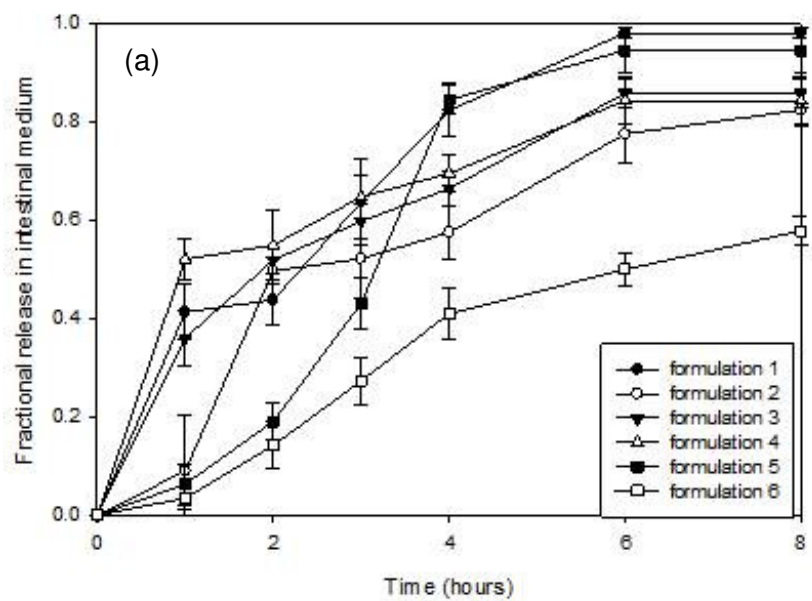


**Figure 4.5a-b:** Fractional release of insulin from CHT-PEGDMA-MAA in intestinal medium a) F1-7, b) F8-13.

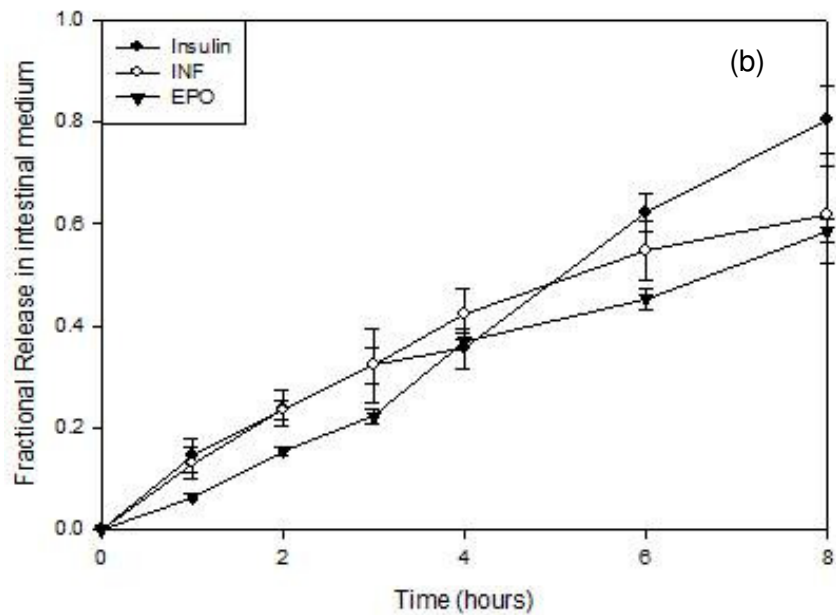
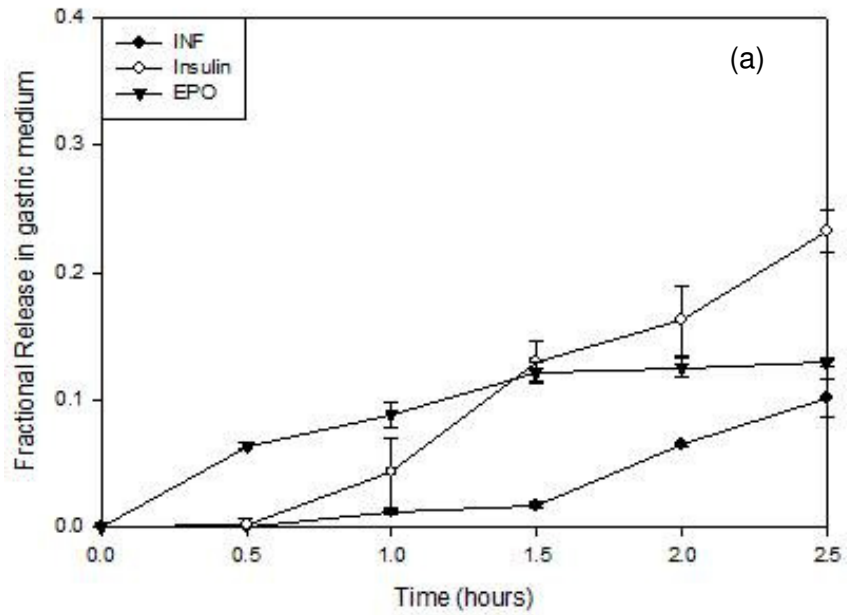


**Figure 4.6:** (a) Fractional release profiles of insulin, INF- $\beta$  and EPO in gastric medium (b) Fractional release profiles of insulin, INF- $\beta$  and EPO in intestinal medium.

### 4.3.3. Concluding Remarks

Protein loading efficiency is proportional in nature to the size of the copolymeric microgel system and a lower loading efficiency can be attributed to the high degree of carboxylic functionalities in the formulation. A significant observation noted was the concentration of CHT and percentage crosslinker increasing in the formulation, resulted in the loading capacity substantially increasing accordingly. Drug loading efficiency studies demonstrated a 25.3% loading efficiency for EPO, 31.5% for INF- $\beta$  and 38.01% for insulin. In gastric medium, insulin showed a maximum release of 23.3% as opposed to EPO and INF- $\beta$ , releasing 12.9% and 10.1% respectively. Drug release profiles in intestinal medium illustrated 80.6% of insulin, 59.6% of EPO and 61.8% of INF- $\beta$  over the specified duration of time. The mechanism of action for drug to be released accordingly can be attributed to the ionization of the particulate bonds in intestinal medium, resulting in significant swelling of the microgel, releasing the loaded protein gradually. EPO demonstrated the lowest drug release profile as well as the lowest drug loading capacity, due to the large size of the protein molecule, in comparison to insulin and INF- $\beta$  protein formulations. These studies clearly demonstrate the significance of particulate size of the protein molecule on the drug loading and release, illustrating the behavior of the copolymeric system in the respective pH conditions. The next Chapter will focus on the *in vivo* evaluation of the microparticulate and microgel protein loaded formulations.

## CHAPTER 5

### EVALUATION OF THE *IN VIVO* RELEASE POTENTIAL OF THE ORAL INSULIN, INF- $\beta$ AND EPO-LOADED TMC-PEGDMA-MAA MICROPARTICULATE AND CHT-PEGDMA-MAA MICROGEL SYSTEMS IN A RABBIT MODEL

#### 5.1. Introduction

*Animal Ethics clearance for this in vivo investigation was approved from the Animal Ethics Screening Committee (AESC) of the University of the Witwatersrand, Ethics Clearance No: 2012/41/05 (Appendix 8.1).*

*In vitro* analysis is essential for determining the release behavior of drug delivery systems. However, it cannot fully simulate physiological conditions to the extent as would in an *in vivo* model. *In vivo* studies are fundamental in order for pharmacokinetic properties to be completely established. In this study, New Zealand White (NZW) rabbit model was selected for evaluation of the *in vivo* release potential of oral insulin, INF- $\beta$  and EPO-loaded TMC-PEGDMA-MAA and CHT-PEGDMA-MAA microgel systems, due to its surrogate gastrointestinal tract and pharmacological volume of distribution for efficient protein drug delivery that is representative of human studies (Tomar *et al*, 2011). The dosing of the oral protein-loaded delivery systems in an *in vivo* model is pertinent for evaluation of safety profiles and potential side-effects that are significant for eventual human clinical trial evaluation. *In vitro* studies proved that the systems were fully responsive with self-sustaining matrices for the delivery of sensitive proteins via the oral route. The aim of this study was to evaluate the ability of the oral protein delivery systems to maintain its integrity *in vivo* and for proteins to be detected. Each delivery system, TMC-PEGDMA-MAA microparticles and CHT-PEGDMA-MAA microgel formulations were loaded with either insulin, INF- $\beta$  or EPO. The insulin-loaded microparticulate and microgel formulations were evaluated in a diabetic rabbit model, in order to determine the reduction in blood glucose levels. EPO and INF- $\beta$ -loaded microparticulate and microgel formulations were evaluated using healthy rabbits, following the same protocol for gastric dosing and blood sampling in all cases. The main areas of focus for pathological evaluation were the GIT, kidney and liver tissue for inflammatory and necrotic responses. The pharmacokinetic (pK) parameters were determined for the various test and competitor formulations.

For purposes of clarity, Results and Discussion section of this chapter has been structured into Part A and Part B. Part A will focus on *in vivo* results of TMC-PEGDMA-MAA microparticulate system and Part B will focus on CHT-PEGDMA-MAA microgel system.

## **5.2. Materials and Methods**

### **5.2.1. Materials**

Ketamine, xylazine, medical oxygen and isoflurane gas (2%) were administered during surgical procedures via attachment of a jelco into the marginal ear vein of the rabbits. Intra-gastric tube (diameter 5mm) was used for dosing the oral system to the rabbits. Phenobarbitone was administered for euthanasia upon completion of the study. All drugs were procured and administered to the rabbits by the Central Animal Services Unit of the University of the Witwatersrand (Johannesburg, South Africa). All other reagents were of standard analytical grade of the highest purity. Table 5.1 provides a detailed list of the treatment doses administered to the rabbits. Table 5.2 lists the dosage of each protein loaded in the microparticulate and microgel systems, as well as the dose of protein administered subcutaneously in the comparator group.

**Table 5.1:** Doses of drugs administered to rabbits during *in vivo* study.

Drug	Route (e.g., I.V., I.M.)	Dose	Frequency
Ketamine HCl (dissociative anaesthetic)	I.M.	40mg/kg	On surgical procedure
Xylazine HCl (analgesia, sedation and muscle relaxation anesthesia)	I.M.	procedure	On surgical procedure
Procaine HCL(topical anesthetic) 0.5% w/w	Topical	1-2 drops	On surgical procedure
Medical oxygen and isoflurane gas (2%)	Inhalation	5-15 min duration	On surgical procedure
Sodium pentobarbitone	I.V.	> 50 mg/kg	On euthanasia

**Table 5.2:** Dosages for protein-loaded microparticulate, microgel and comparator subcutaneous formulations.

Protein	TMC-PEGDMA-MAA microparticulate system	CHT-PEGDMA-MAA microgel system	Subcutaneous comparator dose for each protein
INF- $\beta$	44 $\mu$ g	44 $\mu$ g	44 $\mu$ g (Rebif <sup>®</sup> )
Insulin	100IU	100IU	10IU (Actrapid <sup>®</sup> )
EPO	12000IU	12000IU	5000IU(Recormon <sup>®</sup> )

The differences in experimental and comparator dosage concentrations are due to the maximum concentration the rabbit could be administered as a subcutaneous dosage.

### 5.2.2. Animal study protocol for dosing and blood sampling

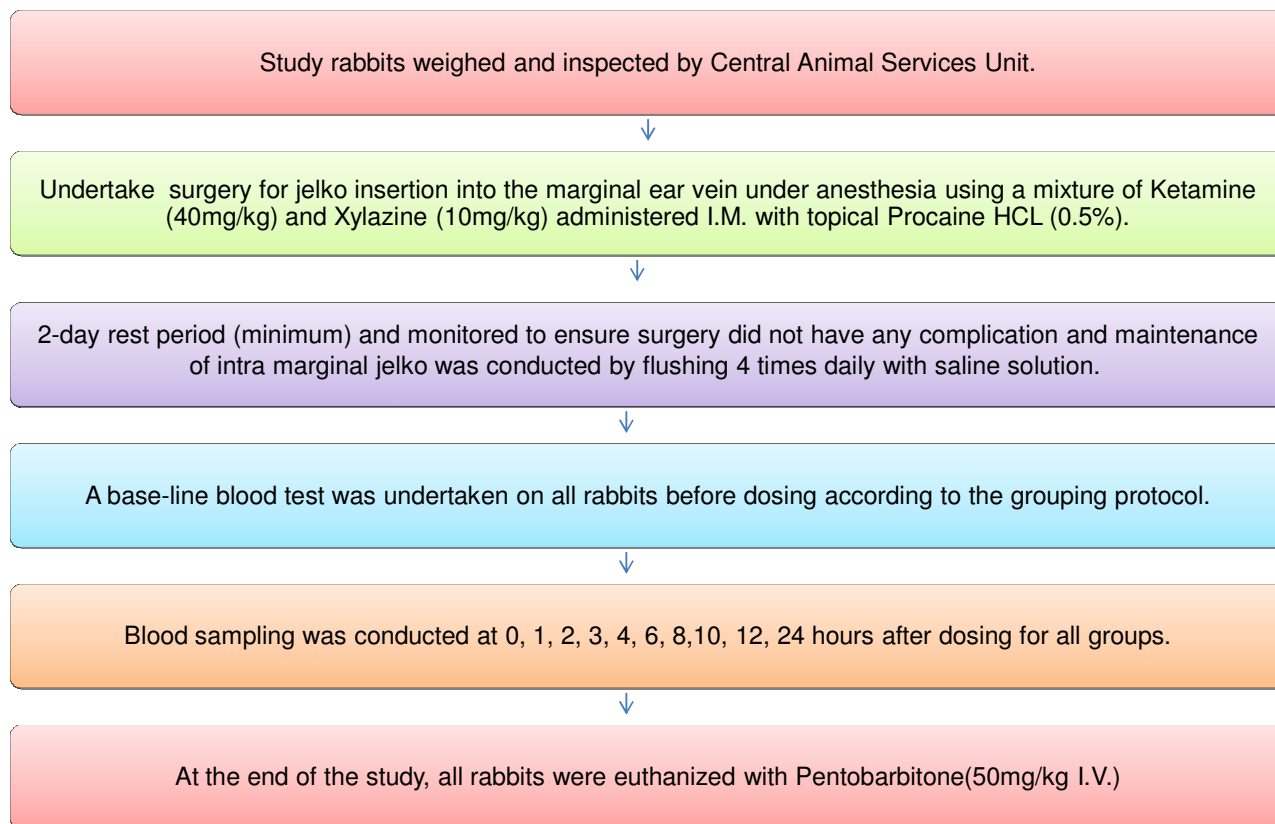
The insulin, INF- $\beta$  and EPO-loaded copolymeric microgel and microparticulate formulations were evaluated in the NZW rabbit model. A total of 9 rabbits were divided in 3 groups each (Group 1: experimental, Group 2: control and Group 3: comparator product evaluation group).

Figure 5.1 provides a summary of the animal study protocol undertaken for each protein-loaded formulation.

Group 1: (Experimental group): The protein-loaded (microparticulate and microgel formulations) were administered to 3 rabbits via gastric gavage using a 5mm diameter intragastric tube. The orally administered dose for this group was evaluated using an ELISA kit for INF- $\beta$  and EPO-loaded formulations and a blood glucose meter was used to evaluate the insulin concentrations respectively.

Group 2: (Control): This group of animals were administered the protein-free (placebo) oral microparticulate and microgel formulations.

Group 3: (Comparator product evaluation): This group of rabbits were administered the commercially available subcutaneous formulations of the respective protein formulations. This study was undertaken to determine the comparator efficiency potential of the oral formulations in comparison to the subcutaneous marketed formulations.



**Figure 5.1:** Summarised flow-chart of the animal study undertaken for *in vivo* evaluation of all protein-loaded formulations of the microgel and microparticulate systems.

All experimental procedures were conducted under anesthesia using ketamine (40mg/kg) and xylazine (10mg/kg), as well as topical procaine HCl (0.5%). The rabbits were maintained under medical oxygen and isoflurane gas (2%) for 5-15 minutes (Fish *et al.*, 2008). A 24 gauge jelko was inserted into the marginal ear vein, and sutured onto the soft cartilage to maintain stability of the jelko during blood sampling. 1000IU heparin in 1L of 0.9% saline was used to flush the jelko 4 times daily and inspections for septicemia were undertaken to assure the rabbit remained healthy throughout the study. Prior to gastric dosing, anesthesia was administered. After dosing, the rabbits were carefully monitored and blood samples were taken at the specified time intervals. Blood samples were collected in lithium heparin vials and centrifuged at 5000rpm for 10 minutes, and the serum was used for evaluation of the respective protein concentrations. Blood samples were taken at 0, 1, 2, 3, 4, 6, 8, 10, 12 and 24 hours after each formulation administration. All rabbits were used once in the study, and were euthanized after the study.

### 5.2.3. Histopathological tissue evaluation postdosing

Histopathological evaluation was undertaken on the GIT, kidney and liver tissues of the rabbit for evaluating the potential for inflammation or tissue necrosis to the epithelial cells, after administration of the protein formulations. Tissue was fixed in formalin and was processed overnight, acquiring sections of 5 $\mu$ m, stained in Haematoxylin and Eosin. Each rabbit was evaluated pathologically to determine the safety of the protein microparticulate and microgel formulations.

### 5.2.4. Pharmacokinetic modeling employing compartmental and non-compartmental algorithms

Pharmacokinetic (pK) compartmental and non-compartmental data analysis was undertaken using PKSolver software (Microsoft Excel add-in) (Visual Basic for Applications, VBA)(Zhang *et al.*, 2010). Data comprising *in vivo* protein concentration released was pharmacokinetically evaluated. Input data comprised release of the INF- $\beta$  from the optimized formulation. Figure 5.2 represents one-compartmental model of the oral microparticulate and microgel systems.

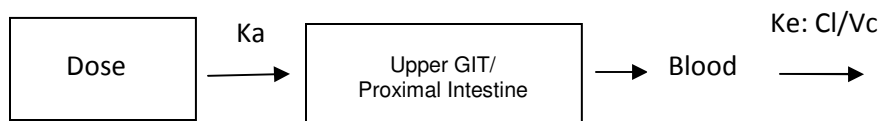


**Figure 5.2:** One-compartmental model representing the pharmacokinetic distribution of protein released from the microparticulate and microgel systems.

## 5.3 Results and Discussion

### 5.3.1. Part A: Evaluation of TMC-PEGDMA-MAA-Loaded Copolymeric Delivery System for *In Vivo* Evaluation

#### 5.3.1.1. Quantitative *in vivo* release analysis

Each rabbit in the experimental group of INF- $\beta$  loaded microparticulate and microgel systems were dosed with a total of 44 $\mu$ g INF- $\beta$  and the same concentration was administered for the comparative subcutaneous dose to another experimental group of rabbits. Both oral and SC formulations were observed to maintain steady state concentration for a period of 24 hours and the peak concentrations in both cases were observed at 2 hour duration. The peak bioavailable

dose in serum for developed copolymeric system was calculated to be 1.3% of INF- $\beta$  in comparison to the SC formulation, having a peak concentration of 0.9%. Due to the slow diffusion of the SC formulation into the systemic circulation, the concentration of INF- $\beta$  increased over a greater duration of time. The microparticulate system showed steady state drug release for 24 hour. *In vitro* release of INF- $\beta$  was obtained up to 8 hours. However, *in vivo* analysis demonstrated release over 24 hour duration. According to guidelines from the manufacturer of Rebif<sup>®</sup>(comparator formulation), the median time of peak serum concentration (T<sub>max</sub>) was documented as 16 hours, with a serum elimination half-life (t<sub>1/2</sub>) of 69 $\pm$ 37 hours resulting in a peak serum concentration (C<sub>max</sub>) of 5.1 $\pm$ 1.7 IU/mL (mean $\pm$ SD) with a dose of 60 $\mu$ g SC injection (www.druglib.com). A 24-hour sustained release profile resulted from the oral microparticulate delivery system can therefore be justified due to the long half life INF- $\beta$  possesses. It can be concluded that the microparticulate system has successfully delivered INF- $\beta$ , via oral administration, with peak concentration over a 24-hour duration greater than the commercial Rebif<sup>®</sup> SC formulation as seen in Figure 5.4a. It was clearly observed that the prepared microparticulate formulation gave remarkable results, greater than the subcutaneous (SC) INF- $\beta$  comparator formulation.

For the insulin-loaded TMC-PEGDMA-MAA formulation, the microparticles significantly decreased the blood glucose by 54.19% within 4 hours, and thereafter a gradual increase occurred. The comparator SC insulin formulation provided a 74.6% decrease in blood glucose within 4 hours. However, a rapid increase in blood glucose occurred thereafter, as shown in Figure 5.4b. EPO-loaded TMC-PEGDMA-MAA microparticles were observed to have a 1.6% peak bioavailable concentration, in comparison to the 6.34% peak concentration after 8 hours from the SC comparator formulation as seen in Figure 5.4c.

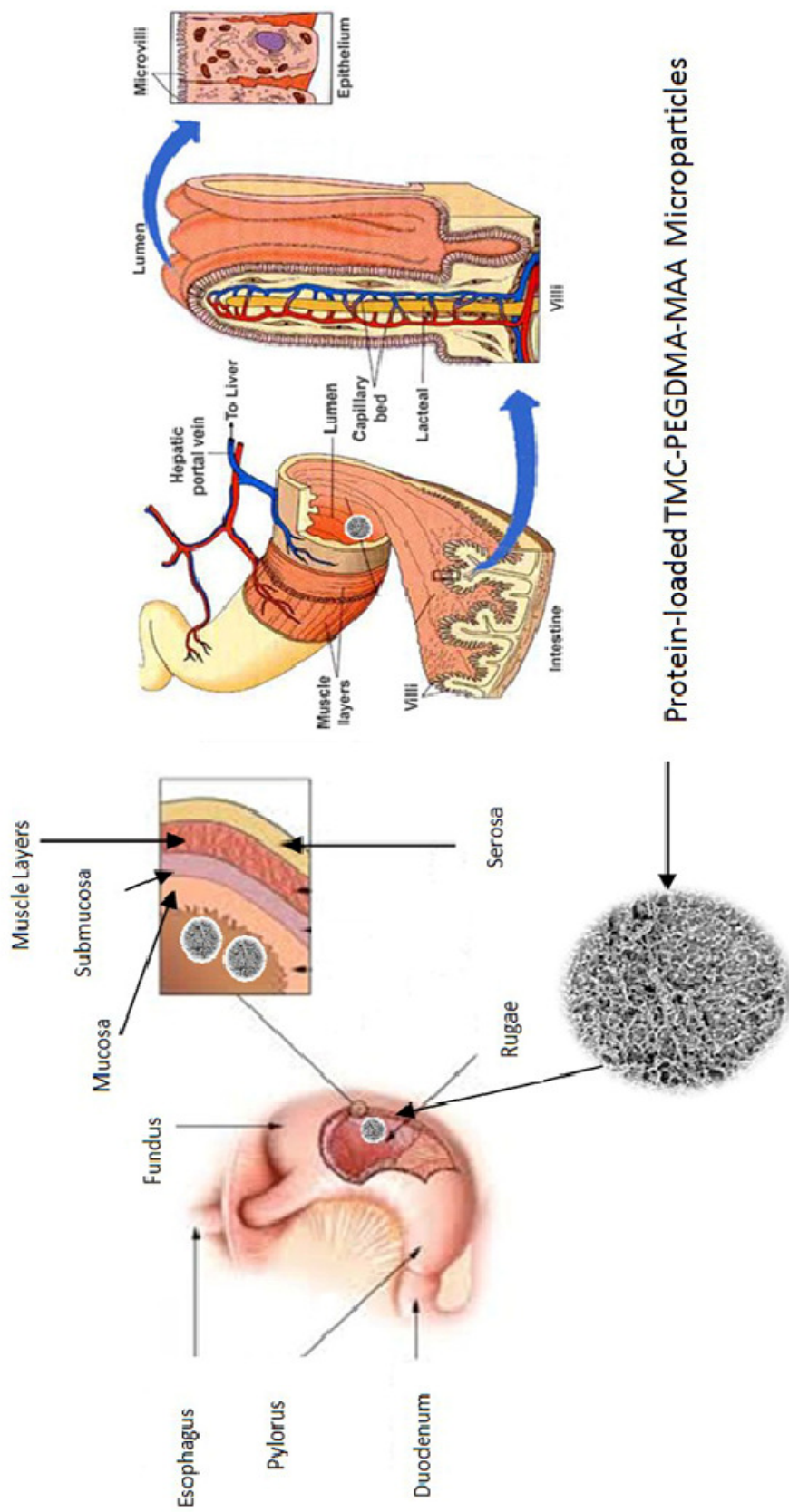


**Figure 5.3:** Mechanism of action depicting the mucoadhesive characteristic of the protein-loaded microparticulate system adhering to the gastric linings of the stomach, forming a site specific directed passage for protein to enter the blood stream.

Initial absorption of the protein from the microparticulate system begins in the stomach, by which the permeation enhancing, mucoadhesive properties of the microparticles adhere to the mucosal lining, releasing the loaded protein passively to be absorbed into the systemic circulation as depicted in Figure 5.3. The microparticles that do not adhere to the mucosal lining of the stomach, passes into the proximal intestine after gastric emptying and swell significantly for protein release and absorption as observed with results from Figure 5.4a, in which peak concentration of the protein was observed within the 1<sup>st</sup> hour, following absorption of the remaining protein-loaded microparticles in the proximal intestine after gastric emptying. The mechanism of absorption of the loaded-protein is challenging for identical replication *in vitro*, therefore indicating the complexity of the microparticulate system.

As seen in Figure 5.4a, INF- $\beta$  has a peak concentration of 560pg/mL after the 1<sup>st</sup>, representing significant gastric absorption. It can be confirmed that the microparticles have a specialized protective mechanism of protein shielding, where denaturing of the protein is minimum, resulting in a high concentration of absorbable protein early on in the GIT.

In addition to the permeation enhancing properties of the particles, PEGylation of a protein molecule modifies the charge distribution, epitope shielding, as well increases the size of the protein molecule which decreases kidney ultrafiltration and increases the passive permeability into tissue (Caliceti *et al*, 2003). Reduced phagocytosis by liver cells are another fundamental aspect due to charge and glycosylation masking, further reducing proteolysis and immune recognition which are essential for elimination identification mechanisms. This effect of PEGylation is further modified by the significant properties of TMC, which complement and enhances passive diffusion of the loaded protein.

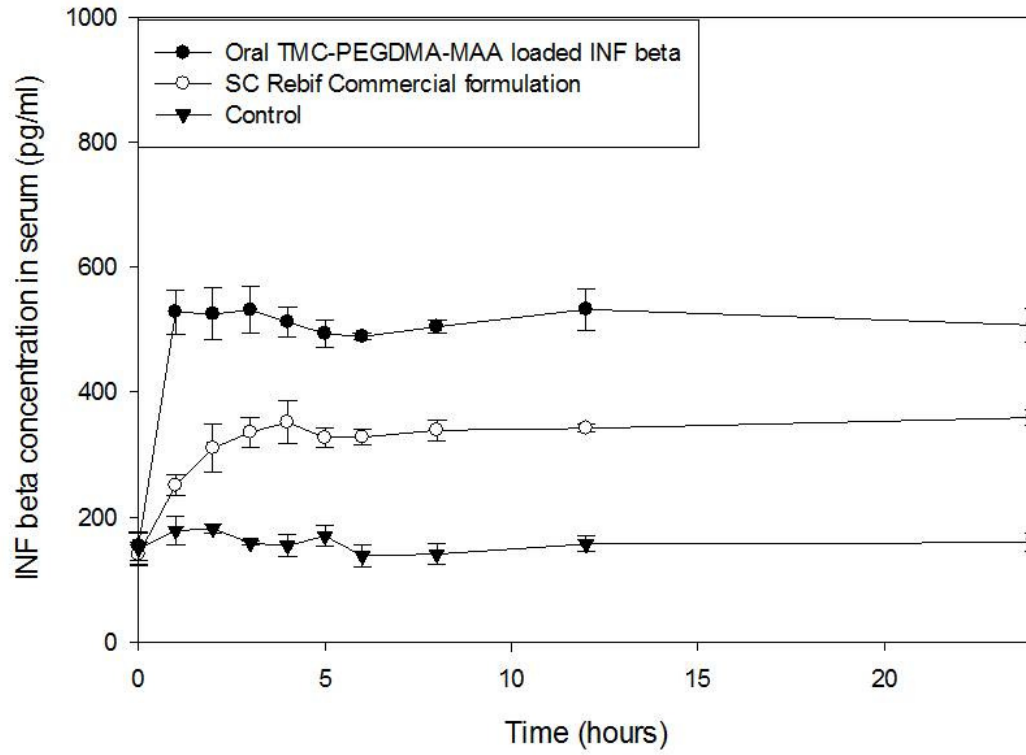


**Fig.5.4a:** *In vivo* release of INF- $\beta$  from the optimized oral microparticles compared to the commercial subcutaneous dose administration.

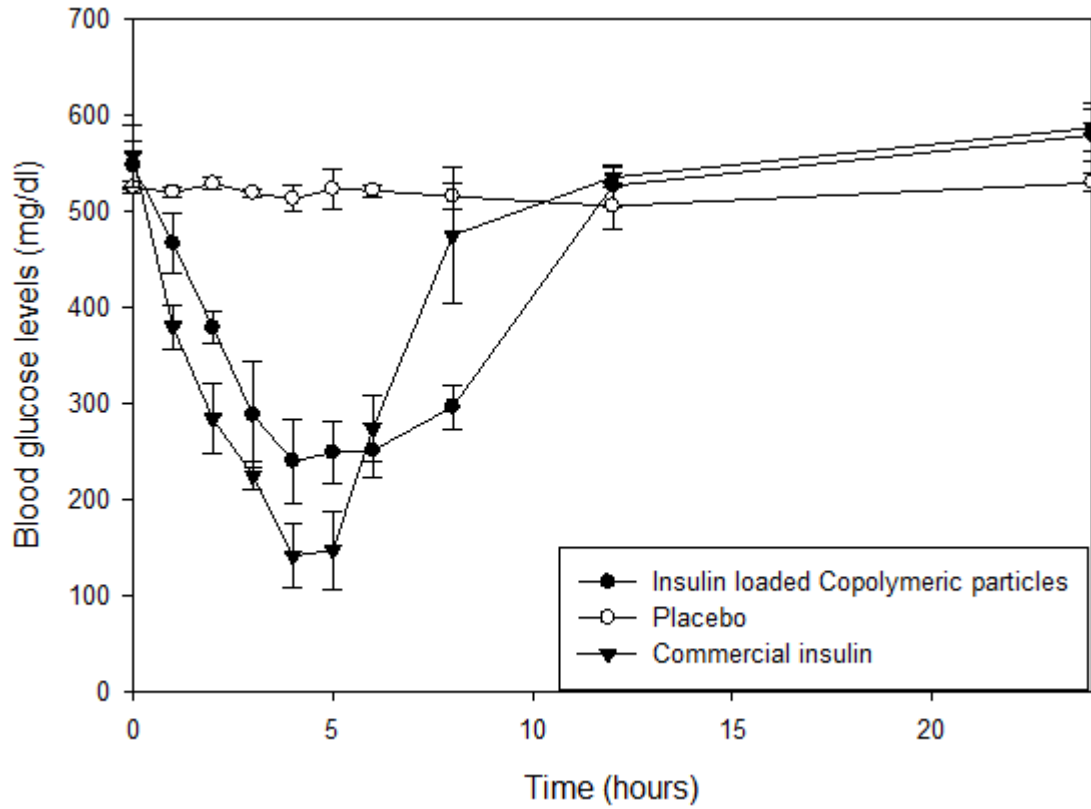


**Figure 5.4b:** Blood glucose response to insulin-loaded microparticles, commercial SC formulation and placebo dose.

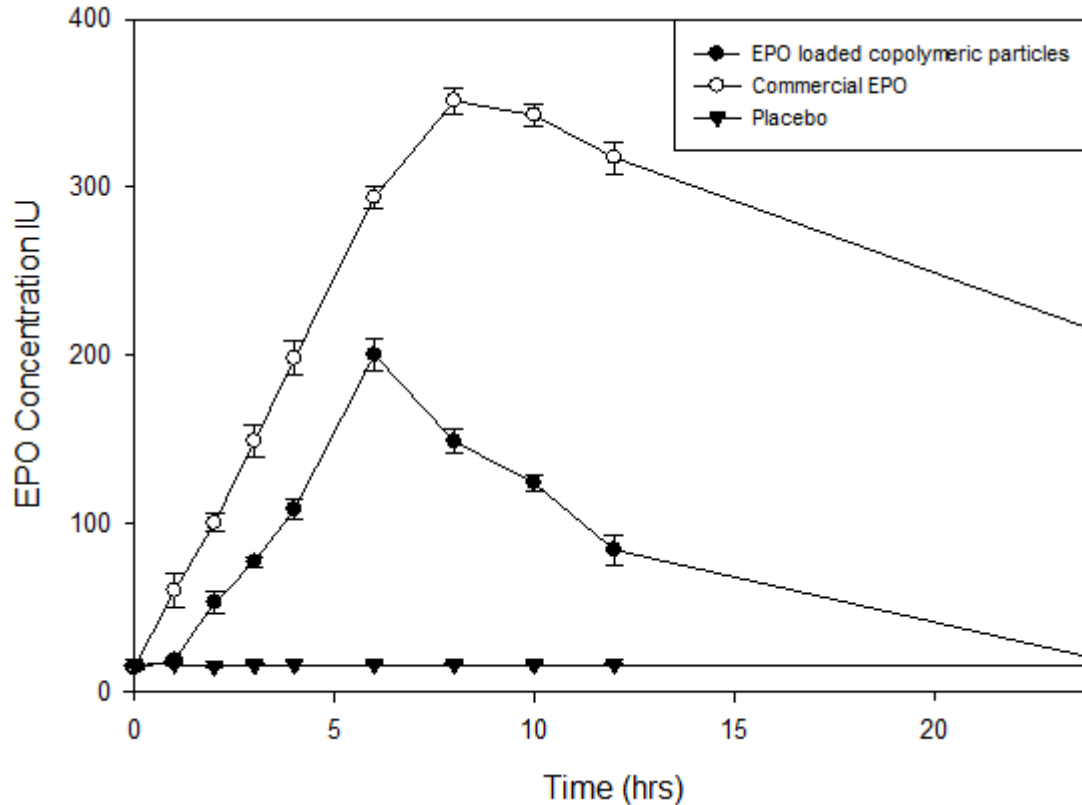


**Figure 5.4c:** EPO-loaded microparticles, commercial SC formulation and placebo *in vivo* studies.

### 5.3.1.2. Histopathological evaluation

Tissue samples from rabbits were evaluated for effects of the protein-loaded microparticles. Rabbits in the insulin study revealed normal kidney and liver tissue. Figure 5.5a represents a GIT intestinal sample, showing normal mucosal crypts and a mild population of lymphoplasmic cells in the lamina propria confirming normal intestinal mucosa. Figure 5.5b depicts a section of intestinal tissue, showing normal epithelium and mucosal intestinal villi. The lymphoplasmic cells in the lamina propria also appeared normal in nature. Figure 5.5c represents the fundic portion of the stomach, showing normality of the fundic glands with no pathology evident. No signs of inflammation or ulceration in any of the GIT tissue samples were noted, therefore confirming the biosafety of the microparticles. Figure 5.5d showed severe loss of cellularity and necrosis in the islet of Langerhans. This was due to the administration of Alloxan<sup>®</sup> to induce diabetes in rabbits. GIT samples were a crucial area of concern, due to direct contact of the microparticles with the GIT tract. Samples from the various protein formulations revealed no pathology in gastric and intestinal tissue. There was absence of inflammation, necrosis or degeneration therefore

proving the oral protein-loaded microparticles completely biodegradable and non toxic for oral administration.

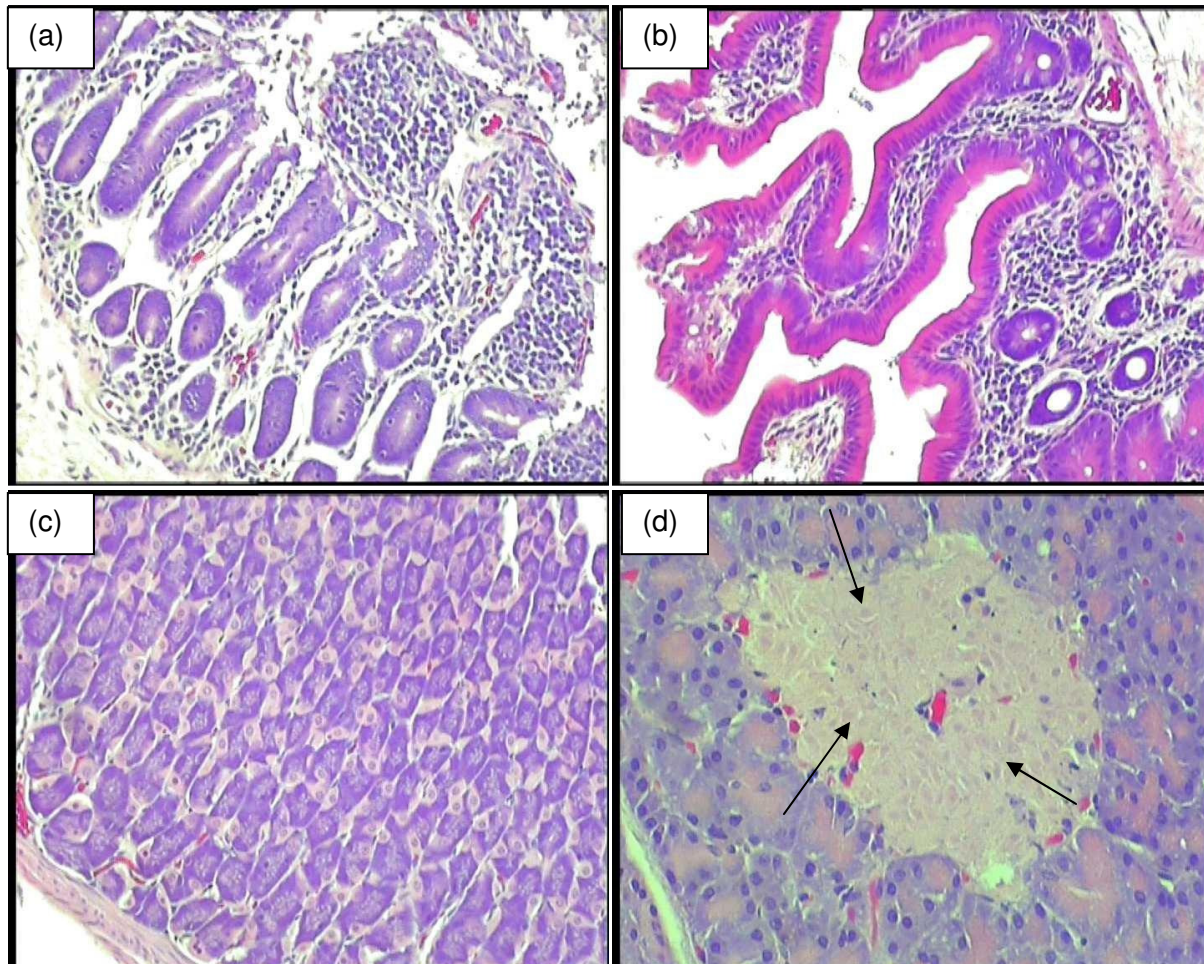
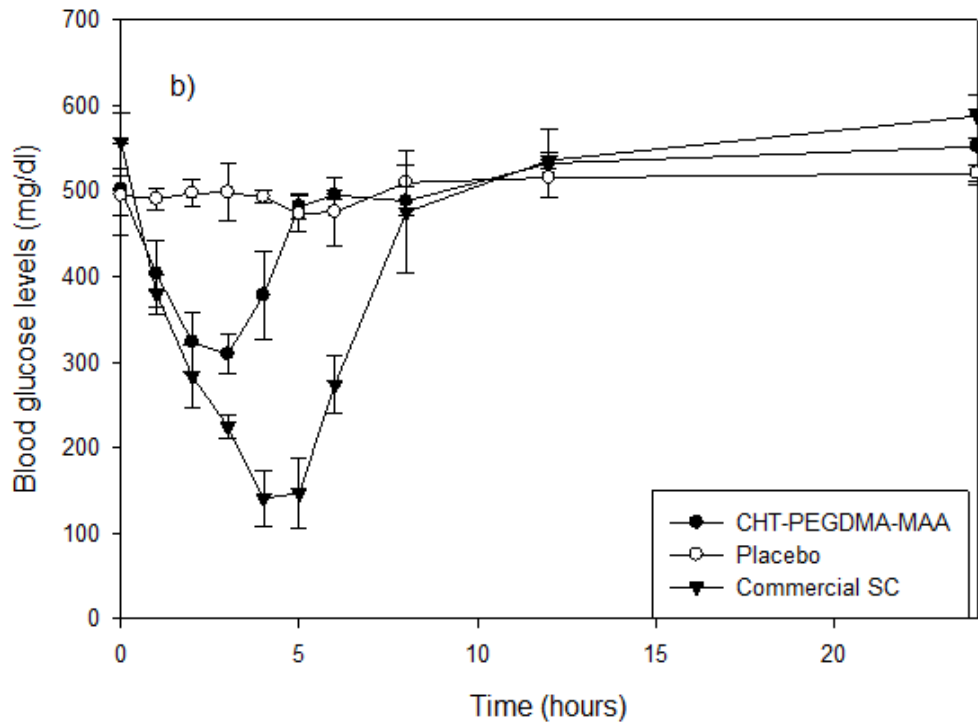
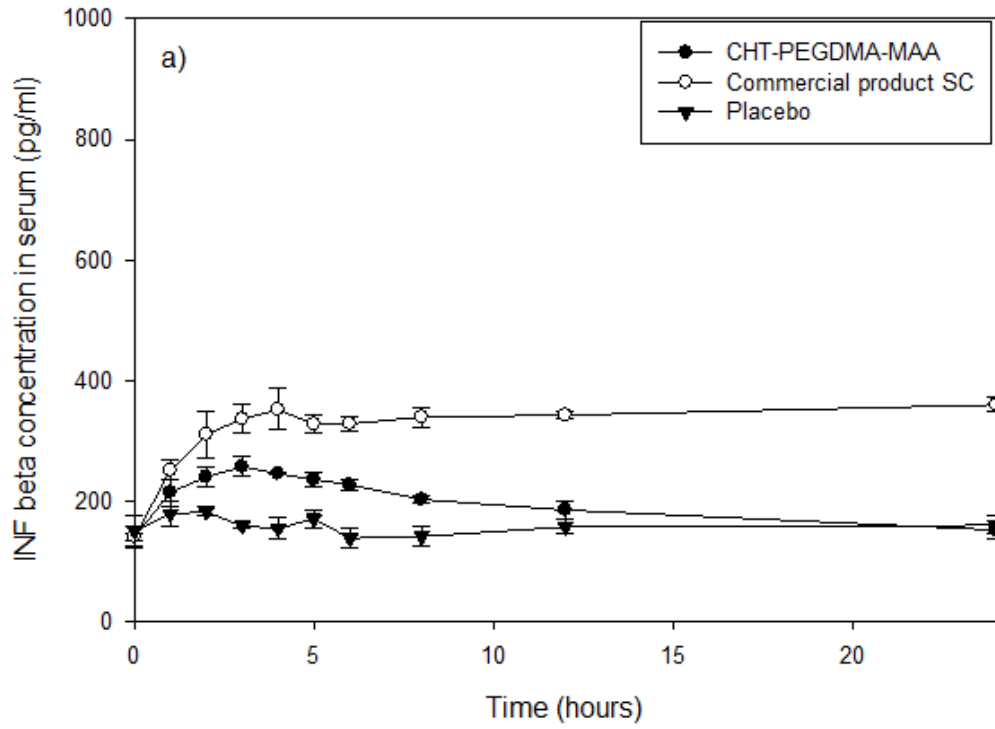


**Figure 5.5:** Histological evaluation of tissue samples from rabbits in the experimental oral microparticles. a) Intestinal mucosal crypts confirm normal intestinal mucosa (X10), b) Intestinal mucosa which shows normal epithelium (X10), c) Fundic portion of the stomach which shows normal fundic glands (X10) d) Severe loss of cellularity and necrosis of the islet cells in the islet of Langerhans (X20).

## 5.4. Part B: Evaluation of CHT-PEGDMA-MAA Protein-Loaded Copolymeric Delivery System for *In Vivo* Evaluation

### 5.4.1 Quantitative *in vivo* release analysis

As discussed in Part A, the same concentrations of the respective proteins were dosed to all rabbits in the various study groups for TMC-PEGDMA-MAA and CHT-PEGDMA-MAA formulations. The microgel protein-loaded formulations were analyzed for a minimum of 24 hours, incorporating a placebo and a SC comparator product on the market in each group of the study. INF- $\beta$  loaded oral microgel system demonstrated a 1.53 times greater concentration than the placebo at 5 hour duration, as opposed to a 2.33 times greater concentration of the comparator Rebit<sup>®</sup> formulation in comparison to the placebo (protein-free microgel formulation) at the same time point (Figure 5.6a). The insulin-loaded microgel formulation revealed a maximum decrease in blood glucose at 3 hours after gastric gavage, showing a 38.2% decrease of blood glucose levels. The commercial formulation of insulin demonstrated a 74.68% decrease in blood glucose in comparison to the placebo, showing 36.36% less efficacy at 10 times less the dose (Figure 5.6b). EPO oral formulation demonstrated a 3.42 times greater increase than the placebo concentration at 8 hour duration as compared to a substantial difference of 22.22 times greater concentration in the SC (commercial SC EPO) formulation than the placebo dose at 8<sup>th</sup> hour duration at 2.4 times lower dose than the oral loaded dose of EPO (Figure 5.6c). Evaluation of the peak concentration of the proteins in the study, confirmed a proportional relationship with size of the protein and the duration for reaching the maximum concentration in the blood. Insulin being the smallest protein molecule in the study, showed the least duration for reaching the maximum effective decrease in blood glucose at 3 hours, as compared to EPO, being the largest protein molecule in the study, being released over an 8 hour duration in which the maximum concentration of EPO was reached. Figure 5.6a-c illustrates the behavior of the respective protein-loaded microgel formulations over the specified time durations.



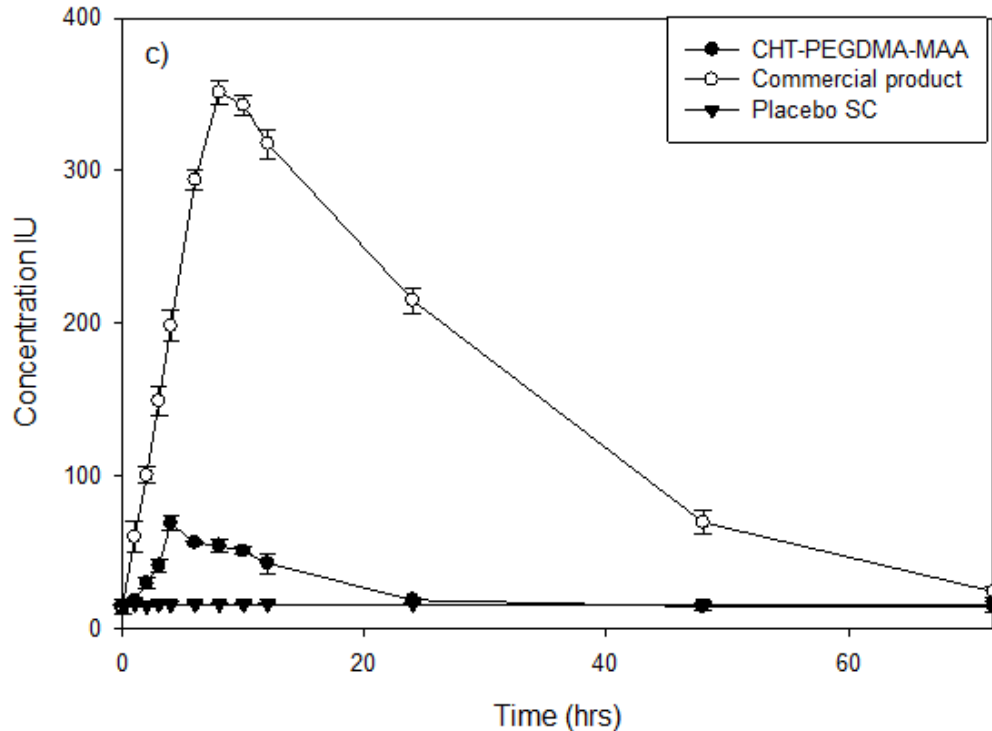


**Figure 5.6:** *In vivo* analysis of the oral protein-loaded microgel system in a rabbit model a) INF- $\beta$ , b) Insulin c) EPO

#### 5.4.2 Histopathological evaluation

After euthanizing rabbits from all groups of the study, histological evaluation was undertaken to determine any pathology occurring due to dosing of the protein-loaded microgel formulation. GIT samples were placed in the highest priority, since confirmation of the safety of the microgel-loaded formulation is essential for an oral dosage form. Figure 5.7a illustrates intestinal mucosa at 10 times magnification, showing normal intestinal villi and a healthy normal variety of cells in the lamina propria. No pathology was observed in all intestinal samples of rabbits in the study. Figure 5.7b shows normal histology of the fundic mucosa of the stomach, demonstrating no inflammation/inflammatory cells in the region of the stomach. Figure 5.7c represents a section from duodenal mucosa, showing normal intestinal crypts and duodenal glands, with no pathology evident in any of the samples. Figure 5.7d of intestinal mucosa appear normal, with gutter cells among epithelial cells in the intestinal villi, with no pathology observed from any samples. Pathology of the kidney was evident in diabetic-induced rabbits, demonstrating necrosis and severe loss of cellularity in the islet of Langerhan cells, as discussed in Figure 5.8d, due to the administration of Alloxan<sup>®</sup>. Evaluation of samples from the kidney, liver, pancreas and heart showed no pathology of any kind, thus proving the oral protein loaded

microgel dosage form safe for oral administration.

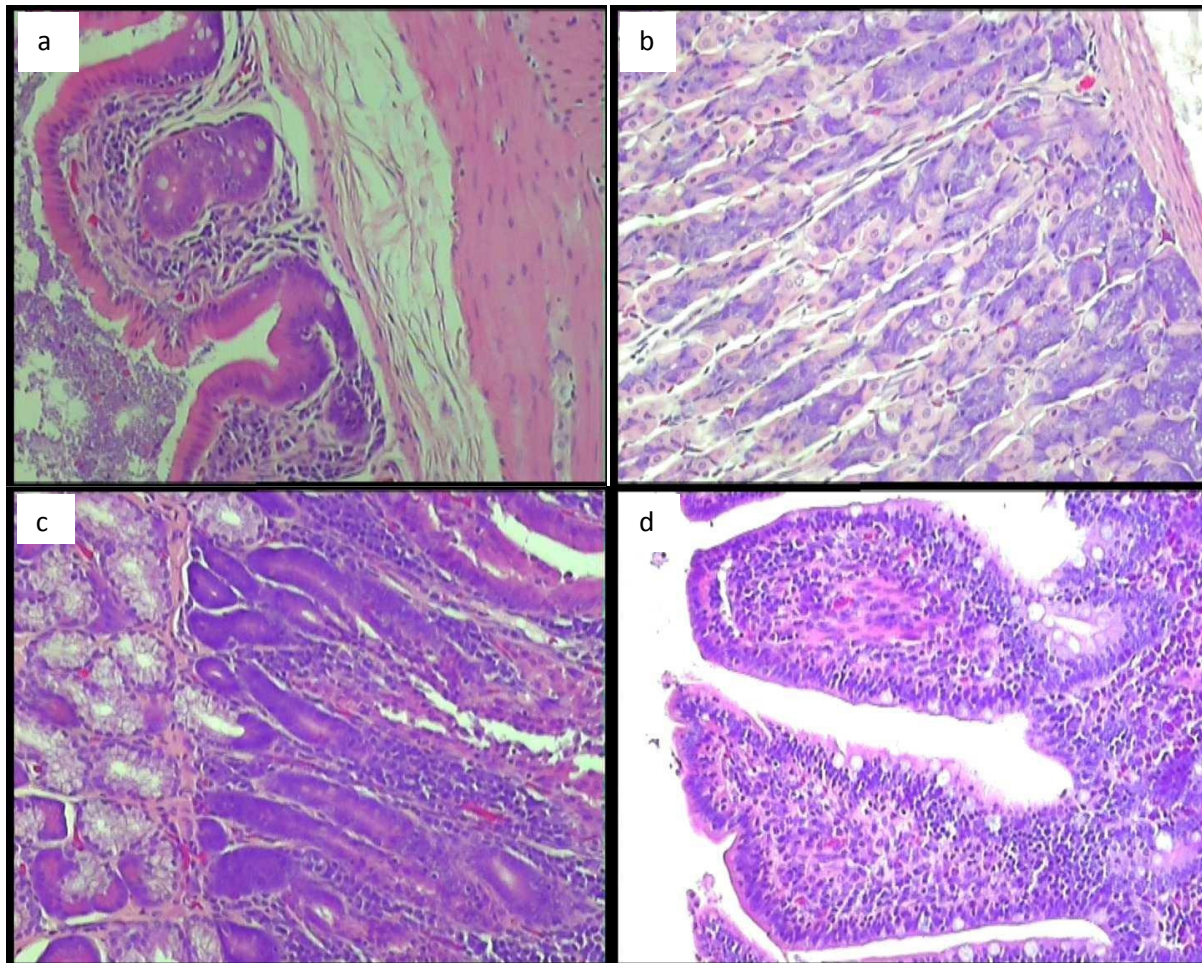


**Figure 5.7:** Histological evaluation of the GIT from rabbits dosed with the protein-loaded microgel formulation. a) Intestinal mucosa showing normal intestinal villi (10X), b) normal fundic mucosa of the stomach (10X), c) duodenal mucosa showing normal glands and intestinal crypts (X10), d) normal intestinal mucosa with goblet cells among epithelial cells (X10)

## 5.5. Comparative pharmacokinetic analysis of the INF- $\beta$ -loaded TMC-PEGDMA-MAA microparticles and CHT-PEGDMA-MAA microgel formulations.

### 5.5.1. INF- $\beta$ non-compartmental and compartmental analysis

TMC-PEGDMA-MAA and CHT-PEGDMA-MAA loaded INF- $\beta$  formulations were compared using pK parameters. The mean serum drug concentration-time curves are shown in Figures 5.8 and 5.9 for the microparticulate and microgel formulations, respectively. The microparticulate formulation peaked with INF- $\beta$  at 1<sup>st</sup> hour postdose, in comparison to the microgel formulation which peaked after 3 hours. The microparticulate system maintained a steady state concentration over 24 hours, in comparison to the microgel formulation which displayed a gradual elimination phase as seen after the 3<sup>rd</sup> hour, with  $t_{1/2}$  of the microparticulate system of 26.4 hours in comparison to the microgel system  $t_{1/2}$  of 13.76 hours as seen in Tables 5.3 and 5.4 respectively.

**Table 5.3:** Results for non-compartmental analysis of INF- $\beta$ -loaded TMC-PEGDMA-MAA microparticles and CHT-PEGDMA-MAA microgel formulations.

Parameter	Unit	TMC-PEGDMA-MAA	CHT-PEGDMA-MAA
$t_{1/2}$	$\mu\text{g/ml}$	26.4	13.76
Ka	h	15.64	1.75
$T_{\max}$	H	0.628	2.42
$C_{\max}$	$\mu\text{g/ml}$	0.516	0.245
AUC <sub>0-inf</sub>	$\mu\text{g/ml}\cdot\text{h}$	615.717	9.975
Cl/F	$(\mu\text{g})/(\text{pg/ml})/\text{h}$	7.1461E-05	4.41E-05

**Table 5.4:** Results for One compartmental analysis with lag of INF- $\beta$ -loaded TMC-PEGDMA-MAA microparticles and CHT-PEGDMA-MAA microgel formulations.

Parameter	Unit	TMC-PEGDMA-MAA	CHT-PEGDMA-MAA
$t_{1/2}$	$\mu\text{g/ml}$	26.4	13.76
Ka	1/h	11.25	1.75
$T_{\max}$	H	0.84	2.42
$C_{\max}$	$\mu\text{g/ml}$	0.516	0.245
AUC <sub>0-inf</sub>	$\mu\text{g/ml}\cdot\text{h}$	615.47	9.975
Cl/F	$(\mu\text{g})/(\text{pg/ml})/\text{h}$	7.149E-05	8.27E-05

Parameters of the non-compartmental and one compartmental analysis were the same for the microgel formulation, with slight differences in the microparticulate formulation of  $K_a$  and  $T_{max}$ , due to its higher sensitivity in pH responsive nature as seen in Tables 5.3 and 5.4. For the one compartmental model, the  $AUC_{0-inf}$  for the micogel system was 61.7-fold higher than the microparticulate system, and the  $C_{max}$  being 2.1-fold greater respectively. The microparticles had a reduced CL/F of 1.15-fold compared to the microgel system, with a 6.42-fold greater  $K_a$  and 1.92-fold greater  $t_{1/2}$ , which was expected from the microparticulate system, due to its significant absorption and sustained release behavior.

These parameters therefore illustrate the superiority composition in relation to its structural activity relationship to its pH sensitive nature, conserving the protein for maximum absorption. This compartmental model with lag demonstrates the slow release behavior of the copolymeric formulations, explaining the time delay response for the transition in pH for desired release kinetics. As seen in Figure 5.8a, a complete match was observed in relation to the observed and predicted concentration of INF- $\beta$  from the microparticulate system. Figure 5.8b demonstrates the observed and predicted concentration for INF- $\beta$  for non-compartmental analysis, demonstrating a significant fitting to the model for the microparticulate system. Equation 5.1 explains the relation of protein concentration absorbed and volume of distribution in a one compartmental model.

$$C = (FD/Vd) (k/k-K) (e^{-Kt} - e^{-kt}) \quad \text{Equation 5.1}$$

F represents the dose fraction absorbed, with dose D, k representing absorption and K representing elimination rate constants, V representing the apparent volume of distribution (Worakul and Robinson, 1997).

The closest fit of the model to one compartmental with lag demonstrates the ability of the formulation to be absorbed across the epithelial membranes via adhering to the mucus membranes, releasing INF- $\beta$  in a constant slow release manner, attaining a distribution in a prolonged, delayed release behavior, displaying a biphasic concentration-time profile. This optimum release behavior is significant for desired responses, demonstrating a prolonged, concentration-absorption profile via GIT membranes.

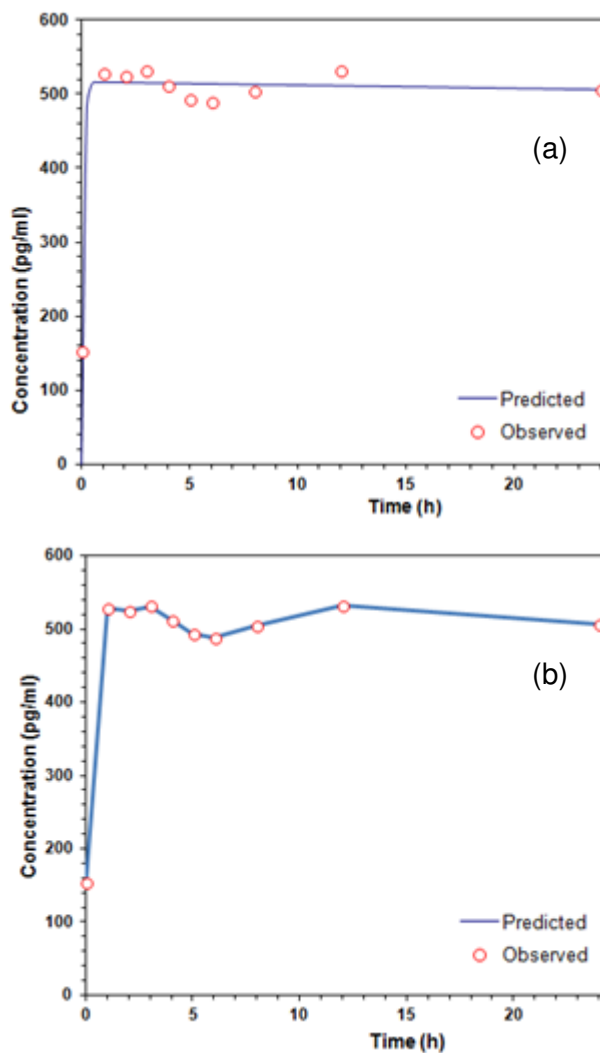


**Figure 5.8:** (a) Concentration-time profiles demonstrating the predicted and observed concentration values from the release profiles of INF- $\beta$  microparticulate system over 24 hours for one compartmental analysis with lag, (b) demonstrating the predicted and observed concentration values from the release profiles of INF- $\beta$  of the microparticulate system over 24 hours for noncompartmental analysis, demonstrating a significant maintenance of slow release behavior of the INF- $\beta$  loaded copolymeric delivery system.

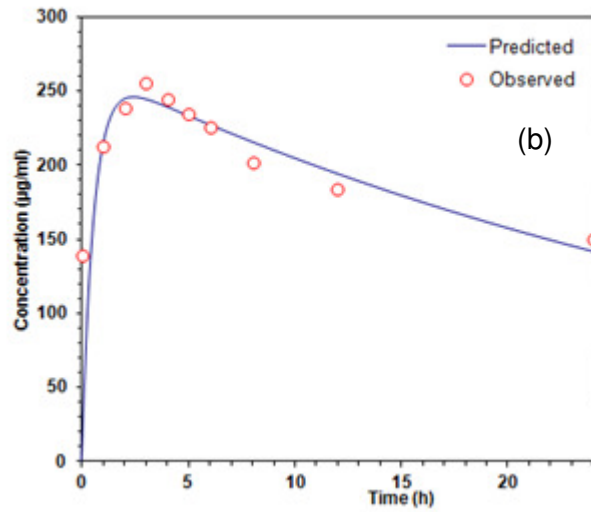
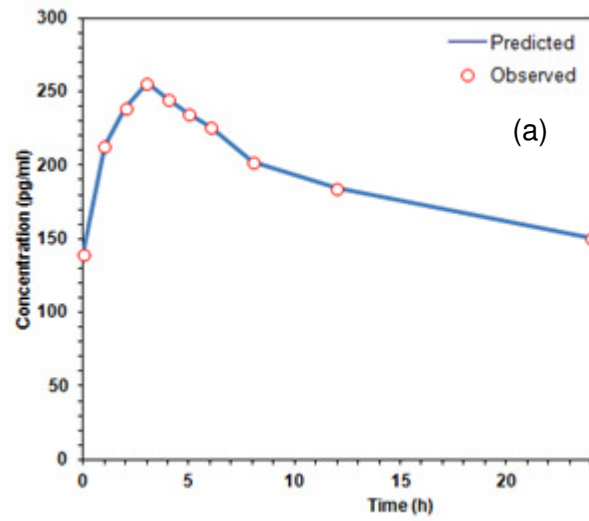


**Figure 5.9:** (a) Predicted and observed concentration values from the release profiles of INF- $\beta$  over 24 hours for noncompartmental analysis (b) Predicted and observed concentration values from the release profiles of INF- $\beta$  over 24 hours for one compartmental analysis with lag.

## 5.6. Concluding Remarks

INF- $\beta$  was administered orally as the experimental formulation and SC Rebit<sup>®</sup> injection as the commercial product. For the microparticulate TMC-PEGDMA-MAA formulation, both oral and SC formulations demonstrated steady state concentration over a period of 24 hours with  $T_{max}$  in both cases at 2 hours. The peak bioavailable dose in serum for the microparticulate system was 1.3% of INF- $\beta$  in comparison to the SC delivery, having a peak concentration of 0.9%. Insulin-loaded microparticles demonstrated a significant decrease of 54.19% within 4 hour duration, in comparison to a 74.6% decrease in blood glucose within 4 hours of the SC formulation. EPO-loaded microparticles demonstrated a 1.6% peak bioavailable concentration, in comparison to the SC formulation demonstrating a 6.34% peak bioavailable concentration.

PK analysis highlighted that the system was best described by a one compartmental analysis with lag based on the slow release behavior of the microparticle formulation, taking into consideration the time delay response for the transition in pH for the desired release outcome.

The CHT-PEGDMA-MAA INF- $\beta$ -loaded microgel formulation demonstrated a 1.53 times greater concentration than the placebo at 5 hours, as opposed to a 2.33 times greater concentration of the commercial product in comparison to the placebo. Insulin studies demonstrated a maximum decrease in glucose at 3 hours after gastric gavage, showing a 38.2% decrease in blood glucose levels in comparison to the commercial formulation demonstrating a 74.68% decrease in blood glucose. EPO oral experimental formulation demonstrated a 3.42 times greater increase than the placebo concentration at 8 hour duration in comparison to 22.22 times greater concentration in the SC formulation than the placebo dose.

Results for pK analysis demonstrated that the one compartmental model with lag is representative of the most fitting model in the study, with parameters which were suitably confined to the pH responsive nature of the microgel system. The half-life and maximum concentration of INF- $\beta$  absorbed was greater in microparticulate formulation in comparison to the microgel, due to the greater mucoadhesive and permeation enhancing properties of the microparticulate system.

## CHAPTER 6

### CONCLUSION AND RECOMMENDATIONS

#### 6.1. Conclusion

The study of oral protein therapeutics encompasses a great deal of innovative research, striving for novel site specific drug release properties, displaying significant potential for a new era of oral dosage forms in protein therapeutics. The pH responsive copolymeric systems were developed to specifically react in accordance to preservation of the centrally loaded drug matrix, thereby conserving the integrity of the protein molecule. Due to the sensitive nature of the protein therapeutic, denaturing is often the most common problem associated with pre-formulation studies, thereby making it most difficult to obtain a composite system with complete efficacy for oral delivery.

Comparative studies of the copolymeric microgel and microparticulate systems clearly demonstrates greater efficacy in the microparticulate formulation of TMC-PEGDMA-MAA, displaying superior *in vitro* and *in vivo* protein concentrations, as well as releasing over a longer duration of time. The microparticles also demonstrated more favorable physical characteristic properties, displaying significant differences in relation to the behavior in the respective pH conditions. The polymer responsible for the significant difference in the behavioral response is attributed to TMC which is well known for its highly mucoadhesive, cationic polyelectrolyte nature. Due to its considerate degree of strong electrostatic interactions with mucus and the charged mucosal surface, its quarternisation properties have significant effects on the absorption enhancing nature of the protein loaded copolymeric system. It is well noted that many positive charges on the polymer are expanded in solution, due to repelling forces between functional groups and is therefore able to transport many hydrophilic compounds easily across the mucosal epithelia by providing easy opening of tight junctions on mucosal linings. Consequently, it has a well defined structural arrangement with improved solubility from its parent polymer chitosan. It can therefore be concluded that the optimized formulation of TMC-PEGDMA-MAA displays significant protein-loading and mucoadhesive properties, thereby enhancing the penetration and absorption of the peptide through the intestinal mucosa, as observed in the results obtained in this thesis.

The copolymeric particles also demonstrated smaller particles size as opposed to the microgel formulation, thereby resulting in greater absorption properties through the mucosal membranes, as seen with substantial degree in the copolymeric particles in comparison to the microgel formulation.

For the copolymeric microparticulate system of TMC-PEGDMA-MAA, the peak bioavailable dose in serum was calculated to be 1.3% of INF- $\beta$  in comparison to the SC formulation, having a peak concentration of 0.9% in comparison to the placebo formulation. Due to the slow penetration of the SC formulation into the blood stream, the concentration of INF- $\beta$  can be expected to increase over a greater duration of time since the dosing intervals are generally 3 injections weekly. Insulin loaded copolymeric particles displayed a significant decrease in blood glucose by 54.19% within 4 hour duration, and thereafter observing an increase in blood glucose levels gradually. The commercial SC insulin formulation showed a 74.6% decrease in blood glucose within 4 hour duration, however displaying a sharp increase in blood glucose thereafter. EPO loaded copolymeric system was observed to have a 1.6% peak bioavailable concentration from oral copolymeric particles, in relation to the 6.34% peak concentration at 8<sup>th</sup> hour duration from the SC commercial formulation.

The copolymeric microgel system of CHT-PEGDMA-MAA displayed a 1.53 times greater concentration of INF- $\beta$  oral delivery system than the placebo at 5 hour duration, as opposed to a 2.33 times greater concentration of the commercial product in comparison to the placebo at the same time point. Insulin studies revealed a maximum decrease in blood glucose at 3 hours after gastric gavage, showing a 38.2% decrease of blood glucose levels due to the oral microgel system. The commercial formulation demonstrated a 74.68% decrease in blood glucose in comparison to the placebo formulation. EPO oral formulation demonstrated a 3.42 times greater concentration than the placebo concentration at 8 hour duration as compared to a substantial difference of 22.22 times greater concentration in the SC formulation at 8<sup>th</sup> hour duration. It can therefore be concluded that the microparticle system has superior properties over the microgel system, displaying many benefits and advantages as discussed in detail in the various chapters of this thesis.

## 6.2. Future Outlook and Recommendations

The avenue of neuroscience has always been a substantially significant platform for continuous development and novel therapeutic drug delivery systems treatment in a wide variety of neurodegenerative diseases. Drug delivery is responsible for determining areas in which we can enhance the application, by substantially providing significant therapy in the most patient acceptable and compliant manner, thereby looking at novel innovative aspects for achieving greatest bioavailability and controlled release formulations.

MS remains as part of a diverse category of diseases in which continuous research is undertaken ranging from selective biomarkers, new anti-inflammatory drug compounds, newly identified specific activation targets, proposed vasodilator treatments and discovery of specific gene targeted therapy. Many studies involving protein therapeutics have been undertaken; however the next stage of achieving greater compliance for various disease states would be the combination of multiple protein therapeutics in a single delivery system, combatting a broad range of problems with a single more efficient system.

Focussing on MS specifically from a diagnostic and therapeutic aspect, a significant area of concern in the advancement of MS treatment is the establishment of selective biomarkers in drug delivery systems, which are fundamental for the establishment of novel therapeutic development to analyze and predict the intensity and progression of the disease state. The use of biomarkers in novel drug formulations will be crucial as an indication of the pathological events and form an optimistic approach to pharmacological intervention. Areas of pharmacokinetic and pharmacodynamic evaluations, will determine the dose quantity and incremental values for the compound advancement, e.g., lymphocytosis with  $\alpha 4 \beta 1$  integrin antagonists. Alteration in the immune system are classical indications of these biomarkers, such as, 'antibodies, adhesion molecules, cytokines, chemokines, BBB disruption; demyelination; oxidative stress and excitotoxicity; axonal and neuronal damage; gliosis; as well as remyelination and repair'. According to Avsar *et al.*, 2012, there appears to be no laboratory markers to date, to enhance the possibility of precise diagnosis and in identifying the degree of MS, however, certain protein markers have been researched to incorporate a procedure of identifying specific subtypes and progression of MS. Areas of analyzing detection of specific protein biomarkers include urine, blood as well as CSF samples with regard to disease

response. Essentially, these biomarkers should correlate with the degree of disease severity and respond to effects of treatment.

Another approach of molecular profiling relating to utility of genomics, proteomics, and metabolomics, will assist in more significantly specified diagnoses and treatment of MS, identifying and validating therapy based targets as well as determining responses from treatment, hence developing specific therapeutic procedures based on the disease progression and outcome. Additionally, translation approaches such as stem cell therapy, although ethically controversial, could be a better alternative to repair the injury in the CNS as proposed by some groups. In view of identifying how people relate to this disease condition and a proposed response in future research pertaining to the alteration of certain genetic pathways, studies conducted by Bieber *et al.*, 2009 (<http://www.sciencedaily.com>) identified that, 'there are two possible genes as potential therapeutic targets in M.S and there may be a small number of strong genetic determinants for CNS repair, in relation to a larger number of weak determinants'. There are however, risks associated with this kind of treatment such as, uncontrolled cells developing with possible manifestations of tumor development. The source of the stem cells, either autologous or allogeneic, also has great significance in the body's response of accepting or rejecting the transplant. Thus, these genes may provide significant future understanding as to why certain people cope better with MS in relation to others.

Drug delivery encompasses major challenges associated with the oral route of peptide delivery including a significantly high acidic pH of the stomach, presystemic enzymatic degradation of peptide and its poor permeation through the intestinal membrane.

The establishment of a versatile oral copolymeric drug delivery system has certainly proved significant oral drug absorption, especially due to the dosage form which was delivered uncoated via gastric dosing. These profound properties and results have not been documented to date to such degree, leaving little scope in the avenue for greater development of oral protein dosage forms as the versatile copolymeric drug delivery system established. Improvements of the system can be designed to increase the half life of the protein formulations, however, since this novelty has been developed with extreme specifications of optimal drug loading and release kinetics, substantial effort would be required to eliminate the limitations which are minimally displayed in this research.

## 7. REFERENCES

A Beginner's Guide, Thermogravimetric Analysis (TGA), 2010, [www.perkinelmer.com](http://www.perkinelmer.com)

Allison, R.S., Millar J.H., 1954. Prevalence of disseminated sclerosis in Northern Ireland. *Ulster Medical Journal* 23, 1–27.

Andersson, P.B., Waubant, E., Gee, L., Goodkin, D.E., 1999. Multiple Sclerosis that is Progressive from the time of onset: clinical characteristics and progression of disability. *Archives of Neurology* 56(9), 1138-42

Angelov, D.N., Waibel, S., Guantinas-Lichius, O., et al., 2003. Therapeutic vaccine for acute and chronic motor neuron diseases: implications for aprocytrophic lateral sclerosis. *Proceedings of the National Academy of Sciences* 100, 4790-4795

Arduini, R.M., Strauch, K.L., Runkel L.A., 1999. Characterization of a soluble ternary complex formed between human interferon-1a and its receptor chains. *Protein Sci.* 8, 1867-1877.

Avsar, T., Korkmaz,D., Tütüncü, M., Demirci, N.O., Saip, S., Kamasak, M., Siva, S., Tahir, E., et al., 2012. Protein biomarkers for multiple sclerosis: semi-quantitative analysis of cerebrospinal fluid candidate protein biomarkers in different forms of multiple sclerosis. *Multiple Sclerosis* 0, 1–11

Axelrod, J and Reichenthal J 1953. The fate of caffeine in man and a method for its estimation in biological material. *J Pharmacol Exp Ther* 107:519-523.

Bar-Or, A., Calabresi, P.A., Arnold, D., Markowitz, C., Shafer,S., Kasper,L.H., Waubant, E, Gazda, S., Fox,R.J., Panzara,M., Sarkar,N., Agarwal,A., Smith,C.H., 2008. Rituximab in relapsingremitting multiple sclerosis: a 72-week, open-label, phase I trial. *Annals of Neurology* 63 (3), 395–400.

Barun, B., Bar-Or, A., 2012. Treatment of multiple Sclerosis with Anti-CD20 antibodies. *Clinical Immunology* 142, 31–37

Bawa, P., Pillay, V., Choonara, Y. E, du Toit, L. C., Ndesendo, L. V. K., and Kumar P., 2011. A composite Polyelectrolytic Matrix for Controlled Oral Drug Delivery. *AAPS PharmSciTech* 12(1), 227-238

Beck and Arnold 1977. Parameter Estimation in Engineering and Science. (Beck JV and Arnold KJ, eds.) John Wiley & Sons Inc., NY, USA.

Beenakker, E.A., Oparina, T.I., Hartgring, A., et al., 2001. Cooling garment treatment in MS: clinical improvement and decrease in leukocyte NO production. *Neurology* 57, 892–894

Bergamaschi, R., Berzuini, C., Romani, A., Cosi ,V., 2001. Predicting Secondary/Progression in Relapsing/Remitting Multiple Sclerosis: A Bayesian Analysis. *Journal of the Neurological Sciences*, 15;189(1-2):13-21

Bjartmar, C., Wujek,J.R., Trapp, B.D., 2003. Axonal loss in the pathology of MS: consequences for understanding the progressive phase of the disease, *Journal of the Neurological Sciences* 206,165– 171

Bowman, K., Leong, K.W., 2006. Chitosan nanoparticles for oral drug and gene Delivery. *Int. J. Nanomedicine*.1, 117–128

Bravo-Osuna, I., Millotti, G., Vauthier, C., Ponchel, G., 2007. In vitro evaluation of calcium binding capacity of chitosan and thiolated chitosan poly(isobutyl cyanoacrylate) core – shell nanoparticles. *Int. J. Pharm.* 338(1-2), 284-290.

Brinkmann,V., Davis,M.D., Heise,C.E., Albert,R., Cottens,S., Hof,R., Bruns,C., Prieschl,E., Baumruker,T., Hiestand,P., Foster,C.A., Zollinger,M.,Lynch,K.R., 2002. The immune modulator FTY720 targets sphingosine 1-phosphate receptors. *Journal of Biological Chemistry* 277, 21453–21457.

Broman, T., Bergmann ,L., Fog, T., et al., 1965. Aspects on classification methods in multiple sclerosis. *Acta Neurologica Scandinavica Supplement*, 2, 543–8.

Bruce D., Trapp, B.D., Nave, K.A., 2008. Multiple Sclerosis:An Immune or Neurodegenerative Disorder?. *The Annual Review of Neuroscience* 31:247–69

Celej, M.S., Dassie, S.A., González, M., Bianconi, M.L. and Fidelio, G.D., (2006). Differential scanning calorimetry as a tool to estimate binding parameters in multiligand binding proteins.

Celej,. M.S., Dassie, S.A., González, M., Bianconi, M.L. and Fidelio, G.D., (2006). Differential

Charles Patrick Davis,. Multiple Sclerosis: Causes, Symptoms and Treatment, 2010. Last accessed on 12<sup>th</sup> April 2013 from [http://www.medicinenet.com/multiple\\_sclerosis\\_pictures\\_slideshow/article.htm](http://www.medicinenet.com/multiple_sclerosis_pictures_slideshow/article.htm),

Chiu, A.W., Ehrmantraut, M., Richert, N.D., Ikonomidou, V.N., Pellegrini, S., McFarland, H.F., Frank, J.A., Bagnato, F., 2007. A case study on the effect of neutralizing antibodies to interferon beta 1b in multiple sclerosis patients followed for 3 years with monthly imaging. *Clin. Exp. Immunol.* 150, 61-67

Claussen, M.C., Korn, T., 2012. Immune mechanisms of new therapeutic strategies in MS—teriflunomide. *Clinical Immunology* 142, 1,49–56

Coisne, C., Mao, W., Engelhard, B., 2009. Cutting Edge: Natalizumab Blocks Adhesion but Not Initial Contact of Human T Cells to the Blood-Brain Barrier In Vivo in an Animal Model of Multiple Sclerosis. *Journal of Immunology* 182, 5909-5913

Compston, A., Coles, A., 2008. Multiple sclerosis. *Lancet* 372, 1502–1517.

Cruise, G.M., Hergre, O.D., Scharp, D.S., Hubbell, J.A., 1998. A sensitivity study of the key parameters in the interfacial photopolymerisation of poly(ethylene glycol) diacrylate upon porcine islets. *Biotechnol. Bioeng.* 57, 655–665.

Davies and Whitting 1972. A modified form of Levenberg's correction. In: *Numerical Methods for*

Dhib-Jalbut, S., 2002. Mechanisms of action of interferons and glatiramer acetate in multiple sclerosis. *Neurology* 58, 3-9

Domard, A., Rinaudo, M., Terrassin, C., 1986. New method for the quaterinization of chitosan. *Int J Biol Macromol.* 8, 105-107.

Domard, A., Rinaudo, M.; Terrassin, C., 1986. New method for the quaterinization of chitosan. *Int J Biol Macromol.* 8, 105-107.

Draper and Smith, 1981. *Applied Regression Analysis*, 2nd ed. John Wiley & Sons, NY, USA.

Dutta, R., Trapp, B.D., 2011. Mechanisms of neuronal dysfunction and degeneration in multiple sclerosis. *Progress in Neurobiology* 93, 1–12

Dutta, S., Reed, R.C., Cavanaugh, J.H., 2004. Absolute bioavailability and absorption characteristics of divalproex sodium extended-release tablets in healthy volunteers. *J Clin Pharmacol* 44:737-742.

Ebers, G.C., Traboulsee, A., Li, D., Langdon, D., Reder, A.T., Goodin, D.S., et al., 2010. Analysis of clinical outcomes according to original treatment groups 16 years after the pivotal IFNB-1b trial. *Journal of Neurology, Neurosurgery, Psychiatry* 81 (8) 907–912.

Eid, P., Meritet J.F., Maury, C., et al., 1999. Oromucosal interferon therapy: pharmacokinetics and pharmacodynamics. *J. Interferon Cytokine Res.* 19, 157–169.

Ellison, C.D., Ennis, B.J., Hamad, M.L., Lyon, R.C., 2008. Measuring the distribution of density and tableting force in pharmaceutical tablets by chemical imaging, *J Pharm Biomed Anal.*, 48: 1-7

Ellison, C.D., Ennis, B.J., Hamad, M.L., Lyon, R.C., 2008. Measuring the distribution of density and tableting force in pharmaceutical tablets by chemical imaging. *J Pharm Biomed Anal.* 48, 1-7

Elovaara, I., 2011. Early treatment in multiple sclerosis, *Journal of the Neurological Sciences* 311, 24–28

Ferguson, B., Matyszak, M.K., Esiri, M.M., Perry, V.H., 1997. Axonal damage in acute multiple sclerosis lesions. *Brain* 120, 393– 399.

Filippi, M., Rovaris, M., Rocca, M.A., et al., 2001. Glatiramer acetate reduces the proportion of new MS lesions evolving into “black holes”. *Neurology* 57, 731-733.

Finger, S., 1998. A Happy State of Mind: A History of Mild Elation, Denial of Disability, Optimism, and Laughing in Multiple Sclerosis. *Archives of Neurology*, 55(2):241-250

Fischer, A., Heesen, C., Gold, S.M., 2011. Biological outcome measurements for behavioral interventions in multiple sclerosis. *Ther. Adv. Neurol. Disord.* ; 4, 217–229.

Fish, R.E., Brown M.J., Danneman, P.J., Karas, A.Z., 2008. Anesthesia and Analgesia in Laboratory Animals. 2nd Ed. New York: Academic Press.

Fontoura, P., Garren, H., 2010. Multiple sclerosis therapies: molecular mechanisms and future. *Results and Problems in Cell Differentiation* 51, 259–85.

Foss, A.C., Peppas, N.A., 2004. Investigation of cytotoxicity and insulin transport of acrylic-based copolymer protein delivery systems in contact with caco-2 cultures. *Eur. J. Pharm. Biopharm.* 57, 447–455.

Foster, C.A., Mechtcheriakova, D., Storch, M.K., Balatoni, B., Howard, L.M., Bornancin, F., Wlachos, A., Sobanov, J., Kinnunen, A., Baumruker, T., 2009. FTY720 rescue therapy in the dark agouti rat model of experimental autoimmune encephalomyelitis: expression of central nervous system genes and reversal of blood–brainbarrier damage. *Brain Pathology* 19, 254–266.

Fox, E.J., 2006. Management of Worsening Multiple Sclerosis with Mitoxantrone: A Review. *Clinical Therapeutics* 28 (4), 461-474

Frischer, J.M., Bramow, S., Dal-Bianco, A., Lucchinetti, C.F., Rauschka, H., Schmidbauer, Frohman, E.M., Racke, M.K., Raine, C.S., 2006. Multiple Sclerosis-The Plaque and Its Pathogenesis. *The new England journal of medicine* 354, 942-955

Fujimori, J., Yoshihashi, Y., Yonemochi, E. and Terada, K., (2005). Application of Eudragit RS to thermo-sensitive drug delivery systems: II. Effect of temperature on drug permeability through membrane consisting of Eudragit RS/PEG 400 blend polymers. *Journal of Controlled Release*, 102, 49-57.

Gafson, A., Giovannoni, G., Hawkes, C.H., 2012. The diagnostic criteria for multiple sclerosis: From Charcot to McDonald, *Multiple Sclerosis and Related Disorders* 1, 9–14

Ghalie, R.G., Edan, G., Laurent, M., Mauch, E., Eisenmann, S., Hartung, H.P., Gonsette, R.E., Butine, M.D., Goodkin, D.E., 2002. Cardiac adverse effects associated with mitoxantrone (Novantrone) therapy in patients with MS. *Neurology* 59, 909–913

Gibaldi, M and Weintraub H 1970. Quantitative correlation of absorption and in vitro dissolution kinetics of aspirin from several dosage forms. *J Pharm Sci* 59:725-726.

Gold, R., Linington, C., Lassmann, H., 2006. Understanding pathogenesis and therapy of multiple sclerosis via animal models: 70 years of merits and culprits in experimental autoimmune encephalomyelitis research. *Brain* 129(8) 1953-1971

Goodin, D.S., Cohen, B.A., O'Connor, P., Kappos, L., Stevens, J.C., 2008. Assessment: the use of natalizumab (Tysabri) for the treatment of multiple sclerosis (an evidence based review).

Report of the Therapeutics and Technology Assessment Subcommittee of the American Academy of Neurology. *Neurology* 71, 766–773.

Goodin, D.S., Frohman, E.M., Garmany, G.P., et al., 2002. Disease modifying therapies in multiple sclerosis: report of the Therapeutics and Technology Assessment Subcommittee of the American Academy of Neurology and the MS Council for Clinical Practice Guidelines. *Neurology* 58(2), 169–178

Goodman, A.D., Cohen, J.A., Cross, A., et al., 2007. Fampridine-SR in multiple sclerosis: A randomized, double-blind, placebo-controlled, dose-ranging study. *Multiple Sclerosis* 13, 357–368.

Goodnow, C.C., Sprent, J., de St Groth, B.F., Vinuesa, C.G., 2005. Cellular and genetic mechanisms of self tolerance and autoimmunity. *Nature* 435, 590-597

Guinesi, L.S., Cavalheiro, É.T.G. The use of DSC curves to determine the acetylation degree of chitin/chitosan samples. *Thermochim Acta*. 2006, 444, 128-133.

Guinesi, L.S., Cavalheiro, É.T.G., 2006. The use of DSC curves to determine the acetylation degree of chitin/chitosan samples. *Thermochim Acta*. 444, 128-133.

Handel, A.E., Ramagopalan, S.V., 2012. Vitamin D and multiple sclerosis: an interaction between genes and environment. *Multiple Sclerosis Journal* 18(1), 2–4

Harder, Y., Hartley, H.O 1961. The modified Gauss-Newton method for the fitting of nonlinear regression

Hauser, S.L., Waubant, E., Arnold, D.L., Vollmer, T., Antel, J., Fox, R.J., Bar-Or, A., Panzara, M., Sarkar, N., Agarwal, S., Langer-Gould, A., Smith, C.H., 2008. Hermes Trial Group, B-cell depletion with rituximab in relapsing-remitting multiple sclerosis. *New England Journal of Medicine* 358 (7), 676–688

Hawker, K., O'Connor, P., Freedman, M.S., Calabresi, P.A., Antel, J., Simon, J., Hauser, S., Waubant, E., Vollmer, T., Panitch, H., Zhang, J., Chin, P., Smith, C.H., 2009. Olympus trial group, Rituximab in patients with primary progressive multiple sclerosis: results of a randomized double-blind placebo-controlled multicenter trial. *Annals of Neurology* 66 (4), 460–471.

Hayes, K.C., 2007. Fampridine-SR for multiple sclerosis and spinal cord injury. *Expert Review on Neurotherapeutics* 7(5), 453–461

Hazime, S., Ryoko T., Kozo O., 1987. High-Resolution Solid-state  $^{13}\text{C}$  NMR Study of Chitosan and Its Salts with Acids: Conformational Characterization of Polymorphs and Helical Structures as Viewed from the Conformation-Dependent  $^{13}\text{C}$  Chemical Shifts, *Macromolecules* ,20, 2424-2430

Hemant, K.S.Y. and Shibakumar, H.G.,2010. A comparative study of N-trimethyl chitosan chloride and chitosan microparticles as novel carriers for the delivery of hypertensive drug. *J Pharm Res.* 3(4):809-813.

Henriksen, K.N., Sorensen, P.S., 2010. The changing demographic pattern of multiple sclerosis epidemiology. *Lancet Neurology* 9, 520–532

Herh, P., Tkachuk, J., Wu, S., Bernzen, M. and Rudolph, B., 1998. The rheology of pharmaceutical and cosmetic semisolids , Application Note, ATS Rheosystems Gerogetown Rd, Bordentown, NJ, USA.

Herrmann, A.M., Göbel ,K., Simon, O.J., Melzer, N., Schuhmann, M.K., Stenner, M.P., Weishaupt, A., Kleinschnitz, C., Bittner, S., Meuth, P., Stuve ,O., Budde, T., Kieseier, B.C., Wiendl, H., Meuth, S.G., 2010. Glatiramer acetate attenuates pro-inflammatory T cell responses but does not directly protect neurons from inflammatory cell death. *American Journal of Pathology* 177(6), 3051-60.

Hong, J., Li, N., Zhang, X., et al., 2005. Induction of CD4+CD25+ regulatory T cells by copolymer-I through activation of transcription factor Foxp3. *Proceedings of the National Academy of Sciences* 3(18): 6449-54

Hori, S., Nomura, T., Sakaguchi, S., 2003. Control of regulatory T cell development by the transcription factor Foxp3. *Science* 14, 1057-6

<https://www2.chemistry.msu.edu/faculty/reusch/VirtTxtjml/polymers.htm>, last updated 05/05/2013, accessed on 30/11/2013.

Huan, J., Culbertson, N., Spencer, L., Bartholomew ,R., Burrows, G.G., Chou, Y.K., et al., 2005. Decreased FOXP3 levels in multiple sclerosis patients. *Journal of Neuroscience Research* 81(1):45-52

Ibrahim, S.M., Gold, R., 2005. Genomics, proteomics, metabolomics: what is in a word for multiple sclerosis. *Current Opinion in Neurology* 18, 231–235.

Ingle, G.T., Sastre-Garriga, J., Miller, D.H., Thompson, A.J., 2005. Is inflammation important in early PPMS? A longitudinal MRI study. *Journal of Neurology, Neurosurgery & Psychiatry* 76(9), 1255-8

Ingwersen, J., Aktas, O., Kuery, P., Kieseier, B., Boyko, A., Hartung, H.P., 2012. Fingolimod in multiple sclerosis: Mechanisms of action and clinical efficacy. *Clinical Immunology* 142, 15–24

Islam, T., Gauderman, W.J., Cozen, W., et al., 2006. Differential twin concordance for multiple sclerosis by latitude of birthplace. *Annals of Neurology* 60, 56–64.

Iwata, A., et al., 1996. Cloning and expression of the canine interferon-beta gene. *J. Interferon Cytokine Res.* 16, 765-770

Jelvehgari, M, Siahi-Shadbad MR, Azarmi S, Martin GP, Nokhodchi A., 2006. The microspoon delivery system of benzoyl peroxide: Preparation, characterization and release studies. *Int J Pharm.* 308:124–32.

Jelvehgari, M., Siahi-Shadbad, M.R., Azarmi, S., Martin, G.P., Nokhodchi, A., 2006. The microspoon delivery system of benzoyl peroxide: Preparation, characterization and release studies. *Int J Pharm.* 308, 124–32.

Johnson, K.P., Brooks, B.R., Cohen, J.A., et al., 1995. Copolymer 1 reduces relapses rate and improves disability in relapsing-remitting multiple sclerosis: results of a phase III multicenter, double blind, placebo-controlled trial. *Neurology* 45, 1268-1276.

Johnson, K.P., Brooks, B.R., Cohen, J.A., et al., 1998. Extended use of glatiramer acetate (Copaxone) is well tolerated and maintains its clinical effect on multiple sclerosis relapse rate and degree of disability. Copolymer 1 Multiple Sclerosis Study Group. *Neurology* 50, 701-708.

Johnson, K.P., Brooks, B.R., Cohen, J.A., et al., 2001. Copolymer 1 reduces relapse rate and improves disability in relapsing-remitting multiple sclerosis: results of a phase III multicenter, double-blind, placebo-controlled trial. *Neurology Supplement* 5, 16-24.

Johnson, W.D., Forman C., Vesey.D.A., 2006. Novel renoprotective actions of erythropoietin: New uses for an old hormone. *Nephrology*, 11(4), 306-312

- Jongen, P.J., Hengstman, G., Hupperts, R., Schrijver, H., Gilhuis, J., et al., 2011. Drug adherence and multidisciplinary care in patients with multiple sclerosis. *BMC Neurology*. 11, 40
- Joseph, M., Cummins, G., Krakowka, S., Thompson, C.G., 2005. Systemic effects of interferons after oral administration in animals and humans. *Am. J. Vet. Res.* 66, 164-176
- Joshi, S., Reif, R., Wang, M., Zhang, J., Ergin, A., Bruce, J.N., L. Fine, R.L., Bigio, I.J., 2011. Intra-arterial Mitoxantrone Delivery in Rabbits: An Optical Pharmacokinetic Study. *Neurosurgery* 69,706–712, 2011
- Jung, S., Siglienti, I., Grauer, O., et al., 2004. Induction of IL-10 in rat peritoneal macrophages and dendritic cells by glatiramer acetate. *Journal of Neuroimmunology* 148 (1-2), 63-73
- Kappos, L., Gold, R., Miller, D.H., et al., 2008. Efficacy and safety of oral fumarate in patients with relapsing-remitting multiple sclerosis: a multicentre, randomised, double-blind, placebo-controlled phase IIb study. *Lancet* 372, 1463–72.
- Kappos, L., Bates, D., Edan, G., Eraksoy, M.U., 2011. Natalizumab treatment for multiple sclerosis: updated recommendations for patient selection and monitoring, *Lancet Neurology* 10, 745–58
- Kataoka, H., Sugahara, K., Shimano, K., Teshima, K., Koyama, M., Fukunari, A., Chiba, K., 2005. FTY720, sphingosine 1-phosphate receptor modulator, ameliorates experimental autoimmune encephalomyelitis by inhibition of T cell infiltration, *Cell. Molecular Immunology* 2 , 439–448.
- Katrych, O., Simone, T.M., Azad, S., Mousa, S.A., 2009. Disease-modifying agents in the treatment of multiple sclerosis: a review of long-term outcomes. *CNS & Neurological Disorders - Drug Targets* 8, 512–519
- Killestein, J., Rudick, R.A., Polman, C.H., 2011. Oral treatment for multiple sclerosis. *Lancet Neurology*, 10, 1026–34
- Kim, H.J., Ifergan, I., Antel, J.P., et al., 2004. Type 2 monocyte and microglia differentiation mediated by glatiramer acetate therapy in patients with multiple sclerosis. *Journal of immunology* 172 (11), 7144-53

Kim, H.J., Miron, V.E., Dukala, D., Proia, R.L., Ludwin, S.K., Traka, M., Antel, J.P., Soliven, B., 2011. Neurobiological effects of sphingosine 1-phosphate receptor modulation in the cuprizone model. *FASEB Journal* 25, 1509–1518.

Kittur, F.S., Prashanth, H., Sankar, K.U., Tharanathan, R.N., 2002. Characterization of chitin, chitosan and their carboxymethyl derivatives by differential scanning calorimetry. *Carbohydr Polym.* 49, 185-193.

Kornek, B., Storch, M.K., Weissert, R., et al., 2000. Multiple sclerosis and chronic autoimmune encephalomyelitis. A comparative quantitative study of axonal injury in active, inactive, and remyelinated lesions. *The American Journal of Pathology* 157, 267– 376

Krishnan (a), A.V., Kiernan, M.C., 2012. Sustained-release fampridine and the role of ion channel dysfunction in multiple sclerosis. *Multiple Sclerosis Journal* 0(0) 1– 7

Krishnan (b), A., Goodman, A., Potts, J., et al., 2012. Health-related quality of life is reduced in multiple sclerosis patients whose walking speed declines over time. *Neurology* 78, 7-96.

Krupp, L.B., Coyle, P.K., Doscher, C., et al., 1995. Fatigue therapy in multiple sclerosis: results of a double blind randomized parallel trial of amantadine, pemoline and placebo. *Neurology* 45, 1956–1961

Kumar, A., Lahiri, S.S., Singh, H., 2006. Development of PEGDMA: MAA based hydrogel micromicrogelfor oral insulin delivery, *International Journal of Pharmaceutics* 323, 117–124.

Kumar, A., Lahiri, S.S., Punyani, S., Singh, H., 2008. Synthesis and Characterization of pH Sensitive Poly(PEGDMA-MAA) Copolymeric Microparticles for Oral Insulin Delivery. *J. Appl. Polym. Sci.* 107, 863-871

Kumar, A., Lahiri, S.S., Singh, H., 2006. Development of PEGDMA: MAA based hydrogel microparticles for oral insulin delivery. *Int. J. Pharm.* 323,117–124

Kumari, A., Yadav, S.K., Yadav, S.C., 2010. Biodegradable polymeric nanoparticles based drug delivery systems. *Colloids Surf. B. Biointerfaces* .75, 1–18

Kuratsune, H., Yamaguti, K., Lindh, G., et al., 2002. Brain regions involved in fatigue sensation: reduced acetylcarnitine uptake into the brain. *Neuroimage* 17, 1256–1265

Kurihara, S., .2013. Greater potency of darbepoetin- $\alpha$  than erythropoietin in suppression of serum hepcidin-25 and utilization of iron for erythropoiesis in hemodialysis patients. *Eur J Haematol*, 90(3):237-244

Lalive, P.H., Neuhaus,O., Benkhoucha, M., Burger,D., Hohlfeld, R., Scott, S., Weber, Z.M.S., 2011. Glatiramer Acetate in the Treatment of Multiple Sclerosis Emerging Concepts Regarding its Mechanism of Action. *CNS Drugs*; 25 (5), 401-414

Lassmann, H., 2004.Recent NeuroPathological Findings In MS - Implications For Diagnosis And Therapy. *Journal of Neurology* 251, Suppl 4:IV2-IV5

le Dung, P., Milas, M., Rinaudo, M., Desbrières, J., 1994. Water soluble derivatives obtained by controlled chemical modification of chitosan. *Carbohydr Polym.* 24(3), 209-214.

Leone, D.R., Giza, K., Gill, A., Dolinski, B.M., Yang, W., Perper, S., et al., 2003. An assessment of the mechanistic differences between two integrin  $\alpha(4)\beta(1)$  inhibitors, the monoclonal antibody TA-2 and the small molecule BIO5192, in rat experimental autoimmune encephalomyelitis. *Journal of Pharmacology and Experimental Therapeutics.* 305, 1150–1162.

Leuner, C., Dressman ,J., 2000. Improving drug solubility for oral delivery using solid dispersions, *Eur. J. Pharm. Sci.* 50, 47-60.

Levin, M., 2006.Pharmaceutical process scale-up. In: *Drugs and the Pharmaceutical Sciences*

Levy, G., Leonards, J and Procknal, J.A., 1965. Development of *in vitro* tests which correlate quantitatively with dissolution rate-limited drug absorption in man. *J Pharm Sci* 54:1719-1722.

Lifshin, E ed. X-ray characterization of materials. 1999, Toronto, Wiley.

Linker, R.A, Lee, D.H, Ryan, S, et al., 2011. Fumaric acid esters exert neuroprotective effects in neuroinflammation via activation of the Nrf2 antioxidant pathway. *Brain* 134, 678–92.

Lovas, G., Szilagyi, N., Majtenyi ,K., et al., 2000. Axonal changes in chronic demyelinated cervical spinal cord plaques. *Brain* 123, 308–317.

Lowman, A.M., Peppas, N.A., 2000. Molecular analysis of interpolymer complexation in graft copolymer networks. *Polymer* 41, 73–80.

M, Laursen, H., Sorensen, P.S., Lassmann, H., 2009. The relation between inflammation and neurodegeneration in multiple sclerosis brains. *Brain* 132, 1175-1189

Mainero, C., Inghilleri, M., Pantano, P., et al., 2004. Enhanced brain motor activity in patients with MS after a single dose of 3,4-diaminopyridine. *Neurology* 62, 2044–2050

Maloney, D.G., Liles, T.M., Czerwinski, D.K., et al., 1994. Phase I clinical trial using escalating single-dose infusion of chimeric anti-CD20 monoclonal antibody (IDEC-C2B8) in patients with recurrent B cell lymphoma. *Blood* 84, 2457–2466.

McAlpine, D., Lumsden, C., Acheson, E., 1972. Multiple sclerosis: a reappraisal. Baltimore: Williams and Wilkins; Book ISBN 0443008256 , 2nd edition, page 653.

McDonald, W.I, Compston, A, Edan ,G., et al., 2001. Recommended diagnostic criteria for multiple sclerosis: guidelines from the International Panel on the diagnosis of multiple sclerosis. *Annals of Neurology* 50, 121–7.

Mecha, M., Francisco, J., Salinas, C., Mestre, L., Feliu´ , A., Guaza, C., 2013. Viral models of multiple sclerosis: Neurodegeneration and demyelination in mice infected with Theiler's virus. *Progress in Neurobiology* 101–102, 46–64

Medline Plus,. Multiple sclerosis. Accessed February 20, 2012, at: <http://www.nlm.nih.gov/medlineplus/ency/article/000737.htm>.

Mettler Toledo Usercom 11, 1998; The University of Southern Mississippi, Differential Scanning Calorimetry, 2005; Silicon Far East, 2005).

Mettler Toledo Usercom 7, 1998; Xua *et al.*, 2000

Miller, A, O'Connor, P, Wolinsky, J.S., et al., 2011. Clinical and MRI outcomes from a phase III trial (TEMSO) of oral teriflunomide in multiple sclerosis with relapses. *Neurology*, 76, S41.002.

Miller, D.H., Khan, O.A., Sheremata, W.A., Blumhardt, L.D., Rice, G.P., Libonati, M.A., Willmer-Hulme, A.J., Dalton, C.M., Miszkziel, K.A., O'Connor, P.W., 2003. A controlled trial of natalizumab for relapsing multiple sclerosis. *New England Journal of Medicine* 348, 15–23.

Miller, D.H., Soon, D., Fernando, K.T., et al., 2007. MRI outcomes in a placebo-controlled trial of natalizumab in relapsing MS. *Neurology* 68, 1390-1401.

Minagar, A., Jy, W., Jimenez, J.J., Sheremata, W.A., Mauro, L.M., Mao, W.W., et al., 2001. Elevated plasma endothelial microparticles in multiple sclerosis. *Neurology* 56(10), 1319-24

Mix, E., Rienecker, H.M., Hartung, H.P., Zettl, U.K., 2010. Animal models of multiple sclerosis- Potentials and limitations. *Progress in Neurobiology* 92, 386–404

Moharreggh-Khiabani, Linker, R.A., Gold, R., Stangel, M., 2009. Fumaric Acid and its Esters: An Emerging Treatment for Multiple Sclerosis. *Current Neuropharmacology*, 7, 60-64

Montalban, X., Tintore, M., Swanton, J., Barkhof, F., Fazekas, F., Filippi, M., et al., 2010. MRI criteria for MS in patients with clinically isolated syndromes. *Neurology* 74, 427–34.

Morishita, M., Peppas, N., 2006. Is the oral route possible for peptide and protein drug delivery. *Drug Discov. Today*. 11, 19-20

Mourya, V.K., Inamdar, N.N., 2009. Trimethyl chitosan and its applications in drug delivery. *J Mater Sci Mater Med*. 20, 1057-1079.

Mourya, V.K., Inamdar, N.N., 2009. Trimethyl chitosan and its applications in drug delivery. *J Mater Sci Mater Med*. 20, 1057-1079.

Multiple sclerosis study identifies genetic causes, <http://www.independent.co.uk/news/science/multiple-sclerosis-study-identifies-genetic-causes-2335615.html>, updated on August 2011, accessed on 24-02-13

Multiple Sclerosis, treatment and drugs :<http://www.mayoclinic.com/health/multiple-sclerosis> accessed on 26-02-13, updated December 2012.

Munger, K.L., Levin, L.I., Hollis, B.W., Howard, N.S., Ascherio, A., 2006. Serum 25-hydroxyvitamin D levels and risk of multiple sclerosis. *Journal of the American Medical Association* 296, 2832–2838.

Mustafa, M., Diener, P., Sun, J.B., et al., 1993. Immunopharmacologic modulation of experimental allergic encephalomyelitis: Low-dose cyclosporin-A treatment causes disease relapse and increased systemic T and B cell-mediated myelin-directed autoimmune. *Scandinavian Journal of Immunology* 38, 499-507.

Mustata, G., Dinh, S.M., 2005. Drug delivery global summit – Evaluating emerging technologies. *Expert Opin Drug Deliv.* 2, 185-187.

Naismith, N.T., Piccio, L., Lyons, J.A., Lauber, J., Tutlam, N.T., Naismith, B.J., Piccio, Lyons, J.A., Lauber, J., Tutlam, N.T., Parks, B.J., Trinkaus, K., Song, S.K., Cross, A.H., 2010. Rituximab add-on therapy for breakthrough relapsing multiple sclerosis: a 52-week phase II trial. *Neurology* 74 (23), 1860–1867.

National Multiple Sclerosis Society. Interferons. Accessed January 31, 2012, at: <http://www.nationalmssociety.org/about-multiple-sclerosis/what-we-know-about-ms/treatments/medications/interferons/index.aspx>.

Neuhaus (a), O., Wiendl, H., Kieseier, B.C., Archelos, J.J., Hemmer, B., Stüve, O., Hartung, H.P., 2005. Multiple sclerosis: Mitoxantrone promotes differential effects on immunocompetent cells in vitro. *Journal of Neuroimmunology* 168, 128 – 137.

Neuhaus (b), O., Stüve, O., Zamvil, S.S., Hartung, H.P., 2005. Evaluation of HMG-CoA reductase inhibitors for multiple sclerosis: opportunities and obstacles. *CNS Drugs*, 19(10), 833-41.

Neuhaus, O., Farina, C., Wekerl, H., et al., 2001. Mechanisms of action of glatiramer acetate in multiple sclerosis. *Neurology* 56, 702-708.

Neuhaus, O., Farina, C., Yassouridis, A., et al., 2000. Multiple sclerosis: comparison of copolymer-1-reactive T cell lines from treated and untreated subjects reveals cytokine shift from T helper 1 to T helper 2 cells. *Proceedings of the National Academy of Sciences* 97 (13), 7452-7

New multiple sclerosis target identified,. <http://www.sciencedaily.com/releases/2011/01/110111171843.htm>. accessed on 11-03-2012. Updated on January 2011

New possibility of reversing damage caused by multiple sclerosis,. <http://www.sciencedaily.com/releases/2010/12/101205202522.htm>. accessed on 11-03-2013. Updated on December 2010.

Newton, R., Broughton LJ, Lind MJ, Morrison PJ, Rogers HJ and Bradbrook ID 1981. Plasma and salivary pharmacokinetics of caffeine in man. *Eur J Clin Pharmacol* 21:45-52.

Nielsen, N.M., Westergaard, T., Rostgaard, K., Frisch, M., Hjalgrim, H., Wohlfahrt, J., et al., 2005. Familial risk of multiple sclerosis: a nationwide cohort study. *American Journal of Epidemiology* 162(8), 774-778.

Nischwitz, S., Müller-Myhsok, B., Weber, F., 2011. Risk conferring genes in multiple sclerosis. *FEBS Letters* 585(23), 3789-97.

Non-linear Optimization. Academic Press, NY, USA, 12.

O'Connor, P.W., Li, D., Freedman, M.S., et al., 2006. A Phase II study of the safety and efficacy of teriflunomide in multiple sclerosis with relapses. *Neurology* 66, 894-900.

O'Connor, P.W., Goodman, A., Kappos, L., et al., 2011. Disease activity return during natalizumab treatment interruption in multiple sclerosis patients. *Neurology* 76, 1858-65.

Oken, B.S., Kishiyama, S., Zajdel, D., et al., 2004. Randomized controlled trial of yoga and exercise in multiple sclerosis. *Neurology* 62, 2058-2064

Okuno, S., Ostrowski, M., Baczek, T., 2010. The Progress on the *In Vivo-In Vitro* Correlation (IVIVC) for Immediate Release Dosage Form as an Alternative to Bioavailability Studies *Curr Pharm Anal*, 6, 289-298.

Ottervald, J., Franzén, B., Nilsson, K., et al., 2010. Multiple sclerosis: identification and clinical evaluation of novel CSF biomarkers. *Journal of Proteomics* 73, 1117-1132..

Palazzuoli, A., Silverberg, D.S., Iovine, F., Calabrò, A., Campagna, M.S., Gallotta, M., Nuti, R., 2007. Effects of beta-erythropoietin treatment on left ventricular remodeling, systolic function, and B-type natriuretic peptide levels in patients with the cardiorenal anemia syndrome, *Am Heart J*. 154(4):645.9-15

Panitch, H.S., Hirsch, R.L., Haley, A.S., Johnson, K.P., 1987. Exacerbations of multiple sclerosis in patients treated with gamma interferon. *Lancet* 1, 893-895.

Paues, J., Vrethem, M., 2010. Fatal progressive multifocal leukoencephalopathy in a patient with non-Hodgkin lymphoma treated with rituximab. *Journal of Clinical Virology* 48 (4), 291-293.

Ping, He., et al., 1998. In vitro evaluation of the mucoadhesive properties of chitosan microspheres. *Int J Pharm.* 166,75–68

Polman, C.H., Reingold ,S.C., Banwell, B., et al., 2011. Diagnostic criteria for multiple sclerosis. *Annals of Neurology* 69, 292–302.

Polnok, A., Borchard, G., Verhoef, J.C., Sarisuta, N., Junginger, H.E., 2004. Influence of methylation process on the degree of quaterization of N-trimethyl chitosan chloride. *Eur J Pharm Biopharm.* 57, 77-83.

Poser , C.M., Brinar, V.V., 2001. Diagnostic criteria for multiple sclerosis. *Clinical Neurology and Neurosurgery* 103, 1–11.

Poser, C.M., Brinar,V.V., 2004. Diagnostic criteria for multiple sclerosis: an historical review, *Clinical Neurology and Neurosurgery* 106, 147–158

Poser, C.M., Paty ,D.W., Scheinberg ,L., et al., 1983. New diagnostic criteria for multiple sclerosis: guidelines for research protocols. *Annals of Neurology* 13, 227–231.

Positive Results from Phase 3 CONFIRM Clinical Trial Show Efficacy and Safety of Oral BG-12 in Multiple Sclerosis; Detailed CONFIRM Data, Presented at 2012 American Academy of Neurology Annual Meeting Regulatory Applications Submitted to the FDA and EMA, [http://www.biogenidec.com/press\\_release\\_details.aspx?ID=5981&ReqId=1686377](http://www.biogenidec.com/press_release_details.aspx?ID=5981&ReqId=1686377), accessed 1/12/2013

Pozzilli, C., Sbardella, E., De Giglio, L., Tomassini, V., 2006. Treatment of multiple sclerosis-related fatigue: pharmacological and non-pharmacological approaches. *Neurological Science* 27, 297–299

Prasad, V, Shah V and Knight P 1983. Importance of media selection in establishment of *in vitro* *in vivo* relationship for quinidine gluconate. *Int J Pharm* 13:1-7.

Prejean, C., Colamonici, O.R., 2000. Role of the cytoplasmic domains of the type I interferon receptor subunits in signaling. *Seminars in Cancer Biology* 10 (2), 83–92.

Promising New Multiple Sclerosis Treatment Under Development, <http://www.sciencedaily.com/releases/2010/11/101118131017.htm>. accessed on 20-03-2013. Updated on Nov. 18, 2010

Prusiner, S.B., 2001. Neurodegenerative diseases and prions. *The New England Journal of Medicine* 344, 1516-1526

Ramagopalan, S.V., Heger, A., Berlanga, A.J., et al., 2010. A ChIPseq defined genome-wide map of vitamin D receptor binding: associations with disease and evolution. *Genome Research* 20, 1352–1360.

Ramazani-Harandi, M.J, Zohuriaan-Mehr, M.J, Yousefi, A.A, Ershad-Langroudi A, Kabiri, K., Rheological determination of the swollen gel strength of superabsorbent polymer hydrogels *Polymer Testing* 25 (2006) 470–474

Ransohoff, R.M., 2006. EAE: pitfalls outweigh virtues of screening potential treatments for multiple sclerosis. *Trends in Immunology* 27, 167–168.

Ratkowsky, D., 1983. *Nonlinear Regression Modeling*. Marcel Dekker, NY, USA.

Romberg, A., Virtanen, A., Ruutiainen, J., et al., 2004. Effects of a 6-month exercise program on patients with multiple sclerosis: a randomized study. *Neurology* 63, 2034–2038

Rose, A.S., Ellison ,G.W., Myers ,L.W., Tourtellotte, W.W., 1976. Criteria for the clinical diagnosis of multiple sclerosis. *Neurology* 26, 20–22

Rossini, P.M., Pasqualetti, P., Pozzilli, C., et al., 2001. Fatigue in progressive multiple sclerosis: results of a randomized, double- blind, placebo-controlled, crossover trial of oral 4-aminopyridine. *Multiple Sclerosis* 7, 354–358

Rudick, R.A., Stuart, W.H., Calabresi, P.A., et al., 2006. A randomized, placebocontrolled trial of natalizumab plus interferon beta-1a for relapsing multiple sclerosis. *New England Journal of Medicine* 354, 911–23.

Rudick, R.A., Fisher,E.,Lee,J.C., Simon,J., Jacobs,L., 1999. Use of the brain parenchymal fraction to measure whole brain atrophy in relapsing–remitting MS. *Multiple Sclerosis Collaborative Research Group. Neurology* 53, 1698–1704.

Rudick, R.A., Cutter, G.R., Baier, M., Weinstock-Guttman,B., Mass,M.K., Fisher,E et al., 2005. Estimating long-term effects of disease modifying therapy in multiple sclerosis patients. *Multiple Sclerosis* 11, 626–634.

Rudicka, R.A., Goelzb, S.E., 2011. Beta-interferon for multiple sclerosis. *Experimental Cell Research* 317, 1301–1311.

RxList, Avonex (interferon beta-1a) drug center. Accessed January 30, 2012, at: <http://www.rxlist.com/avonex-drug/indications-dosage>

Sajeesh, S., Sharma, C.P., 2006. Cyclodextrin-insulin complex encapsulated polymethacrylic acid based nanoparticles for oral insulin delivery. *Int. J. Pharm.* 15, 147-154

Sajeesh, S., Sharma, C.P., 2006. Novel pH responsive polymethacrylic acid-chitosan-polyethylene glycol nanoparticles for oral peptide delivery. *J. Biomed. Mater. Res. B. Appl. Biomater.* 76, 298-305

Sajesh, S., Sharma, C.P., 2006. Interpolymer complex microparticles based on polymethacrylic acid-chitosan for oral insulin delivery. *J. Appl. Polym. Sci.* 99, 506–512.

Sanna, A., Fois, M.L., Arru, G., et al., 2006. Glatiramer acetate reduces lymphocyte proliferation and enhances IL-5 and IL-13 production through modulation of monocyte-derived dendritic cells in multiple sclerosis. *Clinical & Experimental Immunology* 143 (2), 357-62

Schramm, G., (2004). *A Practical Approach to Rheology and Rheometry*. Thermo Electron (Karlsruhe), GmbH, Federal Republic of Germany, volume 2.

Schumacher, G. A., Beebe ,G., Kibler, R.F., et al., 1965. Problems of experimental trials of therapy in multiple sclerosis: report by panel on the evaluation of experimental trials of therapy in multiple sclerosis. *Annals of the New York Academy of Sciences*, 122, 552–68.

Schwab, S.R., Cyster, J.G., 2007. Finding a way out: lymphocyte egress from lymphoid organs. *Nature Immunology* 8, 1295–1301.

Schwarz, G., 1978. Estimating the dimension of a model. *Annals of Stat* 6:461-464.

Sellebjerg, F., Bornsen, L., Khademi, M., et al., 2009. Increased cerebrospinal fluid concentrations of the chemokine CXCL13 in active MS. *Neurology* 73, 2003–2010.

Shah, V.P., Prasad, V.K., Alston, T., Cabana, B.E., Gural, R.P., Meyer, M.C., 1983. Phenytoin I: In vitro correlation for 100mg phenytoin sodium capsules. *J Pharm Sci* 72:306-308.

Shaji, J., Patole, V., 2008. Protein and Peptide Drug Delivery: Oral Approaches. *Indian J.Pharm. Sci.* 70, 269–277.

Sherki, Y. G., Panet, H., Holdengreber, V., Galili, R.M., Offen, D., 2003. Axonal damage is reduced following glatiramer acetate treatment in C57/bl mice with chronic-induced experimental autoimmune encephalomyelitis. *Neuroscience Research* 47, 201-207.

Shim, H., 2011. One target, different effects: a comparison of distinct therapeutic antibodies against the same targets. *Experimental & Molecular Medicine* 43, 539-549.

Sing, K.S.W., Everett, D.H., Haul, R.A.W., Moscou, L., Pierotti, R.A., Rouquerol, J., et al., 1985. Reporting physisorption data for gas/solid systems with special reference to the determination of surface area and porosity. *Pure Appl Chem.*, 57:603–19.

Smith, K.J., 2007. Sodium channels and multiple sclerosis: Roles in symptom production, damage and therapy. *Brain Pathology* 17, 230–242.

Sonia, T.A., Sharma, C.P., 2011. Chitosan and Its Derivatives for Drug Delivery Perspective. *Adv Polym Sci.*, 243: 23–54

Sorensen, P.S., 2011. Balancing the benefits and risks of disease-modifying therapy in patients with multiple sclerosis. *Journal of the Neurological Sciences* 311, 29-34

Sospedra, M., Martin, R., 2005. Immunology of multiple sclerosis. *The Annual Review of Immunology* 23, 683–747

Stem cells, [http://www.mstrust.org.uk/information/publications/factsheets/stem\\_cells.jsp#risks](http://www.mstrust.org.uk/information/publications/factsheets/stem_cells.jsp#risks). Accessed on 7-03-2013. Updated July 2012.

Stewardson, D.J., Whitfield, R.I., 2004. A demonstration of the utility of fractional experimental design for finding optimal genetic algorithm parameter settings. *J.O.R.S.*, 55, 132-138.

Stone, L.A., Frank, J.A., Albert, P.S., Bash, C., Smith, M.E., Maloni, H., McFarland, H.F., 1995. The effect of interferon-beta on blood-brain barrier disruptions demonstrated by contrast-enhanced magnetic resonance imaging in relapsing-remitting multiple sclerosis. *Annals of Neurology* 37(5), 611-9.

Stuart, M., Bergstrom, L., 2011. Pregnancy and Multiple Sclerosis, *J. Midwifery Womens Health*. 56, 41–47.

Stuart, W.H., 2004. Clinical Management of Multiple Sclerosis: The Treatment Paradigm and Issues of Patient Management Supplement to *Journal of Managed Care Pharmacy* 10, 19-25

Taniguchi, T., Takaoka, A., 2002. The interferon-alpha/beta system in antiviral responses: a multimodal machinery of gene regulation by the IRF family of transcription factors, *Current Opinion in Immunology* 14 (1),111–116.

Taus, C., Giuliani, G., Pucci, E., et al., 2003. Amantadine for fatigue in multiple sclerosis. *Cochrane Database Syst Rev* (2):CD00281

Teitelbaum, D., Sela, M., Arnon, R., 1997. Copolymer 1 from the laboratory to FDA. *Journal of Medical Sciences* 33, 280-284.

Tesmer, L.A., Lundy, S.K., Sarkar, S., Fox, D.A., 2008. Th17 cells in human disease. *Immunological Reviews* 223, 87-113.

The New York Times, Health Guide. Multiple Sclerosis. Accessed February 1, 2012, at: <http://health.nytimes.com/health/guides/disease/multiple-sclerosis/overview.html>

Tomar, L.K., Tyagi, C., Lahiri, S.S., Singh, H., 2011. Poly(PEGDMA-MAA) copolymeric micro and nanoparticles for oral insulin delivery. *Polym. Adv. Technol.* 22, 1760–1767

Totoiu, M.O., Keirstead, H.S., 2005. Spinal cord injury is accompanied by chronic progressive demyelination. *Journal of Comparative Neurology* 486(4), 373–383

Two Genes Identified As Potential Therapeutic Targets For Multiple Sclerosis., [http://www.sciencedaily.com /releases/2009/09/090911083327.htm](http://www.sciencedaily.com/releases/2009/09/090911083327.htm).accessed on 11-03-2013. Updated September 2009

Tzartos, J.S., Khan, G., Vossenkamper, A., Cruz-Sadaba, M., Lonardi, S., Sefia, E., Meager, A., Elia, A., Middeldorp, J.M., Clemens, M., Farrell, P.J., Giovannoni, G. , Meier, U.C., 2012. Association of innate immune activation with latent Epstein– Barr virus in active MS lesions. *Neurology* 78, 15–23.

Ure, D.R., Rodriguez, M., 2002. Polyreactive antibodies to glatiramer acetate promote myelin repair in murine model of demyelinating disease. *FASEB Journal* 16 (10), 1260-2

Uze, G., Schreiber, G., Piehler, J., Pellegrini, S., 2007. The receptor of the type I interferon family. *Current topics in microbiology and immunology* 316 , 71–95.

Vajda, F.J.E., 2002. Neuroprotection and neurodegenerative disease. *Journal of Clinical Neuroscience* 9(1), 4-8

van der Voort Maarschalk, K., Zuurman, K., Vromans, H., Bolhuis, G.K., Lerk, C.F., 1996. Porosity expansion of tablets as a result of bonding and deformation of particulate solids, *Int J Pharm.* 140, 185-193

van Boxel-Dezaire, A.H., Rani, M.R., Stark.,G.R., 2006. Complex modulation of cell type-specific signaling in response to type I interferons. *Immunity* 25(3), 361–372.

van den Noort, S., 2005. Signs and Symptoms of Multiple Sclerosis. *Current Clinical Neurology* 1-14.

van der Voort Maarschalk, K, Zuurman K, Vromans H, Bolhuis GK, Lerk CF, Porosity expansion of tablets as a result of bonding and deformation of particulate solids, *Int J Pharm.* 1996; 140: 185-193.

Venkatesan, N, et al., 2005. Liquid filled nanoparticles as a drug delivery tool for protein therapeutics. *Biomaterials* 26 (34) 7154-7163.

Veronese, F.M., Pasut, G., 2005. Pegylation, successful approach to drug delivery. *Drug Discov. Today* .10, 1451-1458.

Viagra could reduce multiple sclerosis symptoms, study suggests. <http://www.sciencedaily.com/releases/2011/05/110519090354.htm>. accessed on 11-03-2013. Updated on May 2011

Virtanen, J.O., Pietilainen-Nickle, J., Uotila, L., Farkkila, M., Vaheri, A., Koskiniemi, M., 2011. Intrathecal human herpes virus 6 antibodies in multiple sclerosis and other demyelinating diseases presenting as oligoclonal bands in cerebrospinal fluid. *Journal of Neuroimmunology* 237, 93–97.

Watson, C.M., Davison, A.N., Baker, D., et al., 1991. Suppression of demyelination by mitoxantrone. *International Journal of Immunopharmacology* 13, 923-930.

Weber, M.S., Starck, M., Wagenpfeil, S., et al., 2004. Multiple sclerosis: glatiramer acetate inhibits monocyte reactivity in vitro and in vivo. *Brain* 127, 1370-8

Wenker, S.D., Wettstein, R., 2013. Secondary burn progression decreased by erythropoietin. *Crit Care Med*, 41(4):963-971.

Wiesemann, E., Klatt, J., Sonmez, D., et al., 2001. Glatiramer acetate (GA) induces IL-13/IL-5 secretion in naive T cells. *Journal of Neuroimmunology* 119 (1), 137-44.

Wingerchuck, D.M., Benarroch, E.E., O'Brien, P.C., et al., 2005. A randomized controlled crossover trial of aspirin for fatigue in multiple sclerosis. *Neurology* 64, 1267–1269

Worakul, N., Robinson, J.R., 1997. Ocular pharmacokinetics/pharmacodynamics. *Eur J Pharm Biopharm*, 44(1627): 71-83.

www.druglib.com, Accessed on 18 june 2013. Last updated on 2005.09.30. [www.druglib.com/druginfo/rebif/description\\_pharmacology](http://www.druglib.com/druginfo/rebif/description_pharmacology)

Yadav, V., Bourdette, D. 2012. New Disease-Modifying Therapies and New Challenges for MS. *Current Neurology and Neuroscience Reports* 12 (5), 489-491

Yamakawa, T., Yang, L., Chu, J.S., Fix, J.A., 2002. Colon-specific drug delivery: new approaches and in vitro/in vivo evaluation. *Int J Pharm.* 235:1–15.

Yang, L., Chu, J.S., Fix, J.A., 2002. Colon-specific drug delivery: new approaches and in vitro/in vivo evaluation. *Int J Pharm.* 235, 1–15.

Yeo, T.W., De Jager, P.L., Gregory, S.G., Barcellos, L.F., Walton, A., Goris, A., et al., 2007. A second major histocompatibility complex susceptibility locus for multiple sclerosis. *Annals of Neurology* 61(3), 228-36.

Yousry, T., Major, E., Ryschkewitsch, C., et al., 2006. Evaluation of patients treated with natalizumab for progressive multifocal leukoencephalopathy. *New England Journal of Medicine* 354, 924–33.

Zhang, Y., Huo, M., Zhou, J., Xie, S., 2010. PKSolver: An add-in program for pharmacokinetic and pharmacodynamic data analysis in Microsoft Excel. *Comp Meth Progr Biomed*, 99(3): 306-314.

Zhou, Z., Ren, Y., Yang, D, Nie, J., 2009. Performance improvement of injectable poly(ethylene glycol) dimethacrylatebased hydrogels with finely dispersed hydroxyapatite, *Biomed. Mater.* 4 035007 (7pp)


Ziemann , U., Wahl, M., Hattingen , E., Tumani , H., 2011. Development of biomarkers for multiple sclerosis as a neurodegenerative disorder. *Progress in Neurobiology* 95, 670–685.

Ziemssen, T., Kumpfel, T., Klinkert, W.E., et al., 2002. Glatiramer acetate-specific T-helper 1 and 2-type cell lines produce brain derived neurotrophic factor (BDNF): implications for multiple sclerosis therapy. *Brain* 125, 238-2391.

## 8. APPENDICES

### 8.1. Animal Ethics Clearance Certificate

AESC3

  
UNIVERSITY OF THE WESTERN CAPE  
FELAMAMETHEC

**STRICTLY CONFIDENTIAL**

**ANIMAL ETHICS SCREENING COMMITTEE (AESC)**

**CLEARANCE CERTIFICATE NO.** 2012/41/05

**APPLICANT:** Mr. P P D Kondiah

**DEPARTMENT:** Department of Pharmacy and Pharmacology

**PROJECT TITLE:** *In Vivo* analysis of an oral polypeptide macromolecular polymeric delivery systems in a rabbit model

**Number and Species**

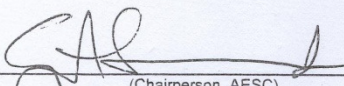
53 female New Zealand White Rabbits

Approval was given for the use of animals for the project described above at an AESC meeting held on **25 September 2012**. This approval remains valid until **30 September 2014**.

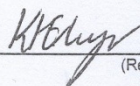
The use of these animals is subject to AESC guidelines for the use and care of animals, is limited to the procedures described in the application and to the following additional conditions:

**Conditions:**

- A glucometer is used in parallel with the stated technique for measuring the development of diabetes
- Three rabbits are used in a pilot test to ascertain the feasibility of administering four anaesthetics in a single day.

Signed:  Date: 5/10/12  
(Chairperson, AESC)

I am satisfied that the persons listed in this application are competent to perform the procedures therein, in terms of Section 23 (1) (c) of the Veterinary and Para-Veterinary Professions Act (19 of 1982)

Signed:  Date: 8/10/12  
(Registered Veterinarian)

cc: Supervisor:  
Director: CAS



Contents lists available at ScienceDirect

International Journal of Pharmaceutics

journal homepage: [www.elsevier.com/locate/ijpharm](http://www.elsevier.com/locate/ijpharm)

## A novel pH-sensitive interferon- $\beta$ (INF- $\beta$ ) oral delivery system for application in multiple sclerosis



Pierre P.D. Kondiah<sup>a</sup>, Lomas K. Tomar<sup>a</sup>, Charu Tyagi<sup>a</sup>, Yahya E. Choonara<sup>a</sup>, Girish Modi<sup>b</sup>,  
Lisa C. du Toit<sup>a</sup>, Pradeep Kumar<sup>a</sup>, Viness Pillay<sup>a,\*</sup>

<sup>a</sup> University of the Witwatersrand, Faculty of Health Sciences, Department of Pharmacy and Pharmacology, 7 York Road, Parktown, Johannesburg 2193, South Africa

<sup>b</sup> University of the Witwatersrand, Faculty of Health Sciences, Division of Neurosciences, Department of Neurology, 7 York Road, Parktown, Johannesburg 2193, South Africa

### ARTICLE INFO

#### Article history:

Received 2 July 2013

Received in revised form 20 August 2013

Accepted 24 August 2013

Available online 1 September 2013

#### Keywords:

Oral delivery system

Interferon- $\beta$  (INF- $\beta$ )

Insulin

Box-Behnken experimental design

Copolymeric microparticulate system

pH-responsive

### ABSTRACT

pH-sensitive microparticles were prepared using trimethyl-chitosan (TMC), poly(ethylene glycol)dimethacrylate (PEGDMA) and methacrylic acid (MAA) by free radical suspension polymerization, for the oral delivery of interferon- $\beta$  (INF- $\beta$ ). The microparticles were subsequently compressed into a suitable oral tablet formulation. A Box-Behnken experimental design was employed for generating a series of formulations with varying concentrations of TMC (0.05–0.5 g/100 mL) and percentage crosslinker (polyethylene glycol diacrylate) (3–8%, w/w of monomers), for establishment of an optimized TMC-PEGDMA-MAA copolymeric microparticles. For pragmatism, insulin was initially employed as the model peptide for undertaking the preliminary experimentation and the optimized formulation was subsequently evaluated using INF- $\beta$ . The prepared copolymeric microparticulate system was characterized for its morphological, porosimetric and mucoadhesive properties. The optimized microparticles with 0.5 g/100 mL TMC and 3% crosslinker had an INF- $\beta$  loading efficiency of 53.25%. The *in vitro* release of INF- $\beta$  was recorded at 74% and 3% in intestinal (pH 6.8) and gastric (pH 1.2) pH from the oral tablet formulation, respectively. The tablet was further evaluated for plasma concentration of INF- $\beta$  in the New Zealand White rabbit, and compared to a known subcutaneous formulation. The system showed an astounding effective release profile over 24 h with higher INF- $\beta$  plasma concentrations compared with the subcutaneous injection formulation.

© 2013 Elsevier B.V. All rights reserved.

### 1. Introduction

Multiple sclerosis (MS) is a chronic neurodegenerative disease that is characterized by its central nervous system effects commonly manifesting as tremors, dizziness, visual disturbances, limb weakness, muscle spasms, loss of sensation, speech impediment and depression (Fischer et al., 2011; Stuart and Bergstrom, 2011). Interferon- $\beta$  (INF- $\beta$ ) is the most effective and widely used peptide drug for the treatment of multiple sclerosis (Jongen et al., 2011). Interferons exist naturally as a globular protein comprising of 5 helices and a molecular weight (Mw) of 20 kDa (Arduini et al., 1999). The fundamental effect of INF- $\beta$  in the treatment of MS is based on reducing the immune response that is directed against myelin of the central nervous system, i.e. the fatty sheath that surrounds and protects nerve fibers. Damage of nerve fibers, resulting in demyelination, consequently causes nerve impulses to be slowed or halted, thus producing symptoms of MS (Jongen et al., 2011).

Presently INF- $\beta$  dose is administered via parenteral route. But, this daily injection therapy (subcutaneously or as intramuscular injections) of INF- $\beta$  has various disadvantages associated with multiple problems of pain, allergic reactions, poor patient compliance and chances of infection (Chiu et al., 2007). To overcome these problems, researchers are investigating alternative routes of delivery such as oral or pulmonary (Shaji and Patole, 2008).

The development of peptide and protein oral formulations has become an increasingly demanding form of drug delivery, and remains an attractive alternative to parenteral formulations. But there are challenges associated with the oral route of peptide delivery which include pre-systemic enzymatic degradation of the peptide and its poor permeation through the intestinal membrane (Morishita and Peppas, 2006). Absorption is the primary concern of the therapeutic in which the small intestine is the targeted area for this to occur, provided the dosage form reaches this site intact without being degraded. Translocation through the mucus layer is also an essential component, since this can severely hinder the absorption if the polymer system does not adhere to the mucus layer and release the peptide concurrently (Mustata and Dinh, 2005).

\* Corresponding author. Tel.: +27 11 717 2274; fax: +27 11 642 4355.  
E-mail address: [viness.pillay@wits.ac.za](mailto:viness.pillay@wits.ac.za) (V. Pillay).

### 8.3. Research Output Presentation

Cross-faculty postgraduate research day, University of the Witwatersrand, Johannesburg, South Africa, 2014

#### Novel pH sensitive oral Interferon- $\beta$ delivery system for application in Multiple Sclerosis

Pierre P D Kondiah<sup>1</sup>, Yahya E. Choonara<sup>1</sup>, Lomas. K. Tomar<sup>1</sup>, Charu Tyagi<sup>1</sup>, Lisa C. du Toit<sup>1</sup>, Pradeep Kumar<sup>1</sup>, Girish Modi<sup>2</sup> and Viness Pillay<sup>1\*</sup>

<sup>1</sup>Department of Pharmacy and Pharmacology, University of the Witwatersrand, 7 York Road, Parktown, Johannesburg 2193, South Africa

<sup>2</sup>Department of Neurology, University of the Witwatersrand, 7 York Road, Parktown, Johannesburg 2193, South Africa

**\*Correspondence:**

**Viness Pillay**

**viness.pillay@wits.ac.za**

#### Abstract

Multiple sclerosis (MS) affects a wide range of individuals with the statistical value of 1.3 in 1000 people affected in developed world countries. There is however, a high degree of correlation between inflammation and axonal injury in all possible stages of MS with axonal and neuronal degenerative lesions in active demyelinating neuronal tissue. Prevalently, the most successful form of therapy is the treatment with Interferon beta (INF- $\beta$ ) injectables. Taking into account the demand for oral drug delivery, an oral pH-sensitive Interferon beta (INF- $\beta$ ) delivery system was prepared by free radical suspension polymerization reaction. A Box-Behnken design program was employed for generating a series of formulations with varying concentrations of polymer and cross-linker, for establishment of an optimized copolymeric microparticulate formulation. Insulin was employed as the prototype peptide for experimental design and the optimized formulation was subsequently evaluated for INF- $\beta$ . The prepared copolymeric system was characterized for morphological, porosimetric and mucoadhesive properties. The optimized copolymeric particulate system had INF- $\beta$  loading efficiency of 53.25% and *in vitro* release of 3% and 74% in gastric (pH 1.2) and intestinal (pH 6.8) simulated conditions, respectively. The oral peptide delivery system was further evaluated for bioavailability of INF- $\beta$  employing New Zealand White rabbit model and compared to the commercial subcutaneous formulation (Rebif<sup>®</sup>) for efficacy and efficiency. The particulate system showed an astounding effective release profile for 24 hours, with higher INF- $\beta$  blood concentration than the commercial subcutaneous injection formulation. This implies successful delivery of INF- $\beta$  orally, providing a platform for advances in the treatment of MS.

**Keywords:** Oral delivery system, Interferon beta (INF- $\beta$ ), Box-Behnken design, copolymeric particulate system